NASA Technical Memorandum 85646

Flight Measurement and Analysis of AAFE RADSCAT Wind Speed Signature of the Ocean

Lyle C. Schroeder, W. Linwood Jones,
Philip R. Schaffner, and John L. Mitchell

JANUARY 1984

NASA

NASA Technical Memorandum 85646

Flight Measurement and Analysis of AAFE RADSCAT Wind Speed Signature of the Ocean

Lyle C. Schroeder
Langley Research Center
Hampton, Virginia

W. Linwood Jones
Satellite Television Corporation
Princeton Junction, New Jersey

Philip R. Schaffner
Research Triangle Institute
Hampton, Virginia

John L. Mitchell
Kentron International, Inc.
Hampton, Virginia

National Aeronautics
and Space Administration

**Scientific and Technical
Information Office**

1984

Use of trade names in this report does not constitute an official endorsement of such products, either expressed or implied, by the National Aeronautics and Space Administration.

CONTENTS

SUMMARY

About 10 years ago, the advanced aerospace flight experiment radiometer scatterometer (AAFE RADSCAT) made its first successful measurements of ocean radar scattering cross section from a NASA C-130 aircraft. This instrument was developed as a research tool to evaluate the use of microwave frequency remote sensors (particularly radars) to provide wind speed information at the ocean surface. The AAFE RADSCAT helped establish the feasibility of the satellite scatterometer for measuring both wind speed and direction. Probably the most important function of the AAFE RADSCAT was to provide a data base of ocean normalized radar cross section (NRCS) measurements as a function of surface wind vector at 13.9 GHz. NRCS measurements over a wide parametric range of incidence angles, azimuth angles, and winds were obtained in a series of RADSCAT aircraft missions from 1973 to 1977.

Presented in this report are analyses of data from 26 of these flights during which the quality of the sensor and the surface wind measurements were felt to be understood. This data base was used to model the relationship between k_u-band radar signature and ocean surface wind vector. The models developed therefrom are compared with those used for inversion of the SEASAT-A satellite scatterometer (SASS) radar measurements to wind speeds. This report represents a comprehensive analysis of the complete RADSCAT data base.

INTRODUCTION

About 10 years ago, the AAFE RADSCAT[1] made its first successful measurements of ocean radar scattering cross section from a C-130 (NASA 929) aircraft. The AAFE RADSCAT instrument, which was similar to the S-193 RADSCAT that flew on Skylab, was developed in part as a research tool to evaluate the use of microwave frequency remote sensors (particularly radars) to provide wind speed information at the ocean surface (ref. 1). The previous data (refs. 2, 3, and 4) were inconsistent; some data predicted very low sensitivities of normalized radar cross section (NRCS) to winds, whereas others indicated sensitivities proportional to the square of the wind speed. The AAFE RADSCAT established that the greater sensitivity prediction was correct (ref. 5), and this helped to establish the feasibility of a satellite scatterometer as a wind sensor. Of equal significance, however, was the demonstration by RADSCAT during circular flight lines over the ocean that the NRCS is anisotropic with respect to surface wind direction, with peaks when the radar looks upwind and downwind, and with minimums near the crosswind directions (ref. 6).

Probably the most important function of the AAFE RADSCAT was to provide a data base of ocean NRCS measurements as a function of surface wind vector at 13.9 GHz. NRCS measurements over a wide parametric range of incidence angles, azimuth angles, and winds were obtained in a series of RADSCAT aircraft missions from 1973 to 1977. Presented herein are analyses of data from 26 of these flights (shown in table I) during which the quality of the sensor and the surface wind measurements were felt to be understood. Data from five of these flights have been previously reported in

---

[1]Compound acronym for advanced aerospace flight experiment radiometer scatterometer.

reference 6, and other analyses of the JONSWAP and 1976 East Coast flights have been published in references 7 and 8. RADSCAT-inferred wind measurements were compared with sonic anemometer measurements in the 1977 West Coast flights (ref. 9). Subsets of this data base were used to model the relationship between k_u-band radar signature and ocean surface wind vector. The models developed therefrom were used for inversion of the SEASAT-A satellite scatterometer (SASS) radar measurements to wind speeds (ref. 10). The present report represents a comprehensive analysis of the complete RADSCAT data base.

SCATTEROMETER DESCRIPTION

A combined microwave radiometer scatterometer (RADSCAT) operating at 13.9 GHz was developed to measure the microwave brightness temperature and scattering cross section of the ocean from aircraft altitudes. The radiometer measurement capability was found to be coarse (±10 K), and is not discussed further in this report. A detailed description of the AAFE RADSCAT and its operation is given in reference 11; therefore, only a brief description of the scatterometer portion from reference 6 is given herein. A simplified block diagram of the scatterometer subsystem is given in figure 1. During normal operation, the radiometer and scatterometer measurements were time shared through the use of a single pencil beam antenna. For the scatterometer measurement, "long" pulses (i.e., 32 μsec at 1524-m altitude) were transmitted to the surface such that the area illuminated was defined by the antenna pattern, that is, beam-limited conditions.

For smooth seas and light winds, the backscattered signal at 13.9 GHz has a dynamic range of approximately 60 dB for measurements from nadir to 55° incidence angle. Since the useful power measurement range of a square-law detector is typically 20 dB, four receiver channels were used in parallel with staggered sensitivities to insure continuous operation over the complete receiver dynamic range. In each channel, the signal was square-law detected and then integrated for a selectable period ranging from 300 to 924 ms. The integrator outputs were analog-to-digital converted and recorded in a PCM format on an analog magnetic tape recorder.

In making scatterometer measurements of the ocean, the quantity of interest is the normalized scattering cross section (NRCS), which is the same as scattering coefficient σ^o. This quantity is independent of the type of radar performing the measurement. In terms of the RADSCAT transfer function, the expression for σ^o is

$$\sigma^o = (16\pi)^2 \frac{A^2}{\lambda^2} \frac{V_{sea}\tau_{cal}}{V_{cal}\tau_{sea}} \frac{\alpha(GXR)}{G^2\beta^2 \cos\theta} \tag{1}$$

where

A altitude of aircraft, m

G antenna gain

GXR receiver calibration loop attenuation

V output voltage of scatterometer integrator, V

α calibration attenuator value for given channel

β equivalent beamwidth, rad

θ incidence angle, deg

λ free-space wavelength, m

τ scatterometer integration time, s

and subscripts are defined as follows:

cal during calibration

sea during sea operation

The measurements presented in this paper were obtained with RADSCAT operating on a C-130 cargo aircraft (NASA 929). The instrument was mounted on the cargo ramp (lower door on the fuselage aft end). For in-flight operation, the ramp was lowered and the RADSCAT extended to its operational position outside the fuselage. In this configuration, the antenna had an unobstructed view of the ocean surface without the use of a radome.

SURFACE MEASUREMENTS

For each flight, the local ocean surface wind vector and temperature (and, at times, wave) conditions were measured by either in situ instrumentation or by onboard aircraft sensors. These measurements are commonly called "surface truth" for remote-sensing measurement missions. A summary of these measurements is given in table II. Extrapolations of these measurements using meteorological analyses and time-space interpolations to the ocean surface at individual flight times is provided in table III. Typical in situ measurements consisted of 10-min averages of wind speed and direction; air temperature and near-surface sea temperature were obtained hourly during the scatterometer experiment. Onboard surface truth was usually obtained at the beginning and the end of the flight, with these observations typically separated by 3 to 4 hours. Flight lines were about 30 km long and were flown in upwind and downwind directions at an altitude of 50 to 150 m. Wind speed and direction measurements were obtained from the aircraft inertial navigation system (Litton LTN-51). Wave measurements were obtained on certain flights using a laser profilometer (Spectra-Physics Geodolite 3A) but were generally not reduced to geophysical values. Wave conditions reported in this document were obtained from weather stations and buoys.

To be consistent with previous investigators, the surface wind measurements are presented at an altitude of 19.5 m. The wind direction measured by the aircraft at altitudes of 100 to 150 m was assumed to be the same as at 19.5 m. The wind speed, however, was extrapolated by using a boundary-layer wind profile model by Cardone (ref. 12). In this model, the wind speed was first extrapolated to the ocean surface value with a profile determined by the air-sea temperature difference, and then extrapolated back to 19.5 with a profile for zero air-sea temperature difference (neutral stability conditions). This wind speed is considered to be proportional to the surface wind stress and is not the actual wind speed at 19.5 m. During the low altitude flight lines, the required temperatures were measured onboard with a Barnes PRT-5 infrared radiometer for sea surface temperature and a Rosemont Model 103 temperature sensor for total air temperature.

NORMALIZED RADAR CROSS SECTION (NRCS) DATA

The experimental data used in these analyses were acquired during aircraft flight missions between 1973 and 1977, as given in table I. The list identifies the aircraft mission and flight number assigned by NASA, the average location of the flight lines, and a characterization of the data which were acquired.

The quality of the sensor measurements varied from flight to flight. In the early missions (1973-1974), the instrument was under development, and henceforth many caveats qualify the use of the data. The most important of these have to do with uncertainties in NRCS caused by lack of temperature stabilization of the radio-frequency (RF) system and band-pass filters and the stability of the periodic gain calibrations. (A discussion of these and other findings during the development and calibration of the instrument is given in ref. 11.) These and other shortcomings in the data are indicated in table I and later in the text where important.

The measurements reported herein came from two basic flight line patterns: straight level lines and circular flight lines. The resulting data are discussed separately.

Straight Level Lines

The straight level lines were flown (fig. 2, upper part) with a level aircraft platform at a constant altitude and with aircraft heading held constant within about ±7.5°. The flight direction was usually selected so that the antenna was pointed in the upwind, downwind, or crosswind direction. The instrument generally operated in the fixed-angle mode (ref. 11) with polarization automatically switched between horizontal (H) and vertical (V). In this mode, the antenna gimbal system automatically scanned the incidence angle through six positions, taking three measurements in each polarization at each position. A summary of data from straight level lines is presented in table IV. These data are organized chronologically by flight. For each entry, the mission, flight, line, and date are presented. The table presents, for each polarization, the average and standard deviation of incidence angle θ, the ratio average and normalized standard deviation of NRCS, an estimate of instrument error, the sample time, and the time-interpolated neutral stability wind speed at 19.5 m above the sea surface. Data are tabulated separately for upwind, downwind, and crosswind measurements.

Since the circular flight lines also provide measurements at upwind, downwind, and crosswind directions, these data are also included in table IV. These data represent an average of all NRCS measurements from the circle flight made at the desired wind azimuth, ±10°.

The trends of the data from table IV were analyzed with regression techniques. The dependence of NRCS on incidence angle was examined in a two-step process. (See fig. 3.) First, each set of measurements was fit by a least-mean-squares polynomial curve of time-weighted NRCS versus incidence angle. Because of the multiple curvatures required to fit these data sets, the regressions were applied piecewise; a third- or fourth-order fit was used for incidence angles from 0° to 40°, and a linear fit was used for incidence angles greater than 40°. Most of the analyses of the straight level flight data were performed in this manner. Even using this piecewise approach, the value of the regression fit was often poor at nadir; for this reason, the value obtained from the regression fit was not used in any subsequent analysis for incidence angles less than 10°. Later, it was determined that for convenience

and uniformity, these piecewise curves could be represented within ±2 dB with a sixth-order regression constructed by sampling the piecewise curves every 1°. The sixth-order regression coefficients are shown in table V and were used in subsequent analysis of the flight data. Except near nadir, the resulting regression fits for NRCS versus incidence angle and the related surface truth wind speed and direction, interpolated to the time of the data set, were assumed to experimentally characterize the radar signature of the ocean.

As the next step, a linear regression of NRCS (dB) values at selected incidence angles versus the log of wind speed was performed. (The NRCS values for every 10° in incidence angle from 10° to 70° were obtained with the curve fits just discussed. Nadir values were obtained from the mean measured value of the near-nadir measurements. These values are given in table VI.) This type of parametric relationship was used in an earlier paper (ref. 6) and as the basis of the SASS I model which converted the SASS NRCS measurements to wind speed (ref. 10). The results of this analysis are provided in figure 4. Trends from the SASS I model function, which is based in part on these data and also on SASS measurements, are shown in these plots for comparison (dashed lines).

The trends exhibited by these data are for the most part consistent. All data at 0° incidence have negative slopes, the data at 10° incidence are nearly flat, and for the data at 20° incidence, the slope is of the order of 10 dB/decade. From 30° to 60° at horizontal polarization and from 30° to 50° at vertical polarization, the slope is near 20 dB/decade. At 60° incidence, there is a trend at vertical polarization to lower slopes. Also, at incidence angles of 30° and above, the magnitude of NRCS tends to decrease uniformly with incidence angle for both vertical and horizontal polarization, but the decrease is considerably less for vertical polarization. All these observations are in agreement with the earlier results (ref. 6) based on only five such aircraft flights. The comparison with the SASS I model shows that the same basic slope trends exist except that the SASS I does not model the decrease in slope at 60° incidence. Both data sets are suspect for this case: the RADSCAT because measurement errors at low signal levels are more likely and because the regression interpolation to 60° may not be accurate, and the SASS I model because of a sparsity of data used in the model. For wind speeds greater than 3 m/s, the plots show biases of from 2 to 3 dB in some cases, with SASS I higher in most cases. The reason for this is not known. Perhaps the dependence of an additional parameter, such as surface water temperature (personal communication from Peter M. Woiceshyn of Jet Propulsion Laboratory), which is present in the aircraft data but has been tuned out from the SASS JASIN (ref. 10) calibrations is responsible for the biases.

In a second analysis, NRCS in ratio form was analyzed as a function of linear wind speed. The advantage of this kind of analysis is that all errors in wind speed are represented as a constant band of errors, independent of wind speed, which is not the case for the first analysis. Since the dynamic range of the instrument is about 60 dB, the NRCS in ratio spans about 6 decades; hence, the analysis for each incidence angle must be plotted separately.

Typical results of this analysis are shown in the plots of downwind horizontal polarization data (fig. 5). In addition to the data points, the least-mean-squares polynomial curve fit (lines) are shown. The curve fits for the other directions and polarizations are shown in appendix A. Linear regression fits appeared best at incidence angles of 0°, 10°, and 20°, whereas second-order fits were better for 30° through 60°. To force the slope of the second-order fit to be 0 at a wind speed of 0, the mirror image of the data (i.e., the same NRCS at negative wind speeds) was input to the regression model. The trends from the SASS I model are also shown as

dashed lines on these plots for comparison. Regression coefficients for all polarizations and directions are given in table VII.

An examination of the plots for 0°, 10°, and 20° shows that, in general, the linear fit describes the data pretty well. The scatter is greater at 10° than for the other angles; this is a surprise, since NRCS at this angle is considered to be somewhat invariant. The nadir data show the least scatter, but at 20°, the trend is also good. The SASS I trend is, in general, higher than the aircraft data by 0.4 to 2.2 dB at nadir, 1 to 2.2 dB at 10°, and 0 to 2.4 dB at 20°. At 30° incidence and above, the scatter appears to be less except for three or so points (outliers) on each plot. These outliers indicate that NRCS measurements from mission 306, FCF (21.5 m/s) and mission 288, flight 5 (22.2 m/s) are too high at 40° and above or that the wind speed measured for these missions is incorrect. For mission 306, FCF both situations are likely since wind speed and direction had to be interpolated in time and space from ships of opportunity and because there were problems in calibrating the receiver during earlier RADSCAT flights. The data from mission 288, flight 5 may be distorted because of shifts in the gain correction characteristics for the bandpass filter.

Circle Flight Lines

The circle flight lines were made with the aircraft flying circles with fixed bank angles and with the antenna set in a fixed antenna gimbal position. (See fig. 2, lower part.) Thus, data were obtained for a complete rotation in azimuth with a nearly constant incidence angle. In a typical flight, such azimuth scans were obtained at up to five different incidence angles, which spanned from about 10° to nearly 70°.

The analysis of these data as illustrated in figure 6 was accomplished in three steps: (1) a ninth-order model in which (NRCS) = $f(\theta, \cos\phi, \sin\phi, \cos 2\phi, \sin 2\phi)$ was used to characterize the data (where ϕ is azimuth angle); (2) the ninth-order model was used to correct the data to the value for the average incidence angle for each circle; and (3) a second-order model in which (NRCS) = $f(\cos\chi, \cos 2\chi)$ was used to fit the data corrected to constant incidence angle (where χ is the wind azimuth relative to upwind). (Previous modeling studies of radar circle flight data are given in ref. 8.) The mathematical model development is given in appendix B. These steps are summarized further in the following paragraphs.

The first step in the analysis of the circle data was to attempt to find a model which could generally be used to fit the data. The model used was

$$(\text{NRCS}) = \sum_{n=0}^{2} \left[\left(a_n + b_n\theta\right) \cos n\phi + \left(c_n + d_n\theta\right) \sin n\phi \right] \qquad (2)$$

(ninth-order model)

$$\begin{aligned}(\text{NRCS}) = {} & A_0 + A_1\theta + A_2 \cos\phi + A_3\theta \cos\phi + A_4 \sin\phi \\ & + A_5\theta \sin\phi + A_6 \cos 2\phi + A_7\theta \cos 2\phi + A_8 \sin 2\phi \\ & + A_9\theta \sin 2\phi \end{aligned} \qquad (3)$$

All data from a circle flight line at a given incidence angle were used to find the least-mean-squares fit for this model. Figure 7 shows a plot of NRCS versus azimuth which results from this process for a typical case. Three separate data sets are shown in this figure. The dots represent the input data. Note that there is considerable scatter in these data, not only from measurement noise but also from normal flight variation in incidence angle. The plus symbol represents values obtained from the input incidence and azimuth angles used with the ninth-order model coefficients. These values provide a judgment of how well the model characterizes the data. The normalized standard deviation (NSD) and the multiple correlation coefficient (R^2) of the differences between input and model data are calculated and printed at the top of the plot along with the regression coefficients. The solid line shows a fairing of the model evaluated at the average incidence angle for 1° increments in azimuth. The critical points of this curve, used to estimate the upwind and downwind peaks and the crosswind minima, are also tabulated.

The ninth-order fit was obtained for all data from circle flight lines reported herein, and the resulting coefficients are given in table VIII. However, the ninth-order model had certain disadvantages; it was too complex, and it showed a tendency for the variation due to wind speed to exceed that due to incidence angle change for variable wind conditions. Prior modelers (ref. 8 and unpublished work done under NOAA Grant No. 04-4-158-11 during 1974 by Willard J. Pierson, Vincent J. Cardone, and J. Arthur Greenwood of City University of New York) have shown that if the incidence angle can be held constant and wind direction is known, the data can be expressed more simply as

$$(\text{NRCS}) = \sum_{n=0}^{2} A_n \cos n\chi \qquad \text{(second-order model)} \tag{4}$$

where χ is the wind azimuth relative to upwind.

The wind direction can be estimated from the maximum in the ninth-order model closest to the surface truth wind azimuth. To remove incidence angle as a parameter, we previously, in reference 6, used upwind, downwind, and crosswind data from the same flight, such as in table IV, to provide a means to correct the data to a constant incidence angle. The corrections to the NRCS data were interpolated in azimuth by calculating the vectorial sum of corrections from the two orthogonal directions (upwind-crosswind or downwind-crosswind) surrounding the azimuth of the data as follows:

$$\Delta\sigma^{o}\big|_{\chi} = \Delta\theta \frac{d\sigma^{o}_{u \text{ or } d}}{d\theta} \cos\chi + \Delta\theta \frac{d\sigma^{o}_{c}}{d\theta} \sin\chi \tag{5}$$

where subscripts are defined as follows:

u upwind

d downwind

c crosswind

However, in this analysis, a more direct calculation of the correction was obtained by calculating from equation (2) or (3)

$$\Delta(\text{NRCS})\Big|_{\chi} = d(\text{NRCS})/d\theta\Big|_{\chi} \Delta\theta \tag{6}$$

It was considered desirable to use this method of correction so that the reduction of circle azimuth scans would be independent of other auxiliary flight lines. The other flight lines represent possible error sources because they are performed at different times and locations. Figure 8 shows an example of a plot of $d(\text{NRCS})/d\theta$ versus azimuth corresponding to the conditions of figure 7. The correction curve shows for this case that the slope is bounded between values of -0.31 to -0.81 dB, as should be expected. Other cases, particularly at conditions of high incidence angle and low wind speed show singular points in the derivative and hence do not model the data well. These cases are pointed out in subsequent discussion or tables but, in general, the behavior of the derivative must be examined before equation (6) is used to correct for incidence angle.

After subtraction of the wind azimuth from ϕ to obtain χ and correction of the NRCS for incidence angle by equation (6), the second-order model of equation (4) was used to fit the data. Figure 9 shows an example of the fits for the azimuth scans at the various incidence angles of mission 335, flight 5. Horizontal and vertical polarizations are shown in figures 9(a) and (b), respectively.

The dots show the NRCS data after having been corrected to the constant average incidence angle by equation (6). The lines are the least-mean-squares fits of these data. The symbols at the maxima of these lines refer to the table at the top of each plot, which indicates the flight conditions, the regression coefficients, the R^2 multiple correlation coefficient, and the normalized standard deviation of the data. In like manner, data from all circle flight lines of this data set were fit with the second-order model, and results are presented in appendix C. The results of the regression fits are provided in table IX. In general, the fits of the second-order model are more stable than those for the ninth-order model, and the fits are quite good. The NSD of the corrected data is usually small except for data for high incidence angle or low wind speed.

To display the trends and check the consistency of the data, measurements of NRCS from circles flown at approximately the same incidence angle were plotted as a function of wind azimuth on the same plot. Circle line data were divided in incidence into groups $\pm 5°$ wide centered at 10°, 20°, 30°, 40°, 50°, 60°, and 70°. The NRCS measurements were corrected to the mean incidence angle. The measurements required corrections as high as 5°. Since this amount of correction generally exceeded the range of incidence angle experienced during a circle flight, sizable errors could result if the corrections were computed with $d(\text{NRCS})/d\theta$ from equation (6). Therefore, the amount of correction was computed by using equation (4).

The resulting plots are given in figures 10 through 16. The horizontal and vertical polarization data are shown as parts (a) and (b), respectively. A legend at the top of each plot identifies each flight line shown, along with the pertinent second-order regression results. (The CHI. SIGMA MIN. refers to the azimuth of σ^o mimima). Shown additionally in these plots for comparison are the trends (dashed lines) predicted from the SASS I model at wind speeds of 5, 15, and 25 m/s.

The 10° circles show a very weak wind dependence. The data (except for mission 306, FCF) are clustered at about 6.0 ± 1 dB at upwind and downwind and 5.5 ± 0.1 dB at crosswind (figs. 10(a) and (b)). Anisotropy is not strongly evident, except for mission 306, FCF; the stronger anisotropic behavior for this flight may be due to data actually being taken at about 15° incidence and, hence, more likely to exhibit anisotropy. Upwind NRCS for a given data set is less than downwind for wind speeds greater than 5.4 m/s (table X). These results agree on the average with the data from the SASS I table, as can be seen by a comparison of the upper and lower plots for these figures.

At 20°, a wind dependence is evident; from the lowest to the highest wind speeds shown, the NRCS increases by about 9 dB for vertical polarization and about 7.5 dB for horizontal polarization. The increase is pretty much monotonic with wind speed, keeping in mind the variance to be expected in wind speed and NRCS. It is noticeable that some circles result in "flatter" responses at crosswind than others. The reason for this has not been determined, but some researchers have suggested a similar effect could be produced by swell. It is also possible that the flatter curves could result when correcting from a lower to a higher incidence angle and, hence, from a lower to a higher wind speed sensitivity. There appears to be a bias such that these NRCS signatures are lower than those of the SASS I by as much as 2 dB at both horizontal and vertical polarization.

At 30°, the wind speed dependence is much stronger. The general trend that NRCS increases with wind speed is violated only by the circle from mission 288, flight 5, for which the NRCS is much lower than expected for a wind speed of 22.5 m/s. This anomalous result could be due to an incorrect band-pass filter (ref. 10) or to an incorrect wind speed measurement, or to both. The rest of these data appear to be biased lower than the SASS I table also.

At 40° and 50°, the results show anisotropy and NRCS wind speed sensitivity at about the same level as for 30°. The winds increase nearly monotonically with wind speed. Some "shallowness" at the crosswind nulls is observed for low wind speeds. The 50° data set consists of only 3 sets of input data, and hence the results may not be general. The high NRCS for mission 306, FCF establishes doubt about the accuracy of the measured wind speed. The trends for the other two cases are slightly lower but within about 1 dB of the SASS I.

At 60°, a much smaller range of wind speeds has been observed because only a few circles fell into this incidence angle bin. This limited data set is also partly due to the dynamic range of the instrument; that is, NRCS values are too low to be sensed by the RADSCAT if the wind speeds were low at these high incidence angles. For the measurements taken, however, the trend was reasonable. The data from mission 306, FCF again clearly lie questionably above the trend of the other data.

At 70°, the trends become more complex. For horizontal polarization (fig. 16(a)), upwind increases monotonically with wind speed but crosswind NRCS shows an extremely shallow level for the 5.5 m/s circle line. This is probably due to the receiver reaching the minimum detectable signal and not responding to lower levels. The vertical polarization data (fig. 16(b)) exhibit the possible effects of some other parameters. It appears that the low (5.5 m/s), the medium (7 to 9 m/s), and the high (10 to 16 m/s) wind speeds, in general, cause increased levels, but the clusters of data do not vary strictly with wind speed. For example, at upwind, the data from four flights are within about 0.5 dB of each other; at crosswind, these same flights show differences as high as 3 dB; at downwind, they show the lowest wind speed point to be about 2 dB higher than the others. The reasons for these results are not known. The

trends of the SASS I model are extrapolations at this incidence angle. The agreement is reasonably close at low wind speeds but diverges to 4 to 5 dB at higher wind speeds.

To further aid in understanding the trends of these groups of circle flight data, a linear least-squares regression fit of NRCS (dB) versus log (Wind speed) was performed at upwind, downwind, and crosswind for each data set. Crosswind calculations were performed at both 90° and at the angle where the second-order fit shows a minimum. These results are given in table X.

In general, the regression coefficients are in reasonable agreement with the results given for straight level lines for incidence angles from 0° through 40°. At 30° incidence, the regression fit was applied including and excluding the data from missions 288 and 306. The results show that the correlation is much higher with the data in question excluded. Regression results for incidence angles at or above 50° show some results in disagreement. In particular, the present wind speed slope factor at 50° is considerably higher (2.5 to 4.0) even when questionable flight data are removed from the analysis. Also, the slope factor is lower at 60° than that at lower incidence angles, with values of 1.2 to 1.8 and 0.4 to 1.0 for horizontal and vertical polarization, respectively. These results should not be taken to be too general since, in all these cases, the number of samples are low.

The regression coefficients A_0 and A_2 for the third-order fit have been observed to vary as a function of wind speed (ref. 8) and show the same trends herein. (See the trend in the tabulation of fig. 14, for example.) This behavior is predictable, since for this model the upwind, downwind, and crosswind values can be determined by inspection to be:

$$(\mathrm{NRCS})_u = A_0 + A_1 + A_2 \qquad (\chi = 0 \text{ or } 2\pi) \tag{7}$$

$$(\mathrm{NRCS})_d = A_0 - A_1 + A_2 \qquad (\chi = \pi \text{ or } -\pi) \tag{8}$$

$$(\mathrm{NRCS})_c = A_0 - A_2 \qquad (\chi = \pi/2 \text{ or } 3\pi/2) \tag{9}$$

Thus, it can be shown that, as in reference 8,

$$A_0 = \frac{(\mathrm{NRCS})_u + (\mathrm{NRCS})_d + 2(\mathrm{NRCS})_c}{4} \tag{10}$$

$$A_1 = \frac{(\mathrm{NRCS})_u - (\mathrm{NRCS})_d}{2} \tag{11}$$

$$A_2 = \frac{(\mathrm{NRCS})_u + (\mathrm{NRCS})_d - 2(\mathrm{NRCS})_c}{4} \tag{12}$$

Since NRCS at upwind and downwind are nearly equal, it is seen from equation (10) that A_0 is near the mean value of NRCS for the circle. Likewise, from equation (12), A_2 is approximately equal to the difference between upwind or downwind

and crosswind NRCS values; for incidence angles 20° or greater, this difference is 3 dB or greater. Hence, the wind speed dependence of A_0 and A_2 should be similar to that shown earlier for NRCS. This result is supported by figures 17 to 20, where A_0 or A_2 is plotted against wind speed on a log-log scale. The first-order regression line and coefficients are given in the plots. Some selected outliers have been removed from certain plots as indicated.

The fits and wind speed sensitivities for A_0 and A_2 are in good agreement with the results from the straight level flights reported earlier for cases where enough points are available (50° and 60° data sets have only 2 or 3 points). The scatter is within reasonable bounds of the expected variance in surface truth wind speeds; this is illustrated in figure 17 for $\theta = 20°$, where boundaries for wind speed errors of ±2 m/s are dashed in around the regression fit line. All the scatter is contained within the ±2 m/s bounds.

The A_1 coefficient trend with wind speed was also examined, but the results were not easily interpreted. Since A_1 can be either positive or negative depending on whether NRCS is higher in the upwind or downwind direction (eq. (11)), linear A_1 was plotted against wind speed. These plots are shown in figures 21 and 22. Whereas there seems to be some consistency in some data sets, no trend stands out. Coding the points by location seems not to be significant. No conclusion can be drawn for this case.

CONCLUDING REMARKS

This report presents a comprehensive analysis of the ocean scattering cross section signature obtained from the AAFE RADSCAT scatterometer sensor. All scatterometer data for which the quality of the sensor and the corresponding surface truth are known are provided in measurement summary form and also in least-mean-squares curve fit studies.

Straight level flight lines in the upwind, downwind, and crosswind directions have been shown to exhibit approximate wind speed sensitivities of -0.5 dB/log decade of wind speed at incidence angle of 0°, 0 at incidence angle of 10°, and increasing values up to 2.2 for incidence angles from 40° to 60°. These values are consistent with earlier flight results (from Jones, Schroeder, and Mitchell, IEEE Journal of Oceanic Engineering, January 1977) based on only five early AAFE RADSCAT (advanced aerospace flight experiment radiometer scatterometer) flights and with the SASS (SEASAT-A satellite scatterometer) I model function. The slopes for wind speed versus NRCS (normalized radar cross section) are about the same level as the earlier data, but the SASS I NRCS is higher by from 2 to 3 dB. This bias indicates that either the SASS I algorithm absolute NRCS values have been compromised by the JASIN calibration or that the AAFE RADSCAT NRCS data has a bias, or both.

Circle flight line NRCS has been modeled by a ninth-order function

$$\text{NRCS} = \sum_{n=0}^{2} \left[\left(a_n + b_n \theta \right) \cos n\phi + \left(c_n + d_n \theta \right) \sin n\phi \right]$$

and a second-order function

$$\text{NRCS} = \sum_{n=0}^{2} a_n \cos n\chi$$

for each circle flight. (The symbols θ and ϕ are defined as incidence angle and azimuth angle, respectively, and χ is the wind direction relative to upwind.) The ninth-order fit is useful to determine and correct the circle flight NRCS data for variations in wind direction and incidence angle but of limited usefulness otherwise because of complexity and instabilities at certain conditions. Also, use of the ninth-order θ dependence for corrections outside the incidence angle limits of the data set was found to be suspect. The second-order fit is more stable and less complex and appears to model the data well but requires knowledge of wind direction and incidence angle dependence. Regression analyses of the upwind, downwind, and crosswind NRCS at a fixed incidence angle show consistent trends with the straight level line data. Plots of NRCS against azimuth for lines corrected to the nearest 10° in θ showed wind speed trends consistent with the straight level line data and earlier RADSCAT data analyses. These plots show that the SASS I model NRCS is biased higher than the RADSCAT data and the bias increases with wind speed. These plots also show variation in the azimuth of minimum NRCS; thus, the actual signature of NRCS versus azimuth may be more complex than this simple model allows.

The wind speed trends of the regression coefficients A_0, A_1, and A_2 of the second-order regression model have been analyzed. The slopes of the A_0 and A_2 coefficients versus wind speed show good agreement with the upwind, downwind, and crosswind NRCS trends, but the trend for A_1 is too complex to be understood by this analysis.

The analyses of these data which were taken over 5 years of intensive flight tests, show gaps at certain parametric ranges and large scatter in others. The trends with wind speed show biases, when compared with the best known model, SASS I. The presence of undocumented second-order parameters are suggested by several results. Thus, it is fair to conclude that these data are but a supplement to a growing data bank on ocean NRCS. For instruments which require these empirical data to be finely tuned such that model function error is removed as a factor from operational satellite scatterometer wind sensors, this data base is still incomplete at this frequency and little known at others.

Langley Research Center
National Aeronautics and Space Administration
Hampton, VA 23665
November 10, 1983

APPENDIX A

REGRESSION FIT RESULTS FOR NRCS VERSUS WIND SPEED IN RATIO FORM FOR RADSCAT STRAIGHT LEVEL LINE DATA

The NRCS versus wind speed data for AAFE RADSCAT straight level lines were obtained as described in the section entitled "Straight Level Lines." The results are given in the plots of figures A1 through A7. A general description of the results can be found in the section of the report referred to earlier.

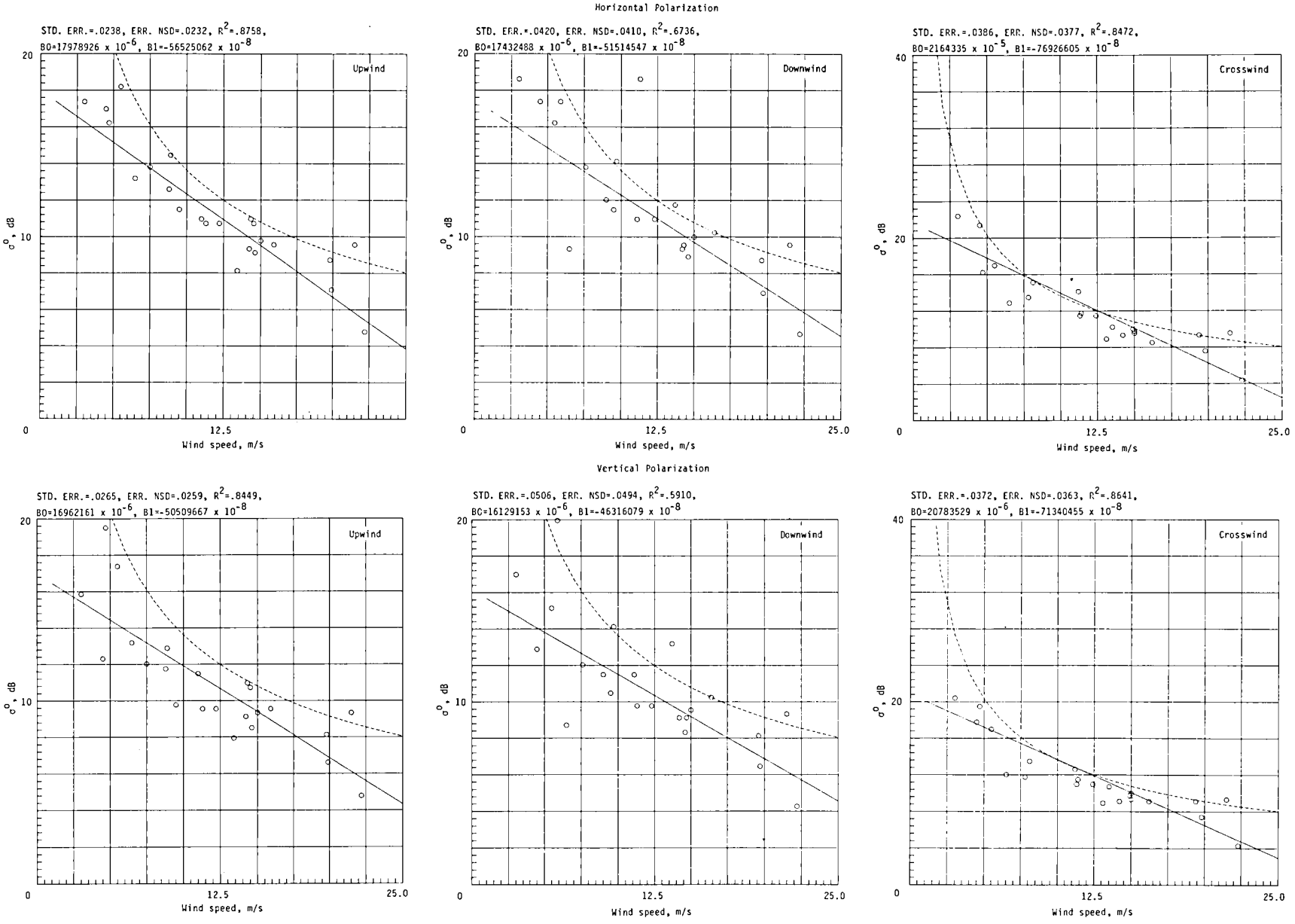

Figure A1.- Regression of NRCS versus wind speed for $\theta = 0°$, with SASS I model function line (dashed) for comparison.

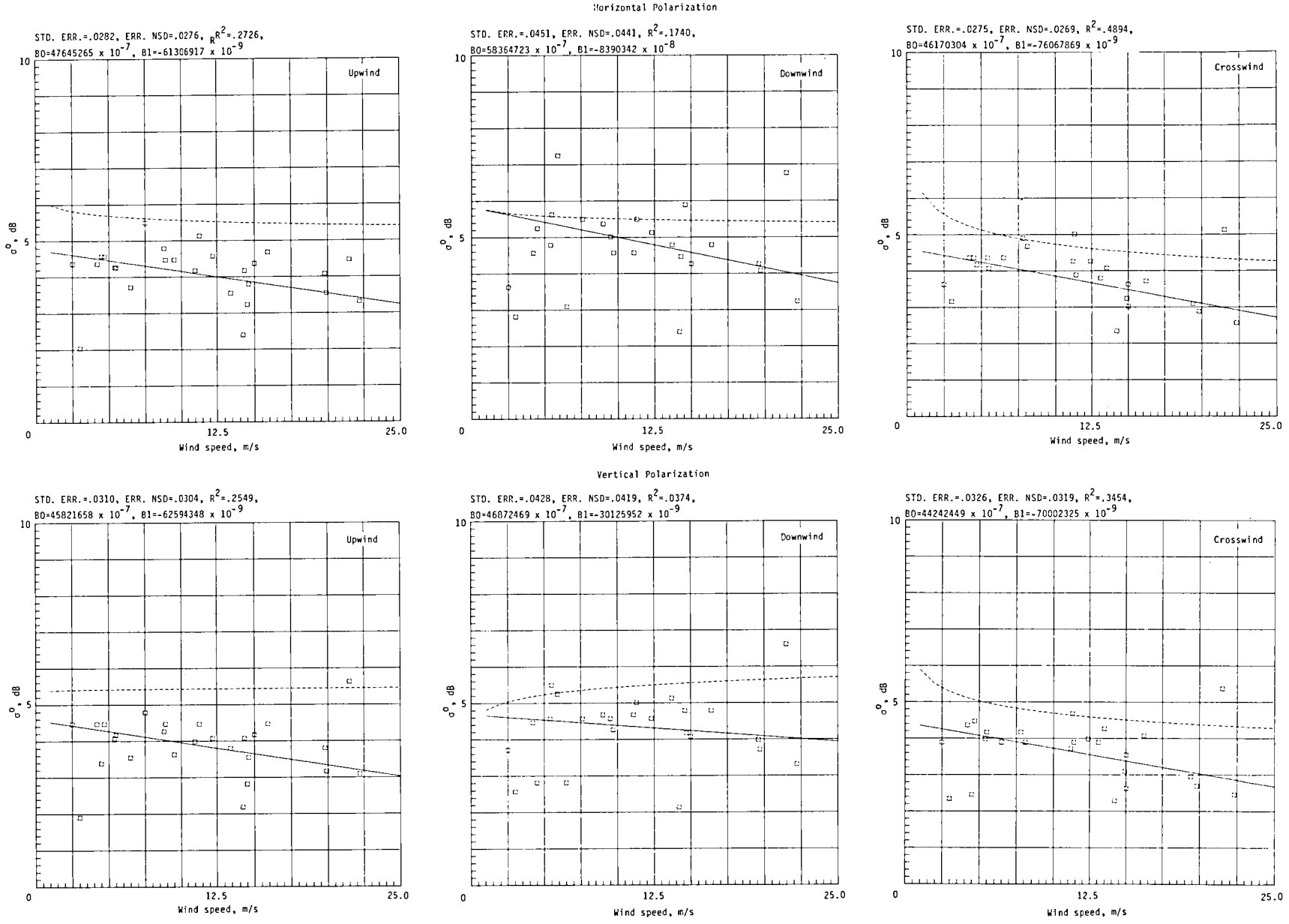

Figure A2.- Regression of NRCS versus wind speed for $\theta = 10°$, with SASS I model function line (dashed) for comparison.

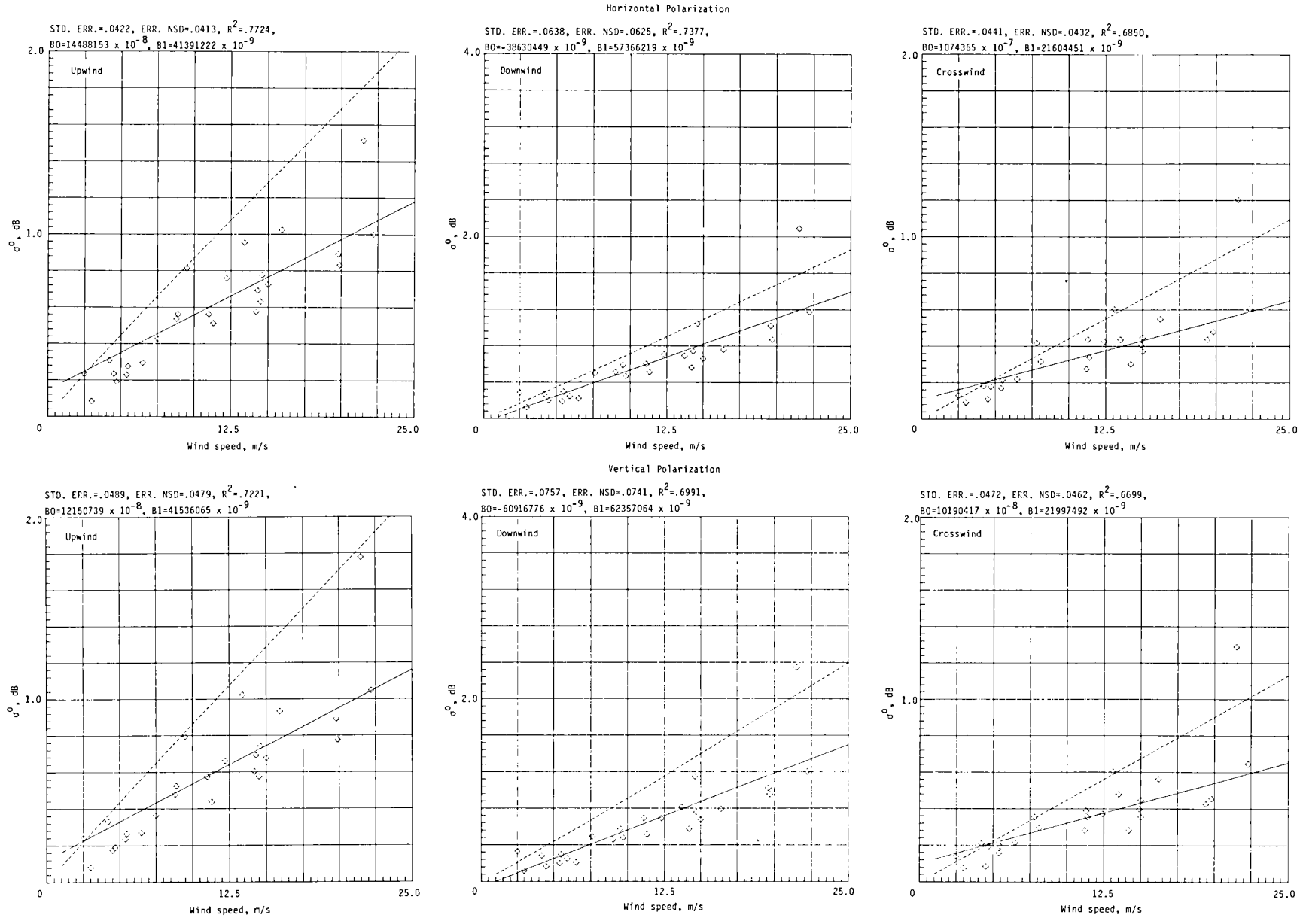

Figure A3.- Regression of NRCS versus wind speed for $\theta = 20°$, with SASS I model function line (dashed) for comparison.

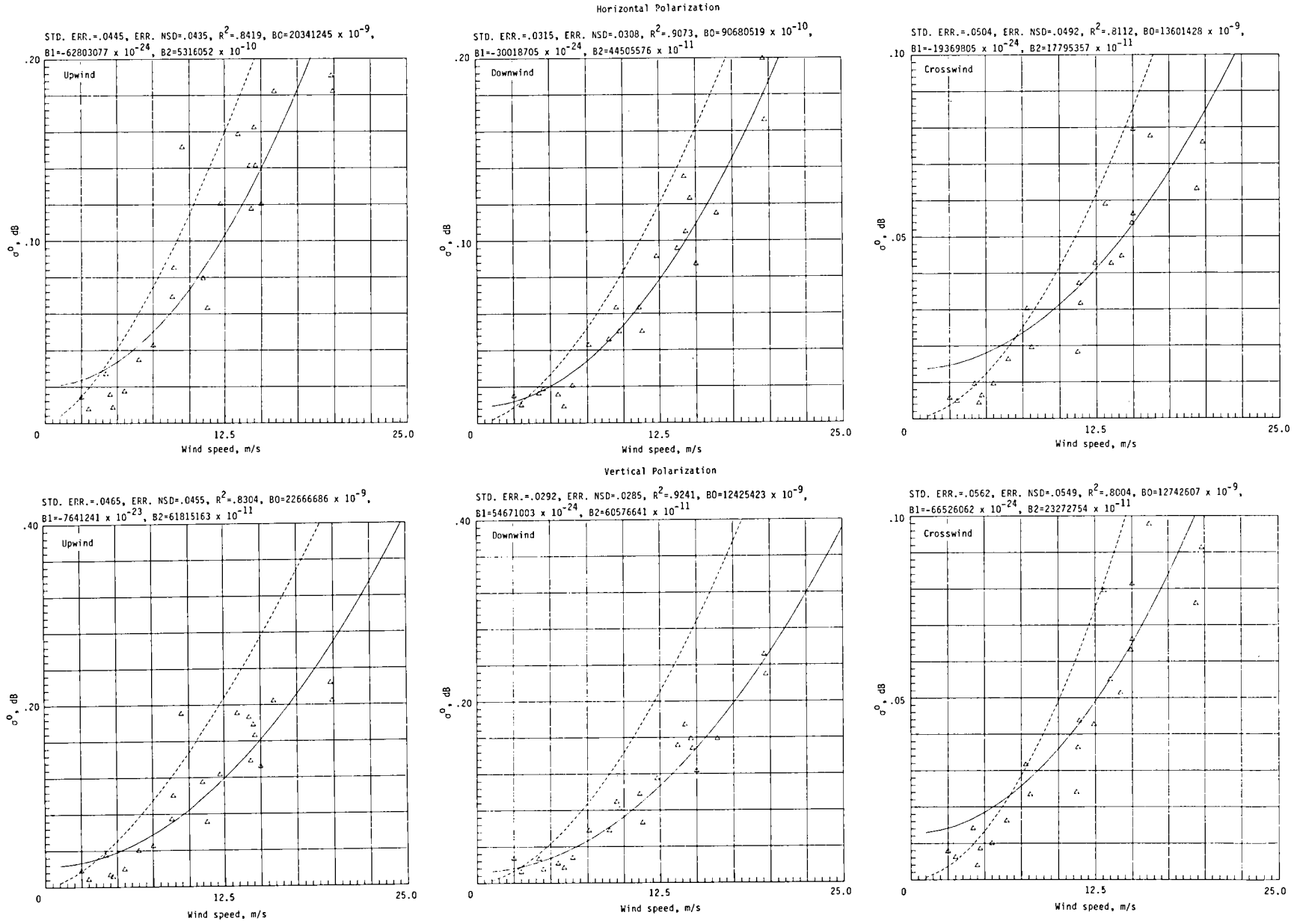

Figure A4.- Regression of NRCS versus wind speed for $\theta = 30°$, with SASS I model function line (dashed) for comparison.

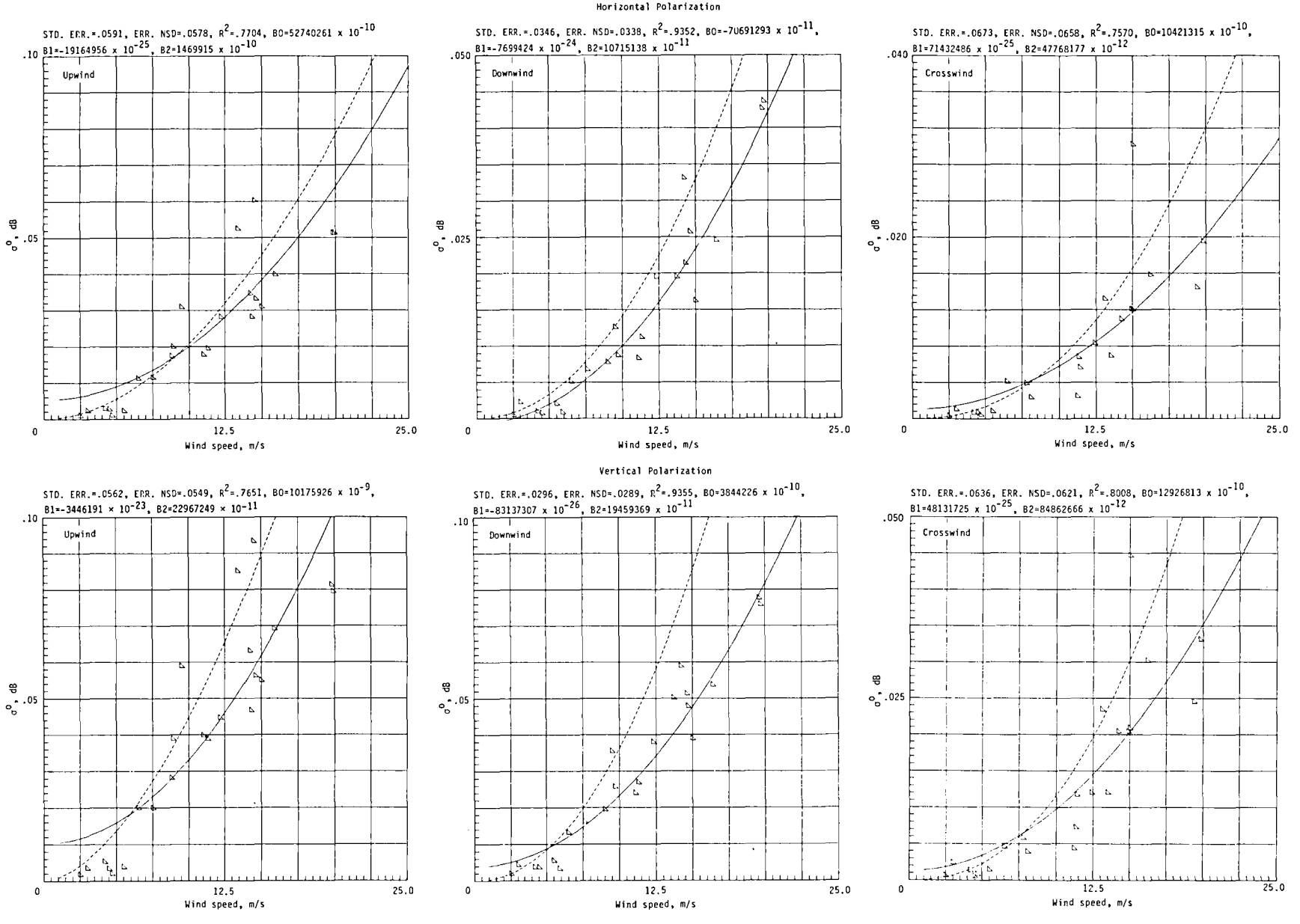

Figure A5.- Regression of NRCS versus wind speed for $\theta = 40°$, with SASS I model function line (dashed) for comparison.

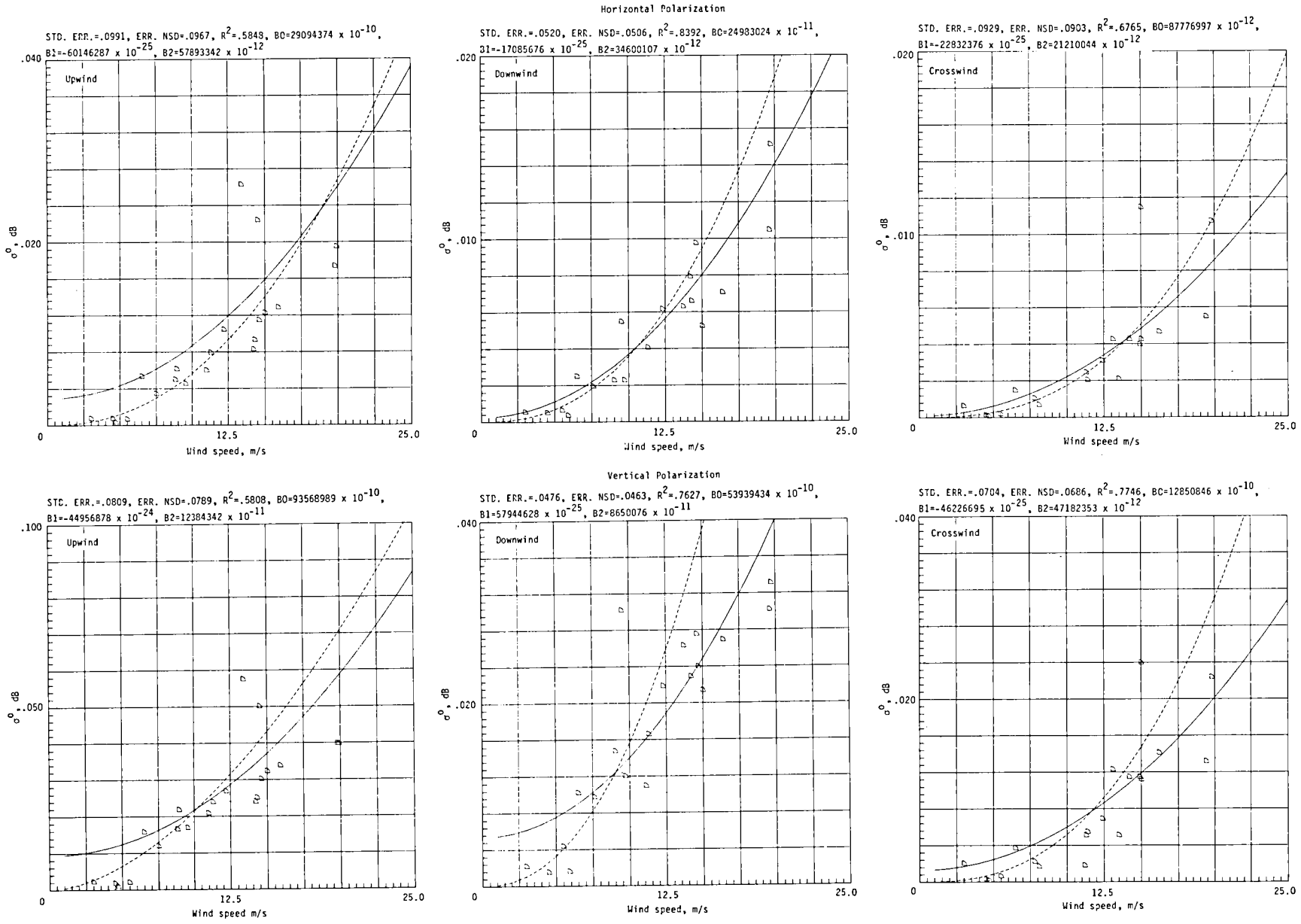

Figure A6.- Regression of NRCS versus wind speed for $\theta = 50°$, with SASS I model function line (dashed) for comparison.

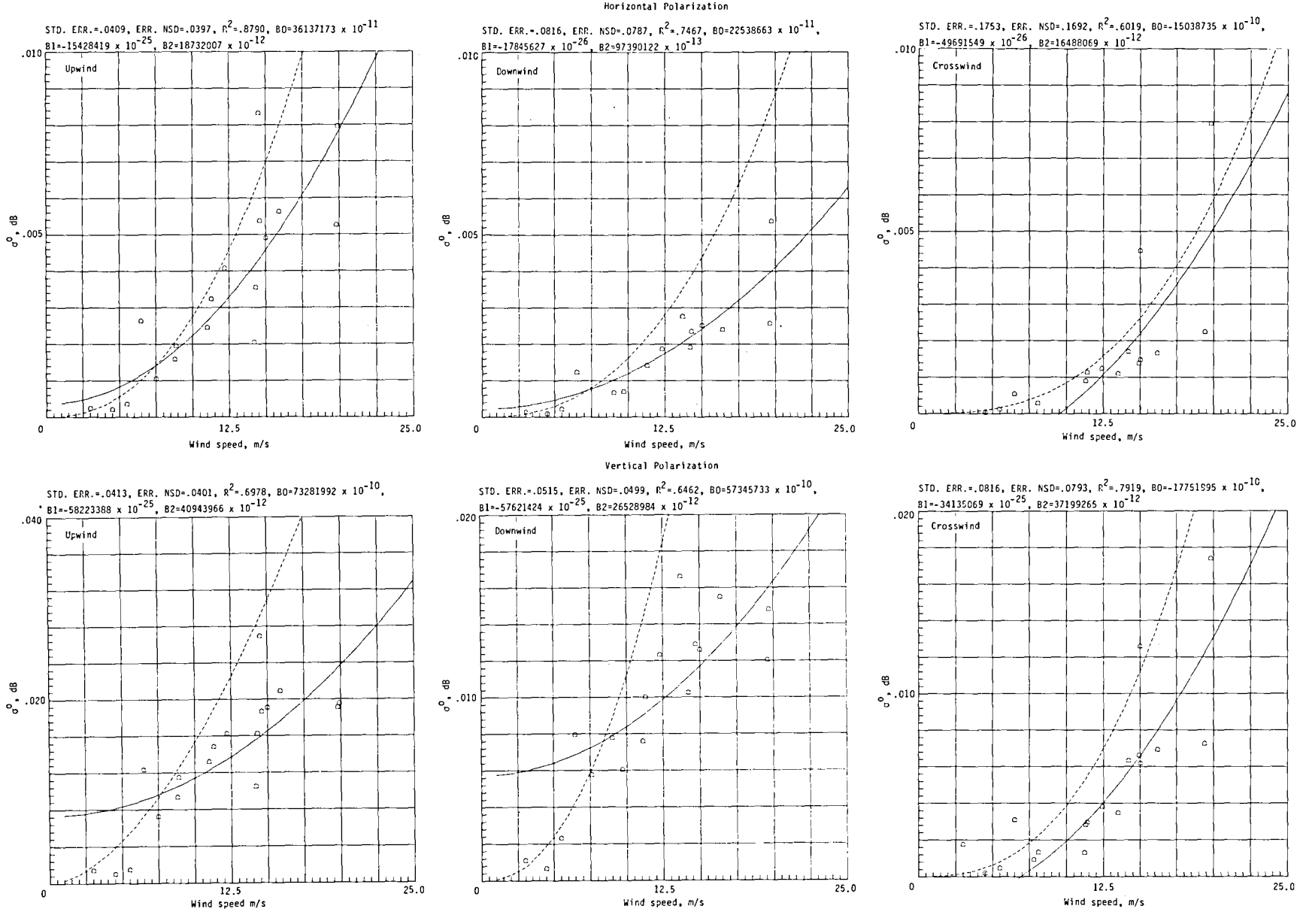

Figure A7.- Regression of NRCS versus wind speed for $\theta = 60°$, with SASS I model function line (dashed) for comparison.

APPENDIX B

REGRESSION MODELS FOR RADSCAT WIND CIRCLES

Philip R. Schaffner
Research Triangle Institute
Hampton, Virginia

The response of the scatterometer has been shown to be a function of incidence and azimuth angles over the ocean surface in the presence of winds of constant direction and speed and can be modeled by an equation of the form (see ref. 8):

$$(\text{NRCS}) = \sum_{n=0}^{2} \left[\left(a_n + b_n \theta \right) \cos n\phi + \left(c_n + d_n \theta \right) \sin n\phi \right] + e \qquad \text{(B1)}$$

where

(NRCS) normalized radar cross section

θ incidence angle

ϕ azimuth angle

a,b,c,d parameters related to actual wind speed and direction

e error in observation of NRCS

Equation (B1) can be rewritten as

$$(\text{NRCS}) = A_0 + A_1\theta + A_2 \cos \phi + A_3\theta \cos \phi + A_4 \sin \phi + A_5\theta \sin \phi$$

$$+ A_6 \cos 2\phi + A_7\theta \cos 2\phi + A_8 \sin 2\phi + A_9\theta \sin 2\phi + E \qquad \text{(B2)}$$

where the coefficients A_i represent linear combinations of a, b, c, and d in equation (B1).

If the dependence on incidence angle is removed from the data and the azimuth angle of the antenna is replaced by azimuth with respect to the wind direction (χ), then an adequate model (ref. 8) is

$$(\text{NRCS}) = \sum_{n=1}^{2} A_n \cos n\chi + E \qquad \text{(B3)}$$

In order to fit experimental data to these models a general least-squares regression technique may be employed. Either of these models may be expressed as a matrix equation of the form:

$$\bar{Y} = \bar{\bar{X}}\bar{B} + \bar{E} \tag{B4}$$

where

$\bar{Y}$ vector of n observations of NRCS

$\bar{\bar{X}}$ $n \times p$ matrix of functions of independent variables

$\bar{B}$ vector of p parameters of model (of order $p - 1$)

$\bar{E}$ vector of n error terms due to random variation in data

It can be shown (ref. 13) that the least-mean-squares-error solution for the coefficient vector B is:

$$\bar{B} = \left(\bar{\bar{X}}'\bar{\bar{X}}\right)^{-1}\bar{\bar{X}}'\bar{Y} \tag{B5}$$

Since a large number of observations were to be included in each regression fit, the computer program would have required a large amount of storage had this equation been implemented directly. As an alternative to the direct matrix manipulation approach, expressions were obtained for the elements of the matrices as follows. Let

$$\bar{\bar{A}} = \bar{\bar{X}}'\bar{\bar{X}} \qquad (p \times p \text{ matrix}) \tag{B6}$$

and

$$\bar{Q} = \bar{\bar{X}}'\bar{Y} \qquad (p\text{-element vector}) \tag{B7}$$

Thus, equation (B5) can be written as

$$\bar{B} = \left(\bar{\bar{A}}\right)^{-1}\bar{Q} \tag{B8}$$

For the ith observation, the ith row of $\bar{\bar{X}}$ can be represented as the vector:

$$\bar{X}_i = \left\{X_{i0}, X_{i1}, X_{i2}, \cdots, X_{ip-1}\right\} \tag{B9}$$

where X_{ij} represents functions of the independent variables.

APPENDIX B

For the model of equation (B2),

$$X_{i0} = 1 \qquad X_{i5} = \theta_i \sin \phi_i$$

$$X_{i1} = \theta_i \qquad X_{i6} = \cos 2\phi_i$$

$$X_{i2} = \cos \phi_i \qquad X_{i7} = \theta_i \cos 2\phi_i$$

$$X_{i3} = \theta_i \cos \phi_i \qquad X_{i8} = \sin 2\phi_i$$

$$X_{i4} = \sin \phi_i \qquad X_{i9} = \theta_i \sin 2\phi_i$$

For the model of equation (B3),

$$X_{i0} = 1$$

$$X_{i1} = \cos \chi_i$$

$$X_{i2} = \cos 2\chi_i$$

An element of $\bar{\bar{A}}$ can then be expressed as

$$A_{ij} = \sum_{k=0}^{n-1} \left(X_{ki} X_{kj}\right) \tag{B10}$$

The vector of n observations, $\bar{Y}$ can be written as

$$\bar{Y} = \left\{Y_0, Y_1, \ldots, Y_{n-1}\right\} \tag{B11}$$

and an element of $\bar{Q}$ can be expressed as

$$Q_i = \sum_{k=0}^{n-1} \left(Y_k X_{ki}\right) \tag{B12}$$

The sums in equations (B10) and (B12) are formed as the data are read, and when the end of the data for a particular run is reached, the $\bar{\bar{A}}$ matrix is inverted and the vector $\bar{Q}$ is premultiplied by the result to arrive at the estimates of the model coefficients in the vector $\bar{B}$. The total sum of squares error (SS), the sum of the

residuals (SR), the multiple correlation coefficient (R^2), and the normalized standard deviation (NSD) are then calculated as follows (ref. 14):

$$(SS) = \sum_{i=0}^{n-1} E_i^2 = \text{Sum of squares error} \tag{B13}$$

$$(SR) = \sum_{i=0}^{n-1} E_i = \text{Sum of residuals} \tag{B14}$$

$$R^2 = \frac{\sum_{j=0}^{p-1} B_j Q_j - \left(\sum_{i=0}^{n-1} Y_i\right)^2 \Big/ n}{\sum_{i=0}^{n-1} Y_i^2 - \left(\sum_{i=0}^{n-1} Y_i\right)^2 \Big/ n} \tag{B15}$$

$$(NSD) = \frac{\left\{\left[n(SS) - (SR)^2\right] \Big/ \left[n(n-1)\right]\right\}^{1/2}}{\left(\sum_{i=0}^{n-1} Y_i\right) \Big/ n}$$

$$= \frac{\text{Sample standard deviation}}{\text{Sample mean}} \tag{B16}$$

where

$$E_i = Y_i - \sum_{j=0}^{p-1} B_j X_{ij} = \text{Error in ith observation (ith residual)} \tag{B17}$$

$$= Y_i - Y'_i$$

B_j = jth element of coefficient vector $\bar{B}$

Y'_i = Model estimate of value of dependent variable for ith set of independent variables

APPENDIX C

SECOND-ORDER REGRESSION RESULTS FOR RADSCAT CIRCLE FLIGHT DATA

After having been preprocessed to correct for effects of incidence angle variations, the RADSCAT circle flight data were fit by the second-order model described in appendix B (eq. (B3)). The results are given in figures (C1) through (C27). A general description of the results can be found in the section "Circle Flight Lines."

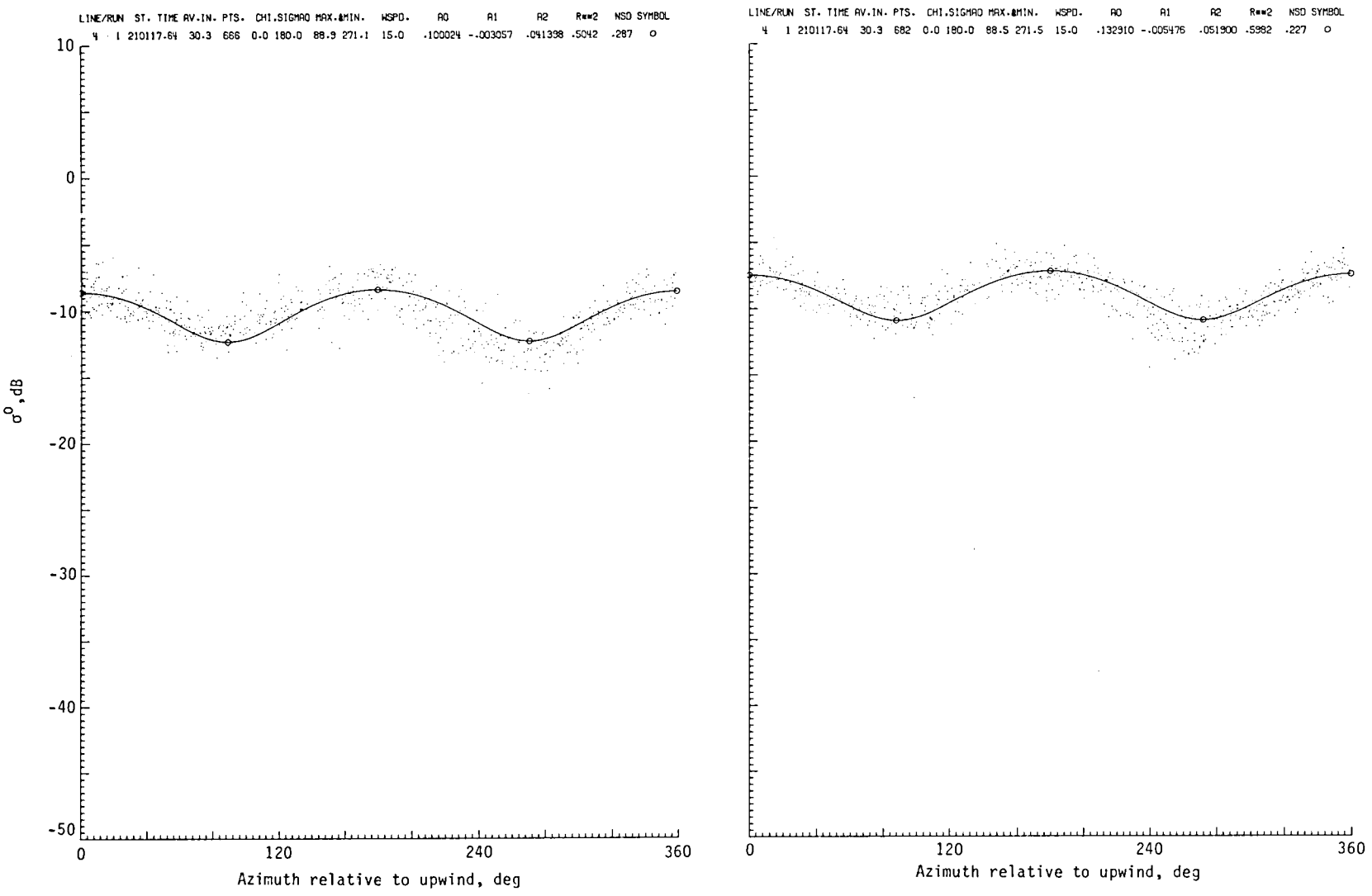

(a) Horizontal polarization.

(b) Vertical polarization.

Figure C1.- Second-order regression fit of NRCS versus azimuth relative to upwind for circle flight line data for mission 230, FCF.

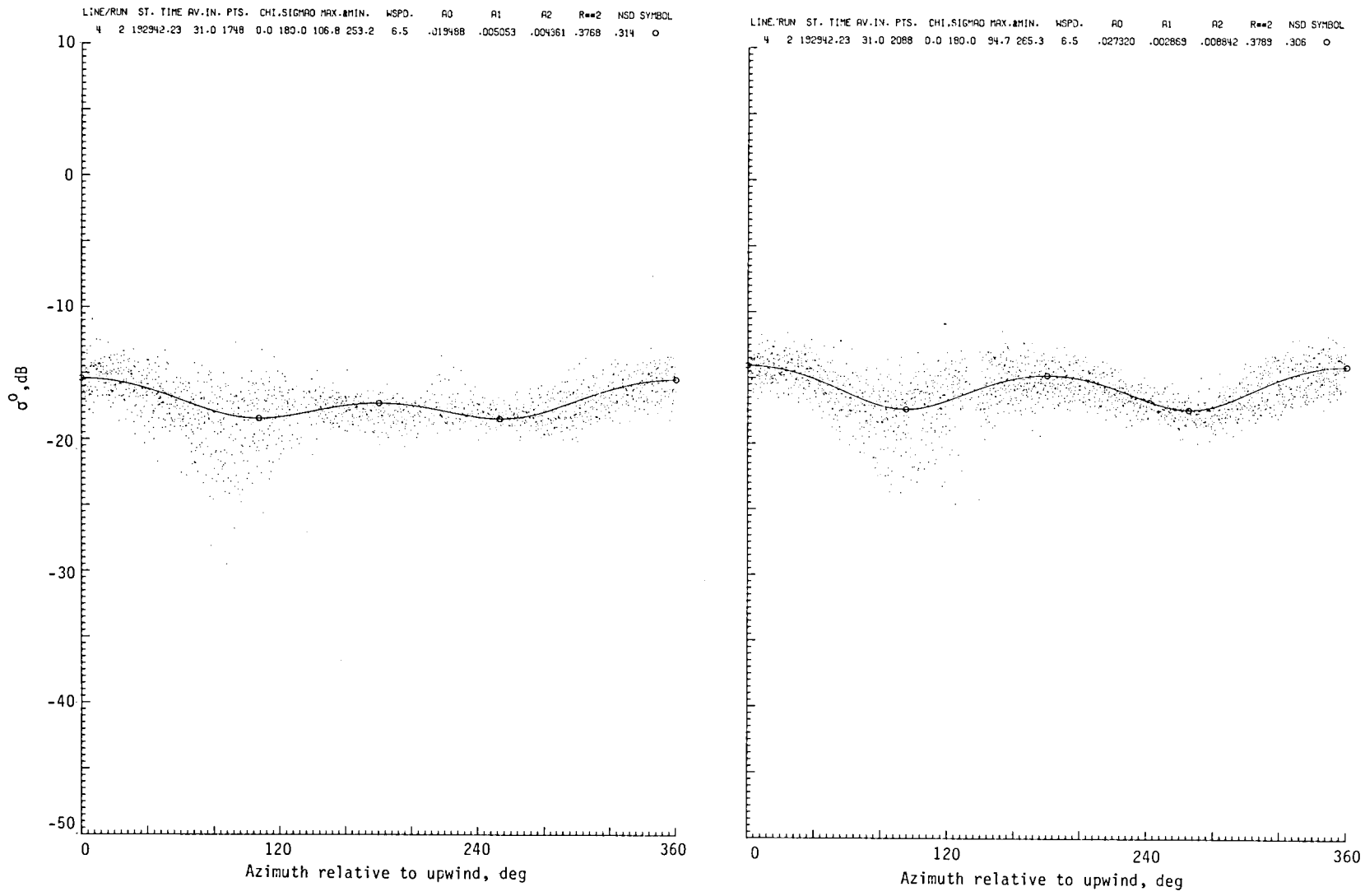

(a) Horizontal polarization.

(b) Vertical polarization.

Figure C2.- Second-order regression fit of NRCS versus azimuth relative to upwind for circle flight line data for mission 238, flight 20.

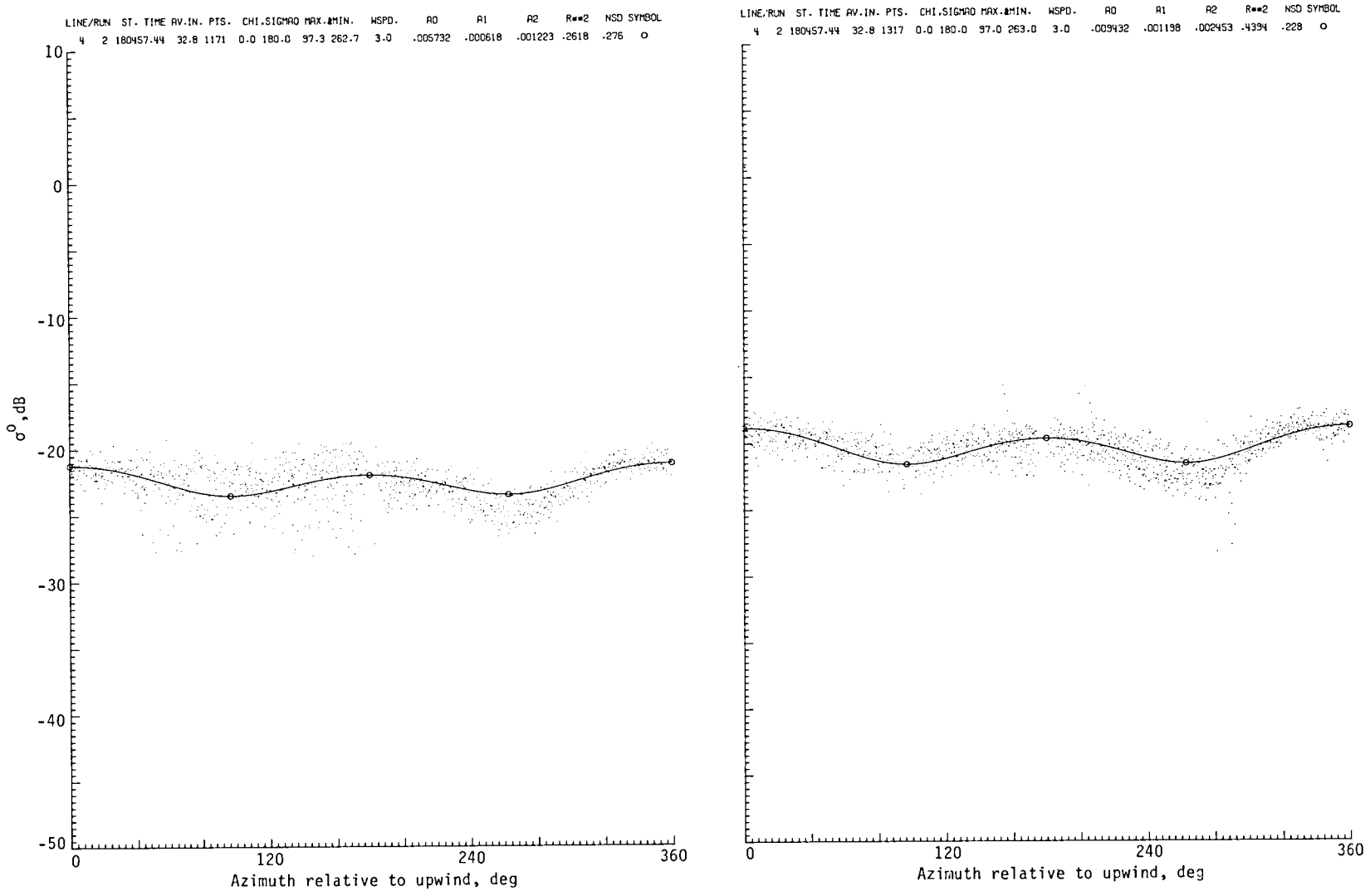

(a) Horizontal polarization.

(b) Vertical polarization.

Figure C3.- Second-order regression fit of NRCS versus azimuth relative to upwind for circle flight line data for mission 238, flight 27.

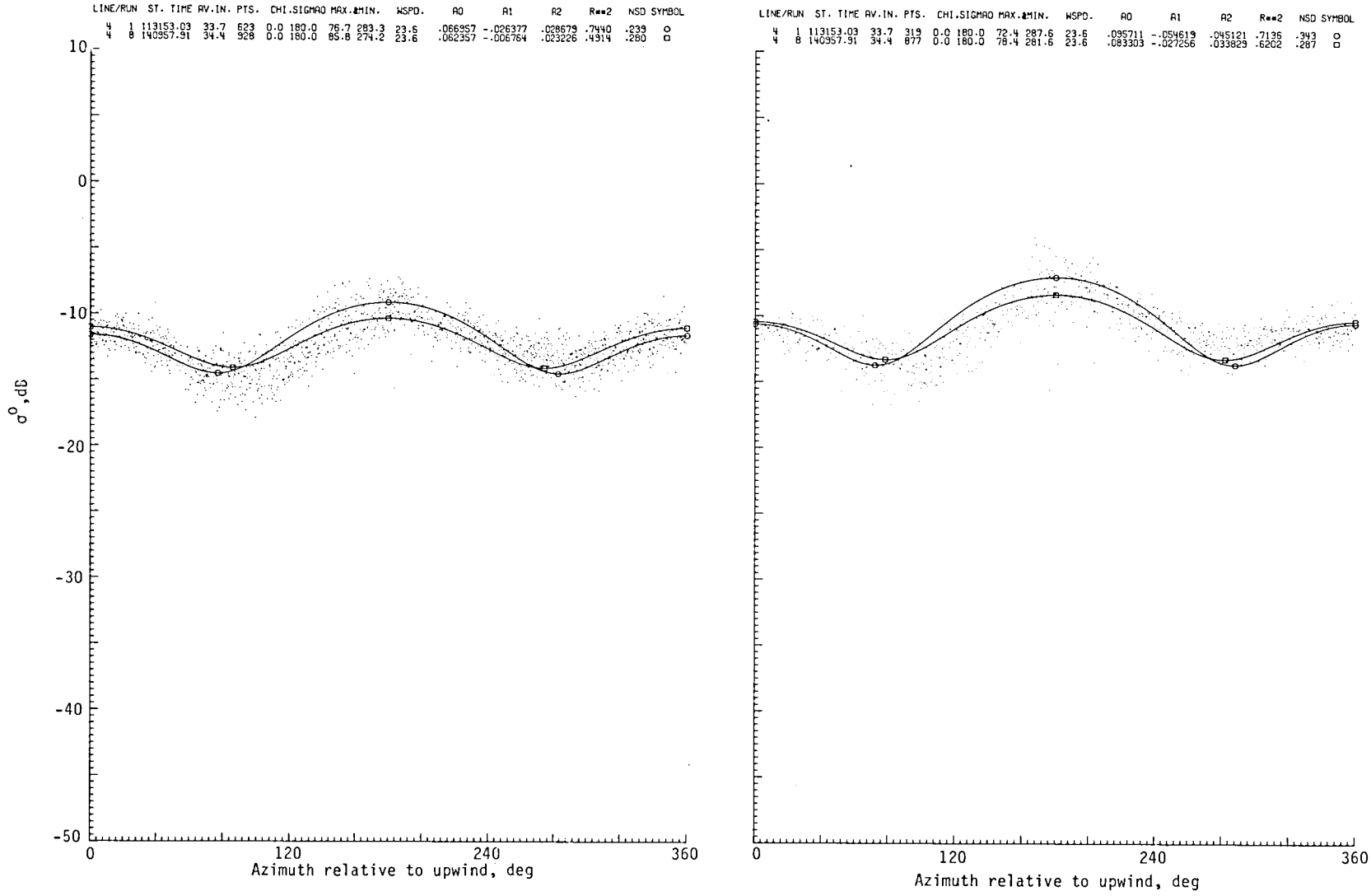

(a) Horizontal polarization.

(b) Vertical polarization.

Figure C4.- Second-order regression fit of NRCS versus azimuth relative to upwind for circle flight line data for mission 288, flight 5.

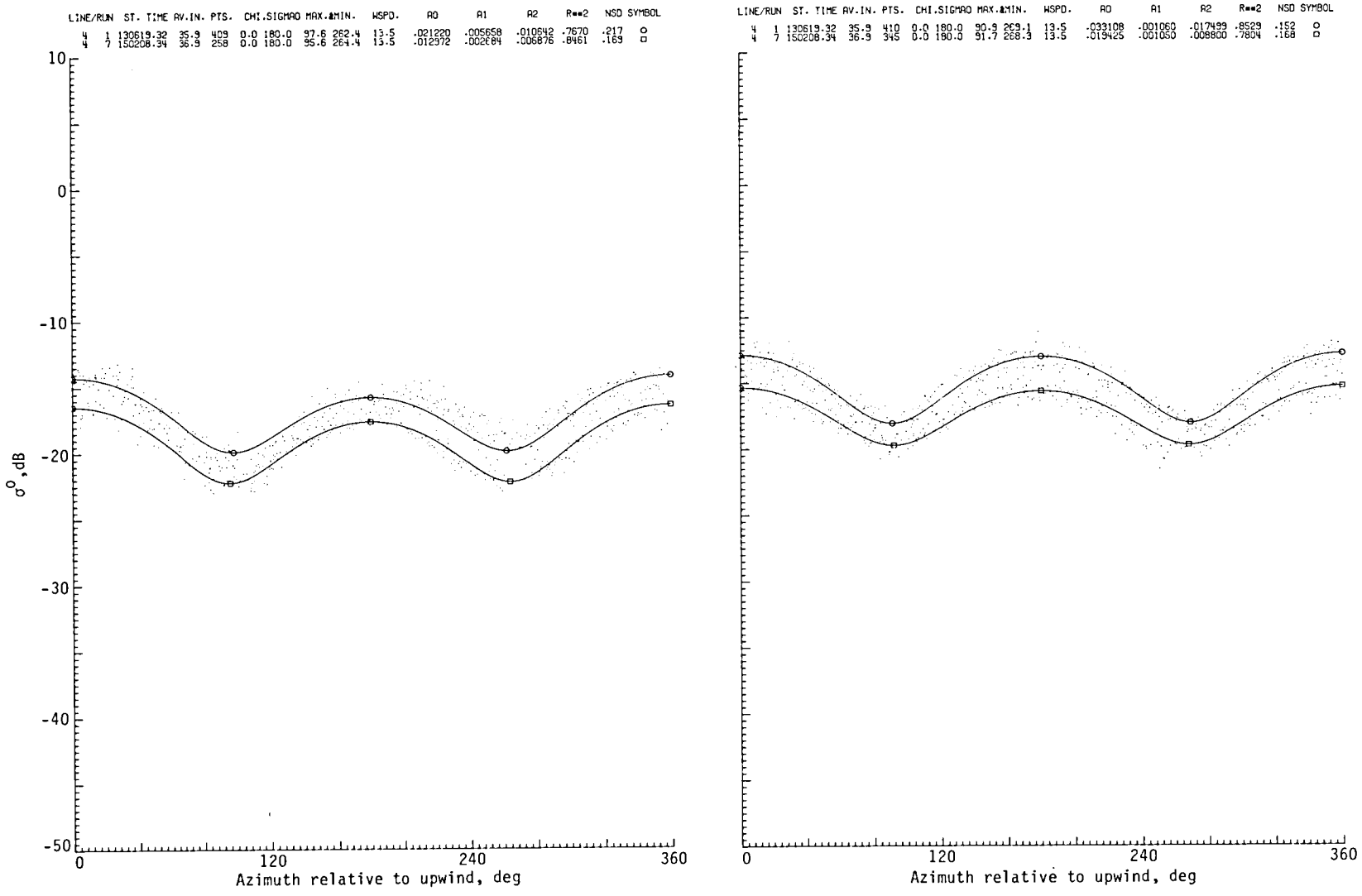

(a) Horizontal polarization.

(b) Vertical polarization.

Figure C5.- Second-order regression fit of NRCS versus azimuth relative to upwind for circle flight line data for mission 288, flight 6.

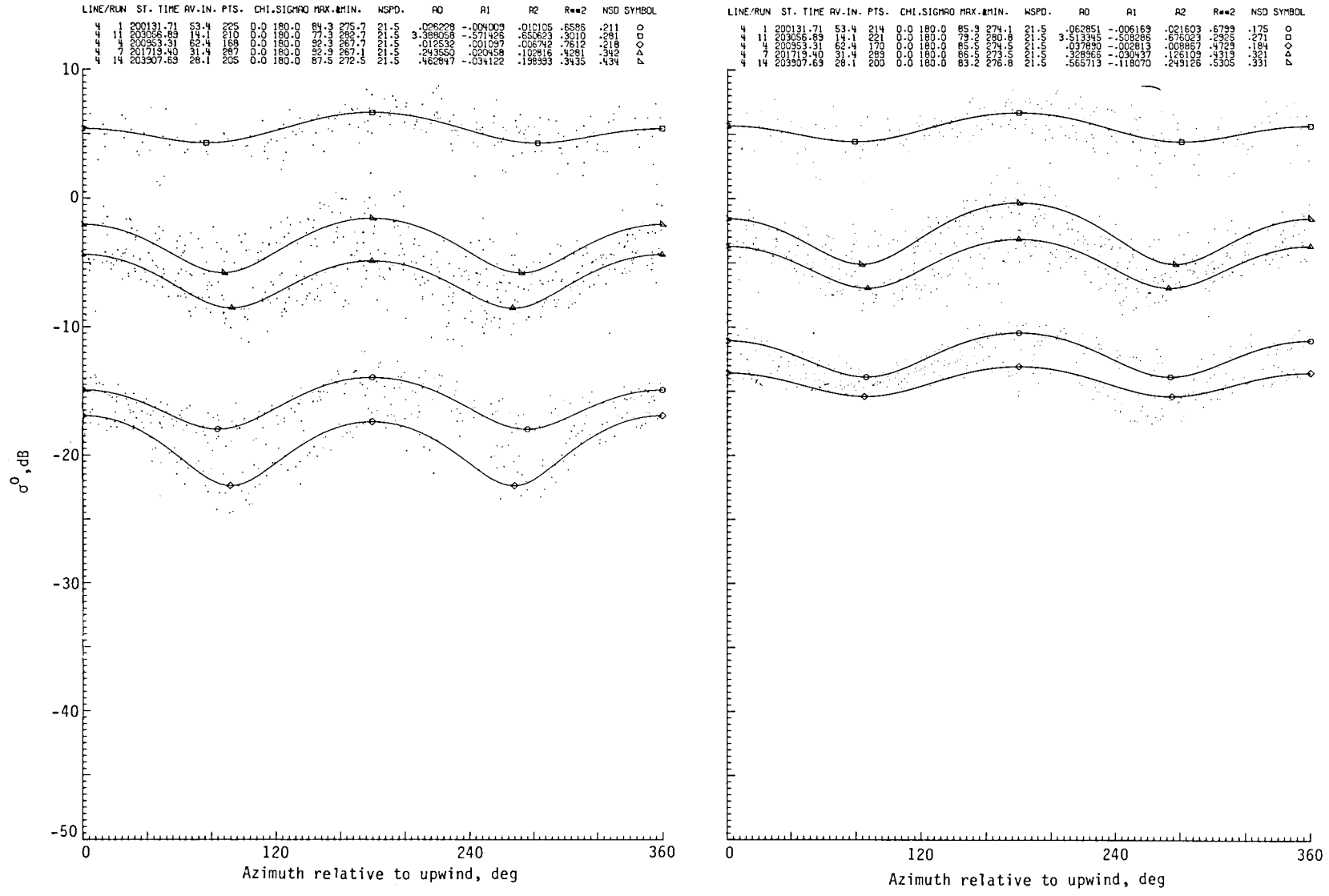

(a) Horizontal polarization.

(b) Vertical polarization.

Figure C6.- Second-order regression fit of NRCS versus azimuth relative to upwind for circle flight line data for mission 306, FCF.

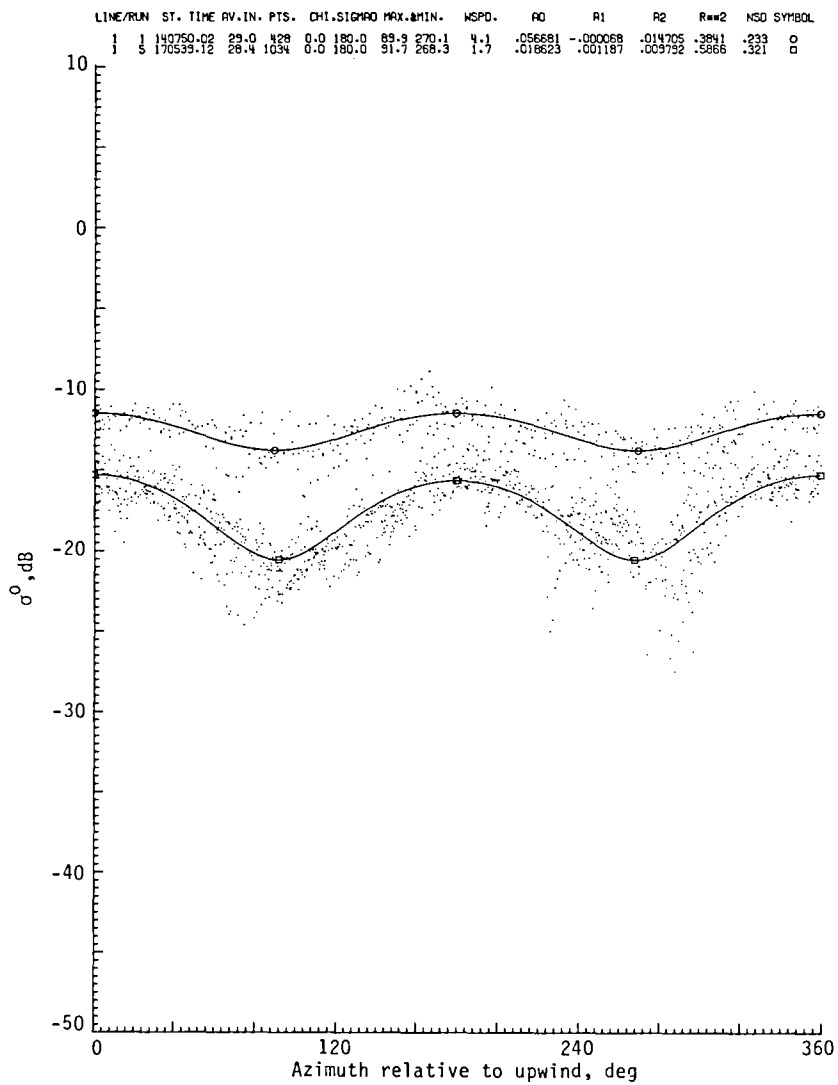

Figure C7.- Second-order regression fit of NRCS versus azimuth relative to upwind for circle flight line data for mission 306, flight 3. Horizontal polarization.

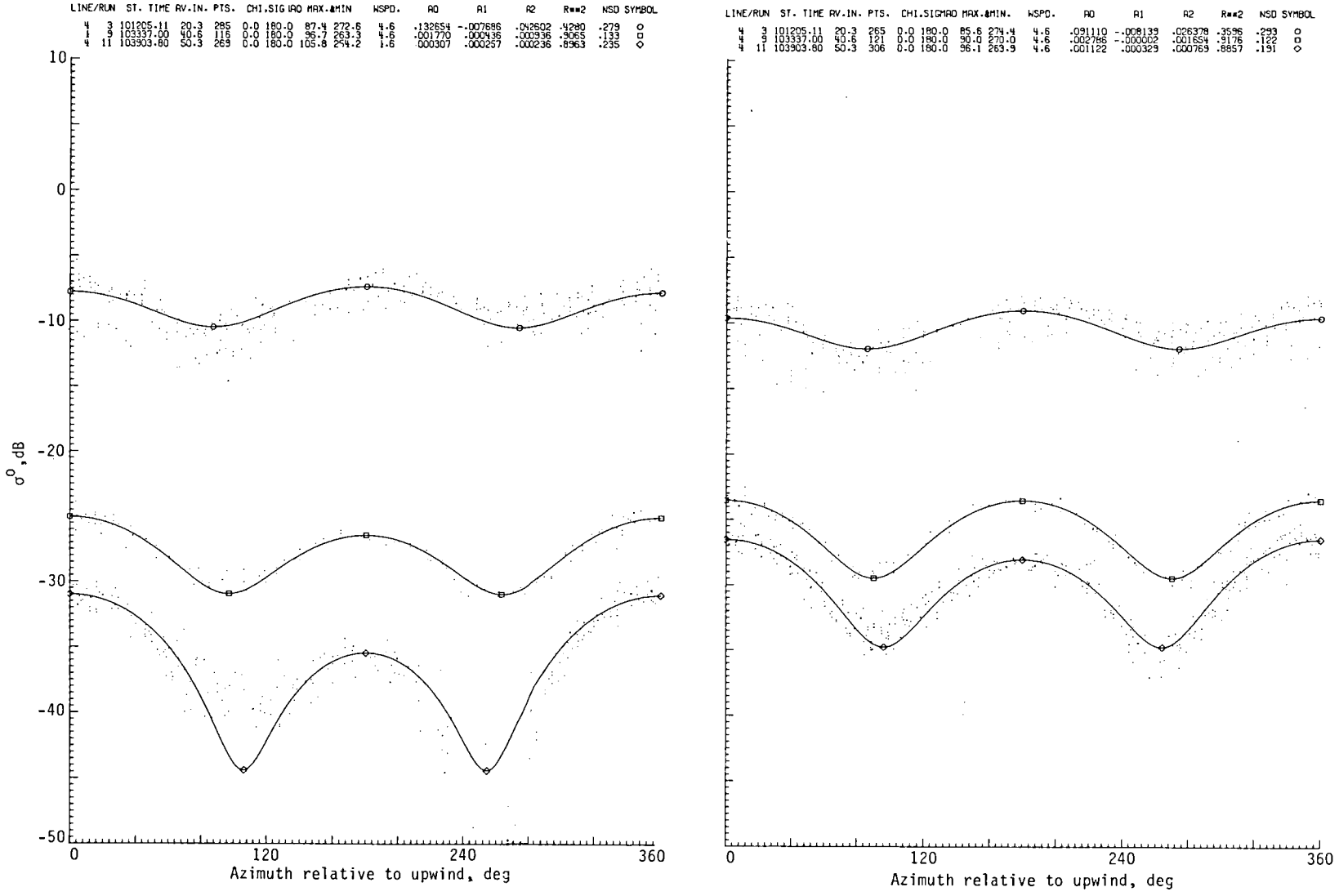

(a) Horizontal polarization.

(b) Vertical polarization.

Figure C8.- Second-order regression fit of NRCS versus azimuth relative to upwind for circle flight line data for mission 318, flight 13.

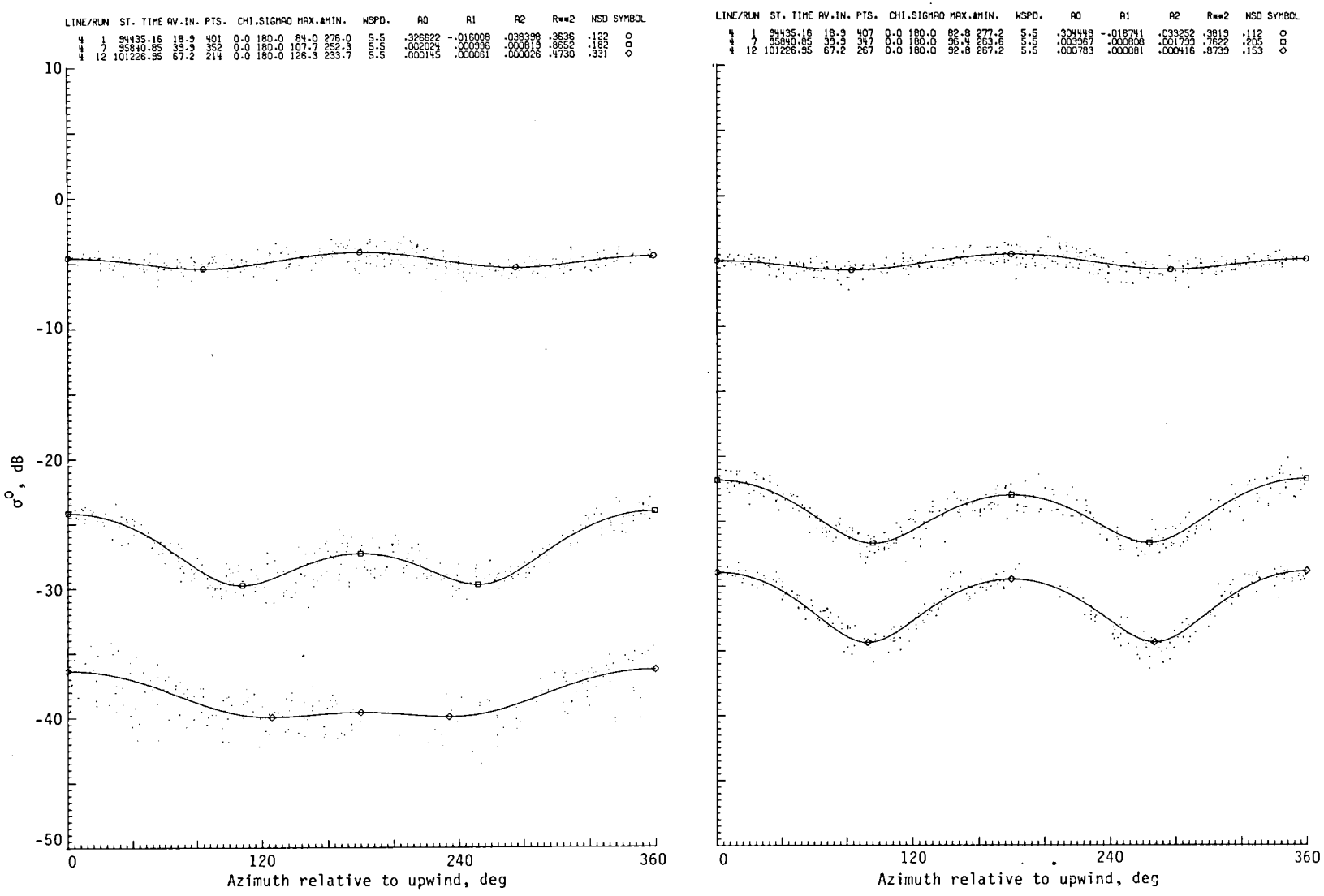

(a) Horizontal polarization.

(b) Vertical polarization.

Figure C9.- Second-order regression fit of NRCS versus azimuth relative to upwind for circle flight line data for mission 318, flight 14.

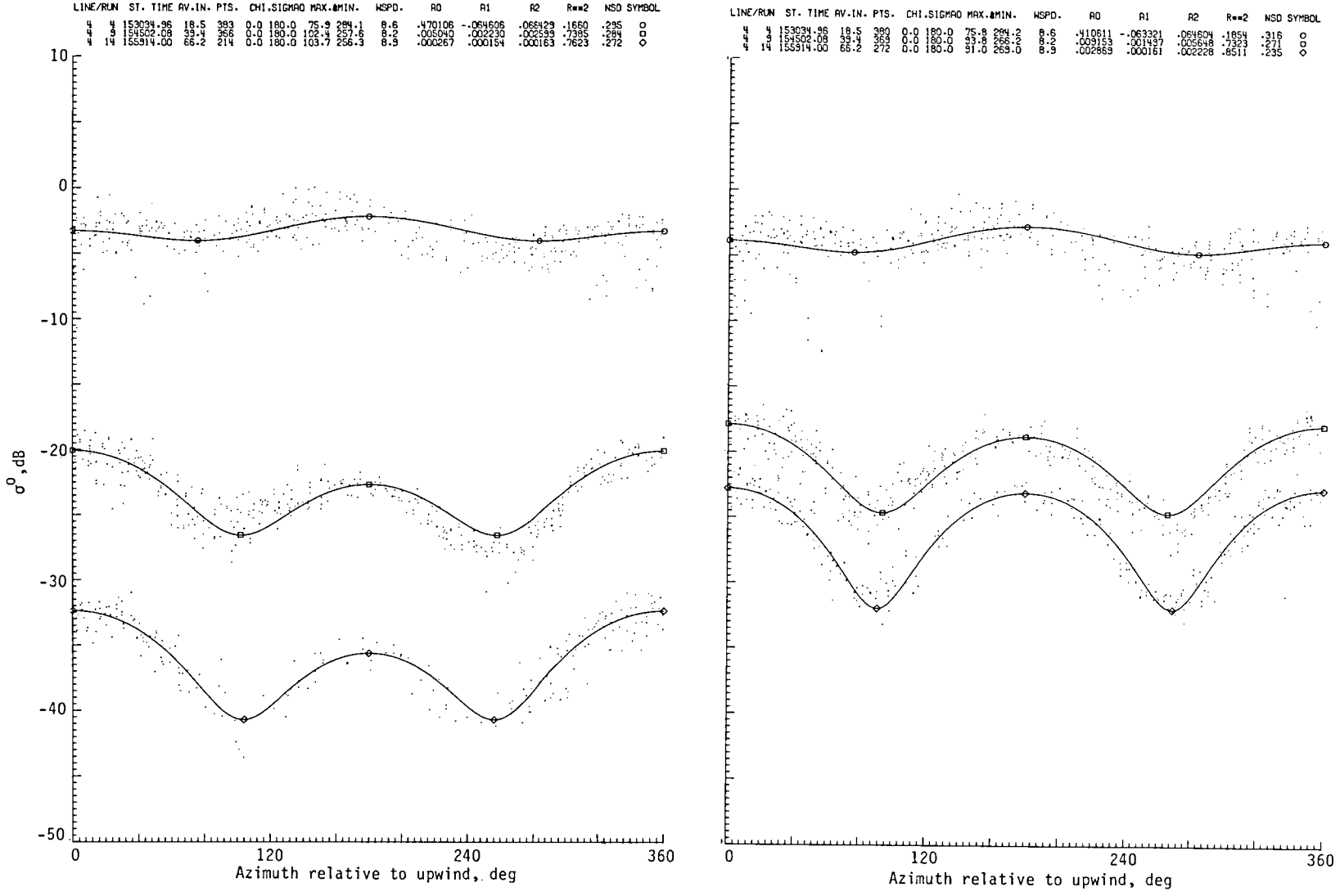

(a) Horizontal polarization.

(b) Vertical polarization.

Figure C10.- Second-order regression fit of NRCS versus azimuth relative to upwind for circle flight line data for mission 318, flight 16.

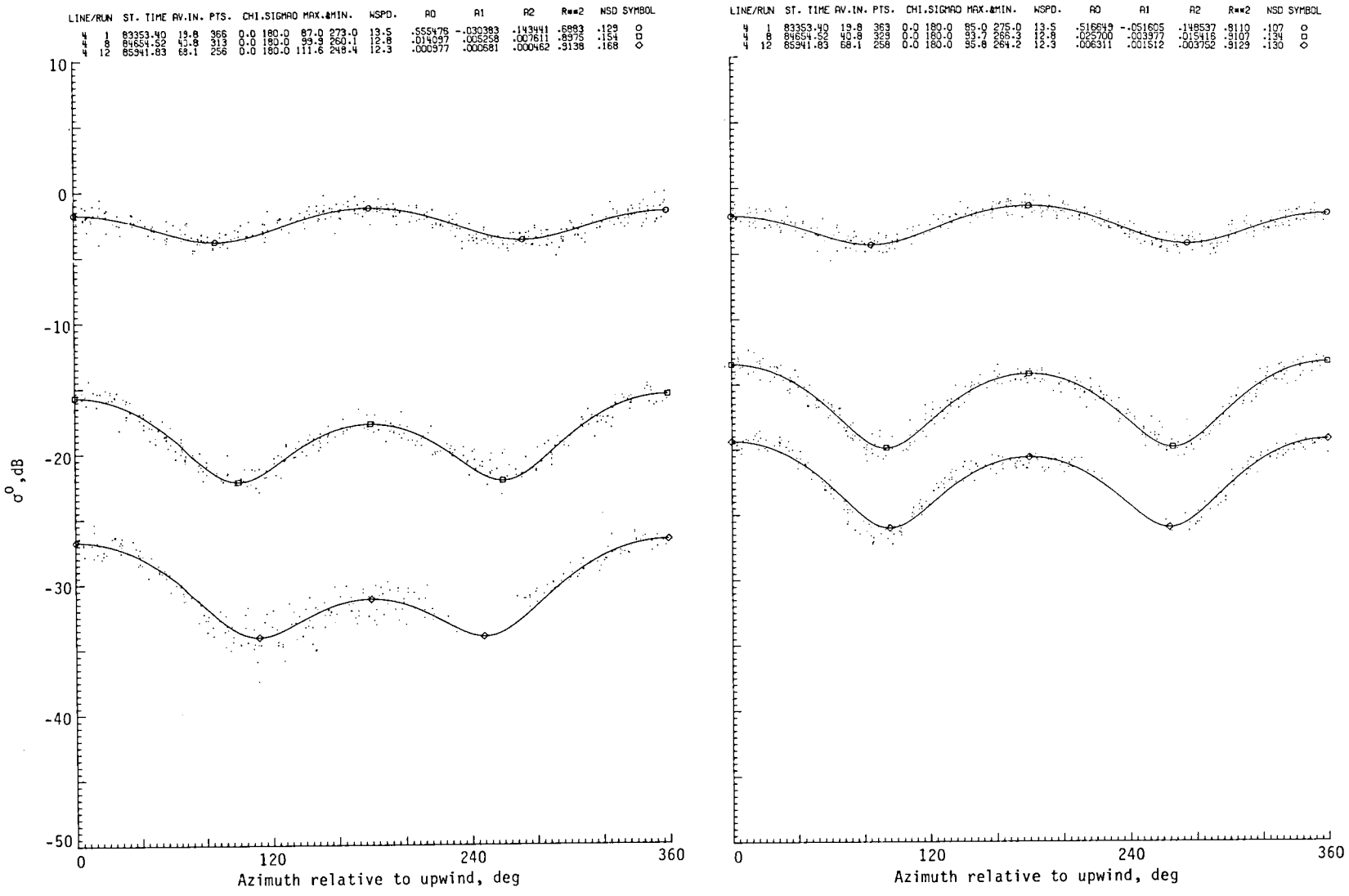

(a) Horizontal polarization.

(b) Vertical polarization.

Figure C11.- Second-order regression fit of NRCS versus azimuth relative to upwind for circle flight line data for mission 318, flight 17.

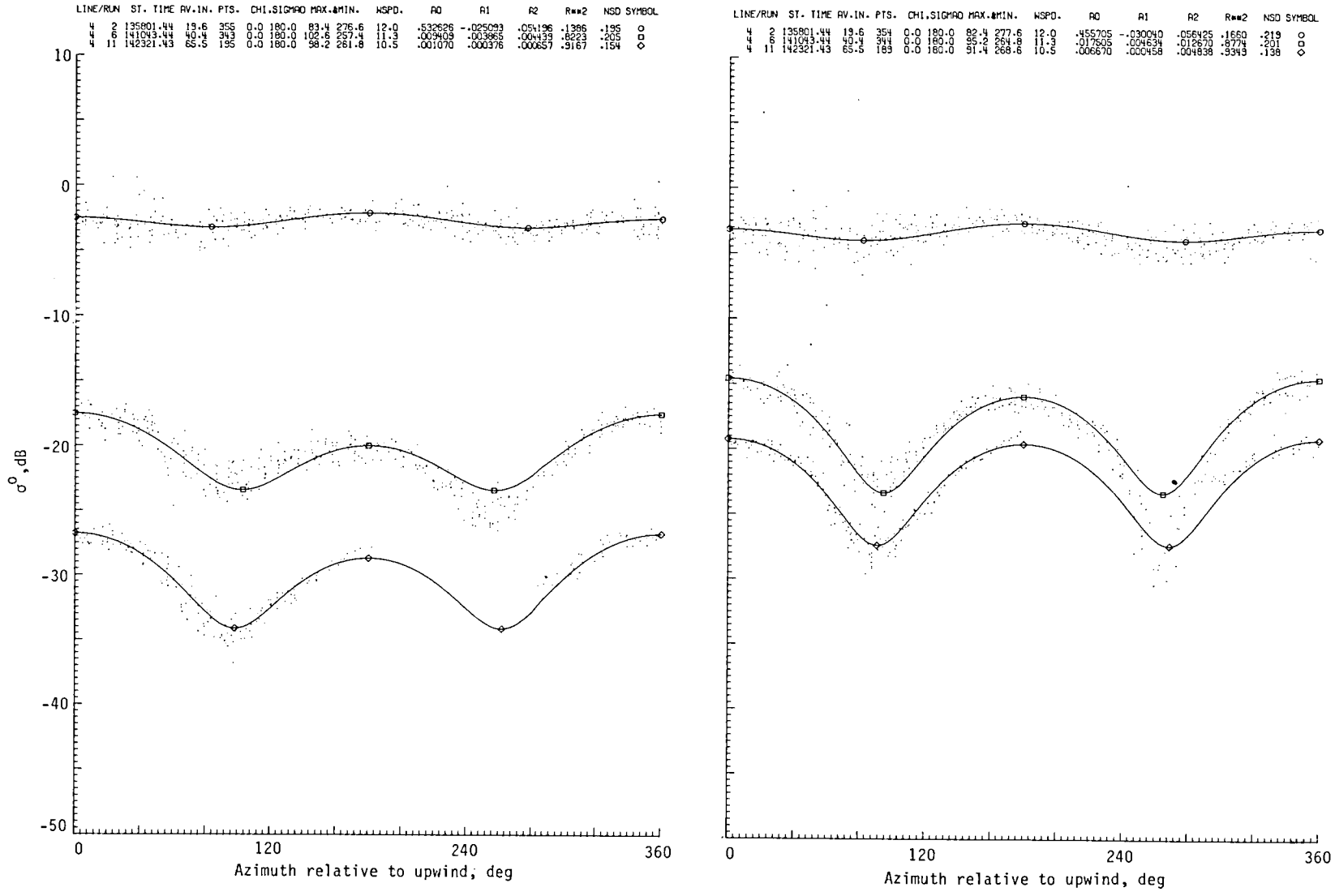

(a) Horizontal polarization.

(b) Vertical polarization.

Figure C12.- Second-order regression fit of NRCS versus azimuth relative to upwind for circle flight line data for mission 318, flight 18.

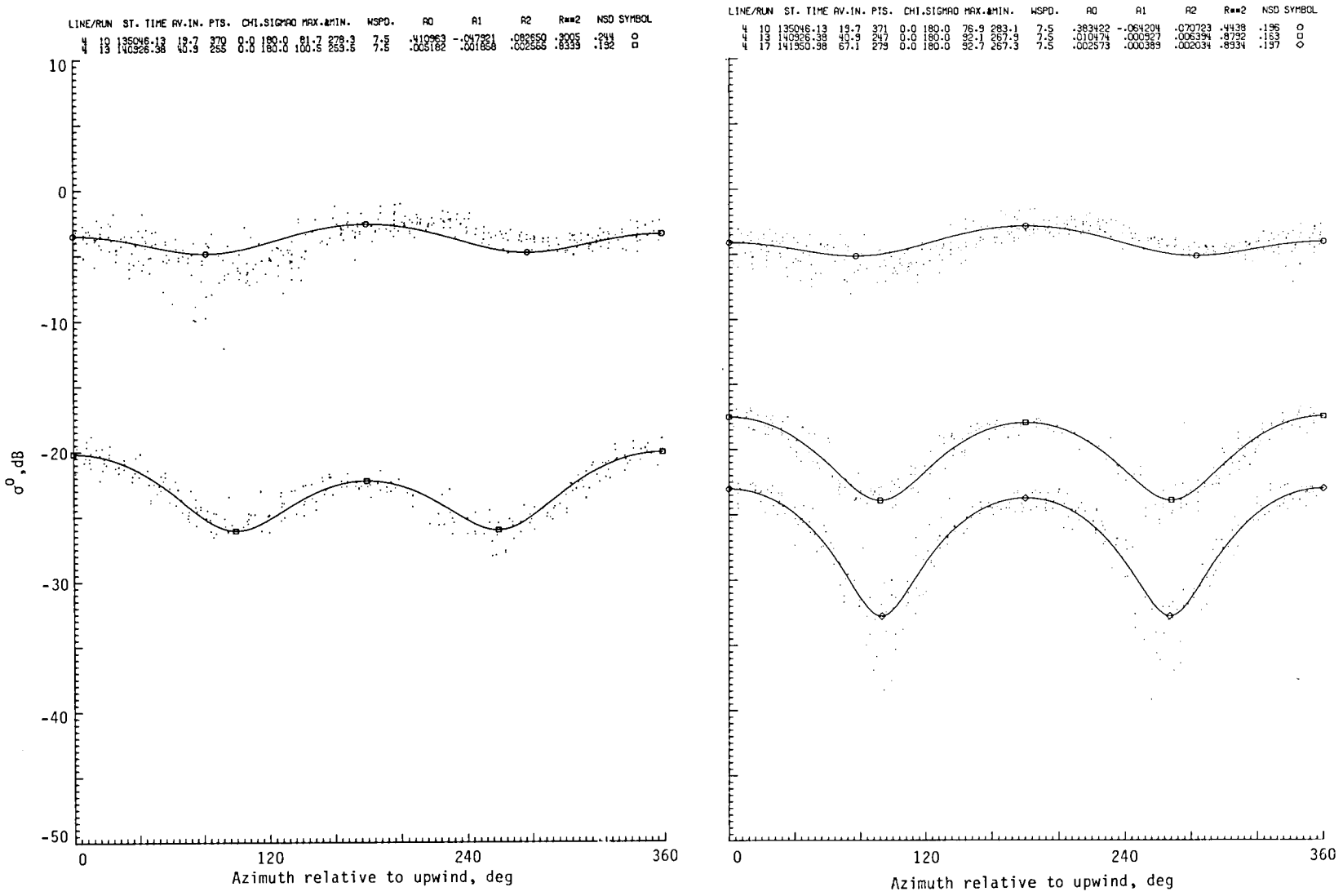

(a) Horizontal polarization.

(b) Vertical polarization.

Figure C13.- Second-order regression fit of NRCS versus azimuth relative to upwind for circle flight line data for mission 318, flight 19.

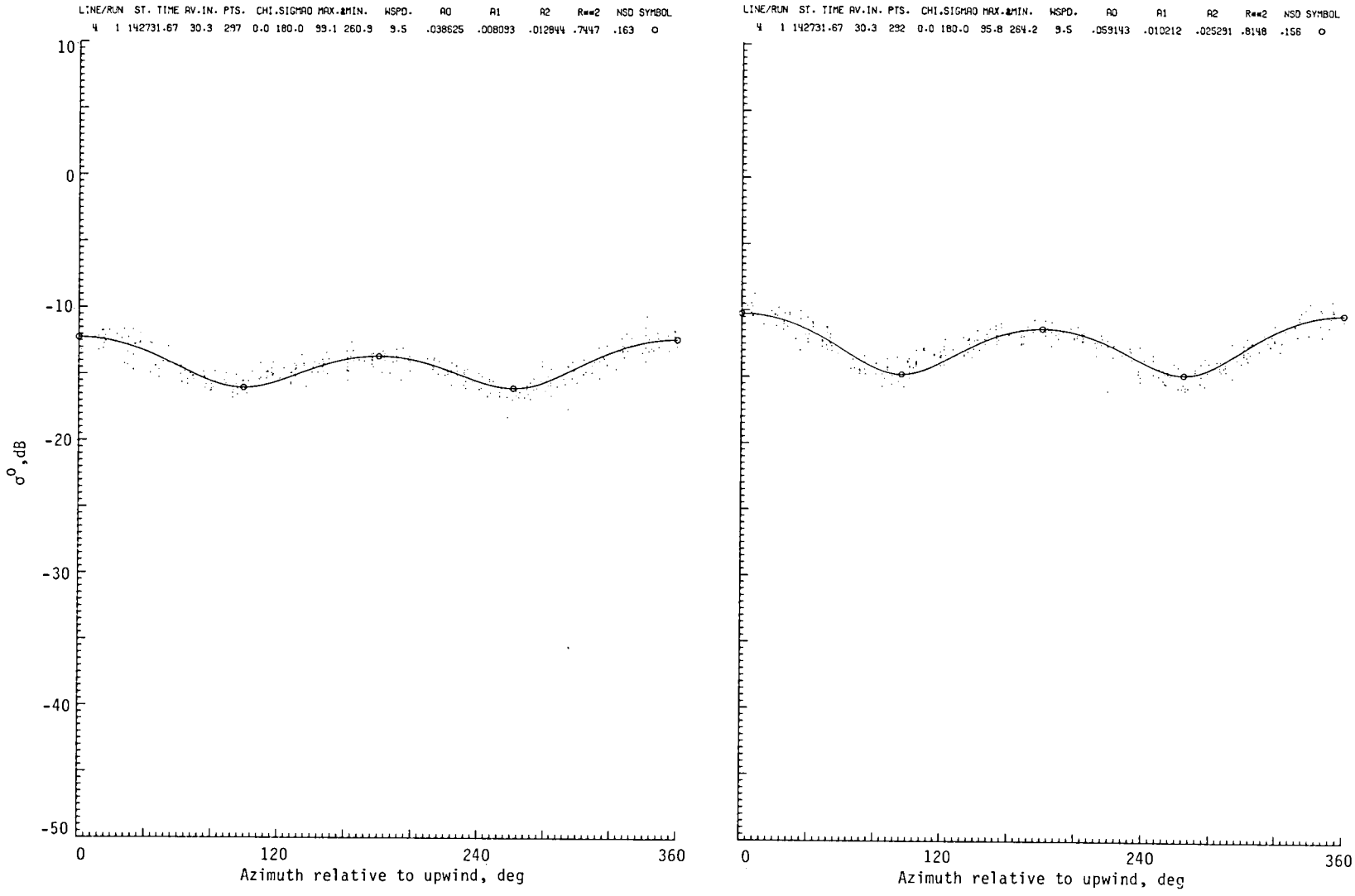

(a) Horizontal polarization.

(b) Vertical polarization.

Figure C14.- Second-order regression fit of NRCS versus azimuth relative to upwind for circle flight line data for mission 318, flight 24.

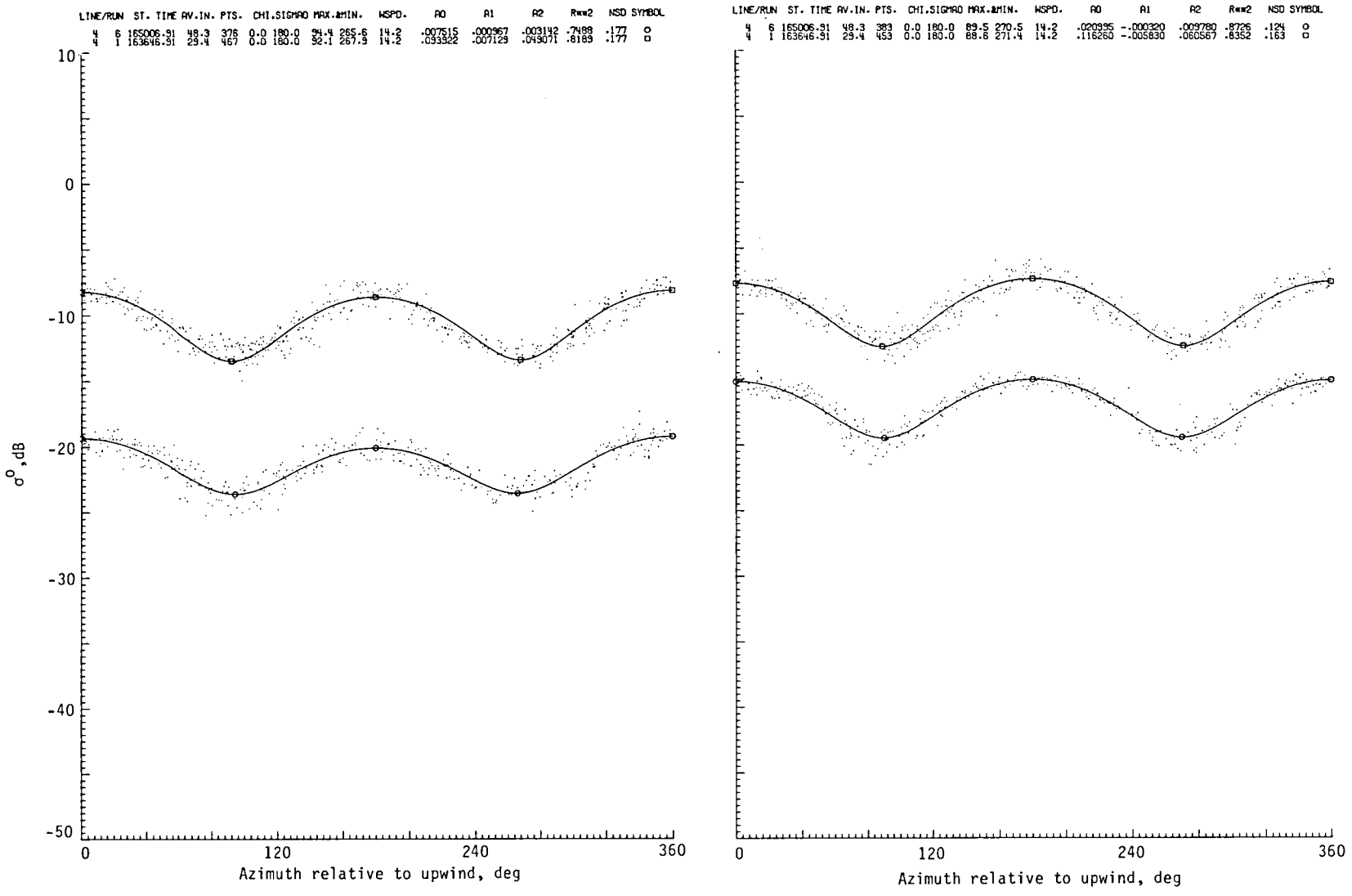

(a) Horizontal polarization.

(b) Vertical polarization.

Figure C15.- Second-order regression fit of NRCS versus azimuth relative to upwind for circle flight line data for mission 335, flight 3.

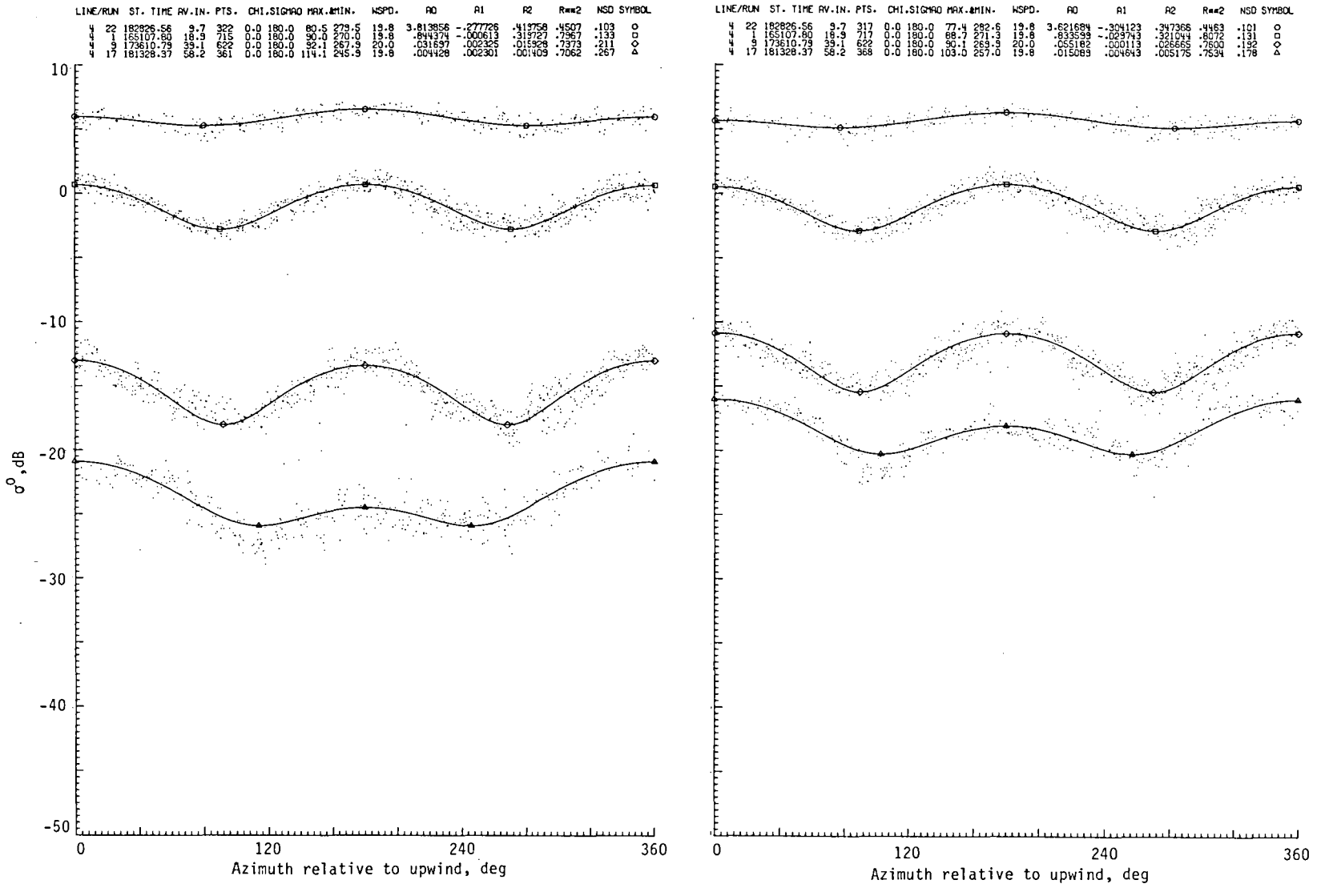

(a) Horizontal polarization.

(b) Vertical polarization.

Figure C16.- Second-order regression fit of NRCS versus azimuth relative to upwind for circle flight line data for mission 335, flight 4A.

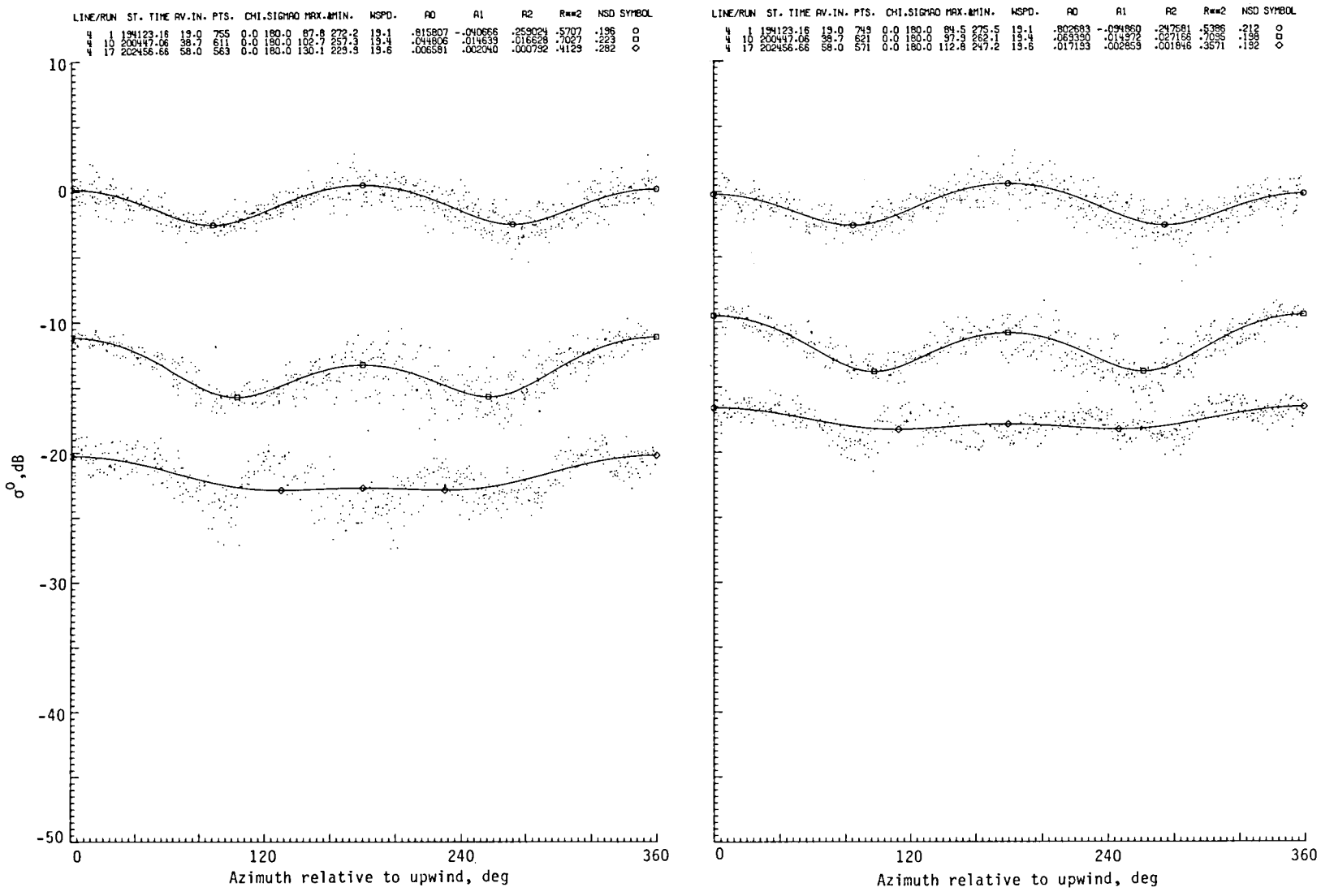

(a) Horizontal polarization.

(b) Vertical polarization.

Figure C17.- Second-order regression fit of NRCS versus azimuth relative to upwind for circle flight line data for mission 335, flight 4B.

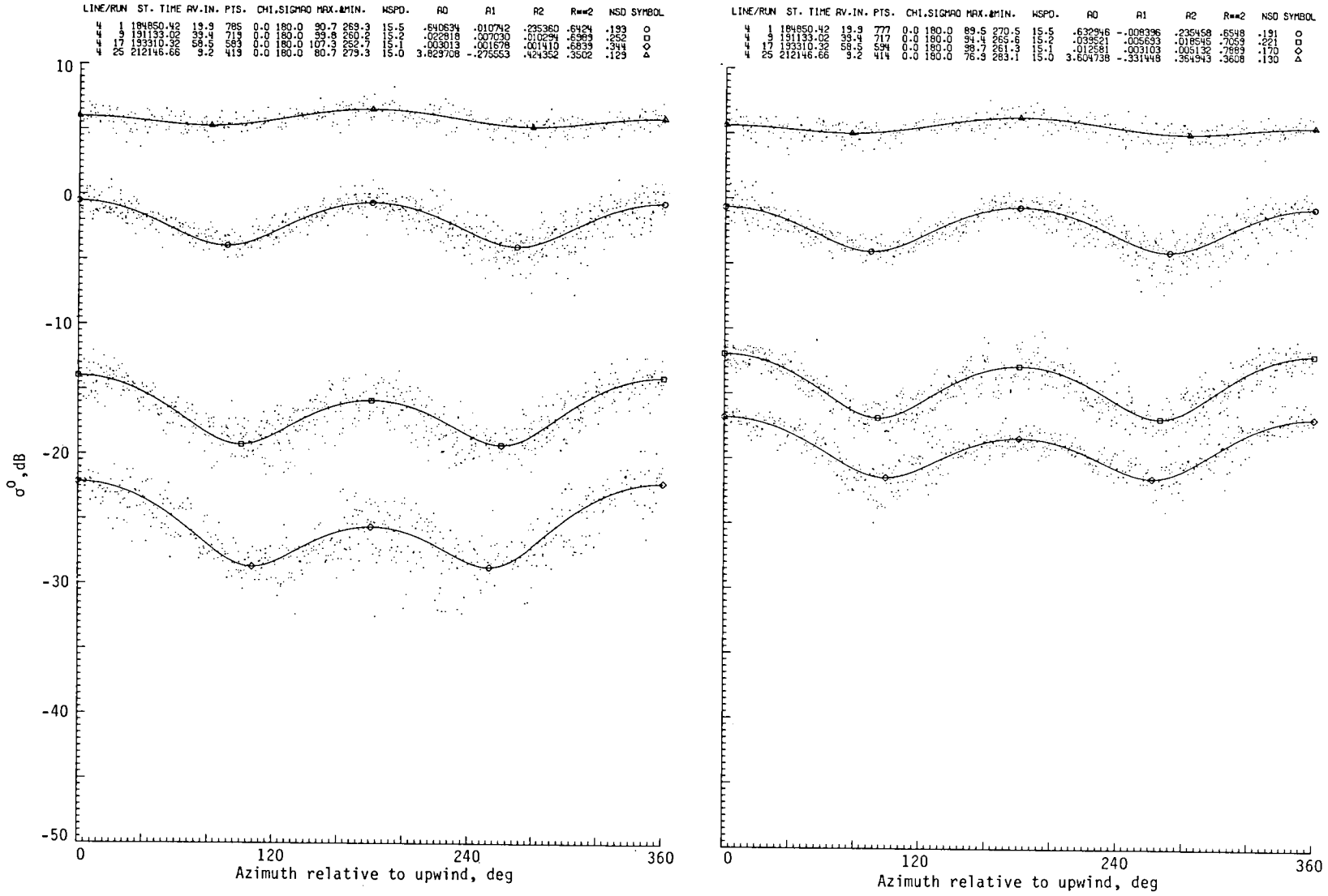

(a) Horizontal polarization.

(b) Vertical polarization.

Figure C18.- Second-order regression fit of NRCS versus azimuth relative to upwind for circle flight line data for mission 335, flight 5.

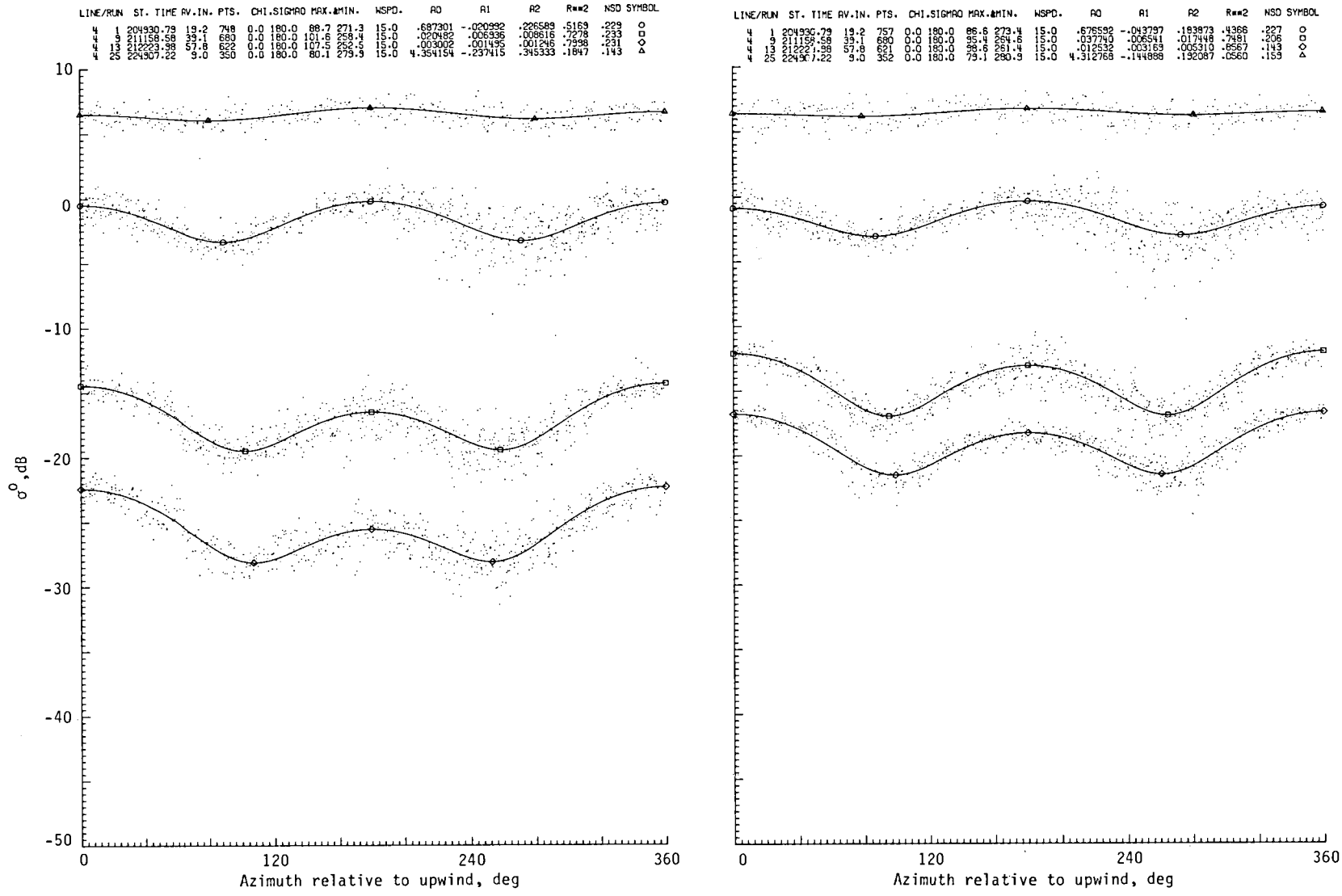

(a) Horizontal polarization.

(b) Vertical polarization.

Figure C19.- Second-order regression fit of NRCS versus azimuth relative to upwind for circle flight line data for mission 335, flight 6.

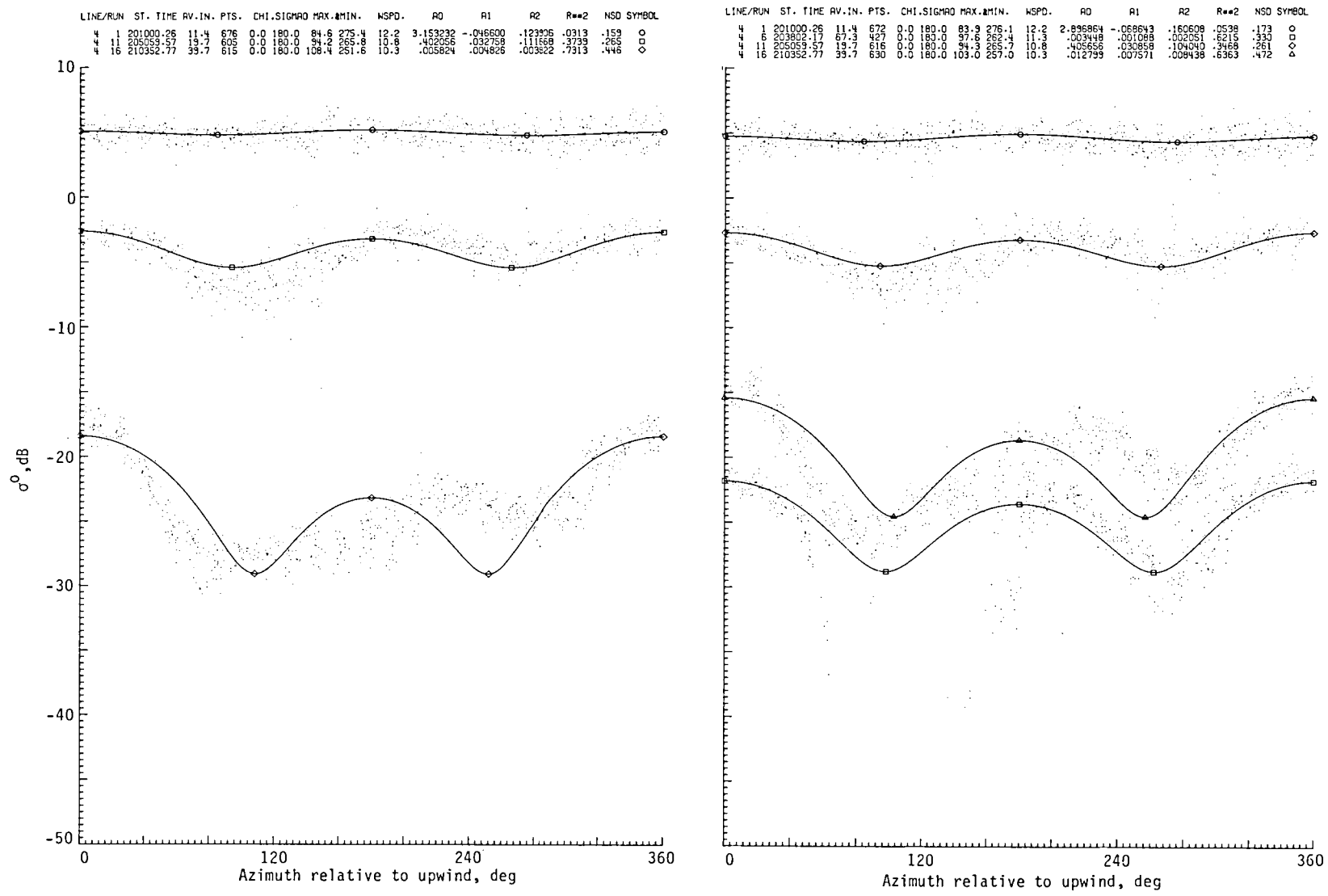

(a) Horizontal polarization.

(b) Vertical polarization.

Figure C20.- Second-order regression fit of NRCS versus azimuth relative to upwind for circle flight line data for mission 353, flight 9.

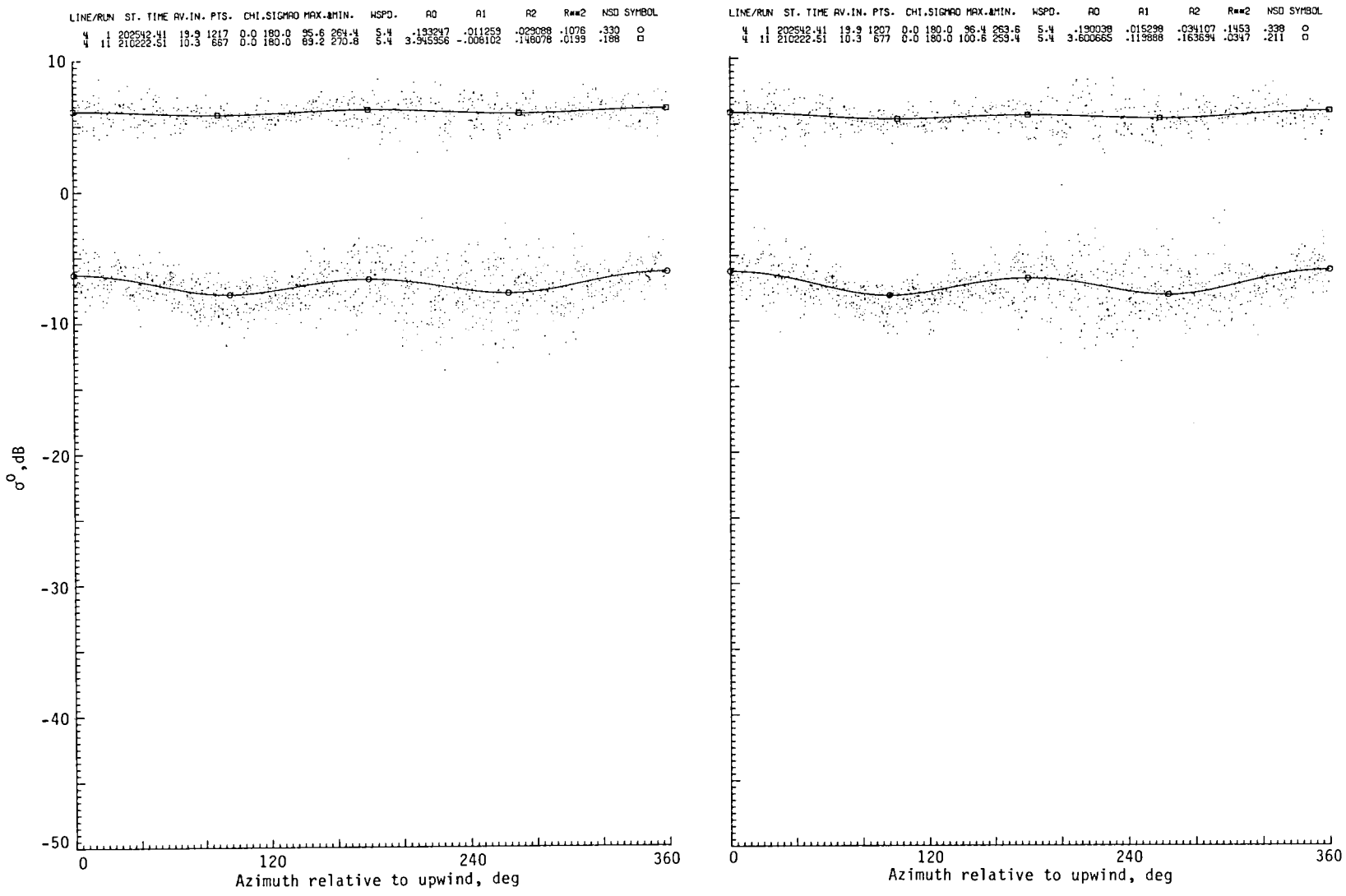

(a) Horizontal polarization.

(b) Vertical polarization.

Figure C21.- Second-order regression fit of NRCS versus azimuth relative to upwind for circle flight line data for mission 353, flight 10.

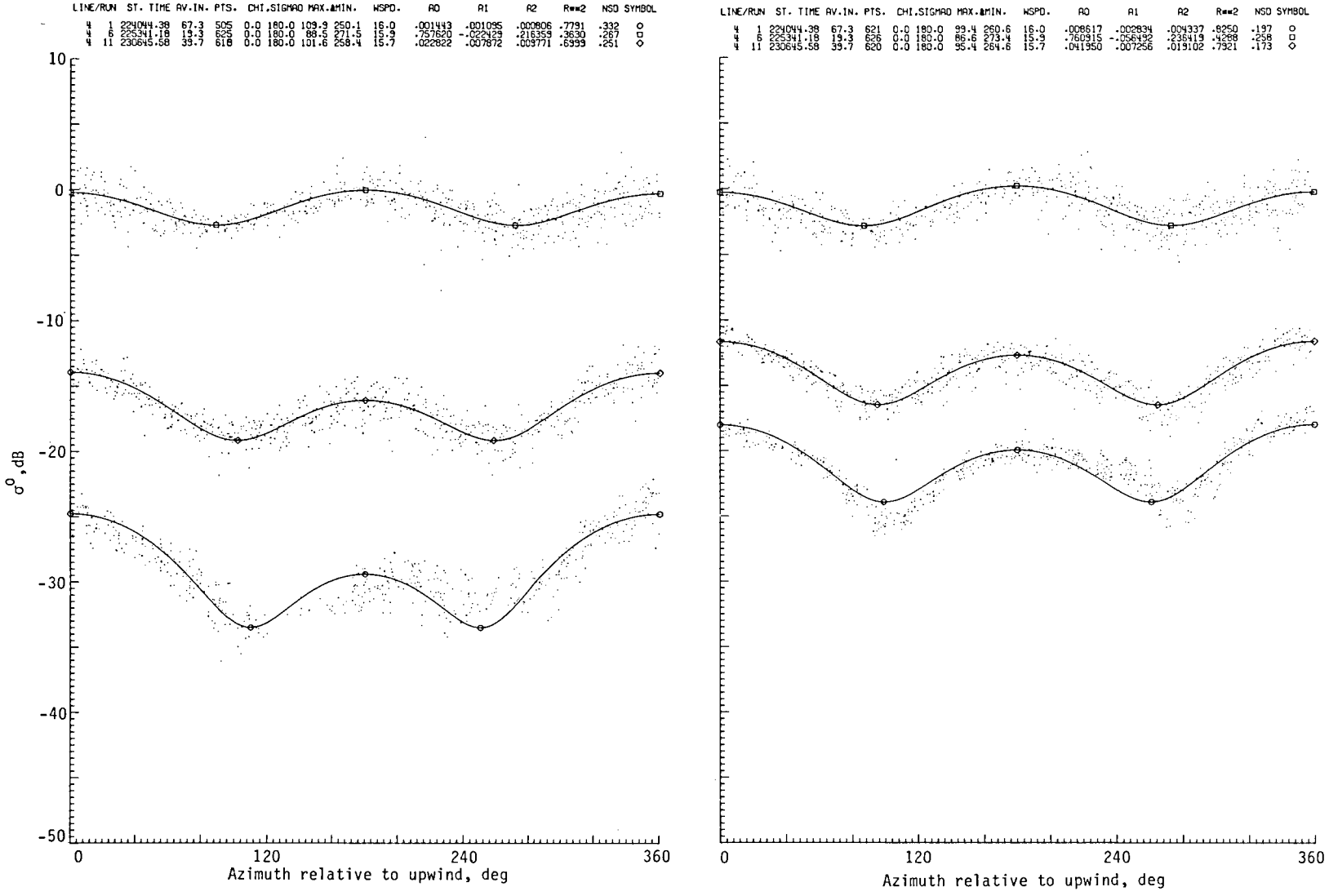

(a) Horizontal polarization.

(b) Vertical polarization.

Figure C22.- Second-order regression fit of NRCS versus azimuth relative to upwind for circle flight line data for mission 353, flight 11.

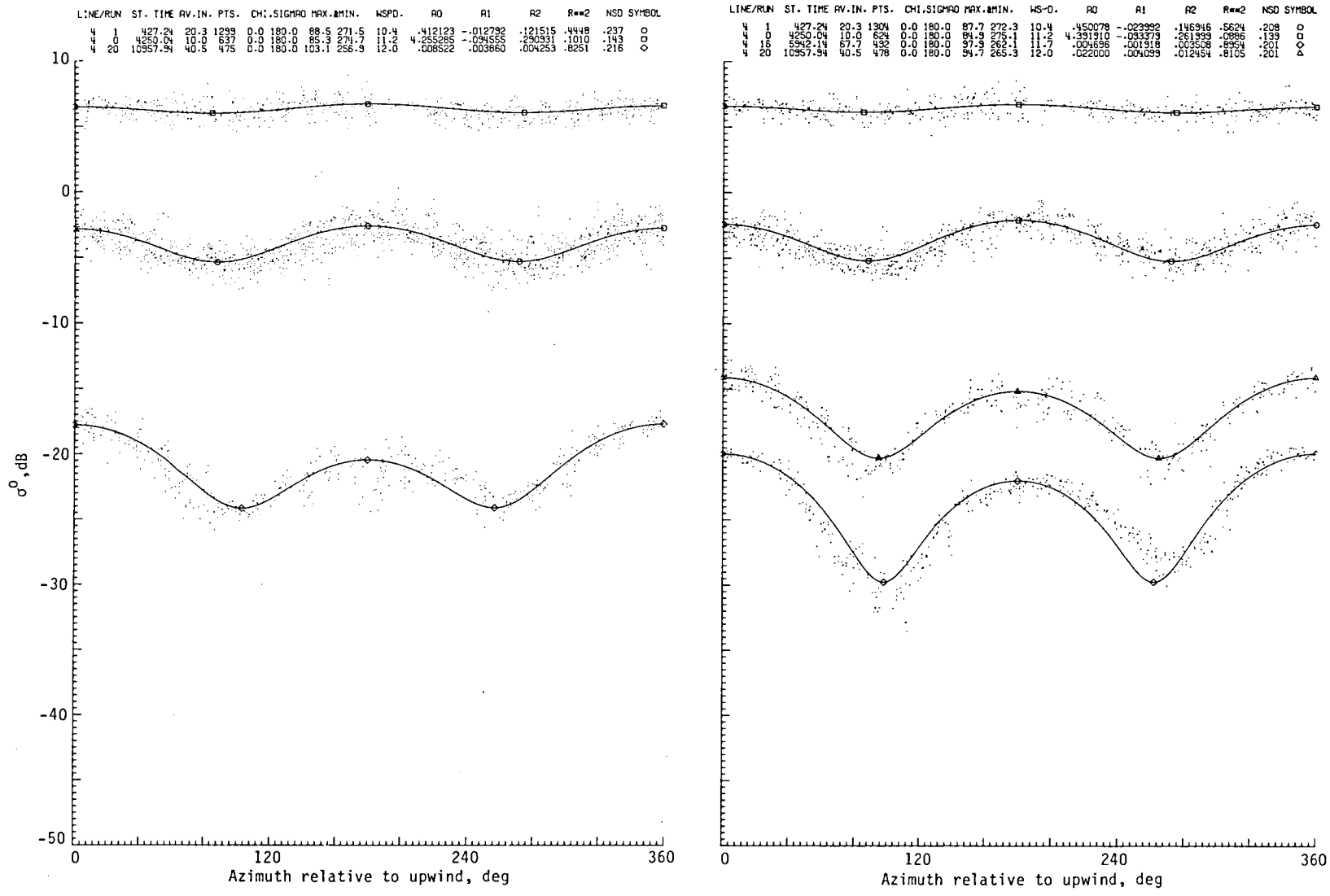

(a) Horizontal polarization.

(b) Vertical polarization.

Figure C23.- Second-order regression fit of NRCS versus azimuth relative to upwind for circle flight line data for mission 353, flight 13.

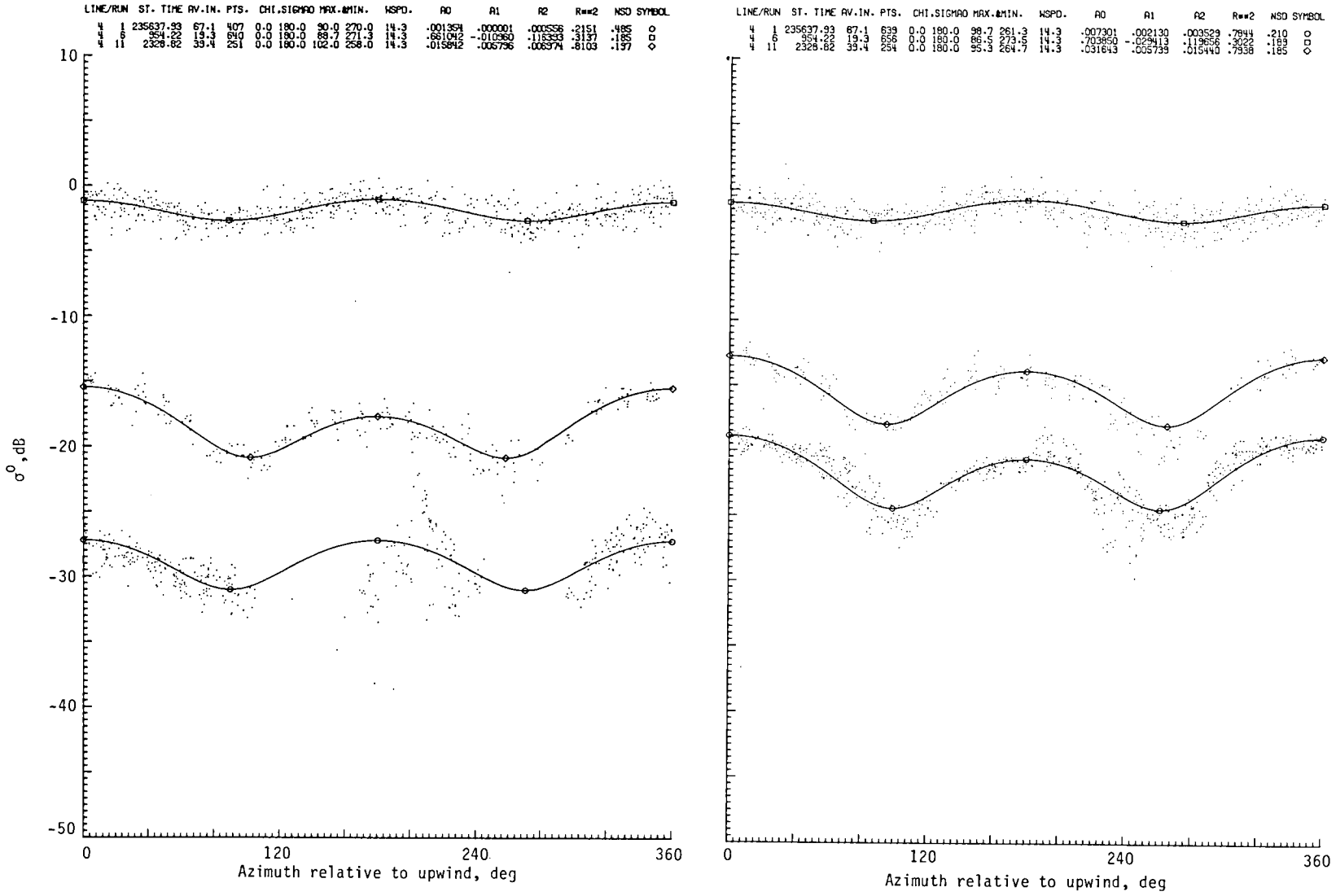

(a) Horizontal polarization.

(b) Vertical polarization.

Figure C24.- Second-order regression fit of NRCS versus azimuth relative to upwind for circle flight line data for mission 353, flight 14.

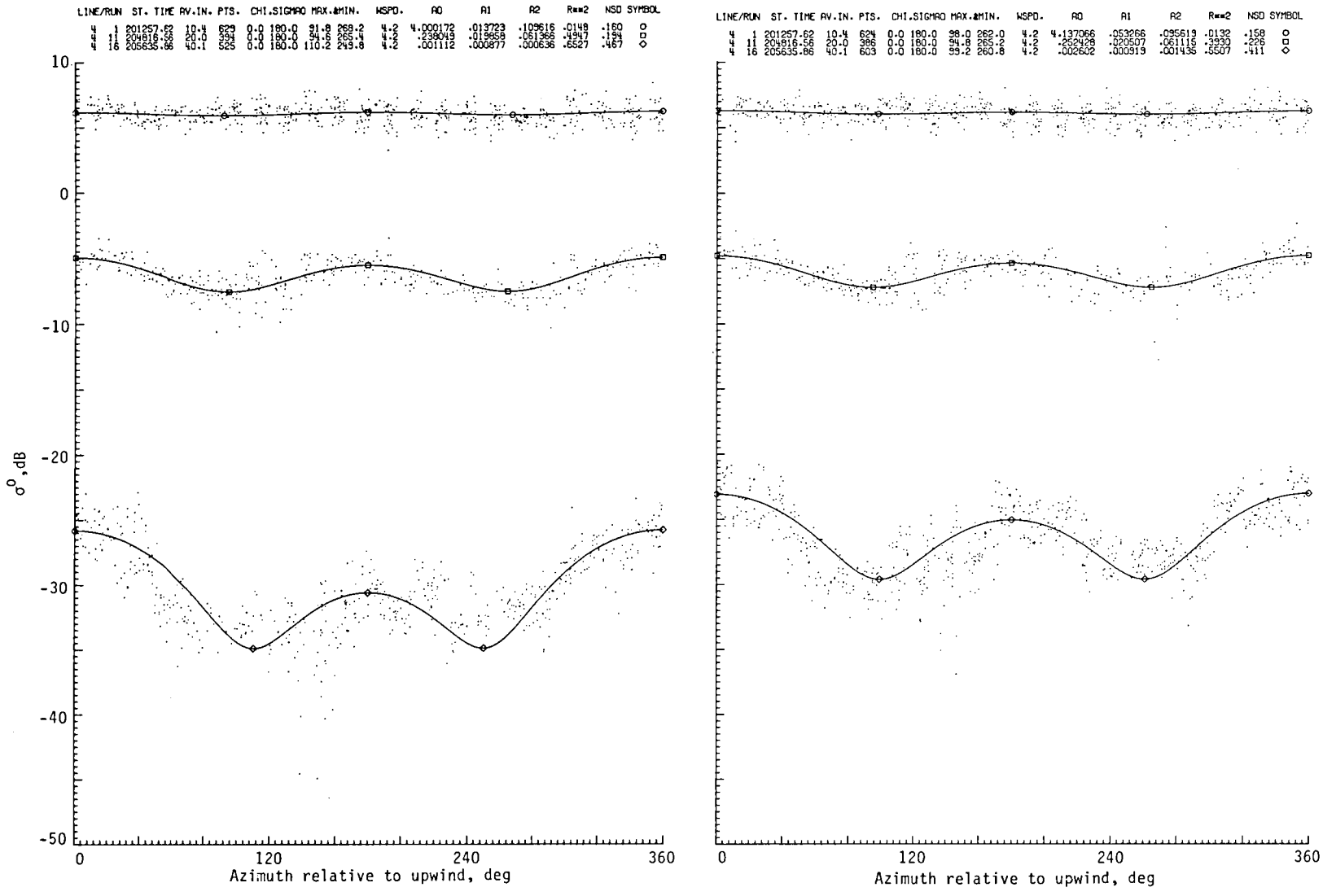

(a) Horizontal polarization.

(b) Vertical polarization.

Figure C25.- Second-order regression fit of NRCS versus azimuth relative to upwind for circle flight line data for mission 353, flight 15.

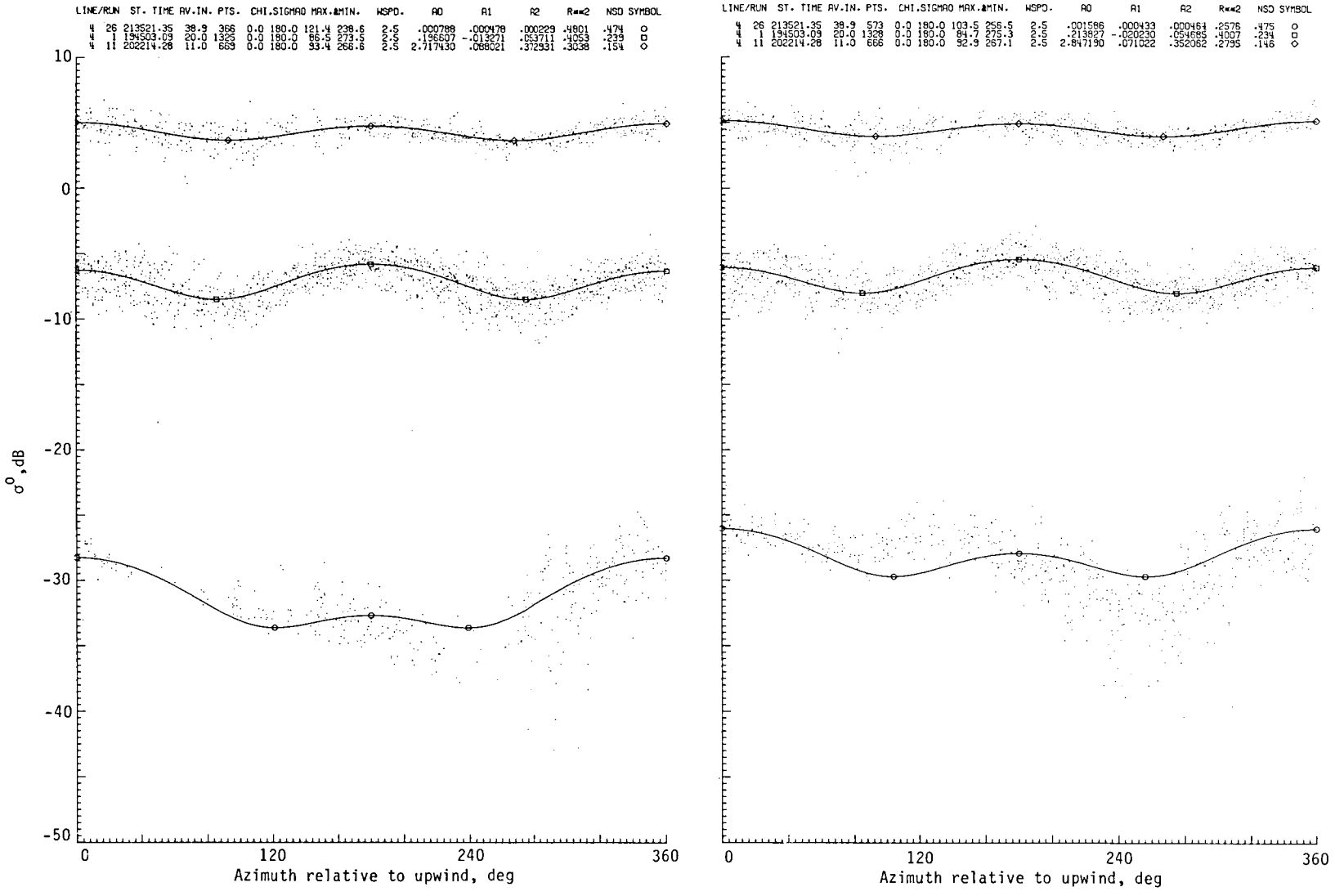

(a) Horizontal polarization.

(b) Vertical polarization.

Figure C26.- Second-order regression fit of NRCS versus azimuth relative to upwind for circle flight line data for mission 353, flight 20.

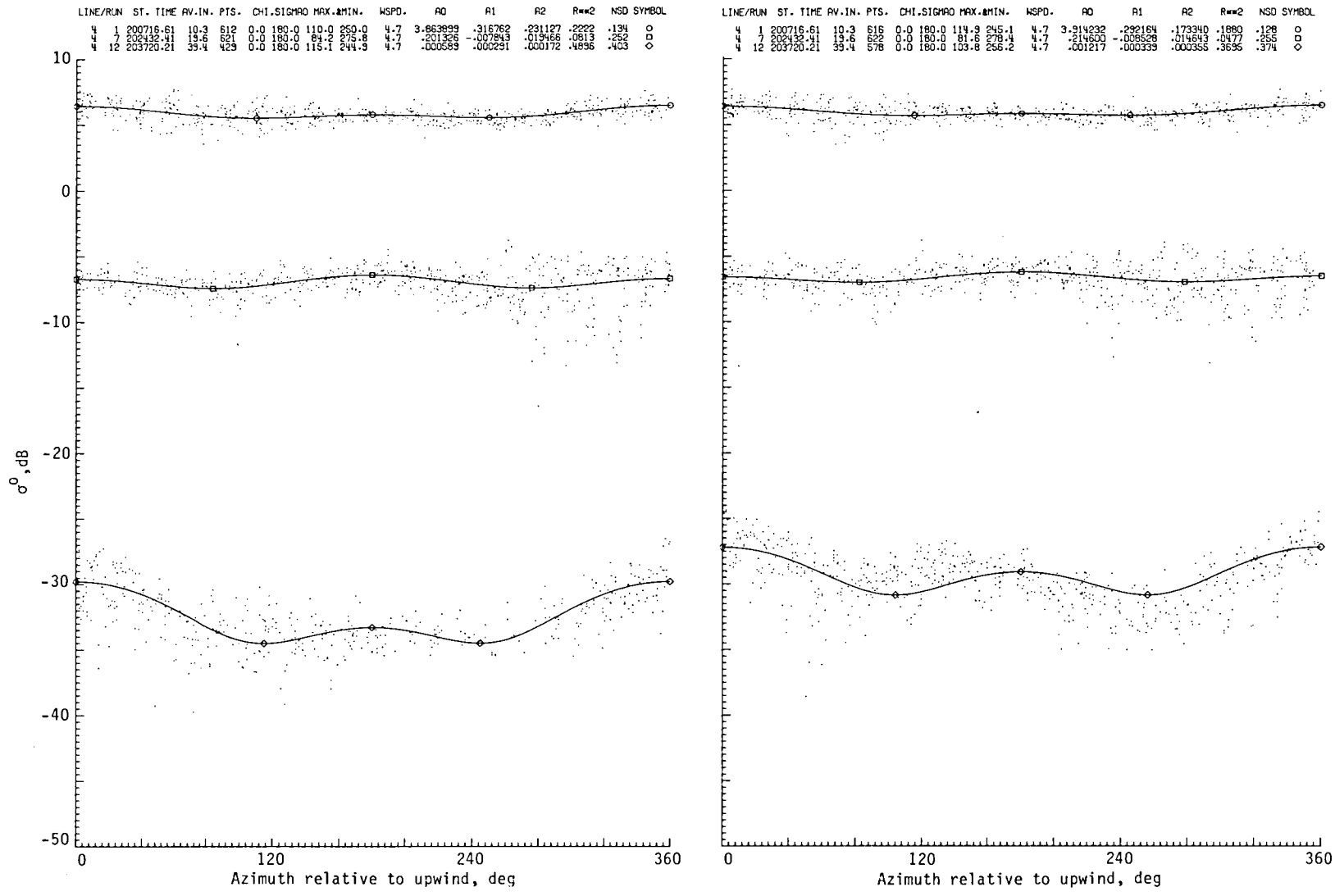

(a) Horizontal polarization.

(b) Vertical polarization.

Figure C27.- Second-order regression fit of NRCS versus azimuth relative to upwind for circle flight line data for mission 353, flight 21.

REFERENCES

1. Moore, Richard K.; and Pierson, Willard J., Jr.: Worldwide Oceanic Wind and Wave Predictions Using a Satellite Radar-Radiometer. J. Hydronaut., vol. 5, no. 2, Apr. 1971, pp. 52-60.

2. Daley, John: An Empirical Sea Clutter Model. NRL Mem. Rep. 2668, U.S. Navy, Oct. 1973.

3. Bradley, G. A.: Remote Sensing of Ocean Winds Using a Radar Scatterometer. Ph. D. Thesis, Univ. Kansas, 1971.

4. Claassen, John P.; Fung, H. S.; Moore, Richard K.; and Pierson, Willard J., Jr.: Radar Sea Return and the RADSCAT Satellite Anemometer. Engineering in the Ocean Environment, IEEE, 1972, pp. 180-185.

5. Jones, W. Linwood; and Schroeder, L. C.: Radar Backscatter From the Ocean: Dependence on Surface Friction Velocity. Boundary-Layer Meteorol., vol. 13, no. 1, 2, 3, 4, Jan. 1978, pp. 133-149.

6. Jones, W. Linwood; Schroeder, Lyle C.; and Mitchell, John L.: Aircraft Measurements of the Microwave Scattering Signature of the Ocean. IEEE J. Oceanic Eng., vol. OE-2, no. 1, Jan. 1977, pp. 52-61.

7. Wentz, Frank J.: A Two-Scale Scattering Model With Application to the JONSWAP '75 Aircraft Microwave Scatterometer Experiment. NASA CR-2919, 1977.

8. Moore, R. K.; Fung, A. K.; Dome, G. J.; and Birrer, I. J.: Wind Speed and Directional Properties of Radar Backscatter at 13.9 GHz. RSL TR 343-3 (Contract NSG 1397), Remote Sensing Lab., Univ. Kansas Center for Research, Inc., 1979. (Available as NASA CR-166090.)

9. Brucks, John T.; Jones, W. Linwood; and Leming, Thomas D.: Comparison of Surface Wind Stress Measurements: Airborne Radar Scatterometer Versus Sonic Anemometer. J. Geophys. Res., vol. 85, no. C9, Sept. 20, 1980, pp. 4967-4976.

10. Schroeder, Lyle C.; Boggs, Dale H.; Dome, George; Halberstam, Isadore M.; Jones, W. Linwood; Pierson, Willard J.; and Wentz, Frank J.: The Relationship Between Wind Vector and Normalized Radar Cross Section Used To Derive SEASAT-A Satellite Scatterometer Winds. J. Geophys. Res., vol. 87, no. C5, Apr. 30, 1982, pp. 3318-3336.

11. Schroeder, Lyle C.; Jones, W. L., Jr.; and Mitchell, John L.: Laboratory Calibration of AAFE Radiometer/Scatterometer (RADSCAT). NASA TM X-73900, 1976.

12. Cardone, Vincent J.: Specification of the Wind Distribution in the Marine Boundary Layer for Wave Forecasting. Geophys. Sci. Lab. TR-69-1 (Contract Nos. Nonr 285(57), N62306-1589, and N62306-68-C-0249), School of Eng. & Sci., New York Univ., Dec. 1969. (Available from DTIC as AD 702 490.)

13. Draper, N. R.; and Smith, H.: Applied Regression Analysis. John Wiley & Sons, Inc., c.1966.

14. Walpole, Ronald E.; and Myers, Raymond H.: Probability and Statistics for Engineers and Scientists. Macmillan Co., c.1972.

SYMBOLS AND ABBREVIATIONS

A	altitude of aircraft, m
AAFE RADSCAT	advanced aerospace flight experiment radiometer scatterometer
AV.IN.	average incidence
A_i, B_i	regression coefficients (Ai and Bi in computer plots)
A_n	nth coefficient of polynomial
a,b,c,d	parameters related to actual wind speed and direction
amp	amplifier
C,D,U	crosswind, downwind, and upwind (XW, DW, and UW in computer plots)
C_1, C_2	angles of crosswind minima for circle NRCS versus χ plots
CUNY	City University of New York
D_{max}	angle of downwind maximum for circle NRCS versus χ plots
dev	deviation
dir	direction
err	error
FCF	functional check flight
f	function
fl,FLT	flight
G	antenna gain
GMT	Greenwich mean time
GXR	receiver calibration loop attenuation
H,V	horizontal and vertical (polarization)
lat	latitude
long	longitude
max	maximum
min	minimum
miss	mission

NASA	National Aeronautics and Space Administration
NRCS	normalized radar cross section (or σ^{o}), dB
NSD	normalized standard deviation
n	integer
PTS	points
pol, P	polarization
R^2	multiple correlation coefficient (R**2 in computer plots)
SASS	SEASAT-A satellite scatterometer
SR	sum of residuals
SS	sum of squares error
ST	start
std	standard
temp	temperature
U	velocity, m/s
V	output voltage of scatterometer integrator, V
WDIR	wind direction
WSPD	wind speed
α	calibration attenuator value for given channel
β	equivalent beamwidth, rad
θ	incidence angle, deg (INC. ANG. in computer plots)
λ	free-space wavelength, m
σ^{o}	scattering coefficient or NRCS, dB (SIGMA0 in computer plots)
τ	scatterometer integration time, s
ϕ	azimuth angle, deg (AZ in computer plots)
χ	wind direction relative to upwind (CHI in computer plots)

Subscripts:

c,d,u	crosswind, downwind, and upwind
cal	during calibration
sea	during sea operation

TABLE I.- AAFE RADSCAT FLIGHT EXPERIMENTAL OCEAN NRCS DATA

Mission	Flight	Date	Line	Run	At line start			At line stop			Number of samples	Average altitude, ft	Mode (a)	Pol (b)	Data quality (c)	Archive tape	
					Time, H M S	N.lat., deg	E.long., deg	Time, H M S	N.lat., deg	E.long., deg						Number	File
230	FCF	4/11/73	2	2	19 12 45	38.9317	-74.5533	19 19 03	39.0801	-74.7533	407	4789	FA	HH,VV	1,2	M230	1
			2	3	19 22 50	39.0317	-74.7626	19 30 30	38.7973	-74.3539	461	4822	FA	HH,VV			2
			2	4	19 34 34	38.7983	-74.4092	19 45 31	39.0583	-74.7617	612	4825	FA	HH,VV			3
			2	5	20 01 00	38.9783	-74.7129	20 07 51	38.7950	-74.3334	314	4840	FA	HH,VV			4
			2	6	20 10 53	38.7066	-74.1783	20 37 52	37.8283	-72.8867	1470	4837	SS,FA,AA	HH,VV			5
			3	1	20 40 56	37.8833	-72.7600	20 52 21	37.9100	-72.6467	600	4824	SS,FA,AA	HH,VV			6
			4	1	21 01 18	37.7533	-72.9972	21 13 48	37.6965	-72.8833	1362	4820	SS	HH,VV			7
238	20	6/5/73	2	3	17 55 26	24.6550	-92.2654	18 07 10	24.9621	-92.7567	660	5423	FA	HH,VV	1,2	M238	1
			2	4	18 10 44	24.9867	-92.7033	18 20 20	24.7867	-92.2838	499	5515	FA	HH,VV			2
			2	5	18 27 28	24.7128	-92.1133	18 33 34	24.6000	-91.8418	345	5451	FA	HH,VV			3
			3	1	18 38 06	24.4314	-91.8750	18 48 50	24.0033	-92.1317	603	5311	FA	HH,VV			4
			5	1	19 04 27	24.5185	-92.0156	19 25 55	25.2761	-92.7533	1189	5271	FA	HH,VV			5
			4	2	19 29 41	25.3100	-92.7730	19 40 03	25.3367	-92.7700	1129	5277	SS	HH,VV			6
			5	2	19 49 36	25.4408	-92.9342	20 11 24	26.2010	-93.6694	1190	5117	FA	HH,VV			7
			4	9	20 15 16	26.3383	-93.7883	20 28 15	26.3709	-93.8317	1421	5372	SS	HH,VV			8
			5	4	21 35 01	27.5722	-95.1639	21 38 15	27.6884	-95.2817	204	5294	FA	HH,VV			9
			5	5	21 40 53	27.7762	-95.3780	22 01 35	28.5496	-96.1147	1066	5193	FA	HH,VV			10
			4	17	22 05 00	28.4850	-96.0383	22 18 47	28.5250	-96.0767	1509	5215	SS	HH,VV			11
238	27	6/11/73	2	3	16 30 32	26.4250	-88.5944	16 40 56	26.2768	-88.0984	584	5489	FA	HH,VV		M238	12
			2	4	16 50 00	26.5241	-88.3986	17 01 10	26.6862	-88.9333	621	5508	FA	HH,VV			13
			3	1	17 03 15	26.5997	-88.9667	17 03 48	26.5752	-88.9750	38	5514	FA	VV			14
			3	1	17 04 21	26.5540	-88.9850	17 16 30	26.1333	-89.2683	684	5512	FA	HH,VV			15
			3	2	17 19 27	26.2683	-89.2233	17 30 40	26.7864	-89.0452	661	5515	FA	HH,VV			16
			5	1	17 39 54	26.7850	-89.4074	18 02 20	27.5966	-90.1683	1235	5522	FA	HH,VV			17
			4	2	18 04 57	27.6267	-90.1500	18 17 37	27.6505	-90.1500	1256	5509	SS	HH,VV			18
			5	2	18 27 13	27.6331	-90.0883	18 48 49	28.4393	-90.7993	1142	5518	FA	HH,VV			19
			4	12	18 51 41	28.4505	-90.7972	19 03 39	28.5083	-90.7800	1306	5488	SS	HH,VV			20

[a]FA indicates fixed angle mode; AA, alternating angle mode; SS, short scatterometer mode. All modes defined in reference 11.

[b]HH is horizontal polarization, transmit and receive; VV, vertical polarization, transmit and receive; VH, vertical polarization transmit and horizontal polarization receive; HV, horizontal polarization transmit and vertical polarization receive.

[c]1 - thermal environment of band-pass filter estimated rather than controlled; 2 - average calibration voltage of flight because periodic calibrations exhibited drift; 3 - bandpass filter characteristics reconstructed subsequent to flight; 4 - additional -2.33 dB added to calibration loop gain to normalize average flight NRCS to 5.5 dB at incidence angle of 10°; 5 - surface truth shows variability or questionable quality.

TABLE I.- Continued

Mission	Flight	Date	Line	Run	At line start			At line stop			Number of samples	Average altitude, ft	Mode (a)	Pol (b)	Data quality (c)	Archive tape	
					Time, H M S	N.lat., deg	E.long., deg	Time, H M S	N.lat., deg	E.long., deg						Number	File
288	5	11/11/74	4	1	11 31 52	57.0533	0.8696	11 40 39	57.0817	1.1363	964	9398	SS	HH,VV	3,4	M288	1
			2	3	11 48 16	57.0773	1.1683	11 59 37	57.5267	2.0326	512	9512	FA	HH,VV			2
			2	4	12 04 24	57.5630	2.1033	12 11 19	57.4226	1.8259	309	9524	FA	HH,VV			3
			2	5	12 18 24	57.2856	1.5556	12 35 16	56.9450	0.8950	834	9585	FA	HH,VV			4
			2	6	12 41 41	57.1027	1.1911	12 56 58	57.6950	2.3666	790	9540	FA	HH,VV			5
			3	1	13 00 44	57.8100	2.2767	13 09 27	58.0383	1.8167	429	9489	FA	HH,VV			6
			3	2	13 12 38	57.9901	1.8532	13 20 30	57.7591	2.3143	386	9474	FA	HH,VV			7
			3	3	13 27 48	57.5665	2.5750	13 31 28	57.4447	2.7986	193	9629	FA	HH,VV			8
			3	4	13 34 05	57.4350	2.7533	13 40 57	57.6067	2.4217	333	9564	FA	HH,VV			9
			2	7	13 43 43	57.6350	2.2700	13 59 10	57.3133	1.6040	745	9606	FA	HH,VV			10
			4	8	14 09 58	57.5067	2.2145	14 26 34	57.6189	2.5978	1816	9582	SS	HH,VV			11
	6	11/14/74	4	1	13 05 44	56.8417	3.9800	13 14 02	56.9496	4.0350	908	9426	SS	HH,VV	3,4	M288	12
			2	3	13 24 20	57.0183	4.0043	13 37 39	56.5708	3.8600	637	9549	FA	HH,VV			13
			2	4	13 41 06	56.4533	3.8200	13 54 30	56.0033	3.6759	633	9568	FA	HH,VV			14
			2	5	14 02 16	55.7615	3.6000	14 14 40	55.3683	3.4790	610	9541	FA	HH,VV			15
			2	6	14 20 10	55.3367	3.4580	14 33 13	56.0349	3.6900	620	9466	FA	HH,VV			16
			2	7	14 37 30	56.2583	3.7583	14 52 11	57.0302	4.0119	699	9450	FA	HH,VV			17
			4	7	14 55 09	57.0800	4.0133	15 07 56	57.2083	4.1283	1387	9380	SS	HH,VV			18
			3	1	15 47 19	56.8129	3.8712	16 01 00	56.9133	2.8867	643	9482	FA	HH,VV			19
			3	2	16 04 09	56.8833	2.9306	16 17 40	56.7512	4.1301	654	9513	FA	HH,VV			20
			2	10	16 26 10	56.5929	3.9003	16 39 30	57.2803	4.0956	626	9458	FA	HH,VV			21
306	FCF	4/4/75	4	1	20 01 32	38.0600	-72.4183	20 09 49	37.9974	-72.2729	444	5327	FA	HH,VV	5	M306	1
			4	4	20 09 53	37.9933	-72.2731	20 17 09	37.9514	-72.1800	347	5333	FA	HH,VV			2
			4	7	20 17 19	37.9433	-72.1800	20 27 04	37.8517	-72.0450	594	5337	FA	HH,VV			3
			4	11	20 30 57	37.8984	-72.1667	20 39 01	37.8219	-72.0751	436	5312	FA	HH,VV			4
			4	14	20 39 08	37.8183	-72.0717	20 48 45	37.7414	-71.9278	414	5307	FA	HH,VV			5
			3	2	20 54 54	37.4817	-72.0183	21 04 49	37.0817	-72.2083	455	5428	FA	HH,VV			6
	3	4/17/75	1	1	14 07 50	40.4752	-73.8567	14 17 49	40.4133	-73.8356	434	9772	FA	HH		M306	7
			7	1	14 34 44	40.4317	-73.4994	14 45 01	40.3667	-73.5148	1049	9790	SS	HH			8
			6	1	14 48 10	40.2150	-73.4767	14 59 10	40.1367	-73.4450	1131	9815	SS	HH			9
			5	1	15 05 02	40.1317	-73.5433	15 15 30	40.0583	-73.5464	1068	9827	SS	HH			10
			13	1	15 19 51	39.8643	-73.5950	15 30 35	39.7717	-73.5647	1121	9834	SS	HH			11
			12	1	15 37 58	40.0489	-73.4500	15 48 15	39.9650	-73.4462	1071	9833	SS	HH			12
			11	1	15 53 58	40.0855	-73.1860	16 04 39	39.9917	-73.1717	1095	9824	SS	HH			13
			10	1	16 11 47	40.2576	-73.2074	16 22 02	40.1733	-73.2250	1066	9831	SS	HH			14
			9	1	16 24 24	40.2533	-73.1733	16 27 59	40.3767	-73.0817	228	9838	SS	HH			15
			9	2	16 29 28	40.4302	-73.0586	16 39 50	40.3508	-73.0900	1079	9844	SS	HH			16
			8	1	16 41 21	40.3940	-73.1532	16 45 30	40.5233	-73.3083	206	9826	SS	HH			17
			8	2	16 46 50	40.5633	-73.3631	16 57 21	40.4817	-73.3967	1097	9841	SS	HH			18
			8	4	17 00 14	40.4442	-73.5717	17 03 29	40.4400	-73.7683	145	9838	SS	HH			19
			1	5	17 05 39	40.4661	-73.8867	17 15 54	40.3850	-73.9049	1048	9898	SS	HH			20

See footnotes on page 58.

TABLE I.- Continued

Mission	Flight	Date	Line	Run	At line start			At line stop			Number of samples	Average altitude, ft	Mode (a)	Pol (b)	Data quality (c)	Archive tape	
					Time, H M S	N.lat., deg	E.long., deg	Time, H M S	N.lat., deg	E.long., deg						Number	File
318	13	8/29/75	3	1	08 22 37	54.9333	7.6117	08 26 03	54.8383	7.8367	157	10247	FA	HH,VV		M318	1
			3	2	08 38 55	55.2067	7.1167	08 42 13	55.3133	6.8983	158	10228	FA	HH,VV			2
			6	1	09 15 27	54.8900	7.1633	09 19 20	54.8900	6.8433	149	10224	FA	HH,VV			3
			2	2	09 55 57	55.1483	7.6267	10 01 17	54.9617	7.3483	217	10193	FA	HH,VV			4
			2	22	10 01 33	54.9533	7.3367	10 02 21	54.9250	7.2933	35	10192	FA	HH,VV			5
			4	1	10 12 05	54.9767	7.8767	10 16 00	55.0117	7.8183	226	10176	FA	HH,VV			6
			4	2	10 16 05	55.0083	7.8167	10 16 55	54.9883	7.8550	48	10179	FA	HH,VV			7
			4	3	10 17 24	55.0078	7.8817	10 22 26	55.0317	7.8783	284	10160	FA	HH,VV			8
			4	9	10 33 36	55.1233	7.8617	10 38 12	55.1217	7.8417	241	10148	FA	HH,VV			9
			4	11	10 39 04	55.1500	7.8733	10 51 31	55.1783	7.7983	614	10158	FA	HH,VV			10
	14	9/2/75	2	3	08 26 16	54.8933	6.7700	08 35 38	55.2267	7.2683	422	10042	FA	HH,VV		M318	11
			3	1	08 51 42	55.3667	7.2750	08 58 42	55.1500	7.7183	318	10040	FA	HH,VV			12
			3	11	08 59 26	55.1260	7.7624	09 01 31	55.0583	7.8883	92	10040	FA	HH,VV			13
			3	2	09 13 29	54.8283	8.1267	09 18 30	54.9783	7.8133	234	10030	FA	HH,VV			14
			3	22	09 19 08	54.9967	7.7717	09 20 38	55.0417	7.6750	64	10022	FA	HH,VV			15
			4	1	09 44 35	54.9800	7.8650	09 58 26	54.9983	7.8250	809	9982	FA	HH,VV			16
			4	6	09 58 41	55.0100	7.8300	10 00 13	54.9800	7.8667	76	10033	FA	HH,VV			17
			4	7	10 00 44	54.9800	7.8283	10 12 15	54.9933	7.7433	624	9970	FA	HH,VV			18
			4	11	10 12 27	55.0033	7.7433	10 13 17	55.0067	7.7950	33	10074	FA	HH,VV			19
			4	12	10 13 32	54.9950	7.8017	10 25 31	54.9667	7.7233	480	10068	FA	HH,VV			20
	15	9/4/75	2	3	08 36 00	54.9400	8.0183	08 39 10	55.0017	7.8363	325	2552	SS	VV		M318	21
			3	1	08 45 02	54.9067	7.9117	08 47 03	54.9817	7.9500	217	2558	SS	VV			22
			2	4	08 51 17	54.9383	8.0933	08 54 35	54.9700	7.8767	343	2541	SS	VV			23
			3	2	08 59 29	54.8750	7.9300	09 02 40	55.0033	7.9517	285	2559	SS	VV			24
			2	5	09 07 33	54.9333	8.0567	09 10 18	54.9650	7.8717	274	2563	SS	HH			25
			3	3	09 14 32	54.8833	7.9100	09 17 06	54.9883	7.9500	219	2575	SS	HH			26
			2	6	09 21 48	54.9767	7.8367	09 24 22	54.9567	8.0367	252	2566	SS	VV			27
			3	4	09 29 56	55.0033	7.9800	09 31 34	54.9383	7.9350	182	2578	SS	VV			28
			2	7	09 35 39	54.9333	8.0750	09 38 34	54.9817	7.8883	293	2572	SS	HH			29
			3	5	09 43 26	54.8883	7.9350	09 46 20	55.0000	7.9733	259	2576	SS	HH			30
	16	9/8/75	2	5	14 52 58	54.7201	7.8517	14 59 20	55.0117	8.1133	280	10129	FA	HH,VV		M318	31
			4	4	15 30 35	54.9550	7.8517	15 44 52	55.0200	7.9519	791	10080	FA	HH,VV			32
			4	9	15 45 02	55.0217	7.9417	15 59 02	55.1283	8.0500	747	10077	FA	HH,VV			33
			4	14	15 59 14	55.1283	8.0350	16 13 13	55.2117	8.0600	535	10044	FA	HH,VV			34
			3	2	16 21 24	55.1414	7.5593	16 23 57	55.1933	7.3817	117	10105	FA	HH,VV			35
			3	22	16 24 23	55.2030	7.3517	16 30 54	55.3217	6.8950	277	10097	FA	HH,VV			36
			3	3	16 35 54	55.2950	6.8267	16 46 37	55.0267	7.6550	416	10094	FA	HH,VV			37

See footnotes on page 58.

TABLE I.- Continued

Mission	Flight	Date	Line	Run	At line start			At line stop			Number of samples	Average altitude, ft	Mode (a)	Pol (b)	Data quality (c)	Archive tape	
					Time, H M S	N.lat., deg	E.long., deg	Time, H M S	N.lat., deg	E.long., deg						Number	File
318	17	9/9/75	2	2	07 50 16	54.9333	7.9467	08 00 22	54.7350	7.7467	416	9878	SS,FA	HH,VV		M318	38
			3	3	08 08 35	55.0083	7.6583	08 15 09	54.8883	8.2083	288	10074	FA	HH,VV			39
			3	4	08 17 54	54.9617	8.1717	08 25 09	55.1467	7.7133	329	10076	FA	HH,VV			40
			4	1	08 33 53	54.8517	7.5689	08 46 23	54.9200	7.6800	731	9989	FA	HH,VV			41
			4	6	08 46 54	54.9233	7.6483	08 53 00	54.9883	7.7000	318	9977	FA	HH,VV			42
			4	8	08 53 08	54.9883	7.7133	08 59 29	54.9683	7.7633	337	9938	FA	HH,VV			43
			4	11	08 59 42	54.9733	7.7517	09 01 12	55.0017	7.8200	73	10169	FA	HH,VV			44
			4	12	09 01 50	54.9783	7.8150	09 12 58	55.0217	7.9283	444	10199	FA	HH,VV			45
	18	9/9/75	4	1	13 58 01	54.8083	7.5960	13 58 55	54.8450	7.5833	61	6165	FA	HH,VV		M318	46
			4	2	13 59 33	54.8600	7.6358	14 10 18	54.9467	7.8100	648	6142	FA	HH,VV			47
			4	6	14 10 43	54.9533	7.7867	14 23 10	55.1000	7.9900	694	6149	FA	HH,VV			48
			4	11	14 23 21	55.1033	7.9783	14 36 06	55.2717	8.1583	493	6140	FA	HH,VV			49
	19	9/10/75	2	6	13 14 57	55.1133	8.2267	13 21 45	54.9883	7.7950	291	9988	FA	HH,VV		M318	50
			3	3	13 27 36	55.0717	7.8433	13 34 19	54.8183	8.1317	297	10017	FA	HH,VV			51
			4	5	13 50 46	54.8883	7.7467	13 52 46	54.9167	7.7320	115	9992	FA	HH,VV			52
			4	6	13 55 22	54.9300	7.7517	13 56 06	54.9100	7.7867	52	9981	FA	HH,VV			53
			4	7	13 56 30	54.9017	7.7733	13 57 59	54.9450	7.7757	100	9937	FA	HH,VV			54
			4	8	13 58 59	54.9183	7.8000	14 01 23	54.9383	7.8283	143	9937	FA	HH,VV			55
			4	10	14 03 13	54.9783	7.8383	14 08 54	54.9967	7.9133	333	9957	FA	HH,VV			56
			4	12	14 09 26	54.9850	7.8933	14 11 08	55.0267	7.9317	107	9942	FA	HH,VV			57
			4	13	14 11 35	55.0117	7.9450	14 18 53	55.0783	7.9967	409	9955	FA	HH,VV			58
			4	17	14 19 51	55.0650	7.9550	14 34 26	55.1917	8.0433	383	9947	FA	HH,VV			59
	24	9/17/75	2	10	14 00 30	55.0317	7.9905	14 11 58	54.7650	7.4567	502	10127	FA	HH,VV		M318	60
			2	11	14 14 19	54.8367	7.5600	14 20 08	55.0417	8.0350	276	10079	FA	HH,VV			61
			4	1	14 27 32	54.8733	7.7867	14 37 26	54.9417	7.9567	589	10028	FA	HH,VV			62
335	3	1/16/76	2	3	16 20 15	36.8586	-72.4433	16 23 02	36.7639	72.3406	162	10054	FA	HH,VV		M335	1
			2	33	16 23 13	36.7600	-72.3333	16 33 35	36.3983	71.9867	955	10062	FA,SS	HH,VV,VH			2
			4	1	16 36 47	36.3167	-71.9467	16 39 42	36.3483	71.9167	216	10011	FA	HH,VV			3
			4	2	16 40 00	36.3550	-71.8977	16 42 46	36.3733	71.8633	213	10033	FA	HH,VV			4
			4	3	16 42 53	36.3721	-71.8550	16 50 00	36.3883	71.8283	494	10010	FA	HH,VV			5
			4	6	16 50 07	36.3950	-71.8217	16 58 10	36.4317	71.7683	503	10016	FA	HH,VV			6
			4	9	16 58 29	36.4400	-71.7483	17 02 50	36.4217	71.7267	238	9984	FA	HH,VV			7
			4	10	17 02 58	36.4250	-71.7317	17 03 15	36.4350	71.7350	18	10032	FA	HH,VV			8

See footnotes on page 58.

TABLE I.- Continued

Mission	Flight	Date	Line	Run	At line start			At line stop			Number of samples	Average altitude, ft	Mode (a)	Pol (b)	Data quality (c)	Archive tape	
					Time, H M S	N.lat., deg	E.long., deg	Time, H M S	N.lat., deg	E.long., deg						Number	File
335	4A	1/22/76	4	1	16 51 08	38.7483	-73.9617	16 53 03	38.7533	73.9050	145	10090	FA	HH,VV		M335	9
			4	2	16 53 10	38.7483	-73.9083	16 56 29	38.7500	73.9050	251	9987	FA	HH,VV			10
			4	3	16 56 49	38.7633	-73.8950	17 00 16	38.7533	73.8100	264	10010	FA	HH,VV			11
			4	5	17 00 36	38.7400	-73.8033	17 05 58	38.7210	73.7367	395	10018	FA	HH,VV			12
			4	7	17 06 19	38.7167	-73.7500	17 09 44	38.7317	73.7117	271	9991	FA	HH,VV			13
			4	8	17 10 04	38.7383	-73.6917	17 11 21	38.7017	73.6700	108	9970	FA	HH,VV			14
			2	3	17 15 52	38.7600	-73.8300	17 31 50	38.9117	74.4533	864	10029	FA	HH,VV,VH			15
			4	9	17 36 11	38.8783	-74.2601	17 40 58	38.8677	74.2017	321	10007	FA	HH,VV			16
			4	11	17 41 17	38.8600	-74.1833	17 51 05	38.8383	74.0667	665	9980	FA	HH,VV			17
			4	15	17 51 25	38.8250	-74.0500	17 53 09	38.8283	74.0539	135	10016	FA	HH,VV			18
			4	16	17 53 37	38.8267	-74.0233	17 55 09	38.8050	74.0333	100	10100	FA	HH,VV			19
			4	19	17 55 35	38.8200	-74.0200	17 56 06	38.8210	73.9867	26	10033	FA	HH,VV			20
			3	1	17 58 12	38.8400	-73.8767	18 08 00	39.2067	73.5217	504	9982	FA	HH,VV			21
			3	11	18 08 11	39.2133	-73.5133	18 11 14	39.3267	73.4017	163	9922	FA	HH,VV			22
			4	17	18 13 28	39.3217	-73.3532	18 17 36	39.3250	73.2400	233	10020	FA	HH,VV			23
			4	18	18 17 42	39.3200	-73.2383	18 26 35	39.2933	73.1333	498	10046	FA	HH,VV			24
			4	22	18 27 58	39.3200	-73.1550	18 39 12	39.2617	72.9517	654	9997	FA	HH,VV			25
	4B	1/22/76	4	1	19 41 23	38.1267	-71.3567	19 50 54	38.1483	71.1633	605	10057	FA	HH,VV		M335	26
			4	5	19 51 12	38.1367	-71.1683	19 54 41	38.1483	71.1583	268	10021	FA	HH,VV			27
			4	6	19 54 59	38.1600	-71.1517	19 56 35	38.1367	71.1050	135	10076	FA	HH,VV			28
			4	7	19 56 54	38.1367	-71.1167	19 58 28	38.1683	71.0683	132	10113	FA	HH,VV			29
			4	8	19 58 52	38.1517	-71.0600	20 00 22	38.1717	71.0797	126	10014	FA	HH,VV			30
			4	9	20 00 43	38.1800	-71.0583	20 03 46	38.1750	71.0067	240	10043	FA	HH,VV			31
			4	10	20 04 47	38.1483	-71.0183	20 08 22	38.1850	70.9900	256	10012	FA	HH,VV			32
			4	11	20 08 53	38.1850	-70.9567	20 10 24	38.1700	70.9800	117	9948	FA	HH,VV			33
			4	12	20 11 02	38.1933	-70.9563	20 12 22	38.1550	70.9283	103	10045	FA	HH,VV			34
			4	13	20 12 42	38.1517	-70.9400	20 17 26	38.1567	70.8783	312	10031	FA	HH,VV			35
			4	14	20 17 31	38.1567	-70.8783	20 20 33	38.1400	70.8733	213	9942	FA	HH,VV			36
			4	16	20 20 52	38.1483	-70.8833	20 24 25	38.1633	70.8283	239	10061	FA	HH,VV			37
			4	17	20 24 57	38.1483	-70.7983	20 45 40	38.1033	70.5267	1140	10025	FA	HH,VV,HV			38
			3	1	20 48 04	38.0056	-70.5233	20 53 34	37.7700	70.5300	316	10099	FA	HH,VV,HV			39
			3	11	20 53 39	37.7683	-70.5267	20 56 16	37.6567	70.5333	149	10145	FA	HH,VV			40
			3	111	20 56 22	37.6517	-70.5317	20 59 01	37.5367	70.5367	155	10165	FA	HH,VV			41
			3	1111	20 59 47	37.5033	-70.5383	21 04 55	37.2917	70.5683	272	10626	FA	HH,VV			42
			2	3	21 07 14	37.2683	-70.6267	21 13 38	37.3783	70.8417	355	11106	FA	HH,VV			43
			2	33	21 13 57	37.3867	-70.8533	21 23 21	37.5333	71.1750	538	11111	FA	HH,VV			44
			3	2	21 24 50	37.5683	-71.2033	21 34 10	37.9583	70.8650	544	11074	FA	HH,VV,HV			45

See footnotes on page 58.

TABLE I.- Continued

Mission	Flight	Date	Line	Run	At line start			At line stop			Number of samples	Average altitude, ft	Mode (a)	Pol (b)	Data quality (c)	Archive tape	
					Time, H M S	N.lat., deg	E.long., deg	Time, H M S	N.lat., deg	E.long., deg						Number	File
335	5	1/23/76	4	1	18 48 50	38.1367	-71.1700	18 53 17	38.1517	71.1150	325	10021	FA	HH,VV		M335	46
			4	3	18 53 42	38.1567	-71.0833	19 11 15	38.1017	70.7950	1258	10062	FA	HH,VV			47
			4	9	19 11 33	38.1033	-70.8050	19 13 22	38.1150	70.7367	141	10167	FA	HH,VV			48
			4	10	19 13 48	38.0983	-70.7383	19 33 03	38.0200	70.3317	1297	9976	FA	HH,VV			49
			4	17	19 33 10	38.0183	-70.3367	19 33 54	38.0417	70.3383	47	10020	FA	HH,VV			50
			4	18	19 34 22	38.0550	-70.3067	19 38 07	38.0067	70.2033	226	9954	FA	HH,VV			51
			4	19	19 38 11	38.0033	-70.2033	19 47 17	37.9733	70.0567	500	10028	FA	HH,VV			52
			4	22	19 47 38	37.9883	-70.0467	19 54 35	37.9433	69.8683	404	10011	FA	HH,VV			53
			2	5	19 59 35	37.9733	-69.8767	20 05 30	38.0717	70.0600	345	10027	FA	HH,VV			54
			2	55	20 06 49	38.0950	-70.1017	20 16 27	38.2500	70.3990	551	9995	FA	HH,VV,VH			55
			3	1	20 19 04	38.1967	-70.4500	20 35 24	37.4217	70.5233	923	10052	FA	HH,VV,HV			56
			3	2	20 38 44	37.4683	-70.5333	20 55 25	38.0817	69.7483	937	9998	FA	HH,VV			57
			4	25	21 21 47	37.8650	-70.7833	21 35 10	37.8033	70.4933	833	9992	FA	HH,VV			58
	6	1/28/76	4	1	20 49 31	38.2567	-71.3600	20 56 24	38.3353	71.2300	479	9945	FA	HH,VV		M335	59
			4	4	20 56 36	38.3283	-71.2233	21 11 33	38.4350	71.1050	1045	9932	FA	HH,VV			60
			4	9	21 11 54	38.4533	-71.0912	21 15 03	38.4700	71.0383	212	9958	FA	HH,VV			61
			4	11	21 15 24	38.4617	-71.0233	21 22 17	38.4890	71.0100	464	9908	FA	HH,VV			62
			4	13	21 22 17	38.4890	-71.0100	21 33 05	38.5349	70.9047	625	9882	FA	HH,VV			63
			4	17	21 33 33	38.5550	-70.8834	21 43 57	38.5933	70.7600	689	9899	FA	HH,VV			64
			4	21	21 44 06	38.6017	-70.7533	21 55 03	38.6567	70.5800	624	9900	FA	HH,VV			65
			3	1	22 00 22	38.5817	-70.6833	22 06 10	38.3667	70.7183	331	9944	FA	HH,VV			66
			3	11	22 06 35	38.3517	-70.7233	22 13 11	38.1100	70.7567	382	9912	FA	HH,VV			67
			2	3	22 15 26	38.1500	-70.8183	22 30 28	38.6933	71.1600	713	9917	FA	HH,VV			68
			3	2	22 33 02	38.6000	-71.1617	22 46 59	38.2067	71.5317	730	9888	FA	HH,VV			69
			4	25	22 49 07	38.2200	-71.4667	23 00 26	38.2400	71.2983	704	9856	FA	HH,VV			70
353	9	3/2/77	4	1	20 10 00	32.7617	-117.5083	20 23 53	32.6633	-117.4218	1348	9684	SS	HH,VV		M3531	1
			4	6	20 38 02	32.9767	-117.6100	20 50 09	32.9000	-117.5433	473	9757	SS	HH,VV			2
			4	11	20 51 00	32.8683	-117.5150	21 03 46	32.7800	-117.4283	1222	9748	SS	HH,VV			3
			4	16	21 03 53	32.7733	-117.4300	21 16 34	32.6933	-117.3633	1245	9728	SS	HH,VV			4
			3	3	22 14 22	32.0133	-117.7983	22 24 19	32.2483	-117.3383	818	9742	SS	HH,VV			5
			3	33	22 26 13	32.2517	-117.3698	22 28 33	32.1617	-117.4517	204	9732	SS	HH,VV			6
	10	3/3/77	4	1	20 25 42	32.7583	-117.4983	20 38 37	32.7083	-117.3833	1272	9528	SS	HH,VV		M3531	7
			4	6	20 42 49	32.8217	-117.4633	20 54 44	32.7600	-117.3683	1168	9513	SS	HH,VV			8
			4	11	21 02 22	32.9100	-117.5633	21 16 16	32.8283	-117.4583	1373	9519	SS	HH,VV			9

See footnotes on page 58.

TABLE I.- Concluded

Mission	Flight	Date	Line	Run	At line start			At line stop			Number of samples	Average altitude, ft	Mode (a)	Pol (b)	Data quality (c)	Archive tape	
					Time, H M S	N.lat., deg	E.long., deg	Time, H M S	N.lat., deg	E.long., deg						Number	File
353	11	3/8/77	2	5	21 45 03	43.4167	-129.8200	21 50 56	43.3200	-129.9917	503	9352	SS	HH,VV		M3531	10
			3	2	22 10 17	42.8517	-129.9083	22 19 45	42.5183	-129.4417	802	9514	SS	HH,VV			11
			2	6	22 27 28	42.5005	-129.6400	22 37 34	42.4050	-129.9800	840	9513	SS	HH,VV			12
			4	1	22 40 44	42.3783	-130.0917	22 53 29	42.5000	-129.8283	1126	9537	SS	HH,VV			13
			4	6	22 53 41	42.5017	-129.8367	23 06 39	42.5983	-129.5900	1251	9539	SS	HH,VV			14
			4	11	23 06 46	42.5983	-129.5950	23 19 22	42.6683	-129.3167	1238	9335	SS	HH,VV			15
	13	3/10/77	4	1	00 04 27	32.8775	-117.7500	00 17 40	32.7183	-117.7117	1302	9583	SS	HH,VV		M3531	16
			4	6	00 27 13	32.9317	-117.5550	00 41 06	32.8283	-117.5300	1374	9535	SS	HH,VV			17
			4	11	00 42 37	32.7750	-117.4933	00 56 10	32.6833	-117.4983	1335	9595	SS	HH,VV			18
			4	16	00 59 42	32.8067	-117.4983	01 09 49	32.7350	-117.4867	560	9645	SS	HH,VV			19
			4	20	01 09 58	32.7400	-117.4867	01 19 58	32.6800	-117.4700	967	9650	SS	HH,VV			20
			2	6	01 21 54	32.7367	-117.5217	01 30 40	32.8967	-117.9283	733	9635	SS	HH,VV			21
	14	3/11/77	2	5	22 57 36	42.5183	-129.9217	23 03 22	42.5780	-130.2167	500	9486	SS	HH,VV		M3532	1
			3	2	23 09 24	42.3733	-130.2467	23 24 00	41.7647	-130.2200	1243	9514	SS	HH,VV			2
			4	1	23 56 38	42.3567	-130.2617	00 09 42	42.4050	-130.1367	1046	9481	SS	HH,VV			3
			4	6	00 09 54	42.4017	-130.1233	00 23 21	42.4533	-129.9883	1304	9473	SS	HH,VV			4
			4	11	00 23 29	42.4533	-129.9783	00 28 42	42.4667	-129.9333	505	9485	SS	HH,VV			5
	15	3/14/77	4	1	20 12 58	32.8650	-117.5450	20 25 45	32.8500	-117.4883	1253	9492	SS	HH,VV		M3532	6
			4	6	20 31 02	32.8333	-117.4517	20 36 29	32.8317	-117.4317	13	9586	SS	VV			7
			4	11	20 48 17	32.9217	-117.5583	20 56 27	32.9283	-117.5150	782	9498	SS	HH,VV			8
			4	16	20 56 35	32.9260	-117.5083	21 09 09	32.9233	-117.4650	1135	9503	SS	HH,VV			9
	20	3/22/77	4	1	19 45 03	32.7500	-117.5583	19 58 43	32.7699	-117.5800	1348	9756	SS	HH,VV	5	M3532	10
			4	6	20 04 13	32.8133	-117.2767	20 18 28	32.8550	-117.3217	1385	9663	SS	HH,VV			11
			4	11	20 22 14	32.8500	-117.5067	20 36 00	32.8683	-117.5450	1335	9687	SS	HH,VV			12
			4	16	21 09 56	32.8983	-117.3317	21 18 07	32.9233	-117.3450	139	9697	SS	HH,VV			13
			4	21	21 21 47	32.9067	-117.3883	21 35 14	32.9300	-117.4317	1305	9729	SS	HH,VV			14
			4	26	21 35 21	32.9300	-117.4383	21 48 41	32.9400	-117.5150	995	9765	SS	HH,VV			15
	21	3/24/77	4	1	20 07 17	32.7617	-117.5867	20 19 46	32.7800	-117.5083	1228	9416	SS	HH,VV,HV		M3532	16
			4	7	20 24 32	32.8333	-117.5533	20 37 11	32.8417	-117.4650	1243	9459	SS	HH,VV			17
			4	12	20 37 20	32.8483	-117.4617	20 49 58	32.8733	-117.3567	1007	9500	SS	HH,VV			18
			3	3	21 57 27	33.0950	-117.4433	22 09 12	32.6150	-117.4333	919	9519	SS	HH,VV,HV			19

See footnotes on page 58.

TABLE II.- SURFACE TRUTH FOR RADSCAT MISSIONS

Mission	Flight	Date	Data source	Location, deg		Time		Neutral stability 19.5-m winds		Temp., °C		Anemometer		Wave height, m	Swell		Data quality (a)
				N.Lat.	E.Long.	H	M	Speed, m/s	Direction, deg	Air	Sea	Height, m	Average time, min		Height, m	Direction, deg	
306	FCF	4/4/75	NASA 929	37.391	-72.730	19	48	21.5	300			135	23				Average
			S.S. Wilmington Geddy	37.6	-73.7	18	00	[b]28.3	290	4.5	13.9			[c]3.0			
				38.1	-74.1	24	00	[b]15.4	330	9.0	12.2			[c]4.5			
306	3	4/17/75	Ambrose Tower	40.444	-73.846	14	00	4.3	315								Good
						17	00	1.7	270								
318	13	8/29/75	Land Station	54.926	8.305	8	45	[b]2.8	124			>20		Smooth			Fair
						9	45	[b]3.0	146								
						10	45	[b]3.8	146								
						11	45	[b]3.8	146								
			List	55.021	8.425	9	45	[b]4.9	149			>20					
						10	45	[b]4.9	149								
						11	45	[b]5.1	149								
318	14	9/2/75	Land Station	54.926	8.305	8	15	[b]4.7	34					1.1			Good
						9	15	[b]5.1	34								
						10	15	[b]5.1	34								
						11	15	[b]4.2	34								
			List	55.021	8.425	8	15	[b]5.4	50								
						9	15	[b]5.6	50								
						10	15	[b]4.7	70								
						11	15	[b]4.1	70								
			Pisa	54.995	7.906	8	15	4.4	45			17	10				
						9	15	5.0	47								
						10	15	5.7	46								
						11	15	5.3	60								
318	16	9/8/75	Land Station	54.926	8.305	14	45	[b]4.9	214					1.1			Good
						15	45	[b]4.5	214								
						16	45	[b]4.5	191								
						17	45	[b]4.2	191								
			List	55.021	8.425	14	45	[b]6.1	240	15.6	17.9						
						15	45	[b]5.5	230								
						16	45	[b]5.6	220								
						17	45	[b]5.7	220								
			Pisa	54.995	7.906	14	45	7.9	198								
						15	45	8.0	198								
						16	45	7.8	188								
						17	45	8.3	184								
			Hornum Pile	54.958	8.210	14	45	5.7	238								
						15	45	5.6	236								
						16	45	5.9	232								
						17	45	6.5	230								
			NASA 929	54.986	7.913	14	45	7.3	212			225.5	258				

[a]Data quality is defined in terms of the standard deviation of wind speed and wind direction, respectively, as follows: Good - 1.0 m/s, 10°; Fair - 1.5 m/s, 15°; Average - 2.0 m/s, 20°.

[b]Measurements uncorrected for height and stability.

[c]Measurements were in World Meteorological Organization units of half-meters, and hence were divided by 2 before entry into this table.

TABLE II.- Continued

Mission	Flight	Date	Data source	Location, deg		Time	Neutral stability 19.5-m winds		Temp., °C		Anemometer		Wave height, m	Swell		Data quality (a)
				N.Lat.	E.Long.	H M	Speed, m/s	Direction, deg	Air	Sea	Height, m	Average time, min		Height, m	Direction, deg	
318	17	9/9/75	Land Station	54.926	8.305	7 45	[b]9.4	214					1.5		240	Good
						8 45	[b]8.8	214								
						9 45	[b]9.4	214								
			List	55.021	8.425	7 45	[b]9.8	230	17.9	17.7						
						8 45	[b]10.9	230								
						9 45	[b]12.1	230								
			Pisa	54.995	7.906	7 45	12.2	209								
						8 45	12.3	205								
						9 45	12.1	206								
			Hornum Pile	54.958	8.210	7 45	11.5	237								
						8 45	11.1	239								
						9 45	11.6	239								
			NASA 929	54.982	7.798	7 45	13.0	233			161.5	52				
318	18	9/9/75	Land Station	54.926	8.305	14 15	[b]7.6	191					1.8		240	Fair
						15 15	[b]7.9	191								
			List	55.021	8.425	14 15	[b]10.6	220	18.7	17.7						
						15 15	[b]10.1	220								
			Pisa	54.995	7.906	14 15	11.3	187								
						15 15	10.9	188								
			Hornum Pile	54.958	8.210	14 15	10.5	237								
						15 15	9.7	236								
			NASA 929	55.029	7.811	14 15	12.5	202			228.6	174				
318	19	9/10/75	Land Station	54.926	8.305	11 15	[b]9.5	214					2.4		240	Good
						13 15	[b]8.5	214								
						14 15	[b]8.6	214								
						15 15	[b]7.8	214								
			List	55.021	8.425	11 15	[b]8.8	270	16.9	17.4						
						13 15	[b]8.2	270								
						14 15	[b]8.0	270								
						15 15	[b]7.6	270								
			Pisa	54.995	7.906	11 15	9.2	248								
						13 15	7.8	245								
						14 15	8.0	245								
						15 15	7.5	244								
			Hornum Pile	54.958	8.210	11 25	7.9	260								
318	24	9/17/75	Land Station	54.926	8.305	13 15	[b]10.4	214								Good
						14 15	[b]10.4	214					2.7		226	
						15 15	[b]8.9	214								
			List	55.021	8.425	13 15	[b]11.8	240	17.0	16 ± 1.0						
						14 15	[b]10.9	240								
						15 15	[b]8.2	250								
			Pisa	54.995	7.906	13 15	13.0	222								
						14 15	12.5	216								
						15 15	9.5	233								

[a]Data quality is defined in terms of the standard deviation of wind speed and wind direction, respectively, as follows: Good - 1.0 m/s, 10°; Fair - 1.5 m/s, 15°; Average - 2.0 m/s, 20°.

[b]Measurements uncorrected for height and stability.

TABLE II.- Continued

Mission	Flight	Date	Data source	Location, deg		Time	Neutral stability 19.5-m winds		Temp., °C		Anemometer		Wave height, m	Swell		Data quality (a)
				N.Lat.	E.Long.	H M	Speed, m/s	Direction, deg	Air	Sea	Height, m	Average time, min		Height, m	Direction, deg	
335	3	1/16/76	NASA 929	36.7	-72.7	16 00	14.6	159	18.0	19.0	137	30	2.0			Fair
335	4A	1/22/76	NOAA buoy EB-41	38.7	-73.6	15 00	17.0	280	-.6	7.9	5	10	3.0			Good
						16 00	26.7	275	-.6	7.9	5	10	3.0			
			NASA 929	38.82	-73.61	16 10	17.5	289	.0	8.5	98	22				
			NOAA buoy EB-41			17 00	16.9	291	-.6	8.0	5	10	3.0			
						18 00	17.0	287	-.5	7.9	5	10	2.6			
335	4B	1/22/76	Weather ship Hotel	38.0	-71.0	15 00	21.6	290	3.7	12.8	21	1	5.5			Good
						18 00	20.2	300	3.4	13.4	21	1	5.5			
			NASA 929	38.06	-71.15	19 15	21.1	290	2.9	13.3	162	18	5.0			
			Weather ship Hotel			21 00	25.2	290	2.1	12.8	21	1	5.5			
						23 00	25.6	30[illegible]			21	1				
						24 00	22.7	290	2.7	12.8	21	1	6.0			
335	5	1/23/76	Weather ship Hotel	38.0	-71.0	15 00	19.5	310	-3.0	11.9	21	1	4.5	5.5	340	Good
			NASA 929	38.07	-71.06	17 45	17.0	295	-.3	11.4	101	24				
				38.07	-71.07	18 10	15.4	293	-.3	12.0	158	30				
			Weather ship Hotel			18 00	18.8	300	-.2	11.5	21	1	4.0	5.0	330	
						19 00	15.2	300	-.3	11.5	21	10	3.0	3.4	285	
						20 00	12.1	294	-.3	11.5	21	10	3.8	1.8	281	
						21 00	13.8	291	-.3	11.5	21	10	3.4	2.3	280	
						21 00	16.8	300	.4	11.5	21	1	3.5	2.7	330	
						22 00	12.1	294			21	10	2.8	2.1	288	
			NASA 929	38.20	-71.29	22 00	12.9	286	1.3	13.2	146	44				
				38.00	-70.70	22 15	13.4	288	1.3	13.2	98	44				
			Weather ship Hotel			24 00	12.1	270	2.0	13.3	21	1	2.5	4.0	300	
335	6	1/28/76	Weather ship Hotel	38.0	-71.0	18 00	17.7	300	9.2	15.0	21	1	2.5	4.0	300	Good
						20 00	16.0	292	9.2	15.0	21	10	1.8	4.6	185	
			NASA 929	38.25	-71.26	20 25	15.0	294	7.9	13.7	101	44				
			Weather ship Hotel			21 00	12.1	250	7.9	13.7	21	10	3.8	3.7	189	
						21 00	16.8	300	7.7	13.4	21	1	2.5	4.0	240	[d]Snow
						22 00	11.3	316	7.7	13.4	21	10	2.4	3.7	180	
						23 00	11.0	315	7.7	13.4	21	10	2.7	2.7	180	
353	9	3/2/77	NASA 929	32.75	-118.57	19 34	13.6	318	10.4	14.3	190.5	20				Good
			Sonic anemometer	32.78	-117.29	21 00	5.4	320	12.5	14.2	8.0					
			NASA 929	32.82	-117.45	22 47	[e]7.1 (6.9)	294	10.5	14.4	175.3	8				
			Sonic anemometer	32.78	-117.29	24 01	6.1		13.6	14.1	8.0					
353	10	3/3/77	Sonic anemometer	32.78	-117.29	20 05	5.2	180	12.8	13.7	8.0					Fair
			NASA 929	32.75	-117.38	21 37	[e]5.6 (5.4)	234	12.4	14.4	100.6	6				
353	11	3/8/77	NASA 929	42.45	-130.08	20 38	17.7	246	10.0	11.0	211.8	11	5.5			Good
			NOAA buoy EB-16	42.50	-130.00	21 00	15.1	250			10.0	8				
			NASA 929	42.67	-130.00	23 38	15.5	277	8.6	10.6	103.6	10				
			NOAA buoy EB-16	42.50	-130.00	24 00	15.6	270			10.0	8	6.0			

[a]Data quality is defined in terms of the standard deviation of wind speed and wind direction, respectively, as follows: Good - 1.0 m/s, 10°; Fair - 1.5 m/s, 15°; Average - 2.0 m/s, 20°.

[d]Snow could affect the quality of RADSCAT data.

[e]Wind speeds in parentheses are from reference 9.

TABLE II.- Concluded

Mission	Flight	Date	Data source	Location, deg		Time	Neutral stability 19.5-m winds		Temp., °C		Anemometer		Wave height, m	Swell		Data quality (a)
				N.Lat.	E.Long.	H M	Speed, m/s	Direction, deg	Air	Sea	Height, m	Average time, min		Height, m	Direction, deg	
353	13	3/10/77	Sonic anemometer	32.78	-117.29	21 25	4.4	315	14.0	14.3	8.0					Good
			NASA 929	32.92	-117.86	22 57	7.9	295	13.0	15.2	85.3	10				
			Sonic anemometer	32.78	-117.29	23 35	5.7	315	14.2	14.5	8.0					
			NASA 929	32.88	-117.53	01 46	13.1	306	11.0	14.4	100.6	11				
353	14	3/11/77	NOAA buoy EB-16	42.50	-130.00	21 00	13.2	290			10.0	8	3.5			Fair
			NASA 929	42.43	-130.25	21 37	10.5	276	5.6	10.2	207.3	18				
			NASA 929	42.75	-130.00	23 45	13.7	252	4.9	10.7	96.0	11				
			NOAA buoy EB-16	42.50	-130.00	24 00	18.9	280			10.0	8	3.0			
353	15	3/12/77	Sonic anemometer	32.78	-117.29	20 10	4.2	270			8.0					Good
353	20	3/22/77	Sonic anemometer	32.78	-117.29	20 05	2.4	245	13.3	15.1	8.0					Variable
						21 00	1.3	245	13.6	15.1						
						21 40	2.5	245								
			NASA 929	32.67	-117.51	22 13	2.8 to 8.3	265	10.2	14.7	86.9	19				
353	21	3/24/77	Sonic anemometer	32.78	-117.29	18 20	5.9	300			8.0					Fair
						19 30	5.5	300								
			NASA 929	32.79	-117.67	21 10	[e]5.4 (4.7)	284	10.1	15.5	71.6	5				
				32.76	-118.11	22 43			10.8	14.2	91.4	30				
				32.78	-118.02	23 00	6.0	282	10.6	14.2	84.4	30				

[a]Data quality is defined in terms of the standard deviation of wind speed and wind direction, respectively, as follows: Good - 1.0 m/s, 10°; Fair - 1.5 m/s, 15°; Average - 2.0 m/s, 20°.

[e]Wind speeds in parentheses are from reference 9.

TABLE III.- NEUTRAL STABILITY WIND VECTOR FOR EACH RADSCAT FLIGHT LINE

Mission	Flight	Line	Run	Date	Start time, GMT			θ, deg	Wind speed at 19.5 m, m/s	Wind direction, deg	Direction relative to wind	Data source	Quality (a)
					H	M	S						
306	FCF	4	1 to 3	4/4/75	20	01	31	52	21.5	300.3	Circle	Inertial navigator with temp from ships	Fair
		4	4 to 6		20	09	53	62					
		4	7 to 10		20	17	19	32					
		4	11 to 13		20	30	56	14					
		4	14 to 17		20	39	07	28					
306	3	1	1	4/17/75	14	07	50	29.0	4.1	315	Circle	Ambrose Tower	Good
		1	5		17	05	39	28.4	1.7	270			
318	13	6	1	8/29/75	09	15	27	0 to 48	4.5	149	Upwind	JONSWAP analysis	Fair
		4	1 to 3		10	12	05	20.3	4.6		Circle		
		4	4 to 9		10	33	37	40.6	4.6		Circle		
		4	11		10	39	04	50.3	4.6		Circle		
318	14	2	3	9/2/75	08	26	16	0 to 48	5.5	50	Crosswind	JONSWAP analysis	Good
		3	1, 11		08	51	42	0 to 48			Upwind		
		3	2, 22		09	13	29	0 to 48			Downwind		
		4	1		09	44	35	18.9			Circle		
		4	6, 7		09	58	41	39.9			Circle		
		4	11, 12		10	12	27	67.2			Circle		
318	16	2	5	9/8/75	14	52	58	0 to 48	7.7	200	Crosswind	JONSWAP analysis	Good
		4	4		15	30	35	18.5	8.6	193	Circle		
		4	9		15	45	02	39.4	8.75	198	Circle		
		4	14		15	59	02	66.2	8.9	205	Circle		
		3	2, 22		16	21	24	0 to 48	8.9	200	Circle		
		3	3		16	35	54	0 to 48	9.1	200	Circle		
318	17	2	2	9/9/75	07	50	16	0 to 48	12.0	190	Crosswind	JONSWAP analysis	Good
		3	3		08	08	35	0 to 48	12.1	190	Downwind		
		3	3		08	17	54	0 to 48	12.0	190	Upwind		
		4	1		08	33	53	19.3	13.5	188	Circle		
		4	6, 8		08	46	54	40.8	12.75	190	Circle		
		4	11, 12		08	59	42	68.1	12.25	193	Circle		
318	18	4	1, 2	9/9/75	13	58	01	19.6	12.0	175	Circle	JONSWAP analysis	Fair
		4	6		14	10	43	40.4	11.3	175	Circle		
		4	11		14	23	21	65.5	10.5	175	Circle		
318	19	2	6	9/10/75	13	14	57	0 to 48	8.0	230	Crosswind	JONSWAP analysis	Good
		3	3		13	27	36	0 to 48	7.7		Downwind		
		4	5 to 8, 10		13	50	46	19.7	7.5		Circle		
		4	12, 13		14	09	26	40.9	7.5		Circle		
		4	17		14	19	51	67.1	7.5		Circle		

[a]Data quality is defined in terms of the standard deviation of wind speed and wind direction as follows: Good - 1.0 m/s, 10°; fair - 1.5 m/s, 15°.

TABLE III.- Continued

Mission	Flight	Line	Run	Date	Start time, GMT			θ, deg	Wind speed at 19.5 m, m/s	Wind direction, deg	Direction relative to wind	Data source	Quality (a)
					H	M	S						
318	24	2	10	9/17/75	14	00	30	0 to 48	9.5	230	Downwind	JONSWAP analysis	Good
		2	11		14	14	19	0 to 47			Upwind		
		4	1		14	27	32	30.3			Circle		
335	3	2	3, 33	1/16/76	16	20	15	0 to 45	14.2	159	Crosswind	CUNY analysis	Fair
		4	3		16	36	47	29.4			Circle		
		4	10		16	50	07	48.3			Circle		
335	4A	4	1 to 8	1/22/76	16	51	07	18.9	19.1	289	Circle	CUNY analysis	Good
		2	3		17	15	51	0 to 44	19.4		Crosswind		
		4	9, 11, 16, 19		17	36	10	39.1	20.0		Circle		
		3	1, 11		17	58	12	0 to 45	19.9		Upwind		
		4	17, 18		18	13	28	58.2	19.8		Circle		
		4	22		18	28	03	9.7	19.7		Circle		
335	4B	4	1, 5 to 9	1/22/76	19	41	23	19.0	19.1	290	Circle	CUNY analysis	Good
		4	10 to 14, 16		20	04	47	38.7	19.4		Circle		
		4	17		20	24	56	58.0	19.6		Circle		
		3	1 to 111		20	48	04	0 to 44	19.8		Downwind		
		2	3, 33		21	07	13	0 to 44	20.0		Crosswind		
		3	2		21	24	50	0 to 44	20.1		Upwind		
335	5	4	1, 3	1/23/76	18	48	50	19.9	15.5	297	Circle	CUNY analysis	Good
		4	9, 10		19	11	33	39.4	15.2		Circle		
		4	17, 18, 19, 22		19	33	10	58.5	15.1		Circle		
		2	5, 55		19	59	35	0 to 44	14.8		Crosswind		
		3	1		20	49	30	0 to 44	14.6		Downwind		
		3	2		20	38	44	0 to 44	14.4		Upwind		
		4	25		21	21	46	9.2	13.9		Circle		
335	6	4	1, 4	1/28/76	20	49	30	19.2	15.0	310	Circle	CUNY analysis	Good
		4	9, 11		21	11	58	39.1			Circle		
			17		21	33	33	39.1			Circle		
		4	13		21	22	23	57.8			Circle		
		4	21		21	44	05	57.8			Circle		
		3	1, 11		22	00	21	0 to 45			Downwind		
		2	3		22	15	25	0 to 44			Crosswind		
		3	21		22	36	45	0 to 45			Downwind		
		4	25		22	49	07	9.0			Circle		
353	9	4	1	3/2/77	20	10	00	11.4	12.19	305	Circle	[b]Inertial navigator	Good
		4	6		20	38	02	67.3	11.28		Circle		
		4	11		20	50	59	19.7	10.84		Circle		

[a]Data quality is defined in terms of the standard deviation of wind speed and wind direction as follows: Good - 1.0 m/s, 10°; fair - 1.5 m/s, 15°.

[b]Data from reference 9.

TABLE III.- Concluded

Mission	Flight	Line	Run	Date	Start time, GMT			θ, deg	Wind speed at 19.5 m, m/s	Wind direction, deg	Direction relative to wind	Data source	Quality (a)
					H	M	S						
353	9	4	16	3/2/77	21	03	53	39.7	10.3	305	Circle	[b]Inertial navigator	Good
		3	3		22	14	22	0 to 48	8.2		Upwind		
		3	33		22	26	13	0 to 48	8.2		Downwind		
353	10	4	1, 6	3/3/77	20	25	42	19.9	5.4	234	Circle	Inertial navigator	Fair
		4	11		21	02	23	10.3					
353	11	3	2	3/8/77	22	10	17	0 to 47	16.5	270	Downwind	Inertial navigator	Good
		2	6		22	27	28	0 to 47	16.3		Crosswind		
		4	1		22	40	44	67.3	16.0		Circle		
		4	6		22	53	41	19.3	15.9		Circle		
		4	11		23	06	46	39.7	15.7		Circle		
353	13	4	1, 6	3/10-11/77	00	04	27	20.3	10.4	305	Circle	Inertial navigator	Good
		4	11		00	42	50	10.0	11.2		Circle		
		4	16		00	59	41	67.7	11.7		Circle		
		4	20		01	09	58	40.5	12.0		Circle		
		2	6		01	21	54	0 to 48	11.7		Crosswind		
353	14	2	5	3/11-12/77	22	57	36	0 to 47	13.0	252	Crosswind	Inertial navigator	Fair
		3	2		23	09	24	0 to 48	13.6		Downwind		
		4	1		23	56	38	67.1	14.3		Circle		
		4	6		00	09	54	19.3	14.3		Circle		
		4	11		00	23	29	39.4	14.3		Circle		
353	15	4	1	3/14/77	20	12	58	10.4	4.2	270	Circle	Sonic anemometer	Good
		4	11		20	48	17	20.0					
		4	16		20	56	35	40.1					
353	20	4	1	3/22/77	19	45	03	20.0	2.5	245	Circle	Sonic anemometer	Variable
		4	6		20	04	13	20.9					
		4	11		20	22	14	11.0					
		4	16		21	09	56	67.8					
		4	21		21	21	47	20.0					
		4	26		21	35	21	38.9					
353	21	4	1	3/24/77	20	07	17	10.3	4.7	282	Circle	Inertial navigator	[c]Fair
		4	7		20	24	32	19.6	4.7		Circle		
		4	12		20	37	20	39.6	4.7		Circle		
		3	3		21	57	27	0 to 47	6.2		Downwind		

[a]Data quality is defined in terms of the standard deviation of wind speed and wind direction as follows: Good - 1.0 m/s, 10°; fair - 1.5 m/s, 15°.

[b]Data from reference 9.

[c]Winds may be high.

TABLE IV.- STATISTICS OF SCATTERING COEFFICIENT, σ°

Line	Run	Antenna position	Horizontal polarization						Vertical polarization						Wind speed, m/s
			θ_{mean}	$\theta_{std\ dev}$	σ°_{mean}, dB	$\frac{\Delta\sigma^\circ}{\sigma^\circ}$	σ°_{error}, ±dB	Sample time, s	θ_{mean}	$\theta_{std\ dev}$	σ°_{mean}, dB	$\frac{\Delta\sigma^\circ}{\sigma^\circ}$	σ°_{error}, ±dB	Sample time, s	
Mission 306, FCF; April 4, 1975															
Upwind															
4	1-3	4	53.24	0.35	-14.82	9.83	0.36	7.8	53.12	0.35	-10.66	9.56	0.59	9.2	21.5
4	4-6	5	62.18	.18	-17.09	17.96	.37	7.2	62.26	.37	-13.74	11.09	.38	8.8	↓
4	7-10	2	32.30	2.08	-4.89	44.06	.37	7.7	32.69	1.58	-4.45	23.80	.37	8.3	
4	11-13	4	13.09	.64	5.2	23.06	.38	7.8	13.06	1.47	5.99	40.14	.39	7.8	
4	14-17	6	28.13	.50	-2.72	31.11	.33	12.0	27.57	1.00	-1.20	36.44	.34	12.0	↓
Downwind															
3	2	1	-0.07	1.88	9.76	15.13	0.48	15.6	0.62	1.78	9.65	18.03	0.48	39.3	21.5
↓	↓	2	11.81	1.02	7.58	35.23	.43	24.3	11.93	.83	7.66	36.23	.47	22.5	↓
		3	22.72	1.02	1.52	57.35	.53	24.1	22.78	1.01	2.20	29.59	.54	24.1	
		4	33.79	.80	-4.37	46.15	.55	22.3	33.73	.62	-2.51	28.87	.55	26.8	
		5	42.76	.48	-8.35	28.78	.80	24.0	42.84	.73	-5.76	29.87	.78	27.2	
↓	↓	6	47.35	.29	-10.43	31.50	.83	30.4	47.36	.33	-7.35	23.31	.79	27.7	
4	1-3	4	53.19	.49	-13.63	26.55	.81	8.5	52.99	.51	-10.09	22.14	.97	9.2	
4	4-6	5	62.67	.26	-16.98	16.43	.85	10.4	62.76	.21	-12.74	45.63	.82	6.4	
4	7-10	2	29.69	1.43	-3.13	35.40	.56	12.5	29.34	1.66	-2.22	35.32	.56	10.1	
4	11-13	4	13.93	.95	6.98	20.54	.42	11.2	14.01	1.19	6.55	29.33	.42	9.2	
4	14-17	6	28.45	.49	-1.73	36.21	.50	12.0	28.60	.58	.00	33.19	.65	10.1	↓
Crosswind															
4	1-3	4	53.47	1.40	-17.64	24.38	0.54	19.7	53.84	1.28	-13.77	21.09	0.51	16.9	21.5
4	4-6	5	62.20	2.44	-20.96	88.48	.59	17.6	61.93	2.55	-16.27	23.59	.57	16.8	↓
4	7-10	2	31.63	2.39	-7.43	46.59	.60	16.6	32.05	2.46	-6.95	15.66	.56	18.4	
4	11-13	4	13.21	1.10	5.23	24.50	.50	16.9	13.18	1.04	5.36	21.09	.51	12.0	
4	14-17	6	27.68	1.67	-4.45	46.79	.50	21.2	27.33	2.30	-3.31	43.51	.51	22.1	↓
Mission 318, Flight 13; August 29, 1975															
Upwind															
6	1	1	0.45	0.23	12.28	5.47	0.40	9.9	0.49	0.07	10.89	5.52	0.28	8.7	4.5
↓	↓	2	10.79	.04	6.18	9.27	.21	6.5	10.81	.00	5.07	4.20	.27	4.2	↓
		3	20.88	.05	-6.58	10.66	.30	10.2	20.89	.07	-7.50	8.97	.34	8.3	
		4	30.85	.03	-18.85	8.31	.35	10.6	30.83	.17	-19.69	9.25	.36	10.6	
		5	40.98	.06	-27.21	17.10	.94	10.4	40.96	.07	-25.94	14.67	.63	10.4	
↓	↓	6	48.13	.07	-31.95	10.74	1.24	6.5	48.16	.06	-29.38	6.82	1.22	6.5	↓
4	1-3	1	19.50	.38	-6.44	29.20	.25	13.9	19.49	.33	-8.03	29.58	.26	12.1	4.6
4	4-9	3	39.30	.52	-24.21	16.33	.52	5.1	39.31	.66	-23.07	11.15	.46	7.0	↓
4	11	4	49.06	.35	-30.08	12.80	2.08	16.9	49.16	.32	-26.25	15.13	1.19	14.1	↓
Downwind															
4	1-3	1	21.12	0.46	-8.80	20.86	0.40	8.7	21.13	0.64	-10.52	30.84	0.45	8.1	4.6
4	4-9	3	43.21	.15	-29.95	7.75	1.10	1.9	43.05	.06	-25.19	8.51	.76	2.5	↓
4	11	4	52.37	.81	-38.05	43.47	2.06	9.2	52.5	.87	-29.04	14.62	1.06	12.0	↓
Crosswind.															
4	1-3	1	20.49	0.77	-10.02	38.28	0.38	20.8	20.39	0.81	-10.98	35.17	0.44	18.5	4.6
4	4-9	3	40.54	.39	-30.37	22.29	1.11	5.1	40.69	.39	-29.09	16.97	1.10	9.5	↓
4	11	4	50.15	.90	-38.87	30.38	2.08	18.3	50.14	.98	-33.79	18.95	1.19	28.2	↓
Mission 318, Flight 14; September 2, 1975															
Upwind															
3	1,11	1	-0.74	0.45	12.61	10.74	0.46	22.6	-0.55	0.65	12.42	11.24	0.40	25.5	5.5
↓	↓	2	10.83	.27	6.32	13.00	.23	19.0	10.87	.28	5.98	9.00	.24	19.6	↓
		3	20.91	.15	-7.62	14.45	.32	22.9	20.92	.16	-7.80	13.52	.32	24.2	
		4	30.69	.05	-18.41	29.16	.35	19.8	30.69	.05	-17.90	30.99	.35	23.3	
		5	40.90	.08	-27.65	43.26	.89	28.9	40.91	.07	-24.91	48.88	.49	29.7	
↓	↓	6	48.10	.05	-31.70	61.97	1.23	24.9	48.08	.05	-27.56	59.43	1.22	24.9	
4	1	1	20.15	.69	-5.87	18.06	.27	12.1	20.12	.63	-6.04	15.65	.26	11.0	
4	6,7	3	41.37	.43	-28.47	16.20	.51	15.2	41.48	.46	-22.37	15.24	.40	14.6	
4	11,12	6	67.02	1.00	-36.54	36.09	1.44	19.4	66.69	.81	-29.23	7.97	1.11	14.8	↓

TABLE IV.- Continued

Line	Run	Antenna position	Horizontal polarization						Vertical polarization						Wind speed, m/s
			θ_{mean}	$\theta_{std\ dev}$	σ^o_{mean}, dB	$\frac{\Delta\sigma^o}{\sigma^o}$	σ^o_{error}, ±dB	Sample time, s	θ_{mean}	$\theta_{std\ dev}$	σ^o_{mean}, dB	$\frac{\Delta\sigma^o}{\sigma^o}$	σ^o_{error}, ±dB	Sample time, s	
Mission 318, Flight 14; September 2, 1975															
Downwind															
3	2,22	1	-0.23	1.04	12.07	6.16	0.35	18.0	-0.56	1.22	11.89	6.88	0.34	20.3	5.5
↓	↓	2	10.75	.10	6.66	10.09	.23	19.0	10.76	.13	6.57	9.89	.23	19.0	↓
		3	20.83	.08	-5.42	11.83	.27	13.4	20.82	.08	-5.43	10.43	.27	14.6	
		4	30.56	.12	-18.66	28.22	.36	21.2	30.57	.08	-17.22	30.34	.36	19.8	
		5	40.79	.06	-26.41	41.98	.56	9.6	40.81	.08	-22.21	44.00	.40	8.8	
↓	↓	6	47.99	.06	-30.62	26.62	1.23	18.5	47.96	.09	-23.31	36.44	.44	21.2	
4	1	1	17.80	.42	-2.88	13.17	.26	19.5	17.90	.38	-3.23	13.77	.26	14.5	
4	6,7	3	38.39	.53	-26.80	21.55	.72	15.2	38.47	.51	-22.74	24.81	.41	14.6	
4	11,12	6	67.04	.79	-40.28	14.31	2.66	6.5	66.87	.78	-29.40	12.63	1.14	11.1	↓
Crosswind															
2	3	1	0.10	0.67	12.41	7.85	0.36	19.7	0.13	0.73	12.19	7.14	0.43	19.1	5.5
↓	↓	2	10.48	.17	6.24	11.17	.22	22.6	10.46	.16	6.02	11.11	.23	21.4	↓
		3	20.63	.13	-8.14	22.61	.38	28.0	20.66	.12	-8.30	21.08	.38	21.7	
		4	30.48	.20	-21.29	29.32	.39	24.0	30.53	.15	-21.08	24.64	.38	27.6	
		5	40.75	.09	-32.90	23.98	1.25	24.9	40.73	.10	-30.07	25.29	1.22	23.3	
↓	↓	6	47.98	.10	-36.86	36.96	1.50	29.6	47.97	.09	-31.95	27.45	1.24	34.2	
4	1	1	19.10	.34	-5.45	12.71	.26	26.6	19.10	.38	-5.77	13.91	.27	26.0	
4	6,7	3	39.81	1.08	-28.97	20.55	1.09	32.4	39.91	1.13	-26.70	20.04	.85	28.6	
4	11,12	6	67.37	1.00	-39.38	26.12	2.48	23.05	67.54	1.19	-34.40	18.13	1.22	25.0	↓
Mission 318, Flight 16; September 8, 1975															
Upwind															
3	2,22	1	-0.06	1.49	10.94	19.48	0.34	15.7	-0.19	1.53	10.72	8.05	0.34	18.6	8.9
↓	↓	2	10.64	.28	6.79	11.38	.21	24.4	10.63	.25	6.23	8.74	.20	24.4	↓
		3	21.01	.30	-3.33	10.50	.24	22.9	20.96	.29	-3.79	11.65	.24	22.3	
		4	30.68	.51	-11.08	16.53	.49	29.0	30.59	.49	-10.56	13.06	.44	25.5	
		5	41.03	.21	-17.39	17.60	.35	28.1	40.12	.22	-14.87	12.86	.36	24.9	
↓	↓	6	48.19	.28	-20.92	7.72	.36	15.7	48.15	.32	-16.51	13.43	.35	19.4	↓
4	4	1	18.33	.58	-2.81	30.13	.24	15.6	18.30	.60	-3.21	29.14	.24	15.0	8.6
4	9	3	37.29	.89	-19.16	23.44	.34	14.0	37.32	.82	-17.27	25.39	.34	15.2	8.2
4	14	6	63.87	1.03	-31.88	18.21	1.14	20.3	63.86	1.00	-22.24	14.88	.44	20.3	8.9
Downwind															
3	3	1	0.92	0.86	11.08	7.99	0.54	27.8	0.86	0.83	10.68	7.27	0.34	28.4	9.1
↓	↓	2	10.92	.29	6.78	10.56	.25	23.2	10.97	.41	6.12	11.80	.24	22.6	↓
		3	21.18	.37	-4.36	22.84	.26	21.7	21.05	.37	-4.55	29.82	.26	22.3	
		4	30.95	.17	-13.64	13.54	.37	21.9	30.94	.14	-12.80	7.88	.38	12.7	
		5	41.16	.16	-20.66	19.27	.38	30.5	41.18	.14	-16.21	15.98	.37	29.7	
↓	↓	6	48.11	.11	-24.66	19.01	.47	23.1	48.07	.13	-17.94	9.00	.37	24.9	↓
4	4	1	19.18	.35	-3.14	30.34	.26	6.4	19.14	.36	-3.48	27.41	.26	6.9	8.6
4	9	3	41.57	.77	-25.08	22.19	.46	12.1	41.34	.59	-20.15	21.78	.38	10.2	8.2
4	14	6	69.30	1.37	-36.90	21.99	1.47	8.3	69.41	.80	-25.05	22.97	.90	12.0	8.9
Crosswind															
2	5	1	-0.74	0.07	11.82	8.51	0.40	15.7	-0.75	0.09	11.35	6.35	0.35	12.8	7.7
↓	↓	2	10.33	.10	7.05	9.69	.21	18.4	10.34	.09	6.62	10.80	.21	19.0	↓
		3	20.56	.08	-6.34	8.83	.26	14.0	20.58	.03	-6.69	10.40	.26	17.2	
		4	30.28	.09	-17.73	13.78	.35	14.8	30.31	.09	-17.36	13.53	.35	11.3	
		5	40.46	.10	-27.76	23.87	.77	18.4	40.48	.10	-25.52	18.46	.54	17.6	
↓	↓	6	47.43	.06	-31.25	18.59	1.22	15.7	47.45	.06	-28.21	20.05	.83	17.6	↓
4	4	1	18.44	1.05	-3.22	56.10	.26	34.7	18.48	1.08	-3.91	60.00	.25	27.2	8.6
4	9	3	39.67	1.76	-24.64	34.17	.57	29.8	39.45	1.83	-22.12	32.64	.52	31.1	8.2
4	14	6	67.14	1.14	-31.26	39.22	2.29	19.4	67.56	.97	-29.52	41.80	1.14	24.9	8.9
Mission 318, Flight 17; September 9, 1975															
Upwind															
3	4	1	-1.21	0.57	10.35	7.87	0.34	25.5	-1.16	0.62	9.83	9.14	0.31	26.1	12.0
↓	↓	2	9.23	.25	7.69	9.36	.25	17.8	9.22	.24	7.13	8.53	.21	16.1	↓
		3	19.46	.25	-1.14	14.81	.25	15.3	19.47	.23	-1.61	10.72	.24	15.9	
		4	29.46	.10	-8.49	12.28	.32	13.4	29.47	.07	-8.64	20.07	.32	14.8	
		5	39.70	.09	-14.90	12.60	.36	20.9	39.76	.11	-13.18	11.34	.36	19.2	
↓	↓	6	46.70	.11	-18.90	14.56	.35	20.3	46.71	.10	-15.09	12.00	.36	20.3	↓
4	1	1	18.59	.77	-.62	19.23	.26	13.9	18.82	.75	-1.35	11.80	.24	13.9	13.5
4	6,8	3	38.84	1.37	-14.77	16.32	.34	9.5	38.91	1.59	-12.71	16.73	.36	9.5	12.8
4	11,12	6	66.92	1.24	-26.69	10.69	1.10	12.0	67.02	1.00	-19.47	7.25	.41	15.7	12.2

TABLE IV.- Continued

Line	Run	Antenna position	Horizontal polarization						Vertical polarization						Wind speed, m/s
			θ_{mean}	$\theta_{std\ dev}$	σ^o_{mean}, dB	$\frac{\Delta\sigma^o}{\sigma^o}$	σ^o_{error}, ±dB	Sample time, s	θ_{mean}	$\theta_{std\ dev}$	σ^o_{mean}, dB	$\frac{\Delta\sigma^o}{\sigma^o}$	σ^o_{error}, ±dB	Sample time, s	
Mission 318, Flight 17; September 9, 1975															
Downwind															
3	3	1	-0.44	0.33	10.37	13.10	0.34	14.5	-0.44	0.33	9.89	6.61	0.31	13.3	12.1
		2	10.88	.62	6.62	10.11	.24	13.7	10.94	.67	6.21	11.40	.24	15.5	
		3	20.71	.10	-2.17	10.18	.28	19.7	20.72	.11	-2.48	10.02	.28	18.5	
		4	30.53	.06	-10.87	12.67	.50	21.9	30.51	.08	-9.64	11.59	.40	18.4	
		5	40.67	.11	-17.03	21.41	.38	15.2	40.65	.10	-13.94	11.37	.39	15.2	
		6	47.67	.11	-20.77	16.09	.39	15.7	47.65	.09	-15.90	8.26	.38	17.6	
4	1	1	20.59	.44	-2.21	13.54	.28	13.3	20.44	.69	-2.07	19.72	.28	12.1	13.5
4	6,8	3	41.51	.80	-18.33	20.80	.36	8.3	42.16	1.21	-15.03	13.99	.36	14.0	12.8
4	11,12	6	67.75	.64	-31.34	24.67	1.14	16.6	67.82	.72	-21.02	8.91	.45	16.6	12.2
Crosswind															
2	2	1	0.19	0.37	10.90	12.46	0.34	15.1	0.18	0.38	10.65	7.30	0.29	14.5	12.0
		2	11.05	.25	6.04	13.93	.33	10.1	11.09	.31	5.67	12.06	.34	10.1	
		3	21.28	.24	-5.27	15.65	.33	16.6	21.31	.26	-5.91	16.03	.28	16.6	
		4	30.86	.09	-14.46	18.14	.38	12.0	30.88	.10	-14.06	17.48	.38	13.4	
		5	41.10	.13	-20.78	17.69	.39	18.4	41.08	.11	-18.77	12.55	.37	19.2	
		6	48.06	.09	-24.81	22.96	.53	12.0	48.03	.05	-21.29	9.40	.40	12.0	
4	1	1	19.97	.48	-3.97	17.91	.26	26.0	19.96	.54	-4.50	18.97	.26	27.7	13.5
4	6,8	3	41.03	.73	-21.50	17.29	.39	19.7	40.94	.77	-19.86	12.65	.36	21.6	12.8
4	11,12	6	68.34	1.41	-32.50	36.23	1.18	23.0	68.08	1.22	-26.26	20.98	1.13	21.2	12.2
Mission 318, Flight 18; September 9, 1975															
Upwind															
4	1,2	1	19.32	0.24	-2.16	24.55	0.27	13.3	19.35	0.18	-2.93	16.00	0.26	15.6	12.0
4	6	3	39.60	.33	-16.93	16.02	.36	10.8	39.58	.26	-13.96	11.90	.52	10.2	11.3
4	11	6	65.68	.42	-27.08	9.76	.50	12.0	65.76	.40	-19.55	7.46	.39	15.6	10.5
Downwind															
4	1,2	1	19.77	0.28	-2.61	15.73	0.31	9.2	19.84	0.22	-2.73	12.20	0.31	11.0	12.0
4	6	3	41.90	.43	-20.25	12.96	.34	10.2	41.71	.42	-16.05	15.29	.41	9.5	11.3
4	11	6	69.35	.44	-32.73	26.01	1.12	8.3	69.23	.34	-22.01	12.03	.40	6.5	10.5
Crosswind															
4	1,2	1	19.74	0.99	-3.28	33.05	0.28	25.4	19.56	1.03	-3.62	35.57	0.28	24.3	12.0
4	6	3	39.70	2.13	-21.57	31.39	.35	21.6	39.70	2.01	-20.33	23.63	.35	22.2	11.3
4	11	6	65.88	3.15	-33.03	46.60	1.12	28.6	66.02	3.41	-27.01	54.12	.54	23.0	10.5
Mission 318, Flight 19; September 10, 1975															
Upwind															
4	5-8,10	1	19.15	0.53	-2.68	27.29	0.24	15.0	19.4	0.59	-3.39	30.72	0.24	12.1	7.5
4	12,13	3	39.25	.76	-19.06	18.37	.34	10.2	39.39	.93	-16.89	14.58	.34	9.5	7.5
4	17	6	65.14	1.74	-32.49	56.75	1.21	20.3	65.08	1.76	-22.50	19.68	.50	18.4	7.5
Downwind															
3	3	1	-0.71	0.17	11.42	8.64	0.35	20.9	-0.70	0.14	10.79	7.96	0.34	21.5	7.7
		2	10.37	.13	7.06	10.21	.24	14.3	10.41	.12	6.40	8.34	.22	14.3	
		3	20.65	.10	-3.78	14.73	.27	12.7	20.66	.12	-3.96	8.27	.27	11.5	
		4	30.46	.09	-14.15	12.82	.38	14.8	30.42	.12	-12.93	15.52	.39	20.5	
		5	40.61	.11	-21.86	17.79	.41	20.0	40.60	.09	-17.58	16.52	.38	20.1	
		6	47.40	.11	-25.75	22.33	.57	18.5	47.40	.13	-19.47	16.20	.39	15.7	
4	5-8,10	1	20.59	.28	-3.73	23.48	.27	13.9	20.49	.30	-3.74	23.44	.28	12.7	7.5
4	12,13	3	43.41	.82	-24.59	23.91	.54	7.0	43.07	.77	-18.99	10.90	.38	7.6	7.5
4	17	6							70.46	1.54	-24.80	20.55	.94	12.9	7.5
Crosswind															
2	6	1	-0.76	0.27	11.25	8.36	0.35	22.6	-0.75	0.27	10.65	6.98	0.34	21.5	8.0
		2	10.48	.23	6.64	10.21	.23	15.5	10.43	.13	6.19	7.80	.23	13.1	
		3	20.78	.55	-5.19	16.90	.31	12.7	20.90	.68	-5.75	13.42	.26	14.0	
		4	30.32	.12	-15.22	11.64	.35	17.7	30.28	.13	-15.16	13.33	.35	17.0	
		5	40.65	.08	-24.18	15.92	.48	18.4	40.63	.07	-22.00	15.01	.39	20.0	
		6	47.61	.12	-28.53	11.31	1.22	11.1	47.59	.15	-25.63	16.75	.57	14.8	
4	5-8,10	1	19.50	1.61	-3.19	46.61	.26	20.8	19.45	1.51	-3.99	38.54	.26	23.1	7.5
4	12,13	3	40.97	1.56	-25.33	29.66	.72	18.4	41.12	1.81	-23.51	18.70	.45	18.4	7.5
4	17	6							67.22	.99	-33.22	49.18	1.32	28.6	7.5

TABLE IV.- Continued

Line	Run	Antenna position	Horizontal polarization						Vertical polarization						Wind speed, m/s
			θ_{mean}	$\theta_{std\ dev}$	σ^o_{mean}, dB	$\frac{\Delta\sigma^o}{\sigma^o}$	σ^o_{error}, ±dB	Sample time, s	θ_{mean}	$\theta_{std\ dev}$	σ^o_{mean}, dB	$\frac{\Delta\sigma^o}{\sigma^o}$	σ^o_{error}, ±dB	Sample time, s	
Mission 318, Flight 24; September 17, 1975															
Upwind															
2	11	1	0.44	0.29	10.59	9.34	0.28	7.0	0.32	0.40	9.86	9.82	0.28	9.3	9.5
		2	10.78	.30	5.97	7.88	.25	17.4	10.78	.29	5.29	12.71	.28	18.4	
		3	20.59	.47	-1.21	19.75	1.92	15.3	20.61	.72	-1.64	27.64	1.92	15.9	
		4	30.49	.30	-6.27	17.97	.87	15.6	30.60	.26	-5.17	12.26	.86	14.1	
		5	40.82	.25	-15.84	20.43	2.57	20.9	40.88	.27	-13.03	24.05	2.32	18.4	
		6	46.81	.19	-20.77	17.84	1.74	21.3	46.82	.14	-15.75	16.03	1.56	21.3	
4	1	1	29.83	.61	-12.07	19.21	.50	8.7	29.88	.54	-10.32	17.30	.34	8.7	
Downwind															
2	10	1	0.67	0.11	10.62	10.48	0.32	18.0	0.71	0.10	10.20	9.10	0.29	19.1	9.5
		2	11.38	.14	5.84	11.61	.24	35.1	11.37	.12	5.43	17.46	.25	31.5	
		3	21.65	.19	-3.82	16.06	.36	35.7	21.69	.20	-3.80	15.02	.36	35.0	
		4	31.54	.29	-12.93	18.44	1.37	26.2	31.48	.27	-11.21	18.92	1.37	30.4	
		5	41.80	.36	-19.80	18.09	2.30	35.3	41.80	.28	-14.68	17.65	1.85	30.5	
		6	47.89	.50	-21.87	18.62	2.06	24.9	47.91	.54	-15.22	15.02	1.68	23.97	
4	1	1	30.69	.98	-14.40	35.85	.36	7.5	30.57	1.01	-12.03	24.76	.34	10.4	
Crosswind															
4	1	1	30.51	0.82	-15.74	25.76	0.36	19.7	30.40	0.78	-14.48	21.96	0.35	15.0	9.5
Mission 335, Flight 3; January 16, 1976															
Upwind															
4	3	1	29.32	0.76	-8.33	16.47	0.49	15.4	29.26	0.87	-7.85	12.95	0.47	16.6	14.2
4	10	4	47.21	.45	-19.01	13.19	.39	17.6	47.34	.36	-15.17	10.87	.37	16.9	14.2
Downwind															
4	3	1	29.59	0.41	-8.98	22.95	0.54	12.5	29.56	0.42	-7.60	19.49	0.77	11.8	14.2
4	10	4	49.82	.45	-20.70	14.98	.43	12.7	49.78	.38	-15.96	9.13	.37	15.6	14.2
Crosswind															
2	[a]33	1	0.83	0.12	9.24	13.96	0.30	27.6	0.13	0.68	9.31	13.89	.29	35.8	14.2
		2	10.58	.21	3.36	13.46	.26	32.2	10.32	.13	3.21	13.80	.25	33.3	
		3	20.20	.18	-5.82	21.79	.43	33.3	20.01	.16	-5.71	14.46	.42	22.0	
		4	29.52	.20	-13.33	17.47	.38	21.5	29.27	.17	-13.25	15.21	.37	34.3	
		5	39.24	.20	-19.32	24.11	.53	33.8	39.14	.14	-17.09	13.47	.39	33.3	
		6	44.72	.14	-21.85	14.34	.91	34.8	44.72	.12	-17.56	12.92	.41	34.3	
4	3	1	29.22	.82	-12.40	18.70	.37	38.6	29.10	.98	-11.62	19.02	.37	32.0	
4	10	4	48.31	.57	-23.04	18.10	.52	28.2	48.40	.62	-18.94	15.28	.37	28.2	
Mission 335, Flight 4A; January 22, 1976															
Upwind															
3	1,11	1	0.14	0.92	9.43	10.15	0.31	34.7	0.52	0.68	9.08	9.44	0.30	27.2	19.9
		2	10.37	.27	6.01	8.63	.23	34.4	10.28	.36	5.78	10.41	.25	38.0	
		3	20.60	1.09	-1.16	19.54	.24	33.7	20.50	.36	-1.28	17.40	.24	31.8	
		4	29.56	.38	-6.85	19.47	.27	47.9	29.53	.39	-6.17	18.26	.25	46.5	
		5	39.13	.89	-12.42	19.33	.59	36.0	39.20	.86	-10.40	21.06	.47	36.8	
		6	44.61	.45	-15.07	14.62	.34	47.9	44.74	.42	-12.45	26.57	.48	44.3	
4	22	5	9.29	.74	6.14	13.56	.24	17.6	9.27	.79	5.87	12.64	.24	12.8	19.7
4	1-8	1	18.86	.71	.63	15.29	.46	24.3	18.65	.63	.60	13.88	.48	23.7	19.1
4	9-16,19	3	38.57	.90	-12.49	20.43	.35	21.0	38.70	1.10	-10.53	16.79	.34	26.0	20.0
4	17,18	5	57.79	.36	-21.48	19.50	.44	9.6	57.86	.18	-16.56	12.31	.36	8.0	19.8
Downwind															
4	22	5	12.79	4.08	5.10	47.96	0.27	16.0	10.01	0.85	6.02	13.76	0.26	14.4	19.7
4	1-8	1	19.25	.78	.57	21.23	.46	23.1	19.22	.76	.55	20.49	.46	22.5	19.1
4	9-16,19	3	39.73	.75	-13.53	22.94	.34	18.4	39.71	.80	-10.94	21.70	.36	19.1	20.0
4	17,18	5	58.02	.78	-24.62	24.39	.55	20.8	57.79	.85	-18.34	8.57	.39	17.6	19.8
Crosswind															
2	3	1	-0.56	0.51	9.71	11.66	0.46	41.6	-0.57	0.51	9.58	9.63	0.46	40.5	19.4
		2	9.80	.65	5.25	13.46	.32	42.1	9.73	.58	5.12	16.45	.34	43.9	
		3	19.51	.49	-3.80	21.84	.28	54.6	19.51	.47	-3.94	22.66	.28	54.0	
		4	28.93	.49	-11.02	24.68	.32	55.7	28.91	.50	-10.25	25.02	.27	52.2	
		5	38.58	.36	-17.52	21.75	.36	43.2	38.62	.33	-15.53	24.07	.38	47.1	
		6	43.73	.67	-20.50	21.28	.36	60.9	43.72	.64	-17.50	22.72	.37	64.5	
4	22	5	9.28	1.31	5.61	20.80	.22	32.8	9.35	.92	5.39	16.97	.23	35.2	19.7
4	1-8	1	19.05	1.27	-2.52	26.67	.27	39.9	18.95	1.38	-2.55	26.42	.26	43.4	19.1
4	9-16,19	3	39.09	1.66	-17.40	30.79	.36	43.2	38.95	1.48	-15.26	21.31	.36	41.3	20.0
4	17,18	5	58.46	.96	-25.79	29.69	.61	37.6	58.31	1.01	-20.92	22.97	.41	30.4	19.8

[a]All are short scan mode, with timing of 0.3 s.

TABLE IV.- Continued

Line	Run	Antenna position	Horizontal polarization						Vertical polarization						Wind speed, m/s
			θ_{mean}	$\theta_{std\ dev}$	σ^o_{mean}, dB	$\frac{\Delta\sigma^o}{\sigma^o}$	σ^o_{error}, ±dB	Sample time, s	θ_{mean}	$\theta_{std\ dev}$	σ^o_{mean}, dB	$\frac{\Delta\sigma^o}{\sigma^o}$	σ^o_{error}, ±dB	Sample time, s	
Mission 335, Flight 4B; January 22, 1976															
Upwind															
3	2	1	-1.33	0.87	8.45	13.19	0.40	30.6	-1.57	0.43	8.17	11.51	0.40	30.1	20.1
		2	9.68	.25	5.63	12.93	.34	32.0	9.73	.22	5.16	24.07	.34	30.2	
		3	19.55	.34	-.68	19.89	.30	32.4	19.54	1.07	-1.13	18.77	.26	31.8	
		4	28.75	.40	-6.52	20.94	.49	28.2	28.74	.44	-6.17	15.95	.48	26.8	
		5	38.54	.77	-12.61	16.05	.38	28.8	38.40	.67	-10.83	12.54	.41	25.6	
		6	43.67	.65	-14.62	23.36	.56	38.7	43.58	.69	-12.18	17.87	.46	35.0	
4	1,5-9	1	18.68	.57	.26	19.52	.27	24.3	18.71	.62	.02	23.72	.27	25.4	19.1
4	10-14,16	3	40.34	.76	-12.39	15.31	.36	19.0	40.34	.70	-10.34	16.31	.38	18.4	19.4
4	17	5	59.69	1.00	-20.87	20.50	.40	26.4	59.56	1.11	-16.99	13.78	.36	28.0	19.6
Downwind															
3	1,11,111	1	0.32	0.93	8.40	11.41	0.27	37.0	0.34	0.95	8.13	11.41	0.27	40.5	19.8
		2	10.32	.61	6.09	18.24	.34	45.1	10.32	.54	5.75	15.02	.34	40.3	
		3	19.82	.61	-.92	23.65	.29	29.2	19.70	.52	-.48	29.23	.31	29.2	
		4	29.16	.51	-6.99	23.43	.26	26.8	29.24	.58	-5.81	16.21	.24	29.6	
		5	38.97	.40	-12.83	25.13	.45	36.8	38.91	.35	-10.26	20.57	.40	35.2	
		6	44.22	.56	-15.76	22.20	.35	32.3	44.49	.56	-13.24	15.92	.51	34.1	
4	1,5-9	1	19.35	.71	-.02	22.09	.31	22.0	19.23	.67	.49	28.45	.46	21.4	19.1
4	10-14,16	3	37.56	1.02	-12.59	31.08	.36	24.8	37.53	.84	-10.46	23.30	.31	24.1	19.4
4	17	5	57.25	.95	-21.44	21.71	.38	20.8	56.98	.99	-17.24	14.63	.36	24.0	19.6
Crosswind															
2	3,33	1	-0.97	1.02	8.71	14.38	0.30	45.1	-0.94	1.10	8.65	14.79	0.30	40.4	20.0
		2	9.72	.85	5.05	21.07	.27	50.4	9.61	.53	4.78	22.77	.28	48.0	
		3	19.52	.50	-3.05	18.78	.27	47.0	19.51	.42	-3.27	22.49	.27	52.7	
		4	28.62	.27	-10.64	24.18	.34	55.7	28.62	.32	-10.03	19.21	.49	55.0	
		5	38.45	.21	-16.52	26.15	.36	53.6	38.53	.18	-14.57	26.01	.36	53.6	
		6	43.84	.31	-18.83	20.27	.36	59.0	43.81	.29	-16.12	19.15	.36	57.2	
4	1,5-9	1	19.00	1.47	-2.17	34.39	.27	53.7	18.87	1.51	-2.16	32.07	.26	52.6	19.1
4	10-14,16	3	38.27	2.19	-14.75	39.96	.36	45.1	37.91	2.08	-12.82	29.91	.38	45.7	19.4
4	17	5	57.96	1.87	-20.82	23.87	.41	48.0	58.30	2.02	-17.42	19.18	.39	43.2	19.6
Mission 335, Flight 5; January 23, 1975															
Upwind															
3	2	1	-0.75	0.72	9.69	13.31	0.43	48.6	-0.76	0.72	9.35	12.92	0.42	50.3	14.4
		2	9.64	1.04	6.05	20.98	.36	52.2	9.66	1.17	5.64	25.11	.36	51.0	
		3	19.28	1.03	-.92	27.81	.32	54.6	19.23	1.06	-.86	26.74	.32	55.9	
		4	28.52	.80	-7.52	26.76	.34	55.7	28.47	.81	-7.03	22.13	.32	57.2	
		5	38.28	.56	-13.88	25.45	.42	54.4	38.28	.58	-11.86	25.40	.50	54.4	
		6	43.99	.46	-16.99	24.58	.48	59.0	43.99	.48	-13.87	18.71	.49	55.3	
4	25	4	10.13	.51	5.63	16.92	.24	21.6	10.02	.72	5.40	12.10	.24	21.6	13.9
4	1,3	1	19.53	.91	-.23	23.53	.26	42.4	19.49	.92	-.33	25.82	.27	39.6	15.5
4	9,10	3	39.64	.71	-14.15	25.27	.34	27.3	39.85	.76	-12.29	13.91	.36	30.5	15.2
4	17-22	5	58.97	1.14	-22.35	24.33	.76	26.4	59.01	1.08	-17.03	11.45	.66	25.6	15.1
Downwind															
3	1	1	-0.76	0.75	9.77	11.71	0.42	46.2	0.79	0.75	9.47	10.80	0.42	43.9	14.6
		2	10.02	.83	6.59	15.07	.36	47.4	10.07	.78	6.30	18.50	.36	48.0	
		3	19.43	1.13	-1.11	25.03	.30	49.5	19.41	1.08	-1.05	27.08	.29	49.5	
		4	28.32	.66	-8.61	25.64	.32	57.1	28.23	.56	-7.49	26.52	.29	57.1	
		5	38.87	.93	-16.17	29.46	.36	60.8	38.90	.96	-12.58	34.13	.42	60.0	
		6	43.70	.64	-18.88	32.73	.37	57.2	43.80	.62	-14.87	22.92	.38	58.1	
4	25	4	8.40	.80	7.20	15.37	.28	18.4	8.29	.90	6.97	12.73	.27	16.8	13.9
4	1,3	1	21.26	1.50	-1.77	31.14	.24	43.3	21.36	1.51	-1.65	26.65	.24	44.3	15.5
4	9,10	3	38.73	1.04	-15.31	28.66	.38	24.1	38.87	1.20	-12.16	27.78	.39	24.8	15.2
4	17-22	5	57.56	1.17	-25.16	30.96	.68	35.2	57.28	1.07	-18.13	14.59	.52	31.2	15.1
Crosswind															
2	5,55	1	-0.28	0.76	9.96	11.65	0.30	34.1	-0.28	0.80	9.87	13.24	0.29	34.7	14.8
		2	9.45	1.22	5.94	22.65	.26	57.5	9.41	1.27	5.77	26.75	.26	55.7	
		3	19.20	.82	-3.70	25.13	.26	55.9	19.22	.83	-3.85	24.07	.25	56.5	
		4	28.14	.72	-11.30	28.08	.46	47.9	28.23	.75	-11.04	29.68	.33	50.1	
		5	38.70	.82	-18.26	24.74	.35	60.0	38.80	.97	-16.27	23.04	.35	58.4	
		6	43.36	.69	-21.47	35.82	.38	59.0	43.30	.78	-18.21	30.38	.35	51.6	
4	25	4	9.02	.77	5.49	13.71	.22	38.4	9.03	.74	5.25	17.27	.22	39.2	13.9
4	1,3	1	19.25	2.39	-2.61	41.89	.27	82.1	19.45	2.52	-2.72	44.89	.27	85.7	15.5
4	9,10	3	39.51	1.06	-18.42	34.54	.37	49.5	39.62	1.10	-16.34	27.86	.36	51.4	15.2
4	17-22	5	58.81	.77	-28.03	31.22	.33	50.4	58.72	.84	-21.48	26.54	.46	55.2	15.1

TABLE IV.- Continued

Line	Run	Antenna position (b)	Horizontal polarization						Vertical polarization						Wind speed, m/s
			θ_{mean}	$\theta_{std\ dev}$	σ^o_{mean}, dB	$\frac{\Delta\sigma^o}{\sigma^o}$	σ^o_{error}, $\pm$dB	Sample time, s	θ_{mean}	$\theta_{std\ dev}$	σ^o_{mean}, dB	$\frac{\Delta\sigma^o}{\sigma^o}$	σ^o_{error}, $\pm$dB	Sample time, s	
Mission 335, Flight 6; January 26, 1975															
Upwind															
4	1,4	1	18.71	0.29	-0.33	21.06	0.26	22.5	18.71	0.28	-0.71	19.66	0.26	22.5	15.0
4	9,11,17	3	39.97	.73	-15.06	23.17	.36	20.3	39.99	.69	-12.61	14.00	.37	21.0	↓
4	13,21	5	59.58	1.00	-22.90	19.06	.49	24.8	59.39	1.36	-17.03	9.41	.36	20.0	
4	25	4	8.14	1.18	7.06	19.58	.27	14.1	8.57	1.29	6.74	23.53	.25	12.0	↓
Downwind															
3	1,2	1	0.01	0.91	9.95	11.61	0.33	33.5	-0.12	0.84	9.78	9.95	0.32	31.8	15.0
↓	↓	2	10.52	.45	5.98	13.89	.23	40.3	10.51	.45	5.92	14.97	.23	40.9	↓
		3	20.12	.43	-2.38	14.99	.29	37.5	20.11	.44	-2.15	15.45	.30	37.5	
		4	29.28	.27	-10.10	24.21	.41	47.9	29.25	.26	-8.76	20.35	.34	45.8	
		5	38.91	.21	-17.74	24.36	.37	43.2	38.90	.24	-13.97	23.60	.28	42.4	
↓	↓	6	44.58	.15	-20.75	25.30	.34	43.3	44.56	.14	-15.91	14.41	.35	49.8	
4	1,4	1	20.19	1.38	-1.31	29.84	.29	24.3	20.17	1.46	-1.09	27.57	.29	24.3	
4	9,11,17	3	38.14	.95	-15.89	24.74	.37	31.8	38.20	.91	-12.65	24.55	.35	33.7	
4	13,21	5	57.64	1.11	-25.28	28.36	.56	26.4	57.66	.90	-18.47	13.70	.37	28.0	
4	25	4	8.79	.84	6.90	18.37	.27	12.0	8.67	.54	6.65	16.24	.26	11.3	↓
Crosswind															
2	3	1	-0.67	0.47	9.81	11.78	0.46	38.7	-0.70	0.44	9.64	9.79	0.46	38.1	15.0
↓	↓	2	10.16	.45	5.45	15.34	.34	40.9	10.17	.53	5.18	19.40	.34	39.1	↓
		3	19.75	.42	-3.56	22.82	.32	28.6	19.84	.55	-3.54	26.46	.32	29.8	
		4	28.99	.39	-11.93	34.22	.46	46.5	29.00	.42	-11.14	25.29	.48	47.9	
		5	38.87	.32	-18.74	26.28	.34	40.8	38.93	.36	-16.47	25.95	.36	42.4	
↓	↓	6	44.26	.21	-21.00	20.07	.36	49.8	44.29	.12	-17.57	15.61	.36	47.0	
4	1,4	1	19.32	2.54	-2.35	64.15	.29	46.2	19.50	2.49	-2.59	58.88	.28	49.7	
4	9,11,17	3	38.93	1.83	-18.59	32.51	.35	55.9	38.92	1.83	-16.73	24.36	.34	58.4	
4	13,21	5	57.40	1.85	-27.08	28.39	1.07	59.2	57.02	1.86	-21.30	20.14	.42	52.8	
4	25	4	8.96	1.07	6.06	26.57	.25	26.8	8.66	1.02	6.47	28.92	.24	25.4	↓
Mission 353, Flight 9; March 2, 1977															
Upwind															
3	3	1	-0.04	0.98	11.55	9.90	0.49	23.5	0.12	1.00	11.06	11.42	0.50	31.2	8.2
↓	↓	2	9.39	.42	7.17	19.66	.46	38.4	9.42	.50	7.31	18.43	.46	35.3	↓
		3	19.46	.49	-1.75	22.75	.47	39.9	19.48	.52	-2.08	18.54	.48	40.4	
		4	30.01	.44	-10.65	20.64	.39	29.2	29.90	.48	-9.98	19.74	.39	32.2	
		5	39.52	.77	-16.38	23.02	.45	35.3	39.69	.70	-13.77	21.05	.38	33.8	
↓	↓	6	47.20	.71	-20.64	31.00	.49	36.9	47.19	.59	-15.68	17.73	.43	34.8	↓
4	1	SS	11.68	1.40	4.65	34.68	.22	18.4	11.89	1.38	4.07	36.80	.22	23.0	12.19
4	6	SS	67.71	.87	-31.11	93.49	1.14	9.7	63.13	1.47	-21.72	16.40	1.14	17.9	11.28
4	11	SS	20.39	1.20	-3.36	23.39	.43	18.9	20.59	1.35	-3.39	24.92	.44	15.4	10.84
4	16	SS	39.60	.89	-17.56	20.27	.54	16.9	39.94	1.16	-14.83	20.68	.43	19.5	10.30
Downwind															
3	33	1	-0.68	0.52	11.35	7.91	0.49	8.7	-0.68	0.76	11.01	10.70	0.50	7.7	8.2
↓	↓	2	8.94	.75	7.85	15.85	.51	10.8	9.02	.79	7.24	17.87	.46	12.3	↓
		3	19.42	.21	-2.68	18.77	.52	7.7	19.49	.28	-1.66	15.89	.48	6.7	
		4	30.08	.05	-12.58	24.14	.50	1.0	30.18	.05	-11.38	8.55	.40	2.6	
		5	39.92	.44	-20.65	42.87	1.15	10.8	39.85	.53	-16.21	29.05	.55	12.3	
↓	↓	6	47.00	.58	-24.70	11.91	1.15	12.3	47.39	.62	-17.94	11.60	.67	11.8	↓
4	1	SS	11.68	.78	4.72	27.93	.32	15.4	11.66	.95	4.58	33.93	.32	15.4	12.19
4	6	SS							66.75	.89	-25.97	77.98	1.14	15.9	11.28
4	11	SS	20.01	1.19	-3.18	34.34	.44	21.0	20.00	.88	-3.40	33.97	.46	17.9	10.84
4	16	SS	39.47	.74	-25.40	33.32	1.14	18.9	39.45	.62	-20.31	51.84	.59	18.9	10.30
Crosswind															
4	1	SS	11.51	1.13	4.70	32.86	0.26	42.5	11.43	0.93	4.26	26.86	0.27	41.5	12.19
4	6	SS							68.69	1.51	-30.03	37.62	1.14	15.9	11.28
4	11	SS	19.40	1.40	-4.82	53.03	.38	38.4	19.21	1.44	-4.62	65.97	.37	37.9	10.84
4	16	SS	39.08	1.73	-25.00	46.51	1.08	36.9	39.01	2.04	-22.99	41.71	1.07	36.4	10.30
Mission 353, Flight 10; March 3, 1977															
Upwind															
4	1,6	SS	19.10	1.34	-6.36	51.82	0.32	32.8	19.15	1.59	-6.38	66.34	0.32	34.8	5.4
4	11	SS	10.83	1.07	5.35	42.93	.24	18.9	10.80	1.03	5.19	37.50	.23	21.0	5.4

[b] SS indicates timing was 0.512 s, independent of antenna position.

TABLE IV.- Continued

Line	Run	Antenna position (b)	Horizontal polarization						Vertical polarization						Wind speed, m/s
			θ_{mean}	$\theta_{std\ dev}$	σ^o_{mean}, dB	$\frac{\Delta\sigma^o}{\sigma^o}$	σ^o_{error}, ±dB	Sample time, s	θ_{mean}	$\theta_{std\ dev}$	σ^o_{mean}, dB	$\frac{\Delta\sigma^o}{\sigma^o}$	σ^o_{error}, ±dB	Sample time, s	
Mission 353, Flight 10; March 3, 1977															
Downwind															
4	1,6	SS	20.21	1.07	-8.42	39.17	0.41	36.4	20.22	1.15	-8.60	38.77	0.41	41.0	5.4
4	11	SS	11.28	1.24	4.60	45.32	.26	21.5	11.11	1.04	4.30	43.73	.26	20.0	5.4
Crosswind															
4	1,6	SS	19.41	1.18	-6.00	47.55	0.36	60.9	19.41	1.29	-5.85	48.53	0.36	59.4	5.4
4	11	SS	9.46	1.81	7.19	48.55	.32	35.3	9.55	1.81	6.70	58.23	.32	35.8	5.4
Mission 353, Flight 11; March 8, 1977															
Upwind															
4	1	SS	67.25	0.35	-24.99	25.39	1.15	15.36	67.04	0.48	-18.05	18.16	1.16	16.4	16.0
4	6	SS	19.12	1.29	-.25	32.15	.38	17.9	19.21	1.21	.17	33.97	.38	20.5	15.9
4	11	SS	39.32	.86	-13.57	30.08	.40	15.9	39.33	.96	-11.36	18.37	.35	18.9	15.7
Downwind															
3	2	1	-0.95	0.45	9.77	13.64	0.50	31.7	-0.84	0.45	9.76	15.1	0.54	26.6	16.5
↓	↓	2	9.34	.47	6.87	18.32	.42	33.8	9.24	.41	7.14	22.87	.42	38.9	↓
		3	19.11	.31	-.85	21.13	.51	36.9	19.01	.35	-.06	23.67	.50	32.3	
		4	29.41	.36	-9.68	22.41	.80	36.9	29.47	.43	-8.17	20.76	.80	32.3	
		5	39.72	.41	-15.97	27.39	1.48	32.3	39.64	.30	-12.49	22.36	1.46	36.9	
		6	46.88	.48	-19.53	30.93	1.83	35.3	46.78	.39	-14.63	20.74	1.72	36.9	↓
4	1	SS	67.77	.57	-30.23	26.21	1.21	20.0	67.75	.56	-20.42	15.58	1.21	17.9	16.0
4	6	SS	20.58	.49	-.76	30.40	.32	16.4	20.55	.58	-1.00	25.99	.29	15.9	15.9
4	11	SS	39.96	.68	-16.25	25.72	.39	18.4	39.78	.77	-12.89	15.77	.38	16.4	15.7
Crosswind															
2	6	1	-0.67	0.45	9.50	13.23	0.54	24.1	-0.61	0.54	9.68	13.30	0.54	21.0	16.3
↓	↓	2	9.38	.54	6.06	18.95	.50	32.3	9.49	.55	6.47	19.50	.50	37.4	↓
		3	19.06	.46	-1.72	23.99	.51	42.0	19.20	.43	-1.36	17.55	.50	39.9	
		4	29.70	.36	-11.18	26.93	.53	46.1	29.74	.48	-10.13	26.37	.52	46.1	
		5	39.72	.46	-18.91	25.66	.76	33.8	39.68	.43	-15.84	20.17	.56	35.3	
		6	46.88	.41	-22.36	24.09	1.14	35.8	46.87	.60	-17.74	19.55	.68	36.4	↓
4	1	SS	67.03	1.18	-31.33	21.63	1.11	31.2	67.40	1.10	-24.40	24.54	1.09	33.8	16.0
4	6	SS	18.71	2.17	-1.54	47.86	.32	34.3	19.12	2.15	-1.78	46.54	.37	33.8	15.9
4	11	SS	39.49	.63	-18.55	22.33	.57	36.4	39.54	.84	-16.51	20.75	.49	33.3	15.7
Mission 353, Flight 13; March 10, 1977															
Upwind															
4	1,6	SS	20.30	1.47	-2.96	33.68	0.39	43.0	20.25	1.62	-2.57	32.20	0.39	34.8	10.4
4	11	SS	11.37	3.30	5.72	71.67	.24	13.8	12.90	2.45	3.61	49.30	.24	7.2	11.2
4	16	SS	68.64	.54	-30.49	12.84	1.09	7.7	69.16	.69	-20.40	9.17	1.08	11.3	11.7
4	20	SS	40.75	1.67	-17.80	28.36	.52	13.8	40.39	1.77	-14.06	22.53	.37	12.8	12.0
Downwind															
4	1,6	SS	20.29	2.23	-2.51	53.58	0.41	36.4	19.99	2.03	-1.62	48.67	0.40	38.4	10.4
4	11	SS	12.12	2.66	4.94	58.58	.29	22.5	12.78	2.77	4.64	52.65	.29	25.1	11.2
4	16	SS							68.20	.79	-22.59	16.90	1.11	14.3	11.7
4	20	SS	38.89	2.77	-19.93	55.97	1.07	12.8	38.30	1.83	-15.04	21.23	1.09	12.8	12.0
Crosswind															
2	6	1	-1.40	1.36	10.38	11.05	0.56	21.5	-1.33	1.20	10.56	14.40	0.54	21.0	11.7
↓	↓	2	9.99	1.32	5.89	34.08	.50	26.1	9.95	1.57	5.98	35.37	.50	31.7	↓
		3	19.32	1.46	-4.05	41.28	.58	35.3	19.38	1.06	-4.03	29.25	.58	30.7	
		4	28.87	1.62	-13.55	36.73	.54	35.3	28.98	1.32	-12.85	32.51	.54	32.8	
		5	39.49	.66	-21.82	22.86	1.15	30.2	39.52	.53	-18.45	17.93	.68	35.8	
		6	47.50	1.55	-25.82	32.57	1.14	37.4	47.43	1.62	-21.11	27.91	1.14	36.9	↓
4	1,6	SS	20.38	2.07	-5.22	66.41	.37	73.2	20.35	2.08	-4.97	59.77	.37	78.3	10.4
4	11	SS	9.20	1.50	6.70	32.87	.23	38.4	9.31	1.52	6.90	30.37	.26	38.9	11.2
4	16	SS							67.81	2.07	-28.75	32.16	1.10	29.2	11.7
4	20	SS	40.94	1.75	-23.85	38.92	1.09	28.2	41.23	1.72	-20.80	29.25	.46	31.2	12.0
Mission 353, Flight 14; March 11, 1977															
Upwind															
4	1	SS	67.53	0.59	-26.58	24.96	1.09	17.4	67.56	0.55	-19.43	10.80	1.09	21.5	14.3
4	6	SS	20.41	.63	-3.11	25.20	.32	18.9	20.64	.93	-3.02	29.15	.31	18.4	14.3
4	11	SS	40.48	.96	-17.43	27.78	.42	5.6	40.56	.61	-15.33	29.45	.38	5.6	14.3

[b] SS indicates timing was 0.512 s, independent of antenna position.

TABLE IV.- Continued

Line	Run	Antenna position (b)	Horizontal polarization						Vertical polarization						Wind speed, m/s
			θ_{mean}	$\theta_{std\ dev}$	σ^o_{mean}, dB	$\frac{\Delta\sigma^o}{\sigma^o}$	σ^o_{error}, ±dB	Sample time, s	θ_{mean}	$\theta_{std\ dev}$	σ^o_{mean}, dB	$\frac{\Delta\sigma^o}{\sigma^o}$	σ^o_{error}, ±dB	Sample time, s	
Mission 353, Flight 14; March 11, 1977															
Downwind															
3	2	1	-0.85	1.07	10.61	13.64	0.32	53.8	-0.45	0.96	11.10	11.73	0.32	15.9	13.6
		2	9.68	.92	7.02	18.55	.29	70.6	10.08	.50	7.22	17.78	.29	21.5	
		3	19.56	1.27	-1.18	30.58	.38	84.5	19.45	1.11	-.12	29.96	.36	33.8	
		4	29.53	1.03	-10.16	27.62	.42	69.1	29.98	.99	-8.52	23.23	.42	47.6	
		5	40.18	1.03	-16.74	30.11	.50	69.1	39.88	.97	-12.65	19.16	.43	47.6	
		6	47.45	1.31	-21.16	35.19	1.12	58.9	47.37	1.33	-15.00	19.73	.46	43.5	
4	1	SS	67.51	.49	-31.45	21.72	1.14	3.1	67.42	1.41	-21.42	11.48	1.14	17.9	14.3
4	6	SS	19.67	1.18	-2.39	31.00	.40	21.5	19.67	1.12	-1.77	33.03	.36	19.5	14.3
4	11	SS	40.56	1.99	-19.33	41.47	.56	9.2	40.80	2.14	-15.42	28.07	.54	6.7	14.3
Crosswind															
2	5	1	-0.15	1.32	10.04	11.48	0.56	23.0	0.02	1.23	10.31	14.25	0.54	23.6	13.0
		2	9.23	.63	6.72	18.45	.47	15.4	9.52	.70	6.61	14.98	.46	16.9	
		3	19.20	.63	-2.86	24.27	.49	22.5	19.22	.71	-2.70	23.81	.55	23.0	
		4	29.89	1.28	-13.83	26.70	.47	23.0	29.87	1.19	-12.81	28.45	.46	23.0	
		5	40.04	.83	-21.72	38.78	1.13	23.0	39.86	.50	-19.11	39.25	.83	23.0	
		6	47.08	.50	-25.79	35.90	1.13	21.0	47.11	.46	-21.93	49.32	1.12	18.4	
4	1	SS	65.91	.91	-29.46	20.93	1.13	20.0	65.72	1.07	-22.54	28.55	1.09	45.1	14.3
4	6	SS	17.84	.98	-.51	21.77	.39	32.3	17.92	.97	-.24	26.55	.38	39.9	14.3
4	11	SS	38.67	1.38	-17.26	31.19	1.08	18.9	38.27	1.44	-14.41	21.35	.58	15.4	14.3
Mission 353, Flight 15; March 14, 1977															
Upwind															
4	1	SS	9.30	0.46	7.13	18.07	0.24	16.4	9.02	0.65	7.68	18.10	0.29	18.4	4.2
4	11	SS	20.19	1.49	-5.35	45.72	.37	10.2	20.41	1.32	-5.02	53.18	.37	10.8	4.2
4	16	SS	39.96	.79	-25.41	23.43	1.13	16.9	39.40	.87	-22.51	34.18	1.13	18.9	4.2
Downwind															
4	1	SS	10.33	1.45	6.35	36.31	0.29	15.9	10.67	1.32	5.79	37.75	0.29	24.1	4.2
4	11	SS	20.10	1.38	-5.65	38.97	.42	12.3	19.84	.95	-5.30	32.76	.42	11.3	4.2
4	16	SS	40.16	1.10	-30.72	61.18	1.14	20.0	40.04	1.16	-24.29	40.01	1.13	16.4	4.2
Crosswind															
4	1	SS	10.29	1.49	5.94	41.32	0.27	36.4	10.12	1.55	6.22	37.20	0.25	33.3	4.2
4	11	SS	19.81	.97	-7.21	42.61	.40	22.5	19.68	1.66	-6.43	77.90	.39	24.1	4.2
4	16	SS	40.63	.88	-32.76	25.44	1.08	20.5	40.89	1.33	-29.45	48.28	1.08	33.3	4.2
Mission 353, Flight 20; March 22, 1977															
Upwind															
4	1,21	SS	19.29	1.22	-5.29	42.03	0.49	41.0	19.38	1.18	-5.19	38.72	0.52	41.0	[c] 2.5
4	11	SS	10.42	.61	5.85	20.24	.23	20.0	10.30	.53	6.07	20.37	.23	20.0	[c] 2.5
4	16	SS													[c] 2.5
4	26	SS	38.65	.64	-28.62	40.45	1.13	21.5	38.46	.40	-26.05	34.35	1.13	17.9	[c] 2.5
Downwind															
4	1,21	SS	20.50	1.77	-6.29	59.33	0.34	40.4	20.79	1.75	-6.17	59.86	0.35	41.0	[c] 2.5
4	11	SS	11.72	.36	3.87	14.58	.24	18.9	11.79	.39	3.85	15.62	.24	20.5	[c] 2.5
4	16	SS	67.76	.63	-15.03	44.91	1.13	12.8	68.01	.44	-15.61	23.72	.59	10.8	[c] 2.5
4	26	SS	39.10	.65	-31.85	37.96	1.12	11.8	39.65	.87	-26.67	21.47	1.13	11.3	[c] 2.5
Crosswind															
4	1,21	SS	20.12	1.80	-8.35	60.02	0.33	73.2	20.04	1.69	-7.95	53.58	0.33	70.7	[c] 2.5
4	11	SS	10.80	1.48	4.43	51.88	.24	42.0	10.71	1.47	4.81	49.63	.24	34.3	[c] 2.5
4	16	SS													[c] 2.5
4	26	SS	39.12	1.59	-33.98	16.88	1.09	3.6	39.15	1.53	-31.07	32.32	1.07	31.2	[c] 2.5

[b] SS indicates timing was 0.512 s, independent of antenna position.
[c] Variable - 1.7 → 5.5 m/s.

TABLE IV.- Concluded

Line	Run	Antenna position (b)	Horizontal polarization						Vertical polarization						Wind speed, m/s
			θ_{mean}	$\theta_{std\ dev}$	σ^o_{mean}, dB	$\frac{\Delta\sigma^o}{\sigma^o}$	σ^o_{error}, ±dB	Sample time, s	θ_{mean}	$\theta_{std\ dev}$	σ^o_{mean}, dB	$\frac{\Delta\sigma^o}{\sigma^o}$	σ^o_{error}, ±dB	Sample time, s	
Mission 353, Flight 21; March 24, 1977															
Upwind.															
4	1	SS	9.65	0.69	6.92	19.14	0.24	20.0	9.55	0.66	6.89	13.08	0.24	15.9	4.7
4	7	SS	19.83	.67	-6.90	29.48	1.13	20.0	20.00	.69	-6.92	17.53	1.13	12.8	4.7
4	12	SS	39.17	.65	-29.91	28.4	.34	14.8	39.76	.70	-27.44	18.57	.36	17.9	4.7
Downwind															
3	3	1	-0.43	0.49	12.81	13.67	0.50	30.2	-0.54	0.40	12.94	10.64	0.50	32.8	6.2
↓	↓	2	9.77	.27	7.47	13.25	.46	40.4	9.77	.24	7.42	12.40	.46	37.4	↓
		3	19.55	.23	-4.96	24.79	.56	46.1	19.48	.28	-4.70	26.50	.60	45.1	
		4	30.07	.33	-19.75	38.52	.94	46.1	30.13	.18	-17.63	39.70	.65	46.1	
		5	40.14	.35	-29.89	51.42	1.14	43.5	40.03	.31	-24.07	54.44	1.14	45.1	
↓	↓	6	47.26	.34	-31.85	35.01	1.14	13.3	47.17	.24	-26.86	75.95	1.14	44.5	↓
4	1	SS	11.36	1.16	4.75	30.88	.29	13.8	11.47	1.07	4.75	26.99	.29	21.5	4.7
4	7	SS	19.59	.70	-6.28	24.63	1.14	16.9	19.52	.59	-6.11	26.17	1.14	22.0	4.7
4	12	SS	39.21	.79	-33.89	20.68	.38	15.4	39.76	.80	-29.55	24.82	.38	13.8	4.7
Crosswind															
4	1	SS	10.56	1.97	6.06	54.17	0.27	40.4	10.46	1.79	6.15	53.43	0.25	34.3	4.7
4	7	SS	19.57	1.05	-7.04	51.86	1.09	36.4	19.45	1.25	-6.64	63.82	1.09	36.9	4.7
4	12	SS	39.37	.80	-33.43	28.43	.40	15.9	39.26	.83	-30.16	45.38	.39	30.2	4.7

[b] SS indicates timing was 0.512 s, independent of antenna position.

TABLE V.- REGRESSION COEFFICIENTS FOR NRCS (dB) VERSUS θ FOR ALL UPWIND, DOWNWIND, AND CROSSWIND STRAIGHT LEVEL LINES

Miss	Fl	Date	Pol	Wind dir	θ, deg		Wind speed, m/s	A_0	A_1	A_2	A_3	A_4	A_5	A_6
					Min	Max								
230	FCF	4/11/73	H	U	0	60	14.5	.1108E+02	-.4112E+00	-.2538E-01	.6730E-03	.4014E-05	-.2848E-06	.2322E-08
230	FCF	4/11/73	V	U	0	60	14.5	.1059F+02	-.4192E+00	-.2649E-01	.7377E-03	.6323E-05	-.3624E-06	.2890E-08
230	FCF	4/11/73	H	D	0	60	14.5	.1108E+02	-.4112E+00	-.2538E-01	.6730E-03	.4014E-05	-.2848E-06	.2322E-08
230	FCF	4/11/73	V	D	0	60	14.5	.1059F+02	-.4192E+00	-.2649E-01	.7377E-03	.6323E-05	-.3624E-06	.2890E-08
230	FCF	4/11/73	H	C	0	60	15.0	.9799E+01	.1266E+00	-.9233E-01	.3326F-02	-.4113E-04	.2104E-07	.1926E-08
230	FCF	4/11/73	V	C	0	60	15.0	.1002E+02	-.1016E+00	-.6715E-01	.2059E-02	-.6488E-05	-.4343E-06	.4203E-08
238	20	6/ 5/73	H	U	0	60	6.5	.1121E+02	.6532E-01	-.7776E-01	.1533E-02	.1922E-04	-.7717E-06	.5550E-08
238	20	6/ 5/73	V	U	0	60	6.5	.1114E+02	.1113E+00	-.8744E-01	.1892E-02	.1999E-04	-.9020E-06	.6678E-08
238	20	6/ 5/73	H	D	0	60	6.5	.9614E+01	.1663E+00	-.7686E-01	.1089E-02	.3104E-04	-.8590E-06	.5540E-08
238	20	6/ 5/73	V	D	0	60	6.5	.9191E+01	.2805E+00	-.9548E-01	.1905E-02	.2503E-04	-.9965E-06	.7195E-08
238	20	6/ 5/73	H	C	0	60	6.5	.1064E+02	.5202E+00	-.1201E+00	.2510E-02	.1843E-04	-.9956E-06	.7525E-08
238	20	6/ 5/73	V	C	0	60	6.5	.1054E+02	.2858E+00	-.8989E-01	.1188E-02	.3918E-04	-.1008E-05	.6220E-08
238	27	6/11/73	H	U	0	60	3.0	.1231E+02	-.2547E+00	-.9166E-01	.2511E-02	.4609E-05	-.8079E-06	.6922E-08
238	27	6/11/73	V	U	0	60	3.0	.1197F+02	-.2754E+00	-.8448E-01	.1936E-02	.2259E-04	-.1006E-05	.7531E-08
238	27	6/11/73	H	D	0	60	3.0	.1265E+02	-.1568E+00	-.8640E-01	.1986E-02	.1568E-04	-.8833E-06	.6946E-08
238	27	6/11/73	V	D	0	60	3.0	.1231E+02	-.1364E+00	-.9021E-01	.2127E-02	.1681E-04	-.9233E-06	.7113E-08
238	27	6/11/73	H	C	0	60	3.0	.1353E+02	-.5269E-01	-.1077E+00	.3001E-02	-.2378E-04	.1707E-13	-.9267E-16
238	27	6/11/73	V	C	0	60	3.0	.1323E+02	-.3073E+00	-.8041E-01	.1269E-02	.4557E-04	-.1285E-05	.8605E-08
288	5	11/11/74	H	U	0	53	22.2	.6837E+01	.2192E+00	-.5094E-01	.1353E-02	-.1112E-04	-.1837E-13	.1147E-15
288	5	11/11/74	V	U	0	53	22.2	.6593E+01	.2257E+00	-.5092E-01	.1369E-02	-.1115E-04	-.1866E-13	.1165E-15
288	5	11/11/74	H	D	0	53	22.2	.6270F+01	.3489E+00	-.5372E-01	.1242E-02	-.9402E-05	-.1333E-13	.8332E-16
288	5	11/11/74	V	D	0	53	22.2	.6252E+01	.3267E+00	-.5170E-01	.1240E-02	-.9559E-05	-.1378E-13	.8604E-16
288	5	11/11/74	H	C	0	53	22.2	.6318E+01	.2296E+00	-.5654E-01	.1381E-02	-.1060E-04	-.2344E-13	.1458E-15
288	5	11/11/74	V	C	0	53	22.2	.6316E+01	.2370E+00	-.5707E-01	.1440E-02	-.1112E-04	-.1859E-13	.1161E-15
288	6	11/14/74	H	U	0	55	8.9	.9062E+01	.8734E-01	-.4927E-01	.1186E-02	-.8703E-05	-.1620E-13	.9628E-16
288	6	11/14/74	V	U	0	55	8.9	.8997E+01	.6640E-01	-.4776E-01	.1184E-02	-.8487E-05	-.1456E-13	.8646E-16
288	6	11/14/74	H	D	0	55	9.7	.9470E+01	.2234E+00	-.5876E-01	.1292E-02	-.8959E-05	-.1305E-13	.7761F-16
288	6	11/14/74	V	D	0	55	9.7	.9344F+01	.2507E+00	-.6256E-01	.1508E-02	-.1112E-04	-.2162E-13	.1286E-15
288	6	11/14/74	H	C	0	55	11.2	.9165E+01	.1774E+00	-.6504E-01	.1504E-02	-.1074E-04	-.2359E-13	.1407E-15
288	6	11/14/74	V	C	1	55	11.2	.9148E+01	.2803E+00	-.7662E-01	.1921E-02	-.1449E-04	.1064E-12	-.6224E-15
306	FCF	4/ 4/75	H	U	0	60	21.5	.9747E+01	-.2131E+00	-.1239E-01	.1601E-03	.2780E-06	-.2208E-15	.1106E-17
306	FCF	4/ 4/75	V	U	0	60	21.5	.9630E+01	.4437E-01	-.3275E-01	.7381E-03	-.5145E-05	.2507E-14	-.1360E-16
306	FCF	4/ 4/75	H	D	0	60	21.5	.9798E+01	.1705E+00	-.3948E-01	.8444E-03	-.5864E-05	.5593E-14	-.3039E-16
306	FCF	4/ 4/75	V	D	0	60	21.5	.9610E+01	.1197E+00	-.3344E-01	.7433E-03	-.5301E-05	.2842E-14	-.1545E-16
306	FCF	4/ 4/75	H	C	0	60	21.5	.9755E+01	.4227E-01	-.3870E-01	.8111E-03	-.5265E-05	.4224E-14	-.2287E-16
306	FCF	4/ 4/75	V	C	0	60	21.5	.9577E+01	.1372E+00	-.4613E-01	.1051E-02	-.7275E-05	.6186E-14	-.3367E-16
318	13	8/29/75	H	U	0	50	4.5	.1227E+02	.1879E+00	-.9986E-01	.2631E-02	-.2115E-04	.1817E-14	-.7798E-17
318	13	8/29/75	V	U	0	50	4.5	.1086E+02	.2408E+00	-.1064E+00	.2864E-02	-.2278E-04	-.7631E-14	.5505E-16
318	13	8/29/75	H	D	0	50	4.5	.1197E+02	.5420E+00	-.1226E+00	.1256E-02	.1139E-03	-.3348E-05	.2637E-07
318	13	8/29/75	V	D	0	60	4.5	.1120E+02	-.7363E-01	-.7429E-01	.1266E-02	.2764E-04	-.8814E-06	.6053E-08
318	13	8/29/75	H	C	0	50	4.5	.1349E+02	.5610E-01	-.7340E-01	-.1769E-02	.1905E-03	-.4083E-05	.2781E-07
318	13	8/29/75	V	C	0	50	4.5	.1246E+02	-.2406E+00	-.8057E-01	.2003E-02	-.1351E-04	.2655E-13	-.1711E-15
318	14	9/ 2/75	H	U	0	67	5.5	.1276E+02	-.1611E+00	-.5802E-01	.9478E-03	.7584E-05	-.2494E-06	.1334E-08
318	14	9/ 2/75	V	U	0	67	5.5	.1262E+02	-.1564E+00	-.5714E-01	.6264E-03	.2599E-04	-.5743E-06	.3186E-08
318	14	9/ 2/75	H	D	0	67	5.5	.1247E+02	.1604E+00	-.7516E-01	.6165E-03	.4212E-04	-.9268E-06	.5430E-08
318	14	9/ 2/75	V	D	0	67	5.5	.1262E+02	.1271E+00	-.6954E-01	-.4269E-04	.7386E-04	-.1456E-05	.8310E-08
318	14	9/ 2/75	H	C	0	67	5.5	.1290E+02	-.1510E+00	-.6556E-01	.1358E-02	-.7763E-05	.7083E-14	-.3338E-16
318	14	9/ 2/75	V	C	0	67	5.5	.1272E+02	-.7184E-01	-.6900E-01	.9134E-03	.2115E-04	-.5060E-06	.2760E-08
318	16	9/ 8/75	H	U	0	65	8.8	.1133E+02	.8602E-01	-.6882E-01	.1582E-02	.3166E-06	-.3507E-06	.2787E-08
318	16	9/ 8/75	V	U	0	65	8.8	.1108E+02	.4708E-01	-.6587E-01	.1313E-02	.1355E-04	-.5665E-06	.3947E-08
318	16	9/ 8/75	H	D	0	70	9.0	.1131E+02	.1616E+00	-.6699E-01	.1033E-02	.1516E-04	-.4756E-06	.2972E-08
318	16	9/ 8/75	V	D	0	70	9.0	.1111E+02	.9127E-01	-.6182E-01	.6075E-03	.3692E-04	-.8439E-06	.4963E-08
318	16	9/ 8/75	H	C	0	70	8.1	.1215E+02	-.3225E-01	-.5960E-01	.6843E-03	.1954E-04	-.4438E-06	.2421E-08
318	16	9/ 8/75	V	C	0	67	8.1	.1172E+02	-.1120E+00	-.5817E-01	.1068E-02	.2775E-05	-.1687E-06	.8607E-09
318	17	9/ 9/75	H	U	0	67	12.2	.1053E+02	-.8015E-01	-.3608E-01	.3584E-03	.1522E-04	-.3408E-06	.1942E-08
318	17	9/ 9/75	V	U	0	67	12.2	.1005E+02	-.2750E-01	-.4298E-01	.4658E-03	.2304E-04	-.5459E-06	.3296E-08
318	17	9/ 9/75	H	D	0	68	12.3	.1053E+02	.1061E+00	-.5284E-01	.6814E-03	.1779E-04	-.4729E-06	.2914E-08
318	17	9/ 9/75	V	D	0	68	12.3	.1005E+02	.8864E-01	-.5110E-01	.6262E-03	.2214E-04	-.5509E-06	.3338E-08
318	17	9/ 9/75	H	C	0	68	12.4	.1108E+02	-.1719E-01	-.5324E-01	.5637E-03	.2421E-04	-.5611E-06	.3287E-08
318	17	9/ 9/75	V	C	0	68	12.4	.1086E+02	.2144E-01	-.6032E-01	.7426E-03	.2838E-04	-.7032E-06	.4275E-08
318	18	9/ 9/75	H	U	0	66	11.3	.1078E+02	.2909E+00	-.8505E-01	.1918E-02	.2536E-05	-.4628E-06	.3552E-08
318	18	9/ 9/75	V	U	0	66	11.3	.1021E+02	.4425E+00	-.1133E+00	.3502E-02	-.3230E-04	-.1170E-06	.2271E-08
318	18	9/ 9/75	H	D	0	70	11.3	.1051E+02	.4025E+00	-.9172E-01	.2105E-02	-.5420E-05	-.2927E-06	.2364E-08
318	18	9/ 9/75	V	D	0	70	11.3	.9927E+01	.5111E+00	-.1068E+00	.2883E-02	-.1849E-04	-.2135E-06	.2294E-08
318	18	9/ 9/75	H	C	0	66	11.3	.1084E+02	.1727E+00	-.6352E-01	.4943E-03	.3630E-04	-.7951E-06	.4673E-08
318	18	9/ 9/75	V	C	0	66	11.3	.1065E+02	.2105E+00	-.6995E-01	.6468E-03	.3970E-04	-.9051E-06	.5414E-08
318	19	9/10/75	H	U	0	65	7.5	.1159E+02	.3427E+00	-.9901E-01	.2383E-02	-.1866E-05	-.5008E-06	.4140E-08
318	19	9/10/75	V	U	0	65	7.5	.1101E+02	.3774E+00	-.1039E+00	.2422E-02	.6509E-05	-.6890E-06	.5295E-08
318	19	9/10/75	H	D	0	50	7.6	.1157E+02	.1577E+00	-.7396E-01	.1726E-02	-.1238E-04	.1406E-13	-.8947E-16
318	19	9/10/75	V	D	0	70	7.6	.1096E+02	.8375E-01	-.6216E-01	.9020E-03	.2108E-04	-.5722E-06	.3482E-08
318	19	9/10/75	H	C	0	50	7.8	.1140E+02	.1107E+00	-.7023E-01	.1535E-02	-.1009E-04	.1573E-14	-.7772E-17
318	19	9/10/75	V	C	0	67	7.8	.1090E+02	.4135E-01	-.5901E-01	.5850E-03	.2845E-04	-.6460E-06	.3772E-08
318	24	9/17/75	H	U	0	50	9.5	.1068E+02	-.1298E+00	-.3175E-01	-.3303E-04	.4439E-04	-.1141E-05	.8641E-08
318	24	9/17/75	V	U	0	50	9.5	.1001E+02	-.1828E+00	-.3407E-01	.9555E-03	-.8462E-05	.7066E-15	-.3222E-17
318	24	9/17/75	H	D	0	50	9.5	.1049E+02	.2031E+00	-.7654E-01	.2603E-02	-.6227E-04	.1087E-05	-.8177E-08
318	24	9/17/75	V	D	0	50	9.5	.1002E+02	.2591E+00	-.7874E-01	.2037E-02	-.1536E-04	-.8094E-15	.8668E-17
318	24	9/17/75	H	C	0	50	7.8	.1002E+02	.2591E+00	-.7874E-01	.2037E-02	-.1536E-04	-.8094E-15	.8668E-17
318	24	9/17/75	V	C	0	50	7.8	.1002E+02	.2591E+00	-.7874E-01	.2037E-02	-.1536E-04	-.8094E-15	.8668E-17

TABLE V.- Concluded

Miss	Fl	Date	Pol	Wind dir	θ, deg		Wind speed, m/s	A_0	A_1	A_2	A_3	A_4	A_5	A_6
					Min	Max								
335	3	1/16/76	H	U	0	50	14.2	.9887E+01	-.6133E+00	-.2047E-09	.1608E-10	-.5900E-12	.1016E-13	-.6640E-16
335	3	1/16/76	V	U	0	50	14.2	.9626E+01	-.6580E+00	.2753E-02	.1224E-10	-.4476E-12	.7692E-14	-.5014E-16
335	3	1/16/76	H	D	0	50	14.2	.9892E+01	-.6182E+00	-.6853E-10	.5825E-11	-.2261E-12	.4062E-14	-.2742E-16
335	3	1/16/76	V	D	0	50	14.2	.9562E+01	-.6366E+00	.2445E-02	.1147E-10	-.4244E-12	.7360E-14	-.4834E-16
335	3	1/16/76	H	C	0	50	14.2	.9729E+01	-.2929E+00	-.4192E-01	.1223E-02	-.1623E-04	.1818E-06	-.1421E-08
335	3	1/16/76	V	C	0	50	14.2	.9463E+01	-.1893E+00	-.5510E-01	.1667E-02	-.1692E-04	.8955E-07	-.7875E-09
335	4A	1/22/76	H	U	0	60	19.8	.9412E+01	-.4036E-01	-.3735E-01	.8614E-03	-.6280E-05	.3861E-14	-.2105E-16
335	4A	1/22/76	V	U	0	60	19.8	.9175E+01	-.7647E-01	-.3122E-01	.3714E-03	.1496E-04	-.3799E-06	.2396E-08
335	4A	1/22/76	H	D	0	60	19.6	.9414E+01	-.5860E-01	-.3088E-01	.6070E-03	-.3992E-05	.1113E-14	-.5984E-17
335	4A	1/22/76	V	D	0	60	19.6	.9140E+01	-.8225E-01	-.2797E-01	.3867E-03	.8015E-05	-.2269E-06	.1421E-08
335	4A	1/22/76	H	C	0	60	19.4	.9733E+01	-.1350E+00	-.4519E-01	.1080E-02	-.7617E-05	.5719E-15	-.3174E-17
335	4A	1/22/76	V	C	0	60	19.4	.9662E+01	-.1691E+00	-.3789E-01	.3119E-03	.2842E-04	-.6644E-06	.4212E-08
335	4B	1/22/76	H	U	0	60	19.9	.8510E+01	-.3124E-01	-.3327E-01	.5714E-03	.2607E-05	-.1301E-06	.7738E-09
335	4B	1/22/76	V	U	0	60	19.9	.8268E+01	-.7106E-01	-.2929E-01	.2282E-03	.2021E-04	-.4666E-06	.2914E-08
335	4B	1/22/76	H	D	0	60	19.7	.8406E+01	.1445E+00	-.4434E-01	.6156E-03	.1151E-04	-.3360E-06	.2123E-08
335	4B	1/22/76	V	D	0	57	19.7	.8156E+01	.6655E-01	-.3806E-01	.7133E-03	.1528E-05	-.1400E-06	.8879E-09
335	4B	1/22/76	H	C	0	60	19.8	.8757E+01	-.5116E-01	-.4850E-01	.1445E-02	-.2551E-04	.3530E-06	-.2320E-08
335	4B	1/22/76	V	C	0	57	19.8	.8696E+01	-.9419E-01	-.4593E-01	.1260E-02	-.1349E-04	.1023E-06	-.6952E-09
335	5	1/23/76	H	U	0	60	14.6	.9627E+01	-.1241E+00	-.3252E-01	.6726E-03	-.4094E-05	.5325E-14	-.2929E-16
335	5	1/23/76	V	U	0	60	14.6	.9289E+01	-.9632E-01	-.3677E-01	.8824E-03	-.6097E-05	.3768E-14	-.2047E-16
335	5	1/23/76	H	D	0	60	14.7	.9846E+01	.6149E-01	-.4977E-01	.1082E-02	-.7289E-05	.8316E-14	-.4557E-16
335	5	1/23/76	V	D	0	60	14.7	.9593E+01	.2231E-01	-.4450E-01	.7466E-03	.8967E-05	-.3027E-06	.1893E-08
335	5	1/23/76	H	C	0	60	14.9	.1005E+02	-.1317E+00	-.4346E-01	.6039E-03	.1487E-04	-.4047E-06	.2513E-08
335	5	1/23/76	V	C	0	60	14.9	.9925E+01	-.1101E+00	-.4627E-01	.5770E-03	.2359E-04	-.5935E-06	.3698E-08
335	6	1/28/76	H	U	0	60	15.0	.9999E+01	-.1368E-01	-.3999E-01	.3714E-03	.2011E-04	-.4566E-06	.2698E-08
335	6	1/28/76	V	U	0	60	15.0	.9827E+01	.7428E-01	-.5124E-01	.6029E-03	.2935E-04	-.7556E-06	.4930E-08
335	6	1/28/76	H	D	0	58	15.0	.1003E+02	-.6650E-02	-.4681E-01	.9686E-03	-.5955E-05	.3520E-14	-.2006E-16
335	6	1/28/76	V	D	0	58	15.0	.9819E+01	.3200E-01	-.4997E-01	.1003E-02	.2552E-05	-.2070E-06	.1291E-08
335	6	1/28/76	H	C	0	58	15.0	.9871E+01	.5809E-02	-.5102E-01	.6701E-03	.1805E-04	-.4732E-06	.2880E-08
335	6	1/28/76	V	C	0	57	15.0	.9735E+01	.3900E-01	-.5530E-01	.8181E-03	.1926E-04	-.5349E-06	.3306E-08
353	9	3/ 2/77	H	U	0	67	8.9	.1156E+02	-.1213E-01	-.6961E-01	.2361E-02	-.3464E-04	.2224E-06	-.4568E-09
353	9	3/ 2/77	V	U	0	68	8.9	.1104E+02	.2394E+00	-.1023E+00	.3881E-02	-.6367E-04	.4806E-06	-.1355E-08
353	9	3/ 2/77	H	D	0	50	9.7	.1145E+02	.4151E-01	-.7078E-01	.2010E-02	-.2267E-04	.8579E-07	.4928E-10
353	9	3/ 2/77	V	D	0	67	9.7	.1114E+02	.1690E+00	-.9522E-01	.3545E-02	-.5814E-04	.4492E-06	-.1335E-08
353	9	3/ 2/77	H	C	0	40	11.2	.1150E+02	.1468E+00	-.8794E-01	.2340E-02	-.2395E-04	.8625E-07	.9037E-15
353	9	3/ 2/77	V	C	0	68	11.2	.1101E+02	.7576E-01	-.8093E-01	.2214E-02	-.2277E-04	.8209E-07	-.2359E-16
353	10	3/ 3/77	H	U	10	20	5.3	.1902E+02	-.1273E+01	-.1537E-05	.1398E-06	-.7074E-08	.1887E-09	-.2074E-11
353	10	3/ 3/77	V	U	10	20	5.3	.1862E+02	-.1248E+01	.1283E-04	-.1177E-05	.6005E-07	-.1614E-08	.1788E-10
353	10	3/ 3/77	H	D	10	20	5.3	.2081E+02	-.1399E+01	.1421E-04	-.1308E-05	.6691E-07	-.1805E-08	.2005E-10
353	10	3/ 3/77	V	D	10	20	5.3	.2015E+02	-.1359E+01	-.1782E-04	.1635E-05	-.8342E-07	.2243E-08	-.2486E-10
353	10	3/ 3/77	H	C	10	20	5.3	.2040F+02	-.1403E+01	.1931E-04	-.1778E-05	.9094E-07	-.2453E-08	.2725E-10
353	10	3/ 3/77	V	C	10	20	5.3	.2001E+02	-.1402E+01	-.1411E-04	.1296E-05	-.6619E-07	.1782E-08	-.1976E-10
353	11	3/ 8/77	H	U	0	67	15.9	.9770E+01	-.1973E-01	-.3334E-01	.4852E-03	.2914E-05	-.9972E-07	.5118E-09
353	11	3/ 8/77	V	U	0	67	15.9	.9770E+01	.7219E-01	-.5475E-01	.1701E-02	-.2330E-04	.1538E-06	-.4053E-09
353	11	3/ 8/77	H	D	0	68	16.4	.1008E+02	.1514E+00	-.6522E-01	.1928E-02	-.2616E-04	.1701E-06	-.4348E-09
353	11	3/ 8/77	V	D	0	68	16.4	.1011E+02	.1976E+00	-.7381F-01	.2408E-02	-.3406E-04	.2207E-06	-.5286E-09
353	11	3/ 8/77	H	C	0	67	16.2	.9268E+01	.1213E+00	-.6339E-01	.1765E-02	-.2110E-04	.1078E-06	-.1711E-09
353	11	3/ 8/77	V	C	0	67	16.2	.9570E+01	.2710E+00	-.8752E-01	.2963E-02	-.4431E-04	.3086E-06	-.8146E-09
353	13	3/10/77	H	U	0	69	11.0	.1060E+02	.1713E-01	-.6067E-01	.1710E-02	-.1912E-04	.7613E-07	-.1035E-15
353	13	3/10/77	V	U	0	70	11.0	.1060E+02	.2739E-01	-.7063E-01	.2510E-02	-.3874E-04	.2853E-06	-.8267E-09
353	13	3/10/77	H	D	0	40	11.1	.1040E+02	.4287E-01	-.5379E-01	.1208E-02	-.1084E-04	.3549E-07	.5816E-15
353	13	3/10/77	V	D	0	68	11.1	.1060F+02	.2802E-01	-.5199E-01	.1095E-02	-.3049E-05	-.9390E-07	.6367E-09
353	13	3/10/77	H	C	0	40	11.4	.1075E+02	.1247E+00	-.8237E-01	.2432E-02	-.3177E-04	.2128E-06	-.6276E-09
353	13	3/10/77	V	C	0	68	11.4	.1105E+02	.1092E+00	-.8612E-01	.2685E-02	-.3235E-04	.1368E-06	-.1004E-16
353	14	3/11/77	H	U	0	68	14.3	.1040F+02	-.3273E-01	-.5140E-01	.1459E-02	-.1671E-04	.6890E-07	-.1548E-16
353	14	3/11/77	V	U	0	68	14.3	.1040E+02	-.4691E-01	-.5307E-01	.1602E-02	-.1832E-04	.7329E-07	-.1977E-16
353	14	3/11/77	H	D	0	68	13.7	.1070F+02	.5258E-01	-.5795E-01	.1517F-02	-.1575E-04	.5865E-07	-.2690E-16
353	14	3/11/77	V	D	0	68	13.7	.1122E+02	.2624E-01	-.5948E-01	.1765E-02	-.1999E-04	.7899E-07	-.1306E-16
353	14	3/11/77	H	C	0	67	13.5	.1007E+02	.1361E+00	-.6887E-01	.1703E-02	-.1626E-04	.5511E-07	-.2433E-16
353	14	3/11/77	V	C	0	67	13.5	.1030E+02	.1584E+00	-.7383E-01	.1984E-02	-.2039E-04	.7356E-07	-.3814E-16
353	15	3/14/77	H	U	10	40	4.2	.1882E+02	-.1289E+01	.4610E-02	-.2486E-08	.7992E-10	-.1318E-11	.8748E-14
353	15	3/14/77	V	U	10	40	4.2	.1931F+02	-.1359E+01	.7633E-02	-.6275E-08	.2014E-09	-.3316E-11	.2197F-13
353	15	3/14/77	H	D	10	40	4.2	.1894E+02	-.1230E+01	-.7572E-08	.4529E-09	-.1460E-10	.2413E-12	-.1605E-14
353	15	3/14/77	V	D	10	40	4.2	.2035E+02	-.1469E+01	.8804E-02	.1738E-08	-.5549E-10	.9096E-12	-.6002E-14
353	15	3/14/77	H	C	10	40	4.2	.2127E+02	-.1538E+01	.5221E-02	-.1538E-08	.4937E-10	-.8133E-12	.5392E-14
353	15	3/14/77	V	C	10	40	4.2	.2121E+02	-.1556E+01	.7706E-02	-.5501E-09	.1840E-10	-.3144E-12	.2152E-14
353	20	3/22/77	H	U	10	40	2.5	.1952E+02	-.1336E+01	.2343E-02	.1031E-08	-.3287E-10	.5381E-12	-.3547F-14
353	20	3/22/77	V	U	10	40	2.5	.2046F+02	-.1466E+01	.6675E-02	.1546E-08	-.4921E-10	.8038E-12	-.5288E-14
353	20	3/22/77	H	D	10	40	2.5	.1465E+02	-.8045E+00	-.9838E-02	-.9123E-10	.3481E-11	-.6578E-13	.4876E-15
353	20	3/22/77	V	D	10	40	2.5	.1577E+02	-.9852E+00	-.2148E-02	-.2666E-08	.8522E-10	-.1398E-11	.9235E-14
353	20	3/22/77	H	C	10	40	2.5	.2114F+02	-.1599E+01	.4864E-02	.1144E-07	-.3670E-09	.6041E-11	-.4001E-13
353	20	3/22/77	V	C	10	40	2.5	.2197F+02	-.1695E+01	.8694F-02	-.5075E-09	.1676E-10	-.2833E-12	.1921E-14
353	21	3/24/77	H	U	0	40	4.7	.1210E+02	.3160E+00	-.1141E+00	.3107E-02	-.3252E-04	.1203E-06	.9971F-15
353	21	3/24/77	V	U	0	40	4.7	.1290E+02	.1545E+00	-.1079E+00	.3126E-02	-.3381E-04	.1275E-06	.1585E-14
353	21	3/24/77	H	D	0	50	5.9	.1242E+02	.7124E+00	-.1456E+00	.3968E-02	-.4231E-04	.1598E-06	.1873E-15
353	21	3/24/77	V	D	0	50	5.9	.1305F+02	.2603E+00	-.1149E+00	.3429E-02	-.3899E-04	.1551E-06	.1507E-15
353	21	3/24/77	H	C	0	40	4.7	.1210F+02	.1154E+00	-.8992E-01	.2098E-02	-.1801E-04	.5261E-07	.6846E-15
353	21	3/24/77	V	C	0	40	4.7	.1290E+02	.8416E-01	-.9481E-01	.2498E-02	-.2526E-04	.9093E-07	.1164E-14

TABLE VI.- NRCS EVERY 10° OF INCIDENCE FOR UPWIND, DOWNWIND, AND CROSSWIND DIRECTIONS

[Data derived from weighted regressions of table IV data]

Miss	Fl	Wind speed, m/s	Pol	Wind dir	NRCS, dB, at incidence angle of -						
					0°	10°	20°	30°	40°	50°	60°
230	FCF	14.50	H	U	10.3	5.1	-2.0	-7.9	-12.2	-16.5	-20.8 *
230	FCF	14.50	V	U	10.3	4.5	-2.4	-7.5	-10.3	-13.0	-15.7 *
230	FCF	15.00	H	C	9.9	4.8	-4.3	-11.0	-15.2	-19.4	-23.5 *
230	FCF	15.00	V	C	10.0	4.2	-4.5	-10.9	-13.5	-16.2	-19.0 *
238	20	6.50	H	U	11.2	5.7 *	-5.3 *	-14.6	-19.5	-22.7	-25.8 *
238	20	6.50	V	U	11.2	5.5 *	-5.7 *	-14.0	-17.0	-18.0	-19.1 *
238	20	6.50	H	D	9.7	4.9 *	-6.5 *	-16.9	-22.9	-26.0	-29.1 *
238	20	6.50	V	D	9.4	4.5 *	-6.8 *	-15.6	-18.8	-19.9	-21.0 *
238	20	6.50	H	C	11.1	6.4 *	-6.6 *	-17.9	-23.9	-28.3	-32.7 *
238	20	6.50	V	C	10.8	5.9 *	-6.7 *	-17.9	-23.4	-24.3	-25.1 *
238	27	3.00	H	U	12.4	3.1 *	-10.7 *	-21.2	-26.3	-31.3	-36.3 *
238	27	3.00	V	U	12.0	2.8 *	-10.9 *	-20.8	-24.5	-26.5	-28.6 *
238	27	3.00	H	D	12.7	4.5 *	-9.0 *	-20.1	-26.5	-32.6	-38.7 *
238	27	3.00	V	D	12.3	4.1 *	-9.3 *	-19.2	-23.6	-26.6	-29.6 *
238	27	3.00	H	C	13.5	5.0 *	-10.4 *	-23.2	-29.8	-31.9	**
238	27	3.00	V	C	13.1	3.7 *	-11.2 *	-22.1	-26.2	-26.9	-27.6 *
288	5	22.20	H	U	6.8	5.2	0.0	-5.0	-7.9	-10.1	**
288	5	22.20	V	U	6.8	4.9	.2	-4.7	-6.6	-8.0	**
288	5	22.20	H	D	6.7	5.1	.7	-5.2	-10.2	-14.1	**
288	5	22.20	V	D	6.3	5.2	.8	-4.6	-8.3	-11.2	**
288	5	22.30	H	C	6.4	4.1	-2.2	-8.9	-13.6	-17.3	**
288	5	22.30	V	C	6.3	3.9	-1.9	-8.0	-11.8	-14.2	**
288	6	13.40	H	U	9.1	5.5	-.2	-8.0	-12.8	-15.8	**
288	6	13.40	V	U	9.0	5.8	.1	-7.2	-10.7	-12.4	**
288	6	14.60	H	D	9.5	7.7	.2	-9.1	-15.9	-20.1	**
288	6	14.60	V	D	9.2	6.8	.6	-8.0	-12.9	-15.6	**
288	6	13.10	H	C	9.5	5.8	-2.2	-12.3	-18.8	-23.7	**
288	6	13.10	V	C	9.5	5.9	-2.2	-11.0	-16.3	-19.1	**
306	FCF	21.50	H	U	9.8	6.5	1.8 *	-3.7	-9.1 *	-13.6	-16.7
306	FCF	21.50	V	U	9.7	7.5	2.5 *	-2.7	-6.9 *	-9.9	-12.8
306	FCF	21.50	H	D	9.8	8.3	3.2	-2.6	-7.5	-11.5	-15.7
306	FCF	21.50	V	D	9.7	8.2	3.7	-1.1	-5.1	-8.2	-11.7
306	FCF	21.50	H	C	9.8	7.1	.8 *	-6.2	-12.0 *	-16.4	-20.1
306	FCF	21.50	V	C	9.7	7.3	1.1 *	-5.3	-10.1 *	-13.0	-15.5
318	13	4.50	H	U	12.3	6.6	-6.3	-18.1	-25.7	-31.3	-36.8 *
318	13	4.50	V	U	10.9	5.3	-7.6	-18.8	-24.8	-27.4	-30.1 *
318	13	4.50	H	D	12.4	7.2	-6.9	-17.3	-31.4	-32.9	-40.7 *
318	13	4.50	V	D	11.1	4.5	-7.8	-18.3	-24.3	-28.1	-31.9 *
318	13	4.50	H	C	13.3	6.4	-9.6	-23.7	-31.4	-39.0	-46.6 *
318	13	4.50	V	C	12.5	3.9	-10.7	-24.1	-32.5	-35.0	-37.6 *
318	14	5.50	H	U	12.6	6.3	-5.6	-17.6	-26.5	-31.6	-34.5
318	14	5.50	V	U	12.4	6.2	-5.8	-17.1	-24.2	-26.8	-28.3
318	14	5.50	H	D	12.1	7.5	-5.3	-18.1	-26.9	-31.9	-36.8
318	14	5.50	V	D	11.8	7.4	-5.3	-16.7	-22.6	-23.6	-26.4
318	14	5.50	H	C	12.3	6.1	-6.7	-20.2	-31.0	-37.3	-39.4
318	14	5.50	V	C	12.3	6.2	-7.1	-20.0	-28.5	-31.9	-33.3
318	16	8.80	H	U	11.0	6.8	-2.7	-11.6	-17.6	-23.0	-28.0
318	16	8.80	V	U	10.7	6.3	-3.2	-11.3	-15.5	-17.8	-20.3
318	16	9.00	H	D	10.8	7.3	-2.9	-13.4	-21.1	-26.4	-31.8
318	16	9.00	V	D	10.6	6.7	-3.4	-12.4	-17.1	-18.3	-21.1
318	16	8.10	H	C	11.8	6.7	-5.0	-17.1	-26.3	-31.6	-35.5
318	16	8.10	V	C	11.3	5.9	-5.3	-16.3	-24.1	-27.7	-28.8
318	17	12.20	H	U	10.3	6.6	-1.2	-9.2	-15.5	-19.8	-23.9
318	17	12.20	V	U	9.8	6.1	-1.8	-9.1	-13.5	-15.7	-17.9
318	17	12.30	H	D	10.4	7.1	-1.5	-10.4	-17.1	-22.1	-27.3
318	17	12.30	V	D	9.9	6.6	-1.6	-9.4	-14.2	-16.6	-19.1
318	17	12.40	H	C	10.6	6.3	-3.7	-13.7	-20.8	-25.1	-29.1
318	17	12.40	V	C	10.4	6.0	-4.3	-13.7	-19.2	-21.6	-24.2
318	18	11.30	H	U	10.3	7.1	-2.9	-12.0 *	-17.1	-21.0 *	-24.9
318	18	11.30	V	U	9.8	6.5	-3.6	-11.5 *	-14.1	-16.2 *	-18.3
318	18	11.30	H	D	12.7	7.4	-2.9	-13.0 *	-19.5	-23.9 *	-28.5
318	18	11.30	V	D	9.9	7.0	-2.9	-11.8 *	-15.7	-17.8 *	-20.0
318	18	11.30	H	C	10.6	7.0	-3.6	-14.3 *	-21.7	-26.1 *	-30.5
318	18	11.30	V	C	10.4	6.7	-4.1	-14.4 *	-21.4	-22.9 *	-25.5
318	19	7.50	H	U	11.4	7.4	-3.7	-13.7 *	-19.4	-24.6 *	-29.8
318	19	7.50	V	U	10.8	6.8	-4.4	-13.5 *	-17.0	-19.2 *	-21.4
318	19	7.60	H	D	11.4	7.4	-3.0	-13.7	-21.7	-27.1	**
318	19	7.60	V	D	10.8	6.6	-3.1	-12.4	-17.9	-20.1	-22.4
318	19	7.80	H	C	11.3	6.9	-3.8	-15.2	-24.1	-29.8	**
318	19	7.80	V	C	10.7	6.2	-4.5	-15.0	-22.4	-26.5	-30.4
318	24	9.50	H	U	10.6	6.5	-.9	-8.2	-15.1	-23.4	**
318	24	9.50	V	U	9.9	5.6	-1.0	-7.2	-12.3	-17.7	**
318	24	9.50	H	D	10.6	7.0	-2.3	-12.0	-19.0	-22.6	**
318	24	9.50	V	D	10.2	6.6	-2.4	-10.5	-14.5	-15.2	**

*Extrapolated from data greater than 5° removed in incidence angle.
**No data.

TABLE VI.- Concluded

Miss	Fl	Wind speed, m/s	Pol	Wind dir	NRCS, dB, at incidence angle of -						
					0°	10°	20°	30°	40°	50°	60°
335	3	14.20	H	U	9.7	3.8	-2.4 *	-8.5	-14.6 *	-20.8	-26.9 *
335	3	14.20	H	D	9.7	3.8	-2.5 *	-8.7	-14.8 *	-21.0	-27.2 *
335	3	14.20	H	C	9.7	3.7	-5.2	-13.5	-19.6	-23.7	-27.7 *
335	3	14.20	V	D	9.6	3.3	-2.4 *	-7.6	-12.3 *	-16.4	-19.9 *
335	3	14.20	V	U	9.6	3.4	-2.2 *	-7.3	-12.0 *	-16.2	-19.8 *
335	3	14.20	V	C	9.6	3.6	-5.5	-12.9	-16.9	-19.4	-22.0 *
335	4A	19.80	H	U	9.4	6.1	-.5	-7.2	-12.9	-17.6	-22.8
335	4A	19.80	V	U	9.1	5.8	-.5	-6.5	-10.9	-14.0	-17.2
335	4A	19.60	H	D	9.4	6.3	.1	-7.0 *	-13.7	-19.8 *	-25.9
335	4A	19.60	V	D	9.1	6.0	.1	-6.0 *	-11.1	-15.2 *	-19.2
335	4A	19.50	H	C	9.7	4.9	-3.6	-12.0	-18.4	-22.6	-26.5
335	4A	19.50	V	C	9.6	4.7	-3.7	-11.2	-16.1	-18.8	-21.4
335	4B	19.90	H	U	8.5	5.5	-.8	-7.4	-12.9	-17.1	-21.0
335	4B	19.90	V	U	8.2	5.0	-1.1	-6.9	-11.0	-14.0	-17.1
335	4B	19.70	H	D	8.4	6.1	-.6	-7.8	-13.6	-18.2	-22.7
335	4B	19.70	V	D	8.1	5.7	-.2	-6.4	-11.2	-14.8	-18.3
335	4B	19.80	H	C	8.8	4.6	-3.2	-11.2	-17.1	-19.7	-21.0
335	4B	19.80	V	C	8.7	4.3	-3.4	-10.4	-14.8	-16.5	-17.6
335	5	14.60	H	U	9.6	5.8	-1.1	-8.5	-14.8	-19.4	-22.7
335	5	14.60	V	U	9.3	5.5	-1.3	-7.8	-12.5	-15.2	-17.3
335	5	14.70	H	D	9.8	6.5	-1.3	-9.8	-16.7	-21.8	-26.3
335	5	14.70	V	D	9.6	6.2	-1.2	-8.3	-13.2	-16.2	-18.9
335	5	14.90	H	C	10.0	5.1	-3.9	-12.7	-19.2	-24.0	-28.6
335	5	14.90	V	C	9.9	4.9	-4.0	-12.0	-16.9	-19.4	-21.8
335	6	15.00	H	U	9.9	6.4	-1.4	-9.2 *	-15.1	-19.1 *	-23.1
335	6	15.00	V	U	9.7	6.2	-1.7	-8.8 *	-12.6	-14.9 *	-17.2
335	6	15.00	H	D	10.0	6.3	-1.8	-10.6	-17.9	-22.8	-26.0
335	6	15.00	V	D	9.8	6.1	-1.7	-9.1	-14.1	-16.7	-19.0
335	6	15.00	H	C	9.8	5.6	-3.5	-12.5	-19.2	-23.7	-28.3
335	6	15.00	V	C	9.7	5.5	-3.5	-11.8	-16.8	-19.5	-22.1
353	9	8.90	H	U	11.6	6.5	-2.5	-10.7	-17.0	-22.1	-27.1
353	9	8.90	V	U	11.1	6.5	-2.8	-10.0	-14.1	-16.6	-19.4
353	9	9.70	H	D	11.5	6.6	-3.3	-13.0	-20.6	-26.4	-31.6 *
353	9	9.70	V	D	11.5	6.3	-3.2	-10.9	-15.9	-19.2	-22.2
353	9	11.20	H	C	11.5	6.3	-5.6	-17.4 *	-26.1	**	**
353	9	11.20	V	C	11.0	5.7	-5.5	-16.2 *	-23.6	-27.4 *	-28.9
353	10	5.40	H	U	**	6.3	-6.4	**	**	**	**
353	10	5.40	V	U	**	6.1	-6.3	**	**	**	**
353	10	5.40	H	D	**	6.8	-7.2	**	**	**	**
353	10	5.40	V	D	**	6.6	-7.0	**	**	**	**
353	10	5.40	H	C	**	6.4	-7.7	**	**	**	**
353	10	5.40	V	C	**	6.0	-8.0	**	**	**	**
353	11	15.90	H	U	9.8	6.7 *	.1	-7.4 *	-14.0	-18.9 *	-22.5
353	11	15.90	V	U	9.8	6.5 *	-.3	-6.9 *	-11.6	-14.7 *	-16.8
353	11	16.40	H	D	10.1	6.8	-1.2	-9.4	-16.1	-21.5	-26.2
353	11	16.40	V	D	10.1	6.8	-1.0	-8.0	-12.7	-15.7	-18.1
353	11	16.20	H	C	9.3	5.7	-2.6	-11.1	-18.0	-23.3	-27.8
353	11	16.20	V	C	9.6	6.1	-2.5	-10.1	-15.2	-18.5	-21.6
353	13	11.00	H	U	10.4	6.2	-2.5	-11.0 *	-17.5	-22.2 *	-26.1
353	13	11.00	V	U	10.6	6.0	-2.4	-9.4 *	-14.0	-16.8 *	-18.8
353	13	11.10	H	D	10.4	6.6	-2.2	-12.0 *	-20.8	**	**
353	13	11.10	V	D	10.6	6.7	-1.6	-10.1 *	-16.2	-19.6 *	-21.2
353	13	11.40	H	C	10.7	5.9	-4.7	-15.0	-22.5	-26.9	-29.5 *
353	13	11.40	V	C	10.6	5.9	-4.5	-13.6	-19.3	-22.6	-25.3
353	14	14.30	H	U	10.4	6.2 *	-1.6	-9.3 *	-15.5	-20.3 *	-24.5
353	14	14.30	V	U	10.4	6.1 *	-1.6	-8.6 *	-13.3	-16.0 *	-17.9
353	14	13.70	H	D	10.7	6.8	-1.6	-10.2	-17.1	-22.0	-25.6
353	14	13.70	V	D	11.2	7.1	-.9	-8.2	-13.0	-15.8	-17.8
353	14	13.50	H	C	10.1	6.1	-3.6	-13.7	-21.6	-26.8	-29.6
353	14	13.50	V	C	10.3	6.3	-3.2	-12.6	-19.2	-22.9	-24.6
353	15	4.20	H	U	**	6.4	-5.1	-15.7 *	-25.4	**	**
353	15	4.20	V	U	**	6.5	-4.8	-14.6 *	-22.8	**	**
353	15	4.20	H	D	**	6.6	-5.7	-17.9 *	-30.2	**	**
353	15	4.20	V	D	**	6.5	-5.5	-15.8 *	-24.3	**	**
353	15	4.20	H	C	**	6.4	-7.4	-20.2 *	-31.9	**	**
353	15	4.20	V	C	**	6.4	-6.8	-18.5 *	-28.7	**	**
353	20	2.50	H	U	**	6.4	-6.3	-18.5 *	-30.2	**	**
353	20	2.50	V	U	**	6.5	-6.2	-17.5 *	-27.5	**	**
353	20	2.50	H	D	**	5.6	-5.4	-18.3 *	-33.3	**	**
353	20	2.50	V	D	**	5.7	-4.8	-15.7 *	-27.1	**	**
353	20	2.50	H	C	**	5.6	-8.9	-22.5 *	-35.1	**	**
353	20	2.50	V	C	**	5.9	-8.5	-21.1 *	-31.9	**	**
353	21	4.70	H	U	12.1	6.6	-7.2	-20.7 *	-30.0	-34.7 *	**
353	21	4.70	V	U	12.9	6.5	-7.2	-19.5 *	-27.0	-29.9 *	**
353	21	5.90	H	D	12.4	8.6	-6.1	-20.5	-30.6	-34.4	**
353	21	5.90	V	D	13.0	7.2	-6.0	-17.8	-24.9	-27.9	**
353	21	4.70	H	C	12.1	6.2	-7.5	-22.0 *	-33.6	-40.7 *	**
353	21	4.70	V	C	12.9	6.5	-7.1	-20.7 *	-30.9	-37.2 *	**

*Extrapolated from data greater than 5° removed in incidence angle.
**No data.

TABLE VII.- REGRESSION ANALYSIS RESULTS FOR NRCS (RATIO) VERSUS WIND SPEED

Wind direction	Pol	θ, deg	B_0	B_1	B_2	Std err	R^2	Comment (a)
U	H	0	17.97893	-0.56525		0.0238	0.8758	
		10	4.76453	-.61307E-1		.0282	.2726	
		20	.14488	.41391E-1		.0422	.7724	
		30	.20341E-1	-.62803E-16	0.53160E-3	.0445	.8419	
		40	.52740E-2	-.19165E-17	.14699E-3	.0591	.7704	2
		50	.29094E-2	-.60146E-17	.57893E-4	.0991	.5848	2, 3
		60	.36137E-3	-.15428E-17	.18732E-4	.0409	.8790	2
D	H	0	17.43249	-0.51515		0.0420	0.6736	
		10	5.83647	-.83903E-1		.0451	.1740	
		20	-.38630E-1	.57366E-1		.0638	.7377	1
		30	.90680E-2	-.30019E-16	0.44506E-2	.0315	.9073	2
		40	-.70691E-4	-.76994E-17	.10715E-3	.0346	.9352	1, 2
		50	.24983E-3	-.17086E-17	.34600E-4	.0520	.8392	2
		60	.22539E-3	-.17846E-18	.97390E-5	.0816	.7467	2
C	H	0	21.64335	-0.76927		0.0386	0.8472	5
		10	4.6170	-.76068E-1		.0275	.4897	2
		20	1.07437	.21604E-1		.0441	.6850	2
		30	.13601E-1	-.19370E-16	0.17795E-3	.0504	.8112	2
		40	.10421E-2	.71432E-17	.47768E-4	.0673	.7570	2
		50	.87777E-4	-.22832E-17	.21210E-4	.0929	.6765	2
		60	-.15039E-2	-.49692E-18	.16488E-4	.1753	.6019	1, 2, 4
U	V	0	16.96216	-0.50510		0.0265	0.8849	5
		10	4.58217	-.62594E-1		.0310	.2549	
		20	.12151	.41536E-1		.0489	.7221	
		30	.22667E-1	.76412E-16	0.61815E-3	.0465	.8304	2
		40	.10176E-1	-.34462E-16	.22967E-3	.0562	.7651	2
		50	.93569E-2	-.44957E-16	.12384E-3	.0809	.5808	2
		60	.73282E-2	-.58224E-17	.40944E-4	.0413	.6978	2
D	V	0	16.12915	-0.46316		0.0506	0.5910	
		10	4.6872	-.30126E-1		.0428	.0374	
		20	-.60917E-1	.62357E-1		.0757	.6991	1
		30	.12425E-1	.54671E-16	0.60577E-3	.0292	.9241	
		40	.38442E-2	-.83137E-18	.19459E-3	.0296	.9355	2
		50	.53939E-2	.57945E-17	.86501E-3	.0476	.7627	2
		60	.57356E-2	-.57621E-17	.26529E-4	.0515	.6462	2
C	V	0	20.78353	-0.71340		0.0372	0.8641	5
		10	4.42424	-.70002E-1		.0326	.3454	
		20	.10190	.21997E-1		.0472	.6699	
		30	.12743E-1	-.66526E-16	0.23273E-3	.0562	.8004	2
		40	.12927E-2	.48132E-17	.84863E-4	.0636	.8008	
		50	.12851E-2	-.46227E-17	.47182E-4	.0704	.7746	2
		60	-.17752E-2	-.34135E-17	.37199E-4	.0816	.7919	1, 2

[a] 1 - NRCS < 0 at low wind speeds; 2 - SASS I line is better at low winds; 3 - SASS I line is better at high winds; 4 - fit is not too good; 5 - higher order fit might be better.

TABLE VIII.- REGRESSION RESULTS FOR NRCS (θ,ϕ) FOR RADSCAT CIRCLE DATA FOR NINTH-ORDER MODEL

$$\left[(\text{NRCS}) = A_0 + A_1\theta + A_2 \cos\phi + A_3\theta \cos\phi + A_4 \sin\phi + A_5\theta \sin\phi + A_6 \cos 2\phi + A_7\theta \cos 2\phi + A_8 \sin 2\phi + A_9\theta \sin 2\phi\right]$$

Miss	Fl	Run	Wind speed, m/s	Pol	θ_{mean}, deg	A_0	A_1	A_2	A_3	A_4	A_5	A_6	A_7	A_8	A_9	No. points	NSD	R^2	ϕ critical points, deg			
																			U_{max}	$C1_{min}$	D_{max}	$C2_{min}$
230	FCF	1	15.0	H	30.3	.592E+00	-.162E-01	.961E-01	-.293E-02	.149E+00	-.458E-02	-.136E+00	.397E-02	-.127E+00	.291E-02	666	.277	.808	307.9	32.2	119.8	215.2
230	FCF	1	15.0	V	30.3	.743F+00	-.202F-01	-.216E+00	.728E-02	.965E-01	-.249E-02	.880E-01	-.343E-02	-.466E+00	.137E-01	682	.212	.659	309.0	34.3	123.4	217.7
238	20	2	6.5	H	31.0	.113E+00	-.303F-02	-.571E-01	.157E-02	-.195E-01	.743E-03	.538E-02	-.166E-03	.102E-01	-.470E-03	1748	.279	.684	136.5	243.4	316.7	29.7
239	20	2	6.5	V	31.0	.151E+00	-.399E-02	-.375E-01	.112E-02	-.841E-01	.276E-02	-.175E-01	.552E-03	-.814E-02	-.236E-04	2088	.297	.532	135.4	228.5	311.8	39.3
238	27	3	3.0	H	32.8	.180E-01	-.374E-03	.987E-02	-.317E-03	-.725E-02	.241E-03	-.182E-01	.519E-03	.167E-01	-.497E-03	1171	.261	.641	87.9	178.9	253.4	345.8
239	27	3	3.0	V	32.8	.956E-02	.275F-04	.333E-01	-.103E-02	-.141E-03	.400E-04	-.311E-01	.875E-03	.210E-01	-.634E-03	1317	.228	.566	91.3	185.4	264.0	351.6
288	5	1	23.6	H	33.7	.327F+00	-.793E-02	.261E-01	-.602E-03	-.119F+00	.363E-02	-.150E+00	.402E-02	.407E-01	-.688E-03	823	.215	.662	247.2	330.8	62.7	158.5
288	5	1	23.6	V	33.7	.346E+00	-.784E-02	.101E+00	-.270E-02	.568E-01	-.107E-02	-.204E-01	.930E-04	.613E-01	-.109E-02	819	.247	.665	241.9	321.7	62.9	163.4
288	5	8	23.6	H	34.4	.253E+00	-.559E-02	.389E-01	-.129E-02	-.850E-02	.333E-03	-.836E-02	.389E-03	.476E-01	-.756E-03	928	.228	.668	214.8	309.9	42.3	126.7
288	5	8	23.6	V	34.4	.307F+00	-.662E-02	.518E-01	-.142E-02	.629E-01	-.147E-02	-.339E-01	.108E-02	.111E+00	-.241E-02	877	.220	.640	217.9	306.8	44.9	137.2
288	6	1	13.5	H	35.9	.220F+00	-.553E-02	-.159E+00	.430E-02	-.212E-01	.716E-03	.791E-01	-.192E-02	-.788E-01	.203E-02	403	.194	.802	165.4	266.3	355.0	71.6
288	6	1	13.5	V	35.9	.635F-01	-.846F-03	.408E-01	-.117E-02	-.329E-01	.896E-03	.589E-01	-.115E-02	.310E-02	-.121E-03	410	.148	.868	178.5	268.8	357.3	87.1
288	6	7	13.5	H	36.9	.634F-01	-.136E-02	.213E-01	-.649E-03	.156E-01	-.441E-03	.399E-01	-.901E-03	.235E-02	-.281E-04	758	.183	.917	186.3	281.3	4.7	90.0
288	6	7	13.5	V	36.9	.781E-01	-.159E-02	-.433E-01	.115E-02	.453E-02	-.160E-03	.560E-01	-.127E-02	.104E-01	-.281E-03	345	.151	.877	182.3	271.9	358.0	88.6
306	FCF	1	21.5	H	53.4	.165E+00	-.259E-02	.550E-01	-.110E-02	-.480E-01	.946E-03	-.268E+00	.496E-02	-.159E-01	.121E-03	225	.207	.701	303.6	30.1	127.5	221.9
306	FCF	1	21.5	V	53.4	.286E+00	-.416E-02	.189E+00	-.366E-02	-.205E+00	.391E-02	-.394E+00	.722E-02	-.343E-01	.280E-03	214	.171	.726	300.7	28.9	125.1	217.6
306	FCF	11	21.5	H	14.1	.769E+01	-.321E+00	-.304E+01	.185E+00	.438E+01	-.279E+00	-.266E+01	.156E+00	.362E+00	-.637E-01	210	.285	.429	288.7	13.8	118.3	217.8
306	FCF	11	21.5	V	14.1	.102F+02	-.474E+00	.176E+01	-.138F+00	.155E+01	-.765E-01	-.325E+01	.193E+00	-.125E+01	.576E-01	221	.275	.378	289.3	9.1	110.2	210.7
306	FCF	4	21.5	H	62.4	.316E-01	-.304F-03	-.129E+00	.204E-02	.115E+00	-.187E-02	-.636E-01	.947E-03	-.461E-02	-.650E-05	168	.204	.746	292.0	26.1	116.5	202.1
306	FCF	4	21.5	V	62.4	.383F+00	-.553E-02	.132E+00	-.207E-02	.111E+00	-.169E-02	-.843E-01	.130E-02	-.923E-01	.119E-02	170	.140	.775	315.0	27.9	116.4	219.7
306	FCF	7	21.5	H	31.4	.138E+01	-.362F-01	-.388E+00	.124E-01	.112E+00	-.428E-02	-.301E+00	.810E-02	-.723E+00	.201E-01	287	.319	.651	300.4	34.5	123.3	208.9
306	FCF	7	21.5	V	31.4	.128F+01	-.303E-01	-.422E+00	.125E-01	.158E+00	-.446E-02	-.839E-01	.119E-02	-.578E+00	.147E-01	249	.301	.639	302.6	30.9	125.6	217.9
306	FCF	14	21.5	H	28.1	.437F+01	-.139F+00	-.833E-01	.502E-02	-.486E+00	.206E-01	-.343E+00	.954E-02	-.223E+01	.727E-01	205	.379	.560	311.8	30.8	117.7	217.2
306	FCF	14	21.5	V	28.1	.346E+01	-.103E+00	-.949E+00	.335E-01	.454E+00	-.114E-01	-.561E+00	.154E-01	-.153E+01	.468E-01	200	.311	.590	303.3	22.1	116.3	215.9
318	13	3	4.6	H	20.3	.111E+01	-.482E-01	-.179E+00	.937E-02	.793E+00	-.384E-01	.327E+00	-.141E-01	-.221E+00	.105E-01	285	.231	.720	169.1	251.9	359.8	88.2
318	13	3	4.6	V	20.3	.826F+00	-.363E-01	-.139E+00	.733E-02	.722E+00	-.352E-01	.507E-01	-.121E-02	-.189E+00	.917E-02	265	.238	.698	170.5	261.6	.6	90.8
318	13	8	4.6	H	40.6	.156F-01	-.342E-03	-.347E-02	.750E-04	-.545E-03	.161E-04	.353E-02	-.722E-04	-.588E-02	.127E-03	116	.125	.953	156.1	251.7	333.5	58.5
318	13	8	4.6	V	40.6	.135E-01	-.264E-03	.174E-02	-.434E-04	-.326E-02	.782E-04	.338E-02	-.572E-04	-.340E-02	.523E-04	121	.123	.922	155.6	244.7	334.2	65.0
318	13	11	4.6	H	50.3	.242E-02	-.422E-04	-.354E-02	.655E-04	-.338E-03	.825E-05	.223E-02	-.417E-04	-.312E-02	.580E-04	269	.200	.960	154.7	258.9	328.6	47.7
318	13	11	4.6	V	50.3	.409E-02	-.591E-04	-.270E-02	.475E-04	-.135E-02	.288E-04	.327E-02	-.547E-04	-.508E-02	.896E-04	306	.186	.899	156.8	252.3	335.4	60.1
318	14	1	5.5	H	18.9	.207E+01	-.919E-01	-.244E+00	.120E-01	-.440E+00	.229E-01	-.281E-02	.475E-03	.237E+00	-.105E-01	401	.115	.883	43.1	124.0	218.3	316.3
318	14	1	5.5	V	18.9	.189E+01	-.834E-01	-.429E+00	.219E-01	-.592E+00	.307E-01	.626E-01	-.301E-02	.281E+00	-.131E-01	407	.105	.908	40.7	122.8	219.7	317.3
318	14	7	5.5	H	30.9	.140E-01	-.299E-03	.164E-02	-.284E-04	.384E-02	-.786E-04	-.328E-03	.602E-05	.194E-02	-.281E-04	352	.185	.801	47.4	155.5	229.3	300.0
318	14	7	5.5	V	30.9	.200E-01	-.401E-03	.133E-02	-.197E-04	-.103E-02	.406E-04	-.825E-02	.205E-03	.146E-02	-.853E-05	347	.204	.751	46.4	142.7	226.1	309.8
318	14	12	5.5	H	67.2	-.147E-03	.432E-05	-.725E-03	.113E-04	-.137E-03	.286E-05	.971E-03	-.145E-04	.219E-03	-.287E-05	214	.324	.438	53.5	185.2	287.5	53.5
318	14	12	5.5	V	67.2	.259E-02	-.270E-04	-.670E-03	.119E-04	.213E-03	-.197E-05	.597E-03	-.994E-05	.132E-02	-.139E-04	267	.151	.880	50.7	142.9	229.1	317.0
318	16	4	8.6	H	18.5	.228E+01	-.982E-01	.741E-02	.367E-02	-.828E+00	.429E-01	-.164E+00	.123E-01	-.980F+00	.547E-01	383	.264	.607	206.7	267.6	5.4	114.6
318	16	4	8.6	V	18.5	.207F+01	-.897E-01	-.722F-01	.748E-02	-.663F+00	.349E-01	.196E+00	-.729E-02	-.977E+00	.562E-01	383	.297	.546	200.2	266.7	6.6	113.9
318	16	8	8.2	H	30.4	.379E-01	-.834E-03	-.178F-01	.404E-03	-.234E-01	.557E-03	.136E-01	-.292E-03	.142E-01	-.320E-03	366	.228	.882	201.9	301.1	12.7	97.7
318	16	8	8.2	V	39.4	.485E-01	-.101E-02	-.316E-01	.771E-03	-.339E-01	.829E-03	.125E-01	-.194E-03	.244E-01	-.542E-03	369	.232	.828	198.2	290.1	13.9	102.6
318	16	14	8.9	H	66.2	.142E-02	-.175E-04	-.156E-02	.216E-04	.452E-03	-.815E-05	.160E-02	-.231E-04	.145E-02	-.197E-04	214	.251	.653	212.7	316.2	31.7	108.9
318	16	14	8.9	V	66.2	.182E-01	-.231E-03	-.776F-02	.116E-03	.468E-02	-.729E-04	.614E-02	-.722E-04	.158E-01	-.212E-03	272	.227	.696	206.8	297.2	25.6	115.3
318	17	1	13.5	H	19.8	.312E+01	-.129E+00	.986E-01	-.307E-02	-.118F+00	.586E-02	.542E+00	-.235E-01	.495E+00	-.189E-01	365	.125	.947	211.2	295.8	27.2	122.2
318	17	1	13.5	V	19.8	.276E+01	-.113E+00	.240E+00	-.953E-02	-.167E-01	.166E-02	.188E+00	-.577E-02	.406E+00	-.140E-01	363	.106	.877	211.3	294.9	29.0	125.0
318	17	8	12.8	H	40.8	.740E-01	-.147E-02	-.229E-01	.447E-03	-.133E-01	.270E-03	.188E-01	-.368E-03	.616E-01	-.135E-02	313	.146	.942	209.3	309.7	30.8	109.7
318	17	8	12.8	V	40.8	.882E-01	-.153E-02	-.789E-02	.108E-03	-.115E-01	.235E-03	.399E-01	-.777E-03	.920E-01	-.194E-02	329	.132	.929	208.9	302.6	28.8	115.2
318	17	12	12.3	H	68.1	.507F-02	-.599E-04	-.124F-02	.929E-05	-.309E-02	.412E-04	-.146E-02	.245E-04	.207E-02	-.245E-04	256	.166	.923	209.4	322.1	35.0	98.1
318	17	12	12.3	V	68.1	.317F-01	-.373E-03	-.111F-02	-.176E-05	-.359E-02	.386E-04	.367E-02	-.275E-04	.132E-01	-.145E-03	258	.129	.920	211.6	306.9	30.1	115.1
318	18	2	12.0	H	19.6	.314F+01	-.133E+00	-.141E+00	.847E-02	-.836E-02	.559E-03	.162E+00	-.568E-02	.375E+00	-.181E-01	355	.195	.528	191.6	274.2	10.4	107.5
318	18	2	12.0	V	19.6	.725F+01	-.915E-01	-.398E+00	.222E-01	-.913E+00	.451E-01	-.391E-01	.507E-02	.294E+00	-.147E-01	354	.201	.725	190.5	262.5	356.0	99.7
318	18	5	11.3	H	40.4	.713E-01	-.153E-02	-.960E-01	.228E-02	-.375E-01	.901E-03	.358E-01	-.773E-03	.746E-02	-.196E-03	343	.157	.907	190.4	290.2	352.0	75.7
318	18	5	11.3	V	40.4	.978E-01	-.199E-02	-.178E+00	.428E-02	-.100E+00	.244E-02	.753E-01	-.154E-02	.112E-01	-.278E-03	344	.152	.905	181.8	275.3	357.8	85.0
318	18	11	10.5	H	65.5	.122E-01	-.169E-03	.205E-02	-.361E-04	-.117E-02	.195E-04	.282E-02	-.354E-04	.407E-02	-.566E-04	195	.162	.932	193.7	293.4	22.8	101.2
318	18	11	10.5	V	65.5	.826F-01	-.114E-02	.228F-01	-.346E-03	.336E-01	-.483E-03	.380E-02	-.487E-05	.430E-01	-.615E-03	189	.111	.952	192.5	286.5	24.6	111.4
318	19	10	7.5	H	19.7	.369E+01	-.166F+00	.121E+01	-.624E-01	-.102E+01	.563E-01	-.460F+00	.212E-01	-.124E+00	.102E-01	370	.164	.810	225.2	320.4	69.1	163.4
318	19	10	7.5	V	19.7	.297F+01	-.131F+00	.676E+00	-.346E-01	-.663E+00	.379E-01	-.504E+00	.233E-01	-.171E+00	.116E-01	371	.152	.804	233.1	321.4	70.5	171.0
318	19	13	7.5	H	40.9	.345E-01	-.716E-03	-.225E-02	.422E-04	-.189E-01	.416E-03	-.788E-02	.156E-03	.220E-01	-.487E-03	255	.174	.922	244.6	343.8	60.1	142.6
318	19	13	7.5	V	40.9	.443F-01	-.827F-03	.159E-02	-.411F-04	-.117E-01	.260E-03	-.177E-01	.338E-03	.338E-01	-.703E-03	247	.158	.907	245.1	336.5	63.4	152.1
318	19	17	7.5	H	67.1	-.936F-01	.146E-02	-.100E+00	.155E-02	-.100F+00	.156E-02	-.623E-02	.854E-04	-.433E-01	.674E-03	69	.091	.834	323.2	52.1	233.2	143.2
318	19	17	7.5	V	67.1	.640F-02	-.570E-04	.298E-02	-.455E-04	-.619E-02	.872E-04	-.110E-01	.145E-03	.120E-01	-.154E-03	279	.198	.904	243.6	336.6	63.9	151.1
318	24	1	9.5	H	30.3	.248F+00	-.692E-02	.218F-01	-.824E-03	-.271F-01	.643E-03	-.518E-01	.151E-02	.855E-01	-.245E-02	297	.163	.835	240.1	338.2	57.3	140.0
318	24	1	9.5	V	30.3	.329F+00	-.890E-02	-.211E-01	.609E-03	.775E-01	-.125E-02	-.277E-01	.498E-03	.151E+00	-.425E-02	292	.153	.862	241.4	335.9	58.1	144.3
335	3	A	14.2	H	48.3	.445E-01	-.766E-03	-.262F-01	.523E-03	.460E-02	-.875E-04	.470E-02	-.712E-04	-.728E-02	.906E-04	376	.168	.810	147.6	241.2	325.8	52.4
335	3	A	14.2	V	48.3	.843F-01	-.131E-02	-.241E-02	.519E-34	-.454E-01	.930E-03	.514E-01	-.964E-03	-.478E-01	.812E-03	383	.123	.869	150.0	239.1	329.0	60.0
335	3	1	14.2	H	29.4	.548F+00	-.154F-01	.746E-01	-.279E-02	-.146E+00	.504E-02	.138E+00	-.393E-02	-.304E+00	.883E-02	467	.175	.828	149.2	240.6	327.8	56.5
335	3	1	14.2	V	29.4	.554E+00	-.149F-01	.152F+00	-.505E-02	-.154E+00	.521F-02	.218E+00	-.651E-02	-.251E+00	.667E-02	453	.162	.839	148.1	236.3	327.3	59.1
335	4A	22	19.7	H	9.7	.912F+01	-.549E+00	-.831E+00	.770E-01	.304E+00	-.374E-07	.855E-01	-.485E-01	-.554E+00	.397E-01	322	.102	.883	280.7	2.5	102.8	201.7
335	4A	22	19.7	V	9.7	.849F+01	-.504E+00	-.567F+00	.511E-01	.448E+00	-.157E-01	.290E+00	-.630E-01	-.558E+00	.435E-01	317	.101	.890	281.0	359.1	102.1	204.5
335	4A	1	19.1	H	18.9	.335E+01	-.132E+00	-.449E+00	.236E-01	.151E+00	-.819E-02	-.116E+01	.474E-01	-.350E+00	.898E-02	715	.131	.836	287.1	17.1	107.3	197.2
335	4A	1	19.1	V	18.9	.326F+01	-.128E+00	-.541F+00	.280E-01	.128F+00	-.532E-02	-.103E+01	.403E-01	-.349E+00	.921E-02	717	.129	.841	286.9	15.1	106.6	197.8
335	4A	9	20.0	H	39.1	.203F+00	-.438E-02	-.150E-01	.396E-03	.371E-01	-.101E-02	-.114E+00	.256E-02	-.637E-01	.141E-02	622	.213	.777	286.1	18.3	106.4	194.2
335	4A	9	20.0	V	39.1	.255E+00	-.511E-02	.345E-01	-.893E-03	.286E-01	-.736E-03	-.153E+00	.337E-02	-.953E-01	.204E-02	622	.195	.785	287.4	17.7	107.9	197.6
335	4A	17	19.9	H	58.2	.235E-01	-.327E-03	.764E-02	-.123E-03	-.348E-02	.211E-04	.562E-02	-.117E-03	-.411E-02	.585E-04	361	.269	.711	284.1	38.5	107.0	170.2
335	4A	17	19.9	V	58.2	.597E-01	-.749E-03	.209E-01	-.343E-03	-.679E-02	.380E-04	.293E-01	-.507E-03	.131E-02	-.729E-04	368	.177	.762	285.1	29.9	109.1	184.0

TABLE VIII.- Concluded

Miss	Fl	Run	Wind speed, deg	Pol	α_{mean}, deg	A_0	A_1	A_2	A_3	A_4	A_5	A_6	A_7	A_8	A_9	No. points	NSD	R^2	Φ critical points, deg			
																			U_{max}	$C1_{min}$	D_{max}	$C2_{min}$
335	4R	1	19.1	H	19.0	.340E+01	-.146E+00	-.803E+00	.416E-01	.376E+00	-.177E-01	-.633E+00	.210E-01	-.207E+00	.493E-02	755	.192	.685	282.8	10.7	103.1	195.2
335	4R	1	19.1	V	19.0	.339E+01	-.136E+00	-.421E+00	.206E-01	.223E+00	-.696E-02	-.535E+00	.170E-01	-.429E+00	.158E-01	749	.210	.642	285.5	10.2	105.8	201.2
335	4R	10	19.4	H	38.7	.277E+00	-.602E-02	-.323E-01	.935E-03	-.102E+00	.228E-02	-.919E-01	.202E-02	-.495E-01	.101E-02	611	.221	.654	286.9	29.8	107.8	184.5
335	4R	10	19.4	V	38.7	.383E+00	-.811E-02	-.538E-01	.158E-02	-.569E-01	.112E-02	-.113E+00	.234E-02	-.817E-01	.175E-02	621	.192	.676	287.3	24.0	103.8	188.1
335	4R	17	19.6	H	58.0	.176E-01	-.190E-03	-.709E-02	.118E-03	.129E-01	-.257E-03	-.288E-01	.485E-03	-.307E-01	.536E-03	563	.278	.352	256.3	346.3	33.6	128.8
335	4R	17	19.6	V	58.0	.535E-01	-.627E-03	-.453E-02	.666E-04	.357E-01	-.665E-03	-.604E-01	.101E-02	-.383E-01	.660E-03	571	.190	.354	266.4	20.4	98.4	155.2
335	5	1	15.5	H	19.0	.322E+01	-.130E+00	-.615E+00	.318E-01	-.476E+00	.238E-01	-.500E+00	.169E-01	-.678E+00	.257E-01	785	.184	.837	293.5	23.3	111.8	207.1
335	5	1	15.5	V	19.0	.299E+01	-.119E+00	-.721E+00	.361E-01	-.483E+00	.247E-01	-.354E+00	.993E-02	-.656E+00	.242E-01	777	.181	.824	294.1	23.7	114.2	204.7
335	5	9	15.2	H	39.4	.118E+00	-.242E-02	-.119E-01	.367E-03	-.280E-01	.543E-03	-.337E-01	.636E-03	-.325E-01	.681E-03	719	.250	.701	287.3	26.5	105.5	186.9
335	5	9	15.2	V	39.4	.154E+00	-.299E-02	-.419E-01	.110E-02	.871E-02	-.360E-03	-.672E-01	.132E-02	-.461E-01	.903E-03	717	.218	.717	287.1	21.6	107.4	192.8
335	5	17	15.1	H	58.5	.216E-01	-.318E-03	-.893E-03	.229E-04	-.117E-02	-.774E-05	.419E-02	-.915E-04	-.102E-01	.161E-03	583	.340	.663	286.7	34.2	107.8	179.6
335	5	17	15.1	V	58.5	.509E-01	-.654E-03	.121E-01	-.194E-03	-.816E-03	-.376E-04	.417E-02	-.139E-03	-.308E-01	.471E-03	594	.168	.791	289.1	28.4	110.6	191.0
335	5	25	13.9	H	9.2	.941E+01	-.606E+00	-.133F+01	.134E+00	.104E+01	-.952F-01	.592E-01	-.420E-01	-.251E+00	-.214E-02	419	.128	.692	289.8	10.4	109.8	209.1
335	5	25	13.9	V	9.2	.842E+01	-.523E+00	-.337E-01	-.916E-02	.118E+01	-.942E-01	.539E-01	-.356E-01	.544E+00	-.853E-01	414	.129	.647	290.7	7.6	110.7	213.8
335	6	1	15.0	H	19.2	.363E+01	-.154E+00	-.957E+00	.494E-01	-.925E+00	.492E-01	-.470E+00	.186E-01	-.614E+00	.218E-01	748	.210	.732	299.9	28.6	119.9	211.2
335	6	1	15.0	V	19.2	.343E+01	-.144E+00	-.731E+00	.374E-01	-.814E+00	.447E-01	-.395E+00	.158E-01	-.527E+00	.192E-01	757	.210	.697	300.9	26.6	119.5	213.6
335	6	9	15.0	H	39.1	.135E+00	-.293E-02	-.181E-01	.534E-03	-.367E-01	.777E-03	-.415E-01	.910E-03	-.314E-01	.642E-03	680	.228	.721	293.4	34.9	113.2	191.7
335	6	9	15.0	V	39.1	.197F+00	-.381E-02	-.238E-01	.667E-03	-.420E-02	-.493E-04	-.101E+00	.225E-02	-.440E-01	.824E-03	680	.203	.763	291.1	26.5	111.2	195.8
335	6	13	15.0	H	57.8	.166E-01	-.235E-03	-.355E-02	.721E-04	-.258E-02	.212E-04	-.650E-02	.975E-04	-.599E-03	-.502E-05	622	.230	.753	293.2	40.4	112.1	185.5
335	6	13	15.0	V	57.8	.514E-01	-.673E-03	-.105E-01	.203E-03	.163E-01	-.332E-03	-.191E-01	.263E-03	-.211E-01	.303E-03	621	.142	.836	291.4	29.8	110.8	192.6
335	6	25	15.0	H	9.0	.105E+02	-.682E+00	.984E+00	-.114E+00	.883E+00	-.717E-01	-.458E+00	.197E-01	.138E+00	-.375E-01	350	.142	.636	289.3	7.5	106.6	207.5
335	6	25	15.0	V	9.0	.104E+02	-.678E+00	.111E+01	-.123E+00	-.551E-01	.258E-01	.549E+00	-.744E-01	.681E+00	-.925E-01	352	.158	.578	303.1	12.6	110.9	214.3
353	9	1	12.2	H	11.4	.121E+02	-.789E+00	-.935E+00	.707E-01	.981E+00	-.833E-01	-.170E+01	.144E+00	.462E+00	-.500E-01	676	.156	.779	298.4	24.4	120.9	215.2
353	9	1	12.2	V	11.4	.120E+02	-.798E+00	-.149E+01	.130E+00	-.278E+00	.317E-01	-.167E+01	.141E+00	.481E+00	-.556E-01	672	.170	.782	306.6	26.1	120.2	219.2
353	9	6	11.3	V	67.3	.184F-01	-.241E-03	-.270E-02	.331E-04	-.779E-02	.683E-04	.888E-02	-.116E-03	-.115E-01	.123E-03	427	.244	.799	313.1	59.2	157.8	226.0
353	9	11	10.8	H	19.7	.254E+01	-.109E+00	-.709F-01	.150E-02	.504E+00	-.291E-01	-.172E+00	.854E-02	.195E+00	-.157E-01	605	.208	.707	304.5	44.2	144.3	220.8
353	9	11	10.8	V	19.7	.244F+01	-.103E+00	-.346E+00	.157E-01	.793E-01	-.720E-02	-.284E+00	.141E-01	-.655E-01	-.202E-02	616	.226	.688	304.1	45.5	143.1	219.8
353	9	16	10.3	H	39.7	.307E-01	-.628E-03	-.921F-03	.468E-04	-.186E-01	.347E-03	-.334E-02	.593E-04	-.641E-02	.659E-04	615	.416	.763	302.8	53.5	137.0	197.5
353	9	16	10.3	V	39.7	.501E-01	-.944E-03	-.210E-01	.556E-03	-.957F-02	.262E-04	.121E-01	-.348E-03	-.975E-02	.288E-04	630	.413	.719	303.3	50.0	139.0	205.6
353	10	1	5.4	H	19.9	.144E+01	-.628E-01	-.244E+00	.117E-01	.157E+00	-.829E-02	-.208E+00	.919E-02	.139E+00	-.625E-02	1217	.316	.720	251.3	349.8	79.0	159.1
353	10	1	5.4	V	19.9	.140E+01	-.606E-01	-.283E+00	.136E-01	-.727E-01	.303E-02	-.221E+00	.951E-02	.158E+00	-.730E-02	1207	.331	.713	255.2	354.7	83.7	162.4
353	10	11	5.4	H	10.3	.150F+02	-.107F+01	-.880E+00	.821E-01	.132E+01	-.125E+00	-.157E+01	.145E+00	.106E+01	-.902E-01	667	.179	.869	235.7	329.2	65.0	151.8
353	10	11	5.4	V	10.3	.140E+02	-.101E+01	-.771E+00	.642E-01	.198E+01	-.199E+00	-.151E+01	.141E+00	.156E+01	-.137E+00	677	.201	.859	232.4	335.7	62.4	135.6
353	11	1	16.0	H	67.3	.879E-03	.815E-05	-.941F-03	.101E-04	-.393E-02	.421F-04	-.979E-02	.134E-03	-.654E-02	.997E-04	505	.330	.784	262.1	13.4	88.1	152.5
353	11	1	16.0	V	67.3	.279E-01	-.787E-03	.138E-01	-.220E-03	.161E-01	-.281E-03	-.381E-01	.502E-03	-.113E-01	.173E-03	621	.183	.859	265.1	6.6	91.7	168.1
353	11	6	15.9	H	19.3	.321E+01	-.127E+00	-.587E+00	.299E-01	.231E+00	-.109E-01	-.318E+00	.550E-02	-.166E+00	.602E-02	625	.258	.579	276.2	5.2	97.1	188.1
353	11	6	15.9	V	19.3	.359F+01	-.147F+00	-.140E+01	.697E-01	.711E+00	-.342E-01	-.864E+00	.324E-01	-.461E+00	.214E-01	626	.241	.669	272.8	2.7	98.5	189.3
353	11	11	15.7	H	39.7	.141E+00	-.297E-02	.182E-01	-.406E-03	-.751E-01	.169E-02	-.862E-01	.193E-02	-.190E-01	.471E-03	618	.251	.746	270.7	12.4	90.8	169.1
353	11	11	15.7	V	39.7	.159F+00	-.295E-02	.693F-01	-.173E-02	-.849F-01	.195E-02	-.100E+00	.204E-02	.425E-01	-.108E-02	620	.174	.809	270.6	5.7	89.9	174.8
353	13	1	10.4	H	20.3	.247F+01	-.101E+00	-.380F+00	.178E-01	.274E+00	-.132E-01	-.356E+00	.144E-01	-.472E+00	.181E-01	1299	.233	.849	297.8	27.9	120.9	211.1
353	13	1	10.4	V	20.3	.249F+01	-.100E+00	-.451E+00	.207E-01	.182E+00	-.835E-02	-.280E+00	.102E-01	-.506E+00	.186E-01	1304	.205	.864	298.6	28.2	122.3	213.0
353	13	11	11.2	H	10.0	.125F+02	-.817E+00	.230E+00	-.326E-01	-.540E+00	.399E-01	-.388E+00	.165E-01	.372E+00	-.553E-01	637	.140	.885	117.2	194.1	24.1	283.3
353	13	11	11.2	V	10.0	.129E+02	-.844F+00	.190E+00	-.162E-01	-.493E+00	.402E-01	.830E-01	-.289E-01	.961E+00	-.112E+00	624	.137	.873	108.9	193.7	23.9	288.6
353	13	16	11.7	V	67.7	.296E-01	-.767E-03	-.259F-02	.486E-04	-.740F-02	.819E-04	-.146E-01	.202E-03	-.168E-01	.198E-03	492	.184	.913	305.2	44.7	129.9	209.2
353	13	20	12.0	H	40.5	.616E-01	-.131F-02	.487E-02	-.724E-04	-.141E-01	.266E-03	-.950E-02	.203E-03	-.338E-01	.735E-03	475	.209	.868	305.0	48.9	127.9	202.7
353	13	20	12.0	V	40.5	.868E-01	-.160E-02	.749F-02	-.135F-03	-.291E-02	-.168E-04	.707E-02	-.275E-03	-.326E-01	.516E-03	478	.199	.839	305.0	40.1	126.0	210.7
353	14	1	14.3	H	67.1	-.211E-02	.514E-04	.706E-02	-.110E-03	-.804E-02	.119E-03	.310E-02	-.531E-04	-.268E-02	.389E-04	407	.466	.270	265.4	6.0	103.9	182.1
353	14	1	14.3	V	67.1	.244E-01	-.255E-03	.532E-01	-.788E-03	-.233E-01	.317E-03	-.297E-01	.392E-03	-.231E-01	.335E-03	639	.217	.804	275.5	13.7	94.1	176.4
353	14	6	14.3	H	19.3	.324E+01	-.135E+00	.691F-01	-.370E-02	-.162E+00	.897E-02	-.432E-01	-.152F-02	-.583E+00	.255E-01	640	.182	.738	296.0	24.4	115.4	207.0
353	14	6	14.3	V	19.3	.352F+01	-.146F+00	.915E-01	-.466E-02	.194E-01	.667E-03	.140E-01	-.517E-02	-.612E+00	.272E-01	656	.184	.741	295.4	20.0	111.8	206.9
353	14	11	14.3	H	39.4	.103F+00	-.221F-02	-.888F-02	.306E-03	-.433F-01	.975E-03	-.297E-01	.637E-03	-.623E-02	.217E-04	251	.196	.809	296.3	37.1	112.7	193.5
353	14	11	14.3	V	39.4	.138E+00	-.270E-02	.138E-01	-.233E-03	-.701E-01	.168E-02	-.387E-01	.712E-03	-.372E-01	.653E-03	254	.177	.801	295.7	28.8	110.9	198.7
353	15	1	4.2	H	10.4	.151E+02	-.107E+01	-.814E+00	.919E-01	-.388E+00	.353E-01	-.850E+00	.724E-01	.414E+00	-.322E-01	629	.157	.850	267.2	336.9	55.8	162.9
353	15	1	4.2	V	10.4	.156E+02	-.110E+01	-.279E+00	.405E-01	-.524E+00	.426E-01	-.649E+00	.571E-01	.427E+00	-.309E-01	624	.154	.863	258.9	329.1	39.5	149.2
353	15	11	4.2	H	20.0	.161E+01	-.647E-01	.197E+00	-.963F-02	-.914E-01	.341E-02	.279E-01	-.367E-02	.406E+00	-.181E-01	394	.187	.859	250.6	342.7	64.8	153.6
353	15	11	4.2	V	20.0	.178E+01	-.767E-01	.799F-02	-.405E-03	-.481F-01	.129E-02	-.113E+00	.345E-02	.439E+00	-.197E-01	386	.220	.814	249.0	342.2	65.1	152.6
353	15	16	4.2	H	40.1	.116F-01	-.262E-03	-.317E-02	.697E-04	-.596F-02	.129E-03	-.285E-02	.562E-04	.509E-02	-.120E-03	525	.448	.706	254.4	5.5	84.9	146.7
353	15	16	4.2	V	40.1	.192E-01	-.388E-03	-.152E-02	.251E-04	-.517E-02	.109E-03	-.623E-02	.123E-03	.251E-02	-.479E-04	603	.403	.627	255.0	356.2	81.7	159.3
353	20	26	2.5	H	38.9	.106F-01	-.252E-03	.166E-02	-.341E-04	-.979E-02	.241E-03	-.101E-02	.209E-04	-.128E-02	.300E-04	366	.471	.499	294.3	24.3	114.3	170.5
353	20	26	2.5	V	38.9	.149E-31	-.391E-03	.152E-02	-.227E-04	-.135E-01	.342E-03	-.612E-03	.329E-05	-.181E-02	.480E-04	573	.407	.497	284.4	4.9	95.0	172.7
353	20	1	2.5	H	20.0	.148E+01	-.643E-01	.154F+00	-.754E-02	-.255E+00	.134E-01	-.369E+00	.160E-01	.926E-01	-.351E-02	1325	.232	.824	257.8	344.0	77.4	171.1
353	20	1	2.5	V	20.0	.158E+01	-.683E-01	.147E+00	-.708E-02	-.282E+00	.151E-01	-.395E+00	.173E-01	.613E-01	-.184E-02	1328	.228	.822	256.9	341.3	76.4	171.9
353	20	11	2.5	H	11.0	.123E+02	-.873E+00	.188F+01	-.169E+00	-.188E+01	.162E+00	-.767E+00	.404E-01	.248E+00	-.539E-02	669	.144	.899	256.3	348.1	73.2	161.7
353	20	11	2.5	V	11.0	.130E+02	-.919E+00	.163E+01	-.146E+00	-.188E+01	.164E+00	-.596E+00	.283E-01	.224E+00	-.132E-02	666	.138	.901	253.6	344.5	69.9	159.3
353	21	1	4.7	H	10.3	.137E+02	-.956E+00	.478E+01	-.450E+00	-.553E+00	.249E-01	.113E+01	-.132E+00	-.117E+00	.763E-02	612	.121	.904	280.6	27.6	83.1	168.0
353	21	1	4.7	V	10.3	.137E+02	-.952E+00	.447E+01	-.419E+00	-.544E+00	.278E-01	.154E+01	-.166E+00	-.296E+00	.224E-01	616	.117	.906	286.3	39.0	169.5	286.3
353	21	7	4.7	H	19.6	.171E+01	-.772E-01	-.632F+00	.324E-01	.152E+00	-.738E-02	.238E+00	-.131E-01	.223E+00	-.113E-01	621	.236	.759	267.8	350.7	85.8	182.5
353	21	7	4.7	V	19.6	.172E+01	-.770E-01	-.470E+00	.241E-01	.351E+00	-.174E-01	.209E+00	-.114E-01	.184E+00	-.934E-02	622	.243	.756	270.2	350.1	87.7	187.1
353	21	12	4.7	H	39.4	.504E-02	-.113E-03	.516E-02	-.128E-03	-.175E-02	.377E-04	-.210E-02	.505E-04	-.122E-02	.275E-04	429	.385	.512	294.2	50.9	113.6	181.1
353	21	12	4.7	V	39.4	.803E-02	-.173E-03	.424E-02	-.993E-04	-.215E-02	.480E-04	-.176E-02	.351E-04	-.764E-03	.159E-04	578	.346	.511	284.4	23.7	87.7	180.0

TABLE IX.- REGRESSION COEFFICIENTS OF NRCS VERSUS χ FOR THE SECOND-ORDER MODEL

$$\left[(\text{NRCS}) = \sum_{n=0}^{2} A_n \cos n\chi\right]$$

Miss	Fl	Run	WSPD, m/s	P	θ, deg	A_0	A_1	A_2	No. points	NSD	R^2	χ_{min}, deg	
												1st	2d
230	FCF	1	15.0	H	30.3	.100E+00	-.306E-02	.414E-01	666	.287	.504	84.3	267.3
230	FCF	1	15.0	V	30.3	.133E+00	-.548E-02	.519E-01	682	.227	.598	85.3	268.7
230	1	13	3.0	H	29.3	.216E-02	.146E-02	.200E-02	515	.714	.354	105.0	198.8
230	1	1	3.0	V	27.3	.279E-01	.112E-01	.582E-02	594	.561	.246	119.4	270.0
230	1	5	3.0	V	29.3	.130E-01	-.104E-01	.672E-02	570	.774	.438	54.2	279.1
230	1	13	3.0	V	29.3	.547E-02	-.695E-03	.333E-02	404	.533	.408	92.6	191.4
238	20	2	6.5	H	31.0	.195E-01	.505E-02	.436E-02	1748	.314	.377	106.9	253.2
238	20	2	6.5	V	31.0	.273E-01	.287E-02	.884E-02	2088	.306	.379	93.1	263.9
238	27	2	3.0	H	31.7	.555E-02	.211E-02	.209E-02	558	.243	.700	106.4	257.3
238	27	12	3.0	H	33.0	.438E-02	.230E-02	.138E-02	613	.329	.636	116.8	270.0
238	27	2	3.0	V	31.7	.809E-02	.350E-02	.314E-02	656	.216	.784	107.1	255.5
238	27	12	3.0	V	33.0	.947E-02	.248E-02	.260E-02	658	.169	.709	103.1	255.6
288	5	1	23.6	H	33.7	.670E-01	-.264E-01	.287E-01	623	.239	.744	73.9	280.9
288	5	8	23.6	H	34.4	.624E-01	-.676E-02	.232E-01	928	.280	.491	92.4	282.5
288	5	1	23.6	V	33.7	.957E-01	-.546E-01	.451E-01	319	.343	.714	73.7	288.0
288	5	8	23.6	V	34.4	.833E-01	-.273E-01	.338E-01	877	.287	.620	85.2	289.8
288	6	1	13.5	H	35.0	.212E-01	.566E-02	.106E-01	409	.217	.767	100.0	266.2
288	6	7	13.5	H	36.9	.130E-01	.268E-02	.688E-02	258	.169	.846	95.0	263.7
288	6	1	13.5	V	35.0	.331E-01	.106E-02	.175E-01	410	.152	.853	90.3	268.6
288	6	7	13.5	V	36.9	.194E-01	.105E-02	.880E-02	345	.168	.780	89.6	266.3
306	FCF	1	21.5	H	53.4	.262E-01	-.401E-02	.101E-01	225	.211	.659	86.5	278.2
306	FCF	11	21.5	H	14.1	.339E+01	-.571E+00	.651E+00	210	.281	.301	84.1	288.1
306	FCF	4	21.5	H	62.5	.125E-01	.110E-02	.674E-02	168	.218	.761	94.1	270.1
306	FCF	7	21.5	H	31.4	.244E+00	.205E-01	.103E+00	287	.342	.428	94.1	268.5
306	FCF	14	21.5	H	28.1	.443E+00	-.341E-01	.199E+00	205	.434	.344	79.0	265.4
306	FCF	1	21.5	V	53.4	.629E-01	-.617E-02	.216E-01	214	.175	.680	88.2	276.9
306	FCF	11	21.5	V	14.1	.351E+01	-.508E+00	.676E+00	221	.271	.253	79.8	281.4
306	FCF	4	21.5	V	62.5	.379E-01	-.281E-02	.887E-02	170	.184	.473	72.9	264.7
306	FCF	7	21.5	V	31.4	.329E+00	-.304E-01	.126E+00	289	.321	.432	88.3	275.2
306	FCF	14	21.5	V	28.1	.566E+00	-.118E+00	.249E+00	200	.331	.531	78.8	272.6
306	3	1	4.1	H	29.0	.567E-01	-.676E-04	.147E-01	428	.233	.384	89.0	269.1
306	3	5	1.7	H	28.4	.186E-01	.119E-02	.979E-02	1034	.321	.587	94.1	270.7
318	13	3	4.6	H	20.3	.133E+00	-.769E-02	.426E-01	285	.279	.428	92.8	279.1
318	13	9	4.6	H	40.6	.177E-02	.436E-03	.936E-03	116	.133	.907	95.6	262.4
318	13	11	4.6	H	50.3	.307E-03	.257E-03	.236E-03	269	.235	.896	104.2	253.0
318	13	3	4.6	V	20.3	.911E-01	-.814E-02	.264E-01	265	.293	.360	91.1	280.3
318	13	9	4.6	V	40.6	.279E-02	-.197E-05	.165E-02	121	.122	.918	89.1	269.4
318	13	11	4.6	V	50.3	.312E-02	.329E-03	.769E-03	306	.191	.886	95.5	263.3
318	14	1	5.5	H	18.9	.327E+00	-.160E-01	.384E-01	401	.122	.364	80.9	273.2
318	14	7	5.5	H	39.9	.202E-02	.096E-03	.819E-03	352	.182	.865	108.1	252.6
318	14	12	5.5	H	57.2	.145E-03	.610E-04	.258E-04	214	.331	.473	131.7	0.0
318	14	1	5.5	V	18.9	.304E+00	-.167E-01	.333E-01	407	.113	.382	82.1	276.6
318	14	7	5.5	V	39.9	.397E-02	.808E-03	.180E-02	347	.205	.762	96.3	263.4
318	14	12	5.5	V	57.2	.783E-03	.812E-04	.416E-03	267	.153	.874	92.2	266.3
318	16	4	8.6	H	18.5	.470E+00	-.646E-01	.664E-01	383	.295	.166	80.9	267.9
318	16	9	8.2	H	39.4	.504E-02	.223E-02	.260E-02	366	.284	.730	99.3	255.4
318	16	14	8.9	H	66.2	.267E-03	.154E-03	.163E-03	214	.272	.762	103.5	256.1
318	16	4	8.6	V	18.5	.411E+00	-.633E-01	.646E-01	380	.316	.185	66.5	273.6
318	16	9	8.2	V	39.4	.915E-02	.150E-02	.565E-02	369	.271	.732	91.9	264.4
318	16	14	8.9	V	66.2	.287E-02	.161E-03	.223E-02	272	.235	.851	90.4	268.5
318	17	1	13.5	H	10.8	.555E+00	-.304E-01	.143E+00	366	.129	.688	84.6	271.0
318	17	8	12.8	H	40.8	.141E-01	.526E-02	.761E-02	313	.154	.809	100.4	260.4
318	17	12	12.3	H	68.1	.977E-03	.681E-03	.462E-03	256	.168	.914	112.7	248.7
318	17	1	13.5	V	10.8	.517E+00	-.516E-01	.149E+00	363	.107	.811	83.6	273.7
318	17	8	12.8	V	40.8	.257E-01	.398E-02	.154E-01	329	.134	.911	93.7	266.3
318	17	12	12.3	V	68.1	.631E-02	.151E-02	.375E-02	258	.130	.913	95.3	263.5
318	18	2	12.0	H	19.6	.533E+00	-.251E-01	.542E-01	355	.195	.139	82.6	275.0
318	18	6	11.3	H	40.4	.941E-02	.386E-02	.444E-02	343	.205	.822	99.8	255.3
318	18	11	10.5	H	65.5	.107E-02	.376E-03	.657E-03	195	.154	.917	99.7	267.5
318	18	2	12.0	V	19.6	.456E+00	-.300E-01	.564E-01	354	.210	.166	72.0	269.2
318	18	6	11.3	V	40.4	.175E-01	.463E-02	.127E-01	344	.201	.877	93.5	263.2
318	18	11	10.5	V	65.5	.667E-02	.458E-03	.484E-02	189	.138	.935	94.0	279.3
318	19	10	7.5	H	19.7	.411E+00	-.479E-01	.827E-01	370	.244	.301	95.2	298.2
318	19	13	7.5	H	40.0	.518E-02	.166E-02	.255E-02	255	.192	.834	99.2	258.0
318	19	10	7.5	V	19.7	.383E+00	-.642E-01	.707E-01	371	.196	.444	86.3	297.9
318	19	13	7.5	V	40.0	.105E-01	.927E-03	.639E-02	247	.163	.879	91.4	267.0
318	19	17	7.5	V	67.1	.257E-02	.385E-03	.203E-02	279	.107	.893	92.8	267.3
318	24	1	0.5	H	30.3	.386E-01	.809E-02	.128E-01	297	.163	.745	98.1	259.9
318	24	1	0.5	V	30.3	.591E-01	.102E-01	.253E-01	292	.156	.815	94.5	262.0
335	3	6	14.2	H	48.3	.752E-02	.967E-03	.314E-02	376	.177	.749	93.6	264.8
335	3	1	14.2	H	29.4	.939E-01	.713E-02	.491E-01	467	.177	.810	91.4	267.3
335	3	6	14.2	V	48.3	.210E-01	-.320E-03	.978E-02	383	.124	.873	89.1	270.0
335	3	1	14.2	V	29.4	.116E+00	-.583E-02	.606E-01	453	.163	.835	88.2	271.0

TABLE IX.- Concluded

Miss	Fl	Run	WSPD, m/s	P	θ, deg	A_0	A_1	A_2	No. points	NSD	R^2	χ_{min}, deg	
												1st	2d
335	4A	22	10.8	H	9.7	.281E+01	-.278E+00	.420E+00	322	.103	.451	81.8	281.0
335	4A	1	10.8	H	18.9	.844E+00	-.613E-03	.320E+00	715	.133	.797	90.0	270.1
335	4A	9	20.0	H	39.1	.317E-01	.233E-02	.159E-01	622	.211	.737	92.2	268.1
335	4A	17	19.8	H	58.2	.443E-02	.230E-02	.141E-02	361	.267	.706	114.4	246.1
335	4A	22	10.8	V	9.7	.362E+01	-.304E+00	.347E+00	317	.101	.446	78.1	283.5
335	4A	1	19.8	V	18.9	.834E+00	-.297E-01	.321E+00	717	.131	.807	88.8	271.5
335	4A	9	20.0	V	39.1	.552E-01	.113E-03	.267E-01	622	.192	.760	90.3	270.2
335	4A	17	19.8	V	58.2	.151E-01	.464E-02	.518E-02	368	.178	.753	103.8	257.9
335	4P	1	19.1	H	19.1	.816E+00	-.407E-01	.259E+00	755	.196	.571	87.9	272.4
335	4P	10	19.4	H	38.7	.448E-01	.146E-01	.166E-01	611	.223	.703	102.9	257.6
335	4P	17	19.6	H	58.0	.658E-02	.204E-02	.792E-03	563	.282	.413	90.0	232.5
335	4P	1	10.1	V	19.1	.803E+00	-.940E-01	.248E+00	749	.212	.539	84.7	275.7
335	4P	10	19.4	V	38.7	.694E-01	.150E-01	.272E-01	621	.198	.710	96.7	260.8
335	4P	17	19.6	V	58.0	.172E-01	.286E-02	.185E-02	571	.192	.357	114.0	248.8
335	5	1	15.5	H	19.9	.641E+00	.107E-01	.235E+00	785	.193	.642	89.8	268.6
335	5	9	15.2	H	39.4	.228E-01	.703E-02	.103E-01	719	.252	.699	99.2	259.6
335	5	17	15.1	H	58.5	.301E-02	.168E-02	.141E-02	583	.344	.684	107.5	252.9
335	5	25	15.0	H	9.2	.383E+01	-.276E+00	.424E+00	419	.129	.350	80.6	279.3
335	5	1	15.5	V	19.9	.633E+00	-.840E-02	.235E+00	777	.191	.655	89.6	270.6
335	5	9	15.2	V	39.4	.395E-01	.569E-02	.185E-01	717	.221	.706	94.5	265.7
335	5	17	15.1	V	58.5	.126E-01	.310E-02	.513E-02	504	.170	.789	99.3	261.9
335	5	25	15.0	V	9.2	.360E+01	-.331E+00	.365E+00	414	.130	.361	76.9	283.1
335	6	1	15.0	H	19.2	.687E+00	-.210E-01	.227E+00	748	.229	.517	88.7	271.3
335	6	9	15.0	H	39.1	.205E-01	.694E-02	.862E-02	680	.233	.728	101.5	258.3
335	6	13	15.0	H	57.8	.300E-02	.150E-02	.125E-02	622	.231	.800	107.2	252.3
335	6	25	15.0	H	9.0	.435E+01	-.237E+00	.345E+00	350	.143	.185	78.2	278.2
335	6	1	15.0	V	19.2	.677E+00	-.438E-01	.184E+00	757	.227	.437	85.7	272.7
335	6	9	15.0	V	39.1	.377E-01	.654E-02	.174E-01	680	.206	.748	95.4	264.7
335	6	13	15.0	V	57.8	.125E-01	.317E-02	.531E-02	621	.143	.857	98.4	261.2
335	6	25	15.0	V	9.0	.431E+01	-.145E+00	.192E+00	352	.159	.056	69.5	273.2
353	9	1	12.2	H	11.4	.215E+01	-.466E-01	.124E+00	676	.159	.031	86.0	276.8
353	9	11	10.8	H	19.7	.402E+00	.328E-01	.112E+00	605	.265	.374	101.7	276.3
353	9	16	10.3	H	39.7	.582E-02	.483E-02	.382E-02	615	.446	.731	110.7	254.7
353	9	1	12.2	V	11.4	.290E+01	-.686E-01	.161E+00	672	.173	.054	79.5	272.6
353	9	6	11.3	V	57.3	.345E-02	.109E-02	.205E-02	427	.330	.622	106.1	272.9
353	9	11	10.8	V	19.7	.406E+00	.309E-01	.104E+00	616	.261	.347	101.4	275.7
353	9	16	10.3	V	39.7	.128E-01	.757E-02	.844E-02	630	.472	.636	106.7	262.3
353	10	1	5.4	H	19.9	.193E+00	.113E-01	.291E-01	1217	.330	.108	98.5	267.8
353	10	11	5.4	H	10.3	.395E+01	-.810E-02	.148E+00	667	.188	.020	93.5	276.1
353	10	1	5.4	V	19.9	.190E+00	.153E-01	.341E-01	1207	.338	.145	99.5	267.2
353	10	11	5.4	V	10.3	.360E+01	.120E+00	.164E+00	677	.211	.035	103.3	263.2
353	11	1	16.0	H	67.3	.144E-02	.110E-02	.806E-03	505	.332	.779	111.3	250.4
353	11	6	15.9	H	19.3	.758E+00	-.224E-01	.216E+00	625	.267	.363	89.0	271.9
353	11	11	15.7	H	39.7	.228E-01	.787E-02	.977E-02	618	.251	.700	101.7	258.4
353	11	1	16.0	V	67.3	.962E-02	.283E-02	.434E-02	621	.197	.825	101.5	263.0
353	11	6	15.9	V	19.3	.761E+00	-.565E-01	.236E+00	626	.258	.429	89.9	276.5
353	11	11	15.7	V	39.7	.410E-01	.726E-02	.191E-01	620	.173	.792	95.1	264.2
353	13	1	10.4	H	20.3	.412E+00	-.128E-01	.122E+00	1299	.237	.445	90.1	273.3
353	13	0	11.2	H	10.0	.426E+01	-.946E-01	.291E+00	637	.143	.101	76.9	166.1
353	13	20	12.0	H	40.5	.852E-02	.386E-02	.425E-02	475	.216	.825	103.9	257.7
353	13	1	10.4	V	20.3	.450E+00	-.240E-01	.147E+00	1304	.208	.562	89.6	274.4
353	13	0	11.2	V	10.0	.439E+01	-.934E-01	.262E+00	624	.139	.089	84.8	179.7
353	13	16	11.7	V	67.7	.470E-02	.192E-02	.351E-02	492	.201	.895	99.5	264.0
353	13	20	12.0	V	40.5	.220E-01	.410E-02	.125E-01	478	.201	.811	95.1	265.7
353	14	1	14.3	H	67.1	.135E-02	.103E-05	.554E-03	407	.485	.215	100.6	276.7
353	14	6	14.3	H	19.3	.661E+00	-.110E-01	.116E+00	640	.185	.314	88.4	271.0
353	14	11	14.3	H	39.4	.158E-01	.580E-02	.697E-02	251	.197	.810	100.8	257.2
353	14	1	14.3	V	67.1	.730E-02	.213E-02	.353E-02	639	.210	.784	98.2	260.9
353	14	6	14.3	V	19.3	.704E+00	-.294E-01	.120E+00	656	.189	.302	84.6	271.5
353	14	11	14.3	V	39.4	.316E-01	.574E-02	.154E-01	254	.185	.794	93.1	263.0
353	15	1	4.2	H	10.4	.400E+01	.137E-01	.110E+00	629	.160	.015	69.7	255.7
353	15	11	4.2	H	20.0	.238E+00	.199E-01	.614E-01	394	.194	.495	92.1	263.0
353	15	16	4.2	H	40.1	.111E-02	.677E-03	.636E-03	525	.468	.653	111.1	252.3
353	15	1	4.2	V	10.4	.414E+01	.533E-01	.956E-01	624	.158	.013	70.2	250.3
353	15	11	4.2	V	20.0	.252E+00	.205E-01	.611E-01	386	.226	.393	93.2	263.6
353	15	16	4.2	V	40.1	.260E-02	.919E-03	.144E-02	603	.411	.551	101.2	263.3
353	20	26	2.5	H	38.9	.788E-03	.478E-03	.229E-03	366	.474	.480	90.0	236.2
353	20	1	2.5	H	20.0	.197E+00	-.133E-01	.537E-01	1325	.239	.405	84.2	273.3
353	20	11	2.5	H	11.0	.272E+01	.880E-01	.373E+00	669	.154	.304	91.8	265.4
353	20	26	2.5	V	38.9	.159E-02	.433E-03	.464E-03	573	.475	.258	80.5	248.3
353	20	1	2.5	V	20.0	.214E+00	-.202E-01	.547E-01	1328	.234	.401	84.4	275.0
353	20	11	2.5	V	11.0	.285E+01	.710E-01	.352E+00	466	.146	.280	90.9	265.7
353	21	1	4.7	H	10.3	.386E+01	.317E+00	.231E+00	612	.134	.222	107.0	247.4
353	21	7	4.7	H	19.6	.201E+00	-.784E-02	.195E-01	621	.252	.081	82.9	274.7
353	21	12	4.7	H	30.4	.589E-03	.291E-03	.172E-03	429	.403	.490	114.7	244.9
353	21	1	4.7	V	10.3	.391E+01	.292E+00	.173E+00	616	.128	.188	112.7	0.0
353	21	7	4.7	V	19.6	.215E+00	-.853E-02	.146E-01	622	.255	.048	79.9	276.9
353	21	12	4.7	V	30.4	.122E-02	.330E-03	.355E-03	578	.374	.370	95.3	252.2

TABLE X.- REGRESSION OF UPWIND, DOWNWIND, AND CROSSWIND NRCS VERSUS 10 LOG (WIND SPEED) FROM CORRECTED CIRCLE LINES

θ, deg	Pol	Wind dir or χ, deg	B_0	B_1	R^2	Wind speed, m/s		NRCS, dB		No. points	No. cases U > D	Comments
						Low	High	Low	High			
10	H	U	6.728	-0.0346	-0.1729	2.5	21.5	5.41	7.68	10	3	U < D for speeds >5.4 m/s
		D	5.673	.1001	.3770			5.97	8.94			
		90	5.775	-.0083	-.0459			4.83	6.34			
		79.6	(a)	(a)	(a)			4.80	6.34			
	V	U	6.875	-.0584	-.2229			5.01	7.95	10	3	U < D for speeds >5.4 m/s
		D	5.811	.0734	.2555			5.74	8.94			
		90	6.004	-.0345	-.1784			4.62	6.52			
		88.4	(a)	(a)	(a)							
20	H	U	-11.756	0.865	0.9258	2.5	19.1	-7.41	-.29	18	14	
		D	-11.549	.863	.9240			-7.04	-.29			
		90	-12.697	.750	.9232			-10.00	-3.19			
		87.8	(a)	(a)	(a)			-10.00	-3.2			
	V	U	-12.082	.875	.8773			-9.30	-.406	18	14	
		D	-11.946	.900	.8876			-8.68	-.142			
		90	-12.801	.750	.8658			-11.50	-2.94			
		86.2	(a)	(a)	(a)			-11.50	-2.94			
30	H	U	-26.225	1.501	0.911	3.0	22.5	-18.7	-3.14	9	6	
		D	-28.498	1.660	.912			-19.5	-2.71			
		90	-28.511	1.371	.904			-21.5	-6.89			
	V	U	-23.616	1.346	.886			-17.1	-2.63	9	3	
		D	-26.123	1.593	.913			-17.9	-1.32			
		90	-27.869	1.327	.887			-19.8	-5.92			
		C	(a)	(a)	(a)			-20.0	-6.0			
30	H	U	-26.205	1.494	0.995	3.0	15.0	-18.7	-8.45	5	4	Miss 306 and 288 data removed
		D	-28.247	1.621	.971			-19.5	-8.27			
		90	-27.490	1.233	.989			-21.5	-12.2			
		C	(a)	(a)	(a)			-21.5	-12.2			
	V	U	-24.104	1.405	.994			-17.1	-2.63	5	3	
		D	-25.896	1.558	.990			-17.9	-7.10			
		90	-25.789	1.180	.977			-19.8	-10.8			
		C	(a)	(a)	(a)			-20.0	-10.8			
40	H	U	-39.079	2.034	0.9600	2.5	20.0	-30.3	-11.8	18	18	
		D	-44.687	2.364	.9671			-34.2	-13.9			
		90	-44.727	2.062	.9634			-34.2	-16.2			
		102.7	-36.744	2.179	.9656			-35.1	-16.4			
	V	U	-36.744	2.036	.9600			-27.7	-9.9	18	18	
		D	-38.759	2.146	.9628			-29.5	-11.2			
		90	-41.557	1.988	.9642			-30.9	-14.2			
		95.1	-41.849	2.004	.9637			-31.1	-14.4			

[a]Not computed because NRCS within 0.1 dB of value at 90°.

TABLE X.- Concluded

θ, deg	Pol	Wind dir or χ, deg	B_0	B_1	R^2	Wind speed, m/s		NRCS, dB		No. points	No. cases U > D	Comments
						Low	High	Low	High			
50	H	U	-47.308	2.444	0.9926	4.6	21.5	-30.8	-13.9	3	1	
		D	-57.193	3.259	.9933			-35.2	-12.7			
		90	-64.855	3.564	.9993			-41.1	-17.0			
		94.3	-70.412	3.998	.9999			-43.9	-17.1			
	V	U	-42.197	2.354	.9968			-26.4	-10.3	3	2	
		D	-46.111	2.703	.9975			-28.0	-9.6			
		90	-55.726	3.170	.9979			-34.5	-12.9			
		90.3	-56.332	3.218	.9982			-34.8	-12.9			
50	H	U	-45.016	2.145	1.0	4.6	14.2	-30.8	-20.3	2	0	Miss 306 data removed
		D	-54.290	2.880				-35.2	-21.1			
		90	-63.845	3.432				-41.1	-24.3			
		100.2	-70.300	3.983				-43.9	-24.4			
	V	U	-40.751	2.165				-26.4	-15.8	2	1	
		D	-44.653	2.513				-28.0	-15.7			
		90	-54.131	2.962				-34.5	-20.0			
		92.8	-54.837	3.023				-34.8	-20.0			
60	H	U	-63.826	3.431	0.8445	15.0	21.5	-23.5	-16.3	4	4	
		D	-84.115	4.853	.7914			-26.6	-16.3			
		90	-68.504	3.385	.9097			-28.5	-22.1			
		104.5	-72.891	3.695	.8935			-29.3	-22.1	4	3	
	V	U	-45.073	2.337	.8275			-17.5	-12.6			
		D	-57.120	3.212	.7580			-19.1	-12.0			
		90	-64.292	3.581	.8100			-21.9	-14.4			
		96.2	-65.096	3.635	.8040			-22.1	-14.4			
60	H	U	-37.606	1.227	0.9305	15.0	19.8	-23.5	-21.7	3	3	Miss 306 data removed
		D	-38.393	1.010	.9925			-26.6	-25.3			
		90	-49.673	1.802	.9980			-28.5	-26.3			
		109.4	-50.336	1.799	.9900			-29.3	-27.0			
	V	U	-25.804	.718	.9622			-17.5	-16.5	3	3	
		D	-23.452	.382	.8763			-19.1	-18.5			
		90	-32.705	.926	.9909			-21.9	-20.7			
		100.2	-32.380	.886	.9755			-22.1	-20.9			
70	H	U	-55.478	2.497	0.9406	5.5	16.0	-36.7	-26.2	5	5	
		D	-54.427	2.085	.8420			-39.5	-29.2			
		90	-54.826	1.766	.8078			-41.1	-33.0			
		106.6	-52.826	1.569	.7708			-41.6	-34.4			
	V	U	-44.074	2.194	.9297			-29.4	-19.0	8	6	
		D	-40.294	1.749	.7948			-30.0	-18.8			
		90	-52.561	2.338	.9245			-34.7	-24.2			
		93.5	-52.338	2.300	.9102			-34.8	-24.4			

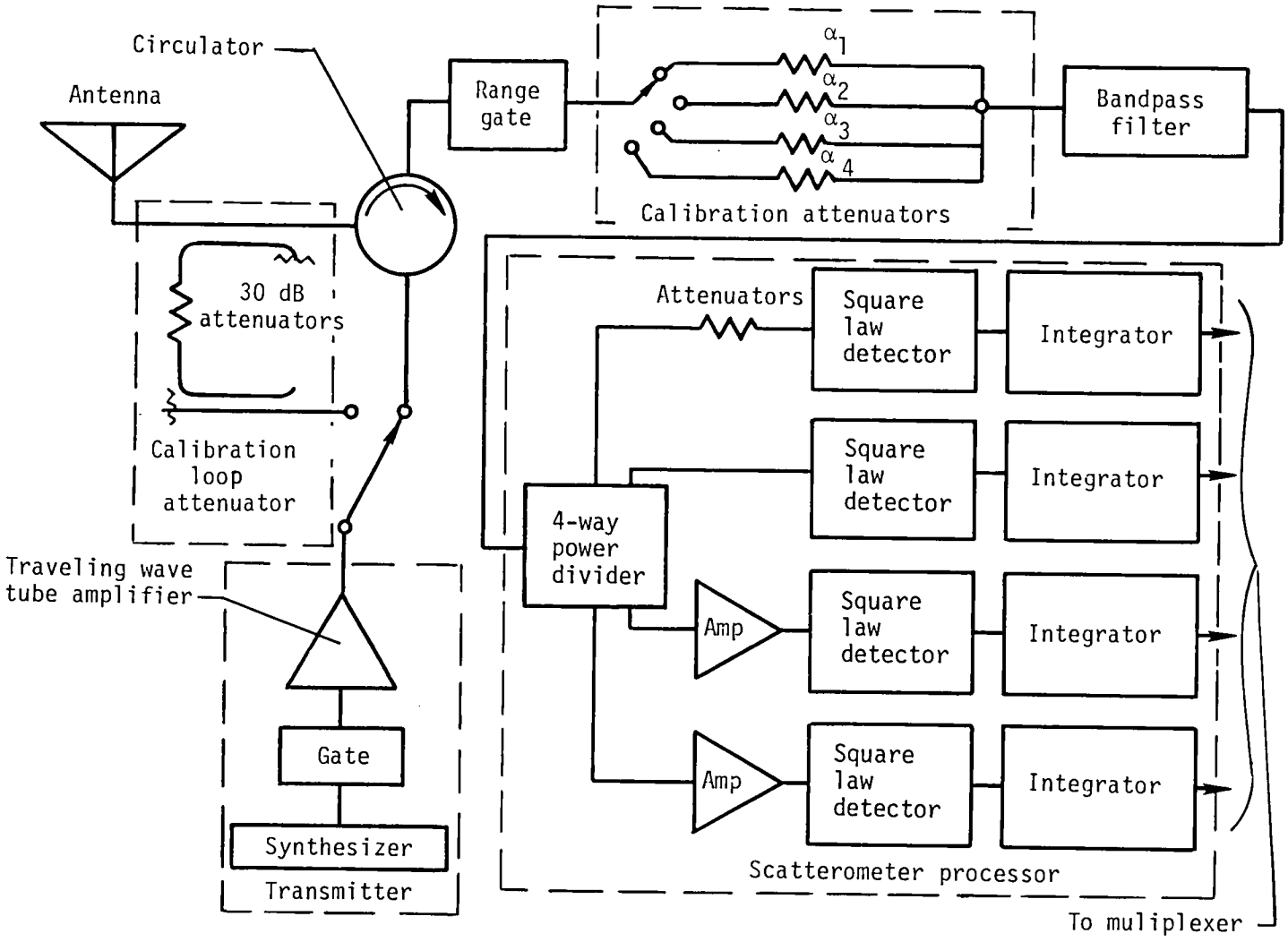

Figure 1.- Block diagram of scatterometer.

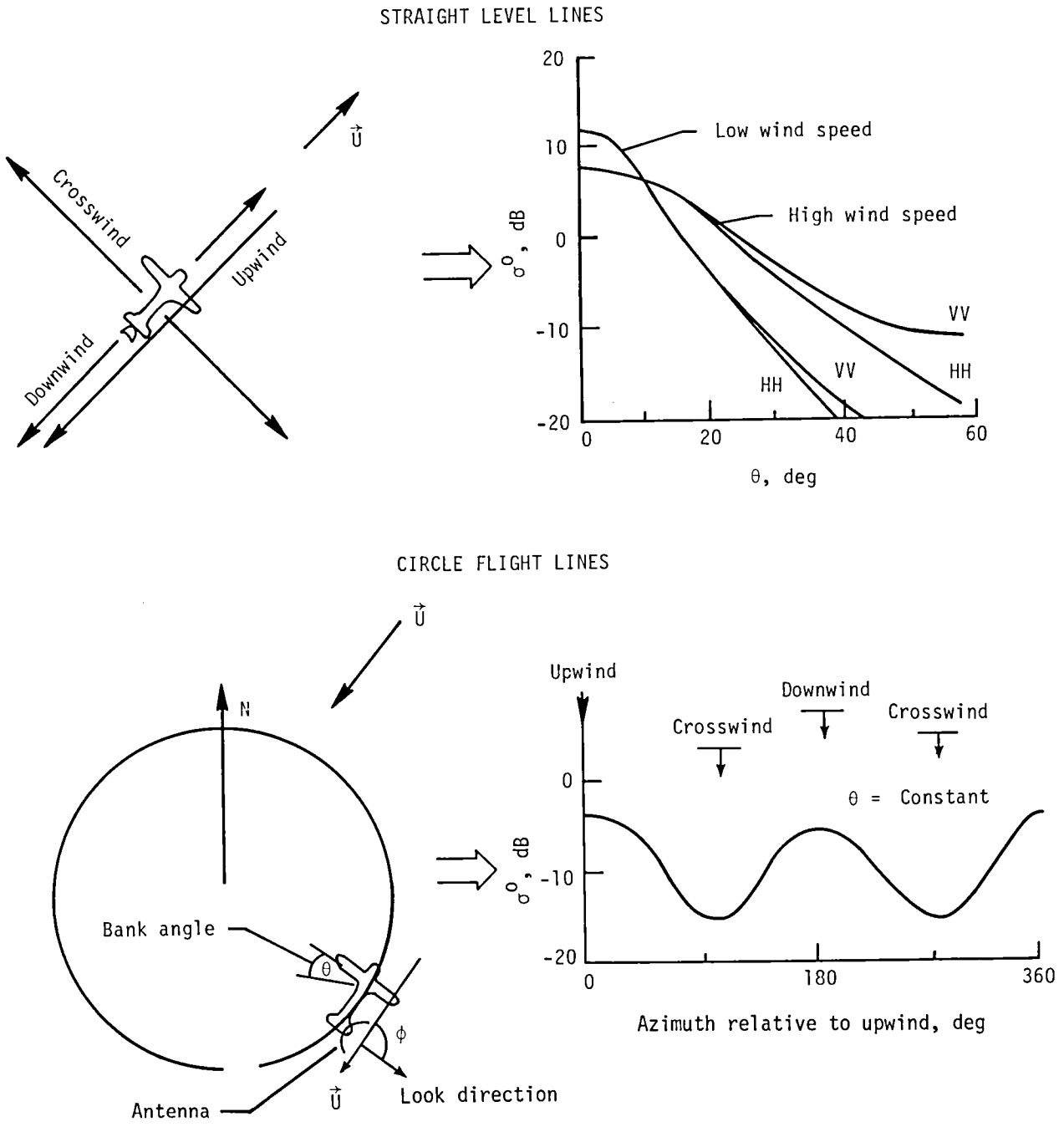

Figure 2.- Flight line (course) and resulting ocean signature scenario for RADSCAT flights.

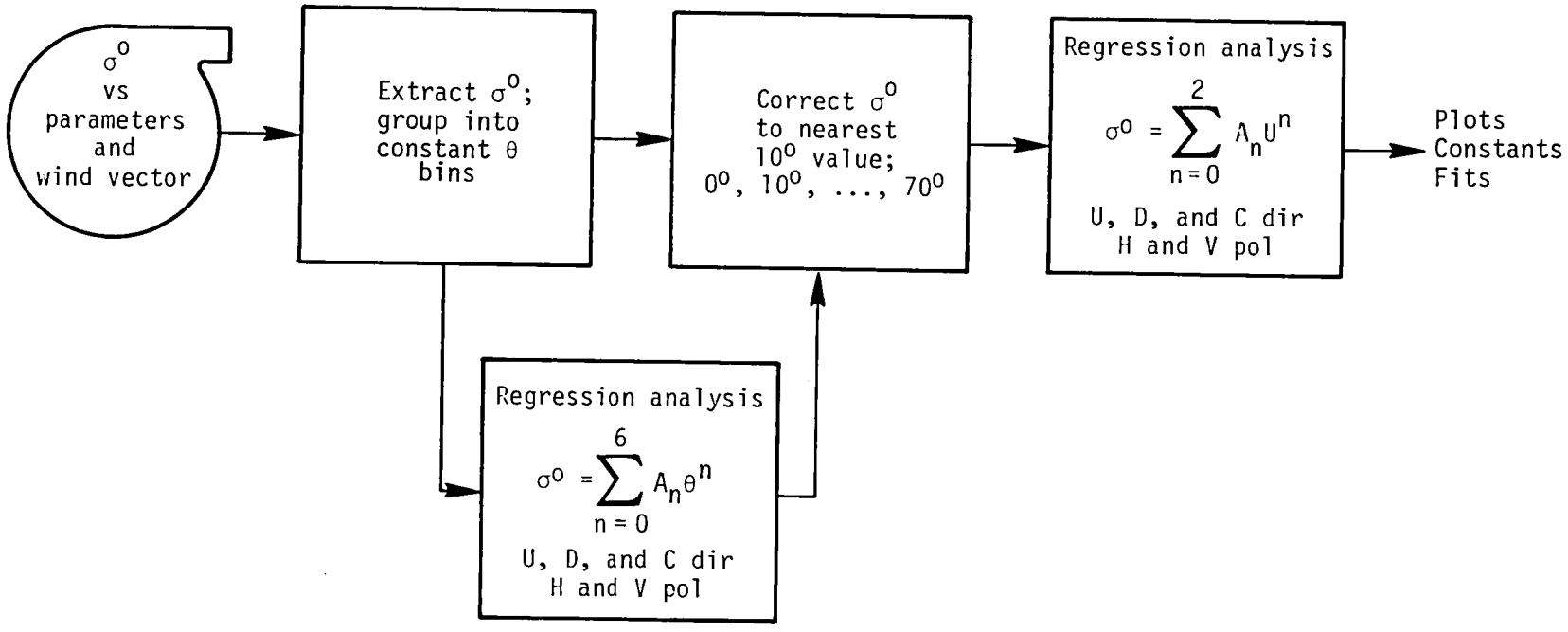

Figure 3.- Data processing flowchart for straight level flight line analysis.

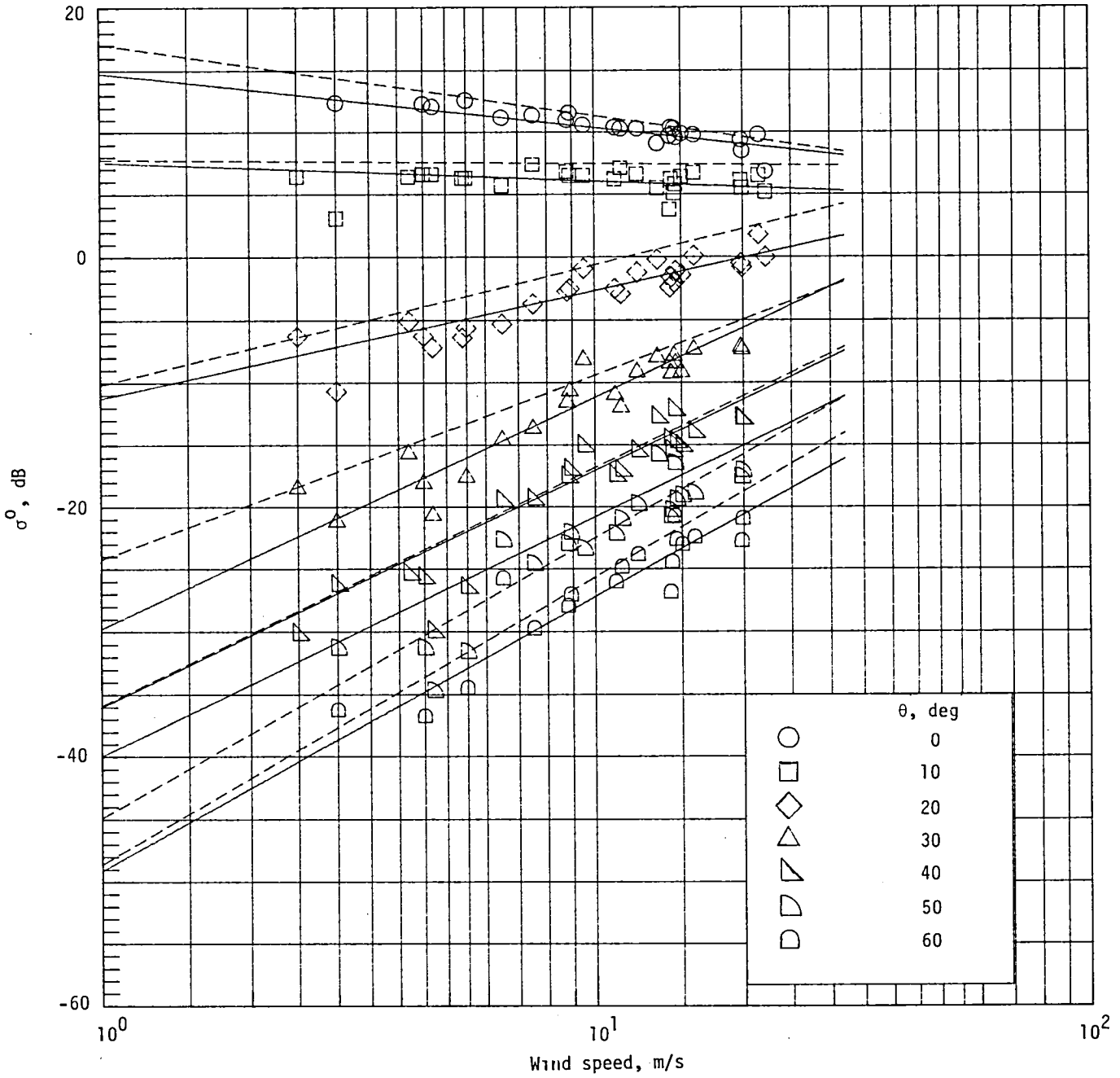

(a) Upwind; horizontal polarization.

Figure 4.- Linear regression of RADSCAT NRCS versus log (Wind speed), with SASS I model function line (dashed) for comparison.

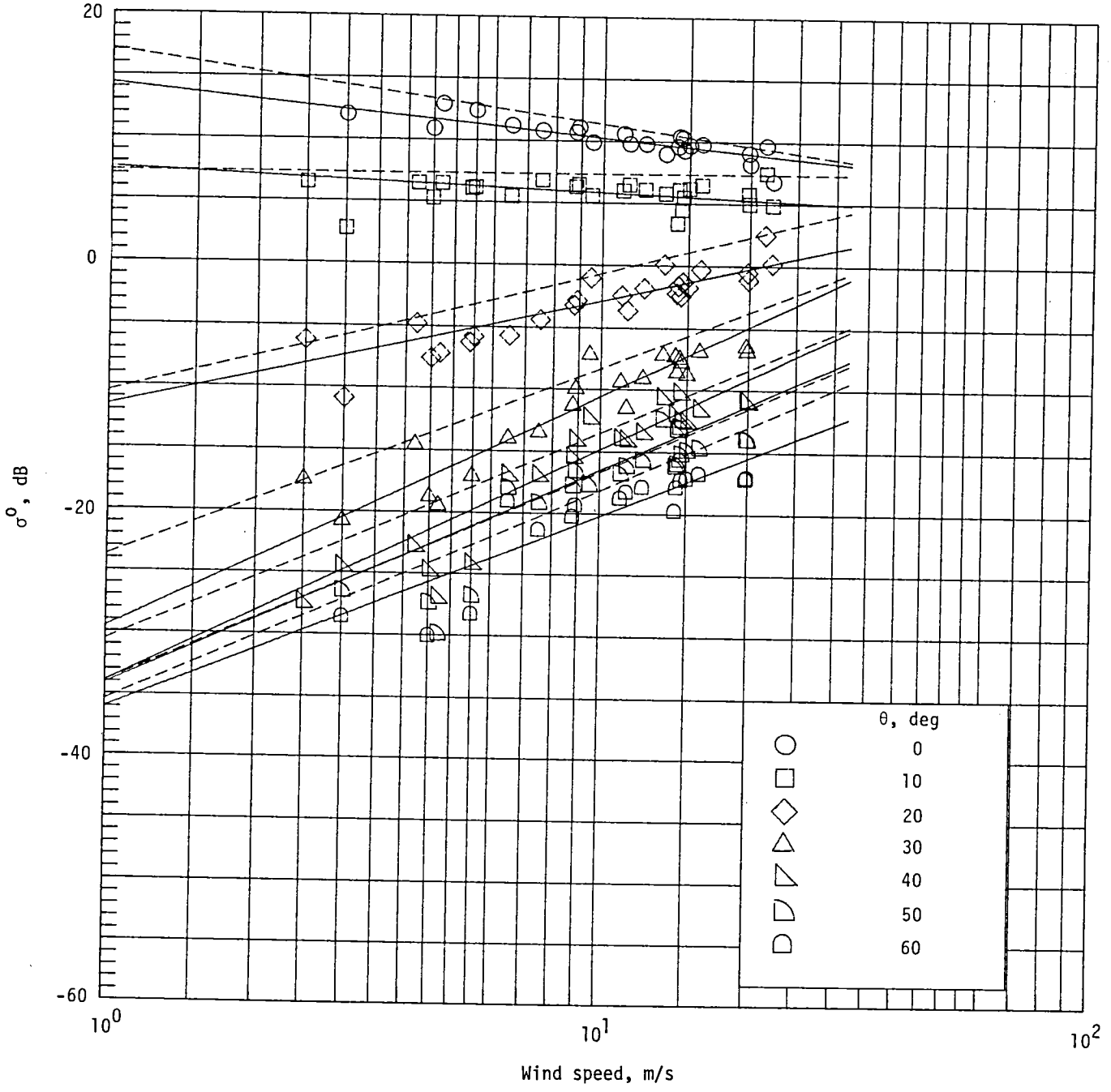

(b) Upwind; vertical polarization.

Figure 4.- Continued.

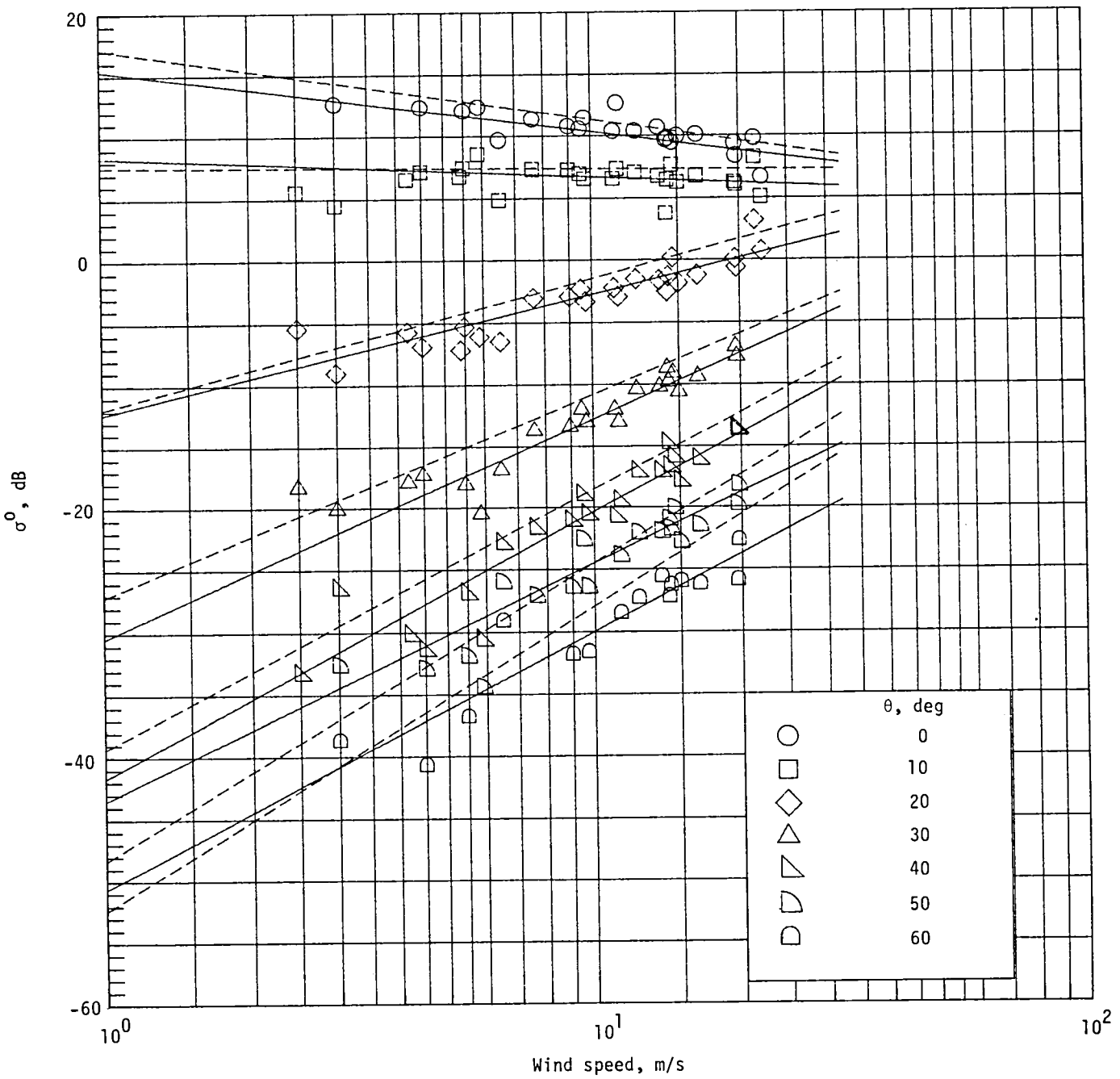

(c) Downwind; horizontal polarization.

Figure 4.- Continued.

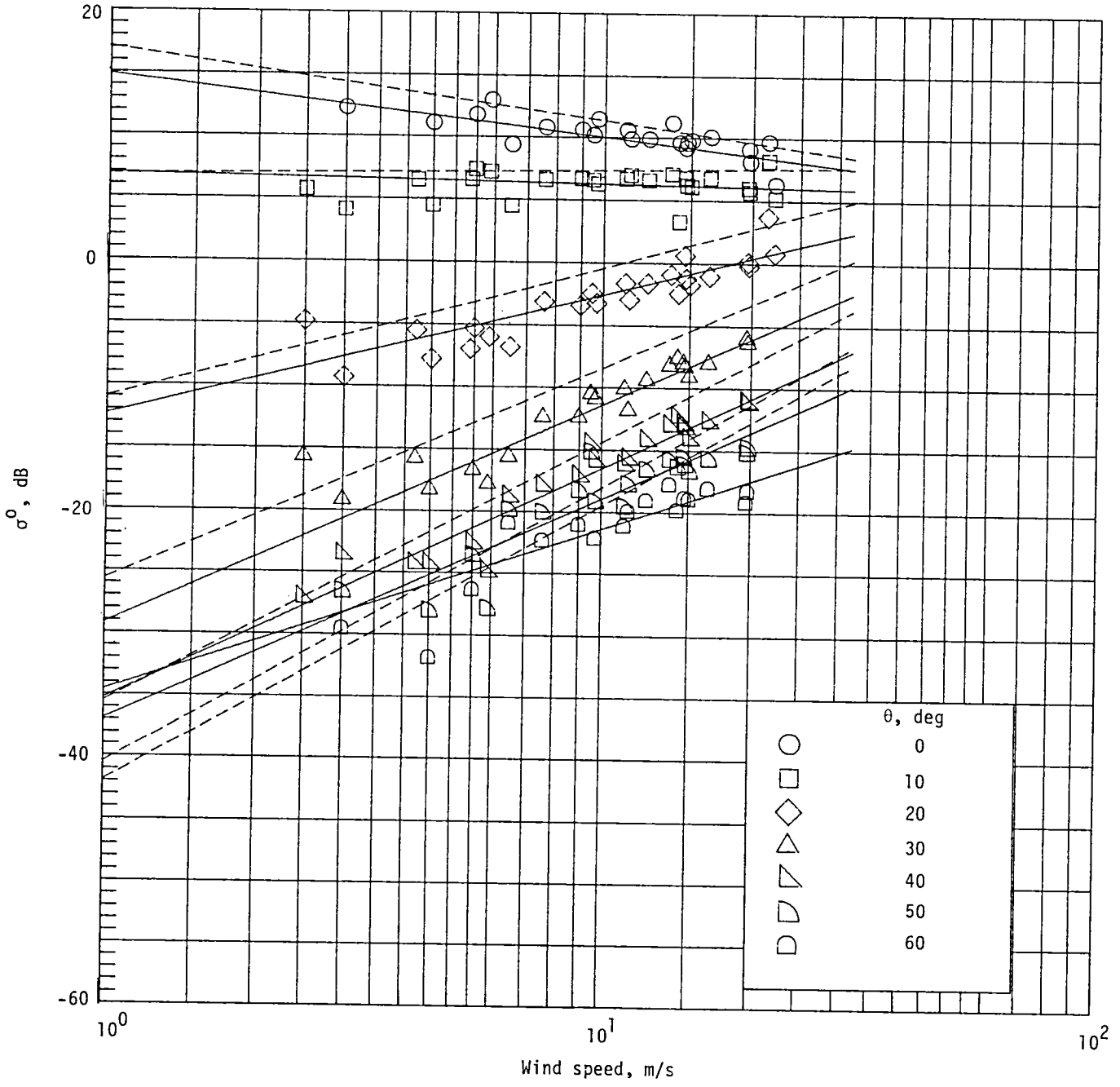

(d) Downwind; vertical polarization.

Figure 4.- Continued.

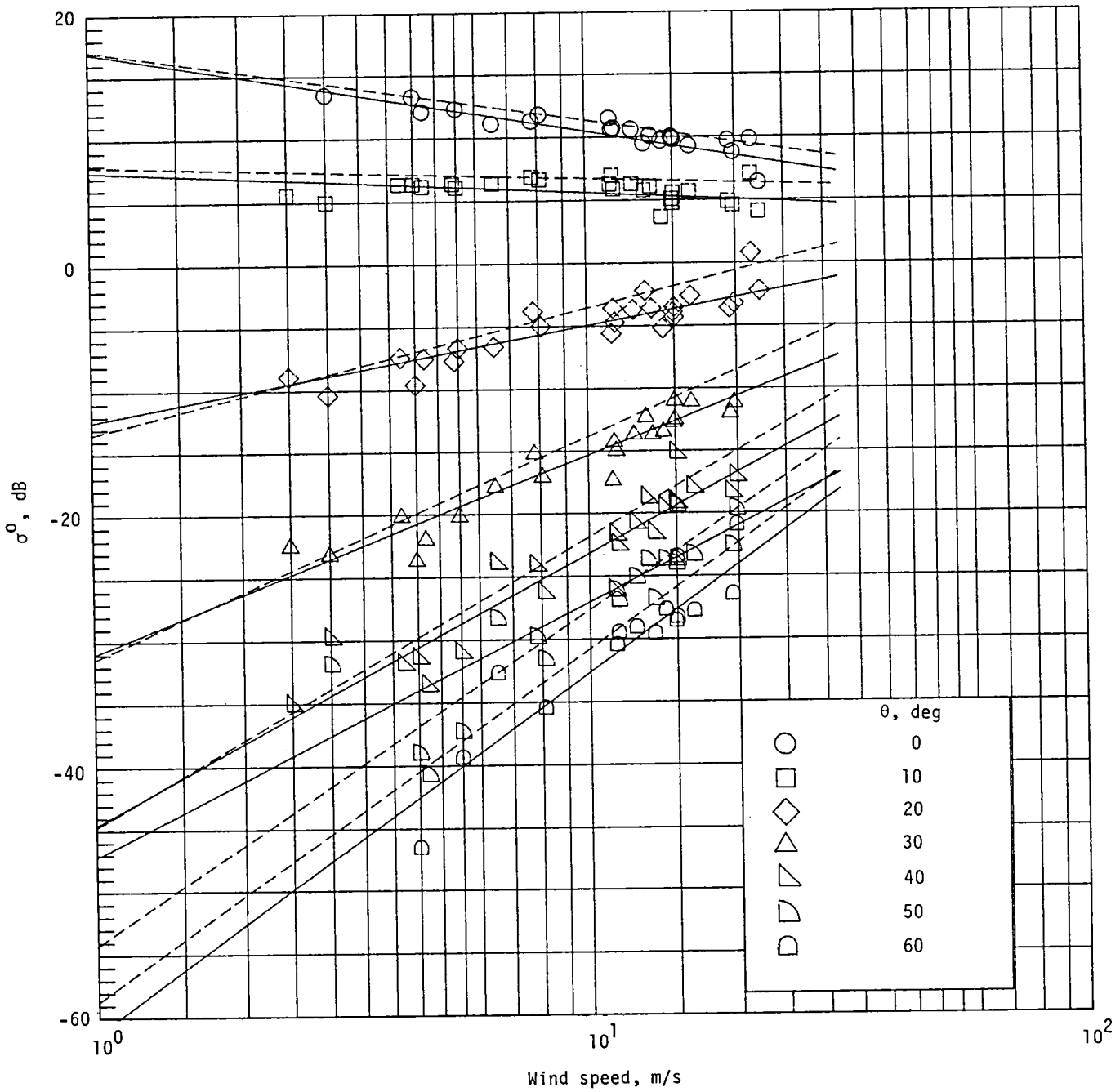

(e) Crosswind; horizontal polarization.

Figure 4.- Continued.

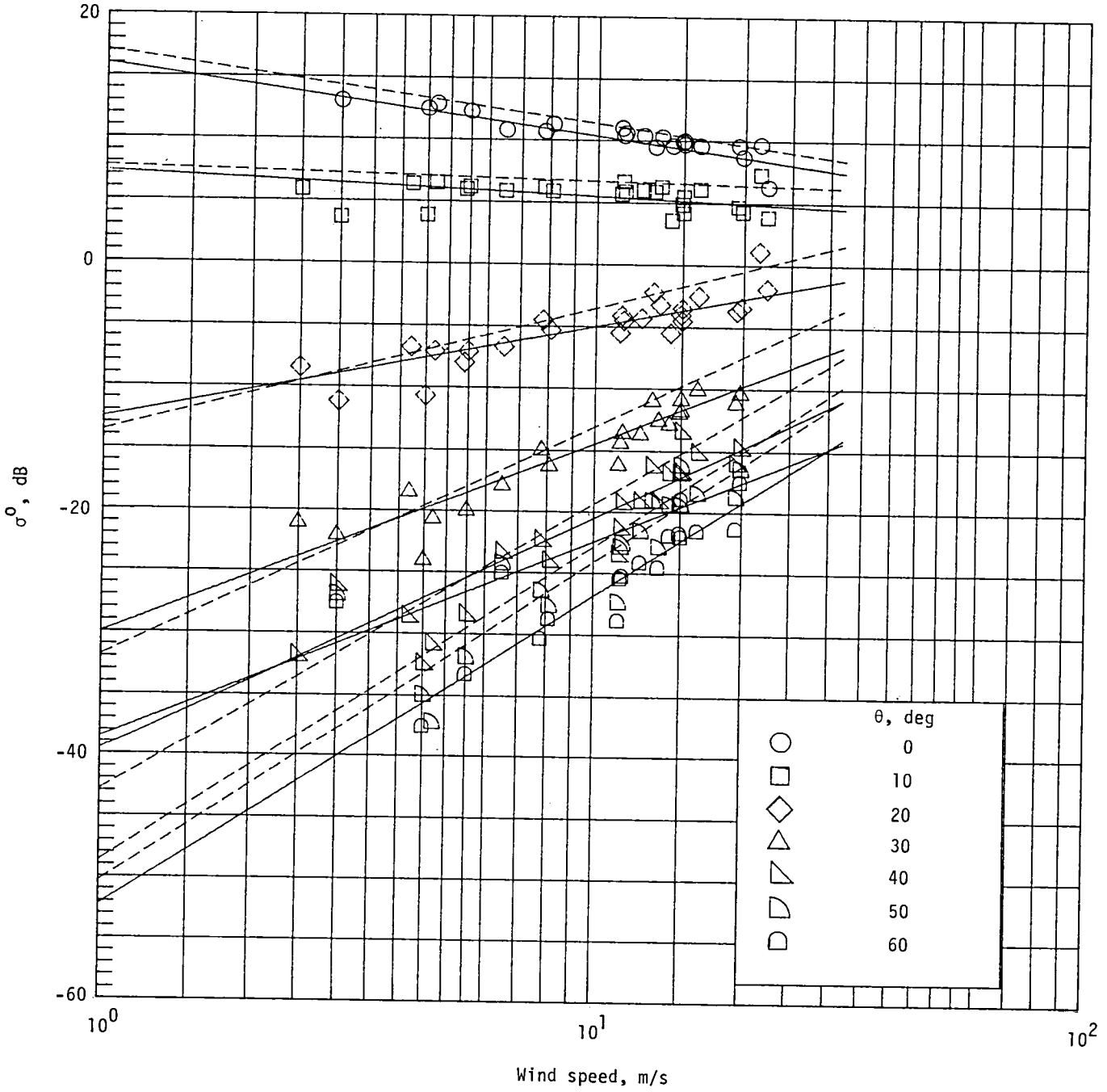

(f) Crosswind; vertical polarization.

Figure 4.- Concluded.

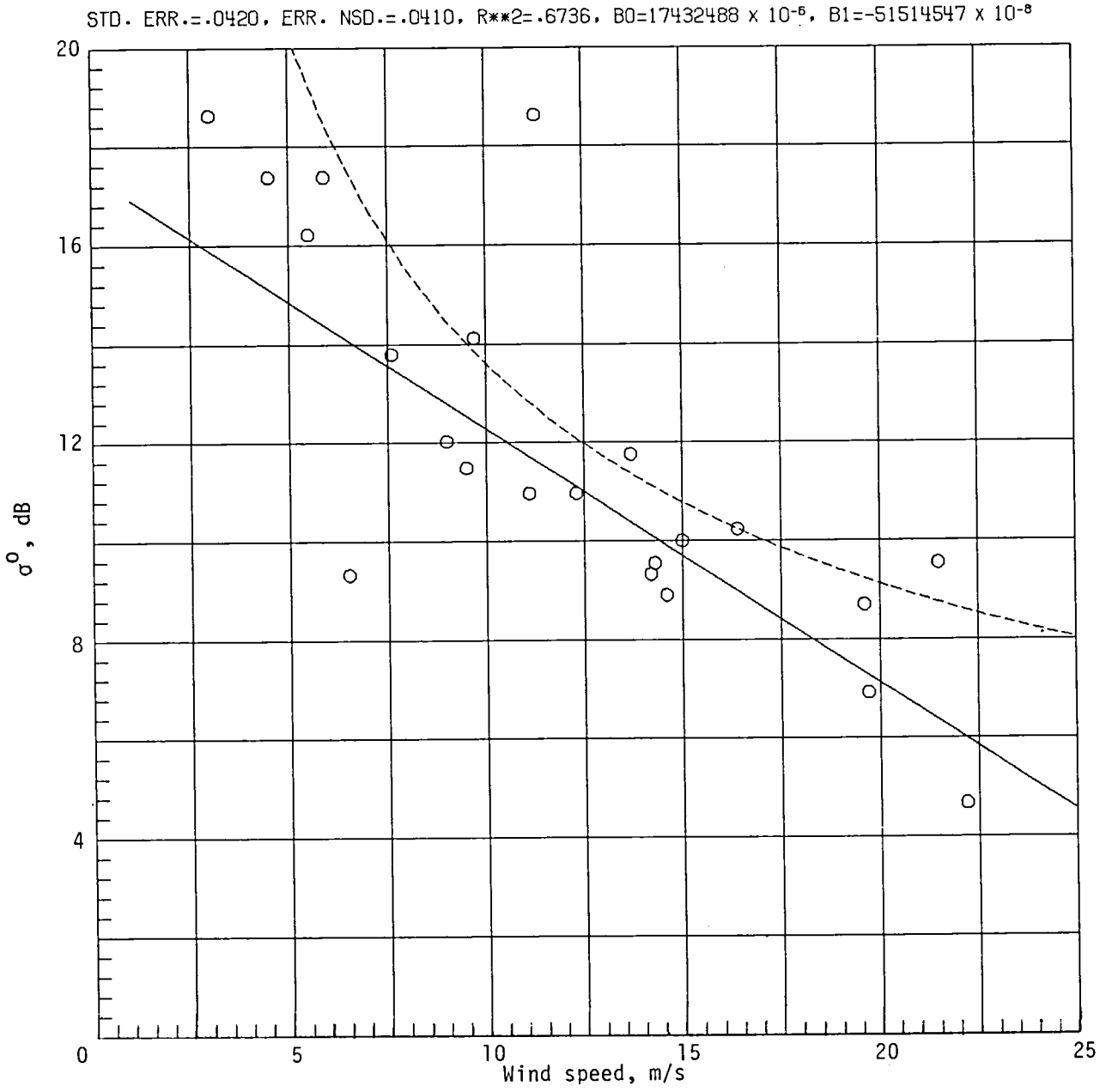

(a) $\theta = 0°$.

Figure 5.- Regression of NRCS versus wind speed, with SASS I model function line (dashed) for comparison. Downwind; horizontal polarization.

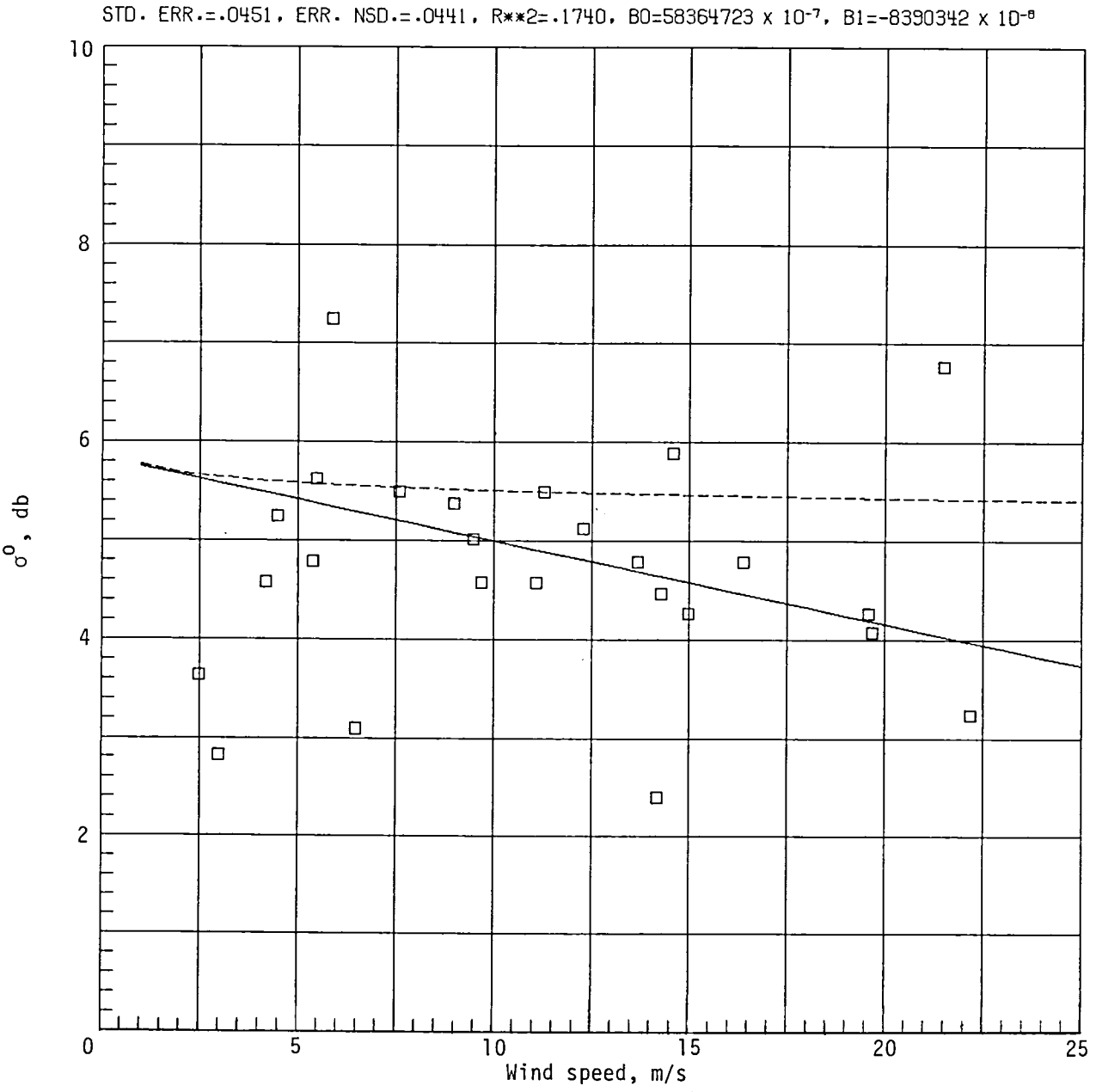

(b) $\theta = 10°$.

Figure 5.- Continued.

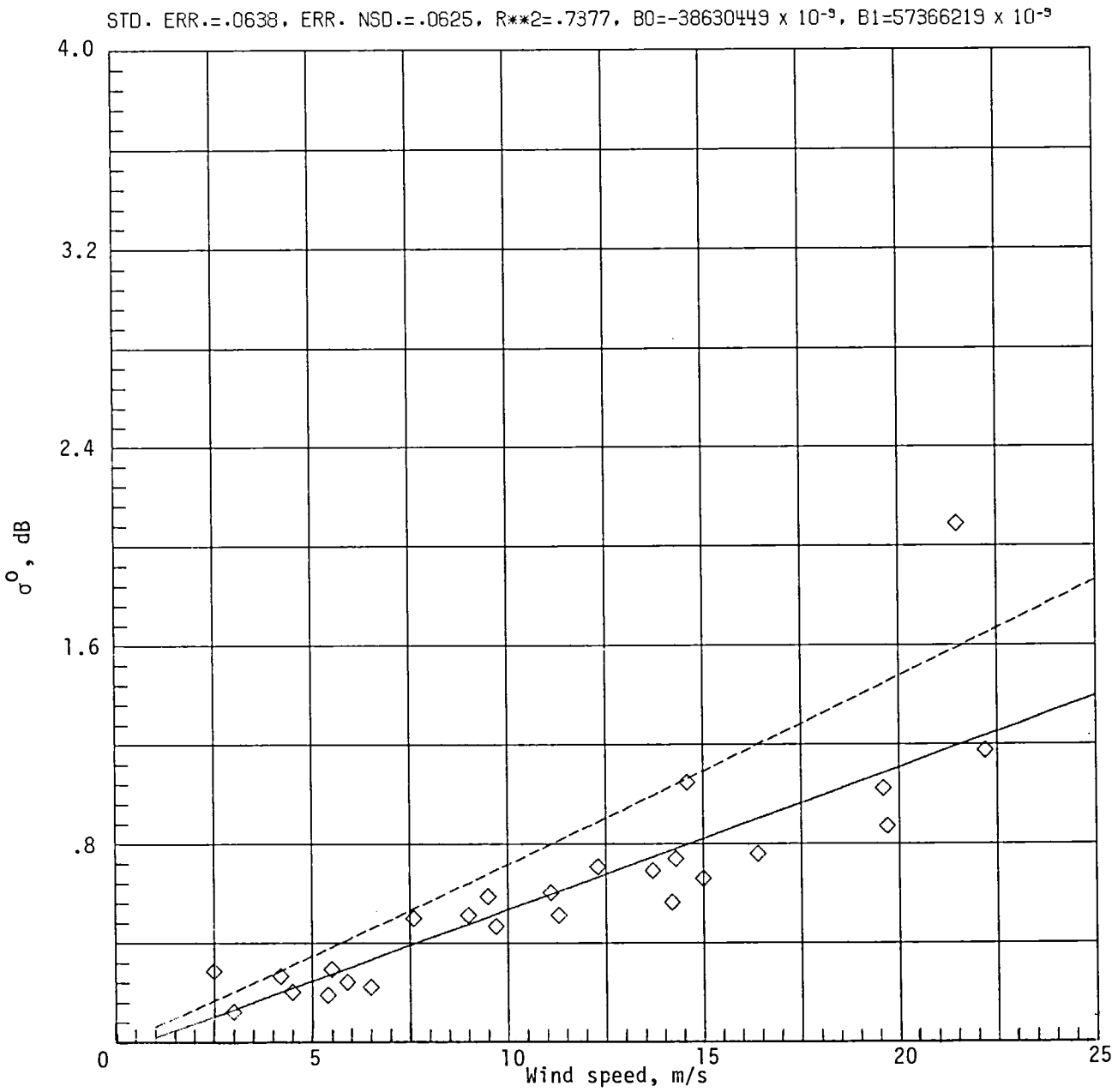

(c) $\theta = 20°$.

Figure 5.- Continued.

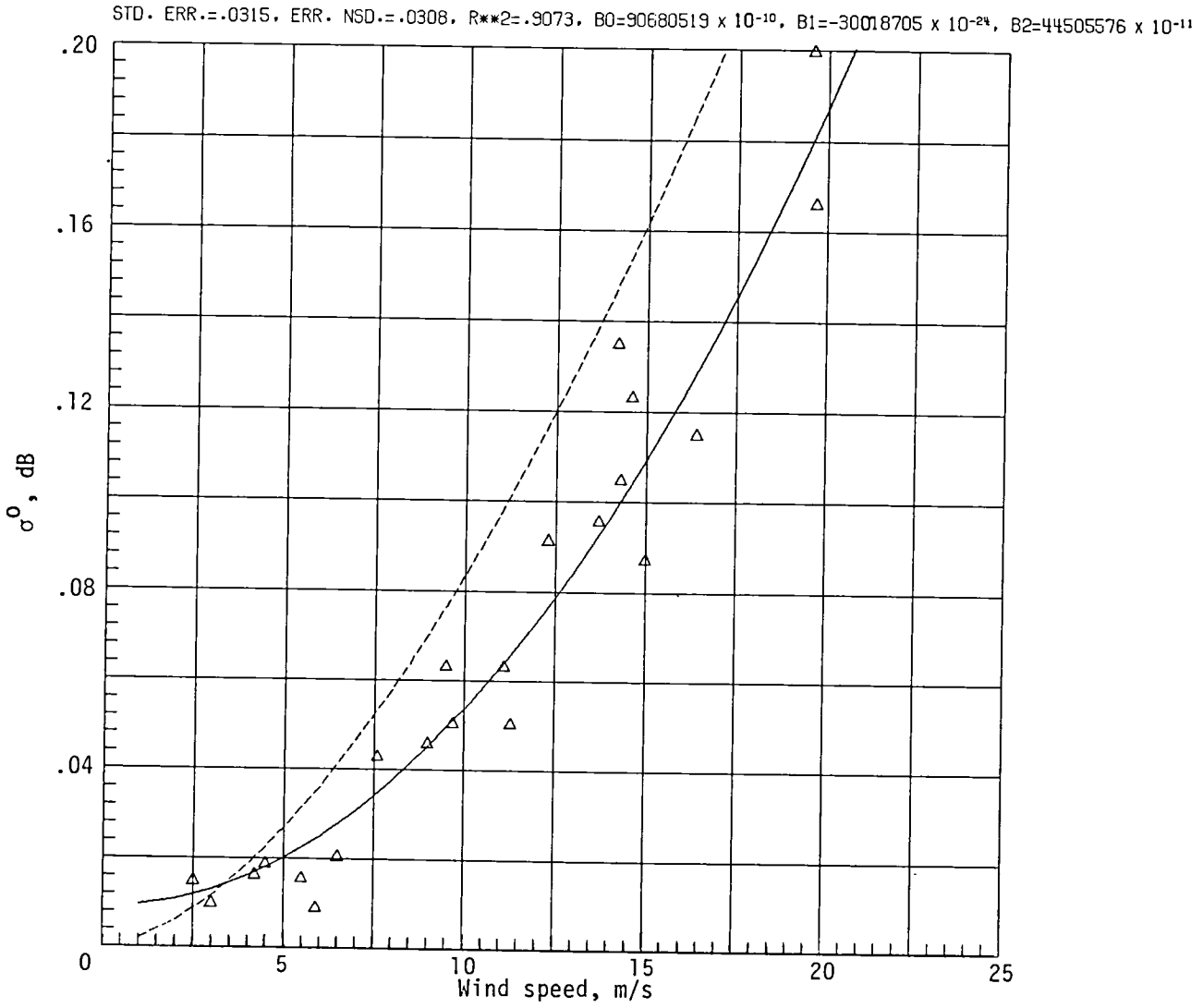

(d) $\theta = 30°$.

Figure 5.- Continued.

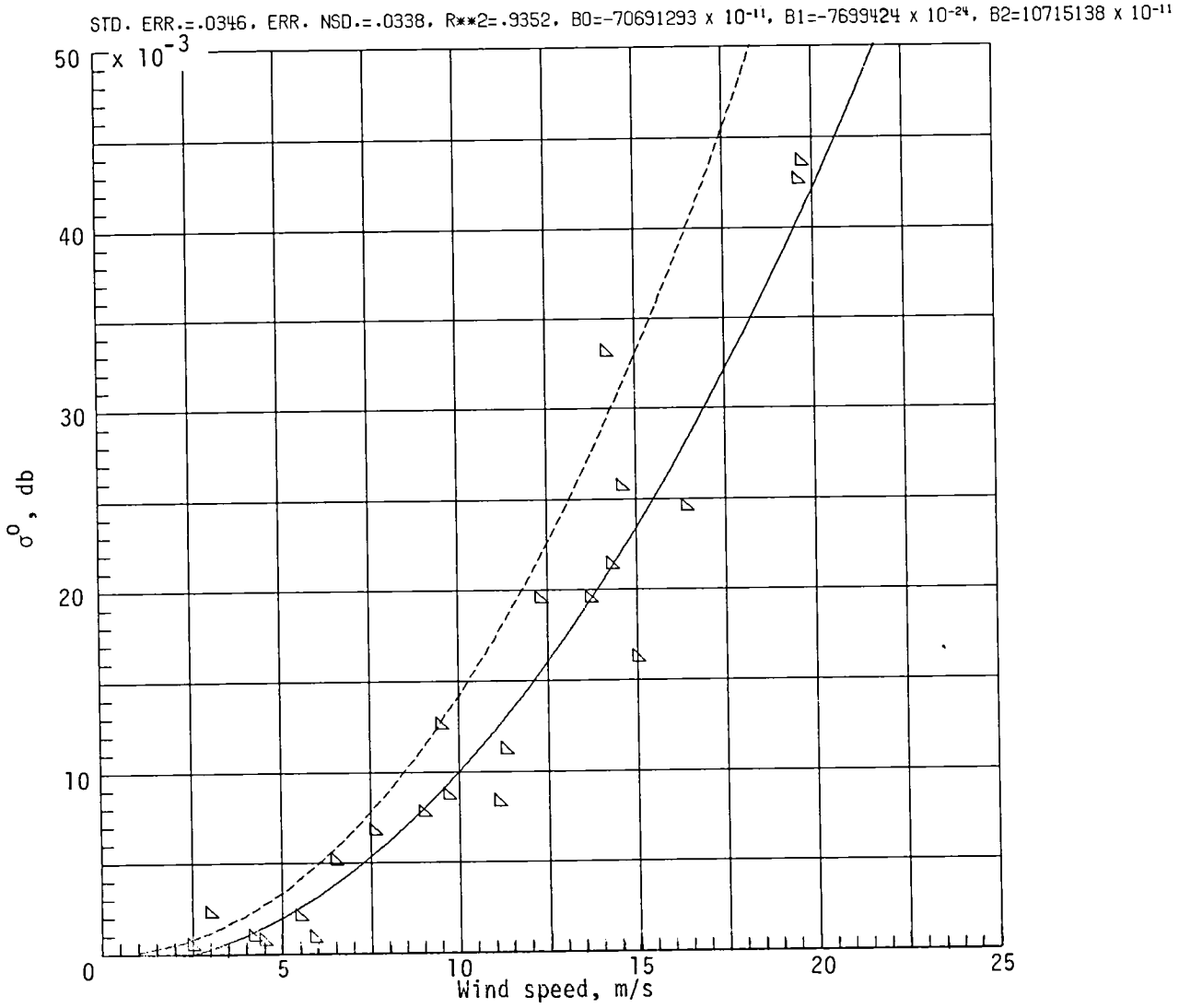

(e) $\theta = 40°$.

Figure 5.- Continued.

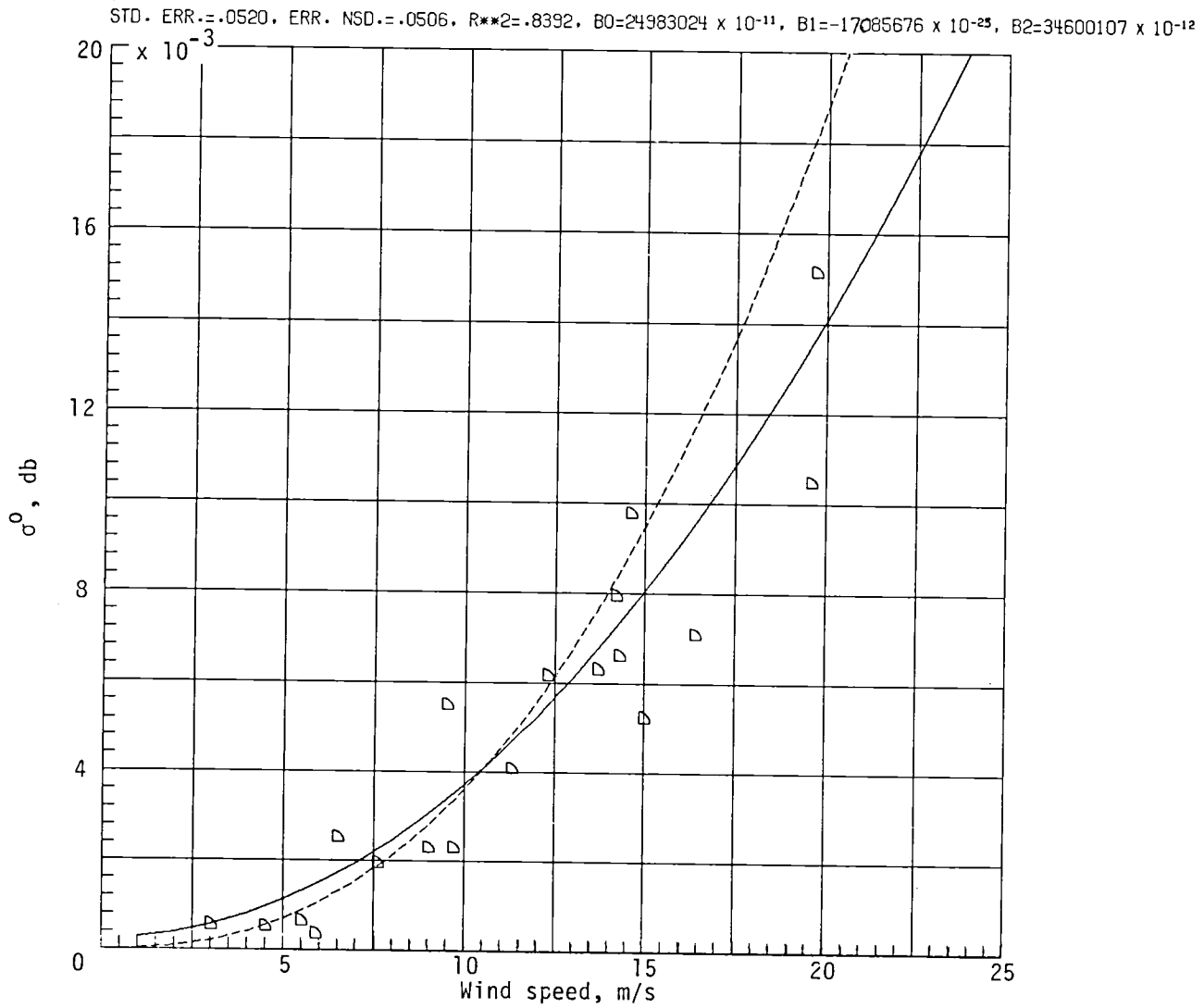

(f) $\theta = 50°$.

Figure 5.- Continued.

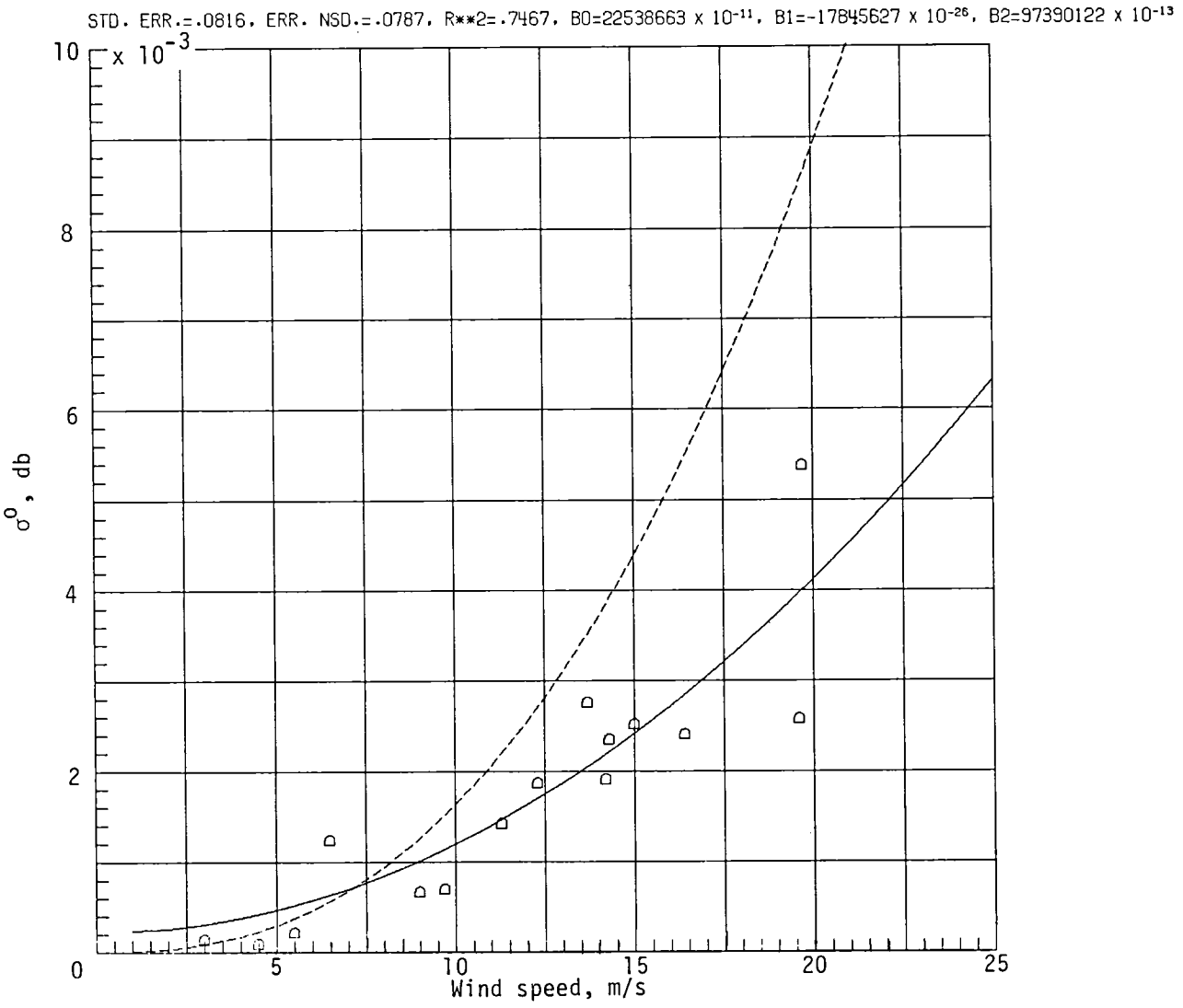

(g) $\theta = 60°$.

Figure 5.- Concluded.

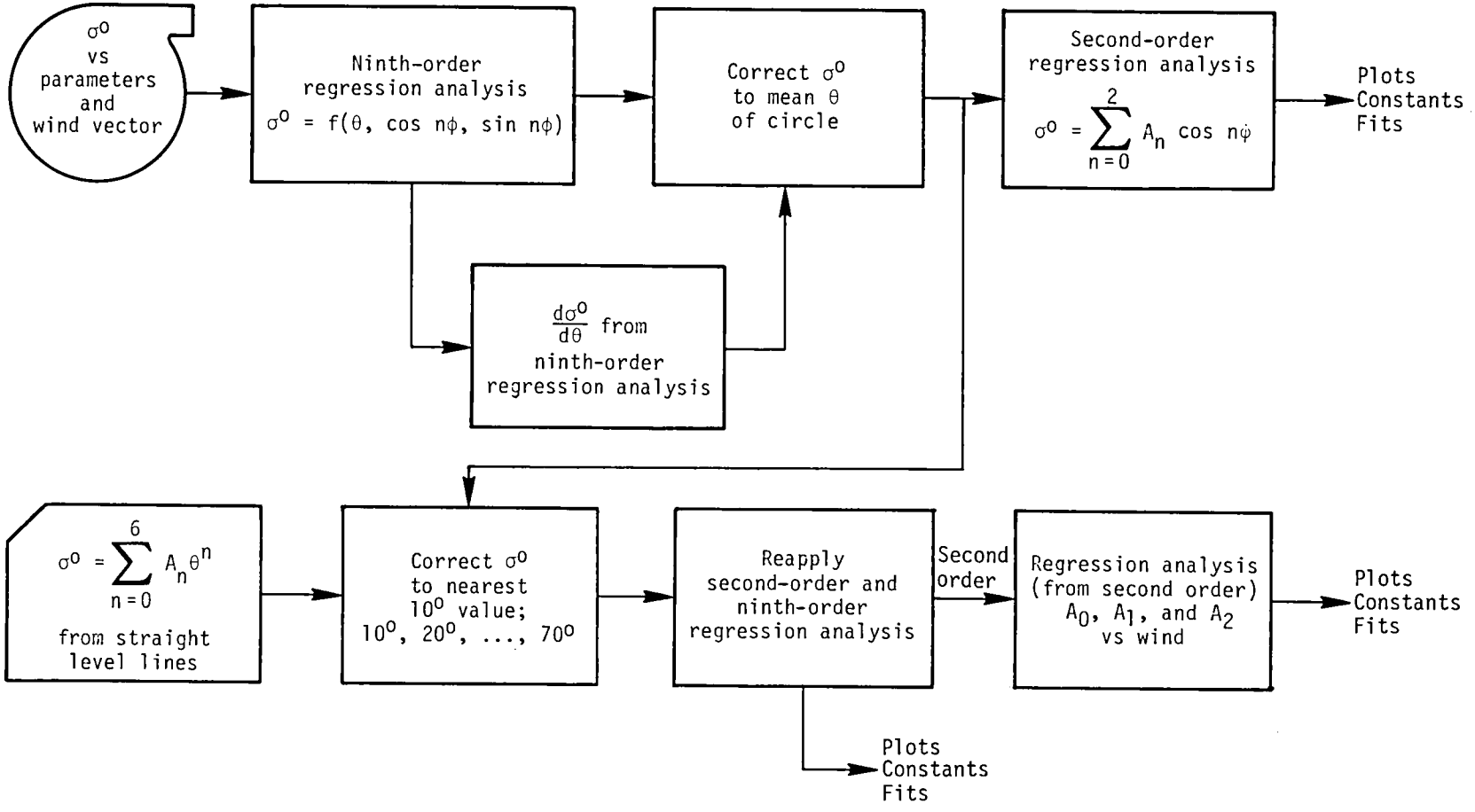

Figure 6.- Data processing flowchart for circle flight line analyses.

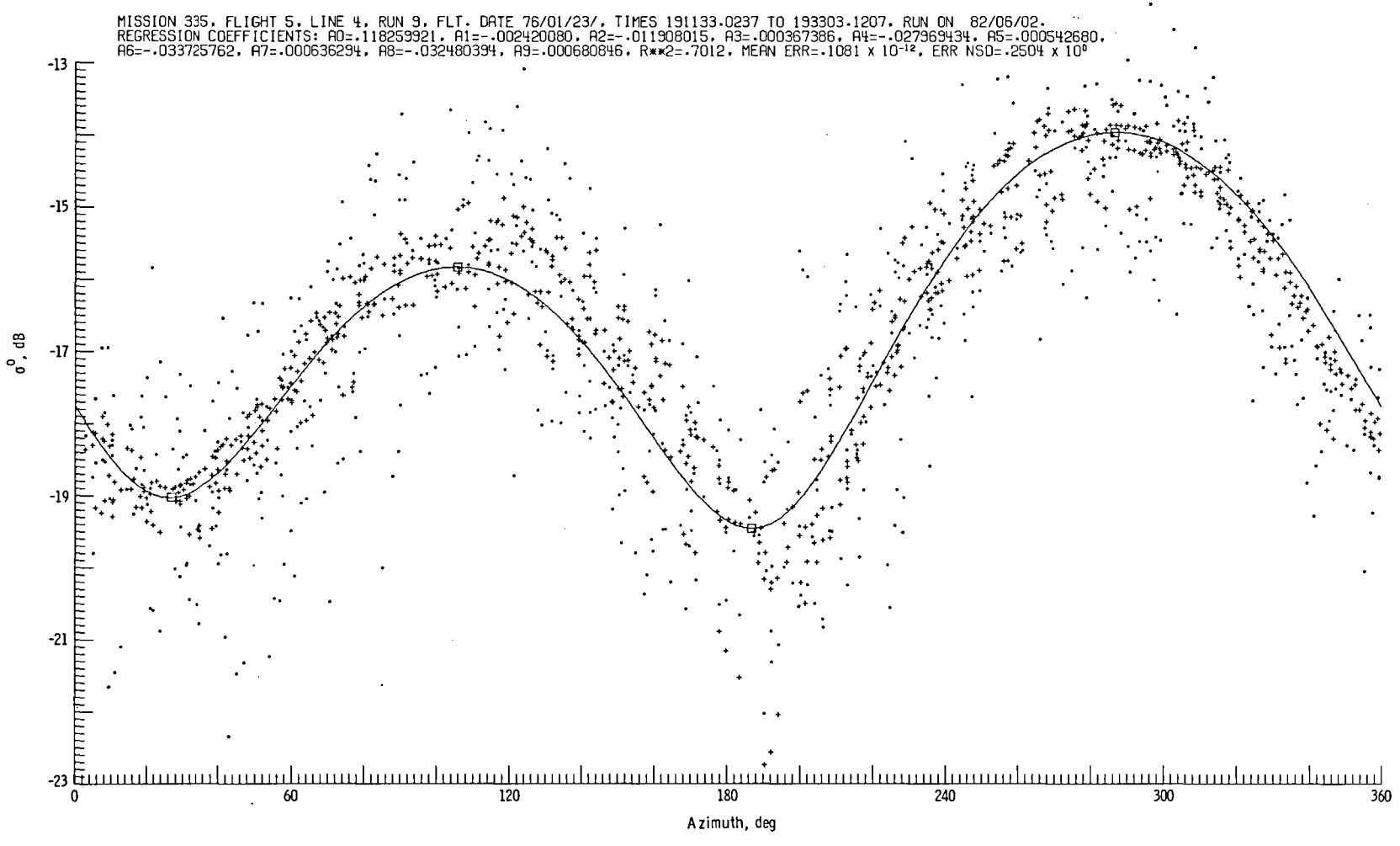

Figure 7.- Ninth-order regression fit of NRCS versus azimuth for typical RADSCAT circle flight line. Mission 335, flight 5; $\theta = 39°$; horizontal polarization.

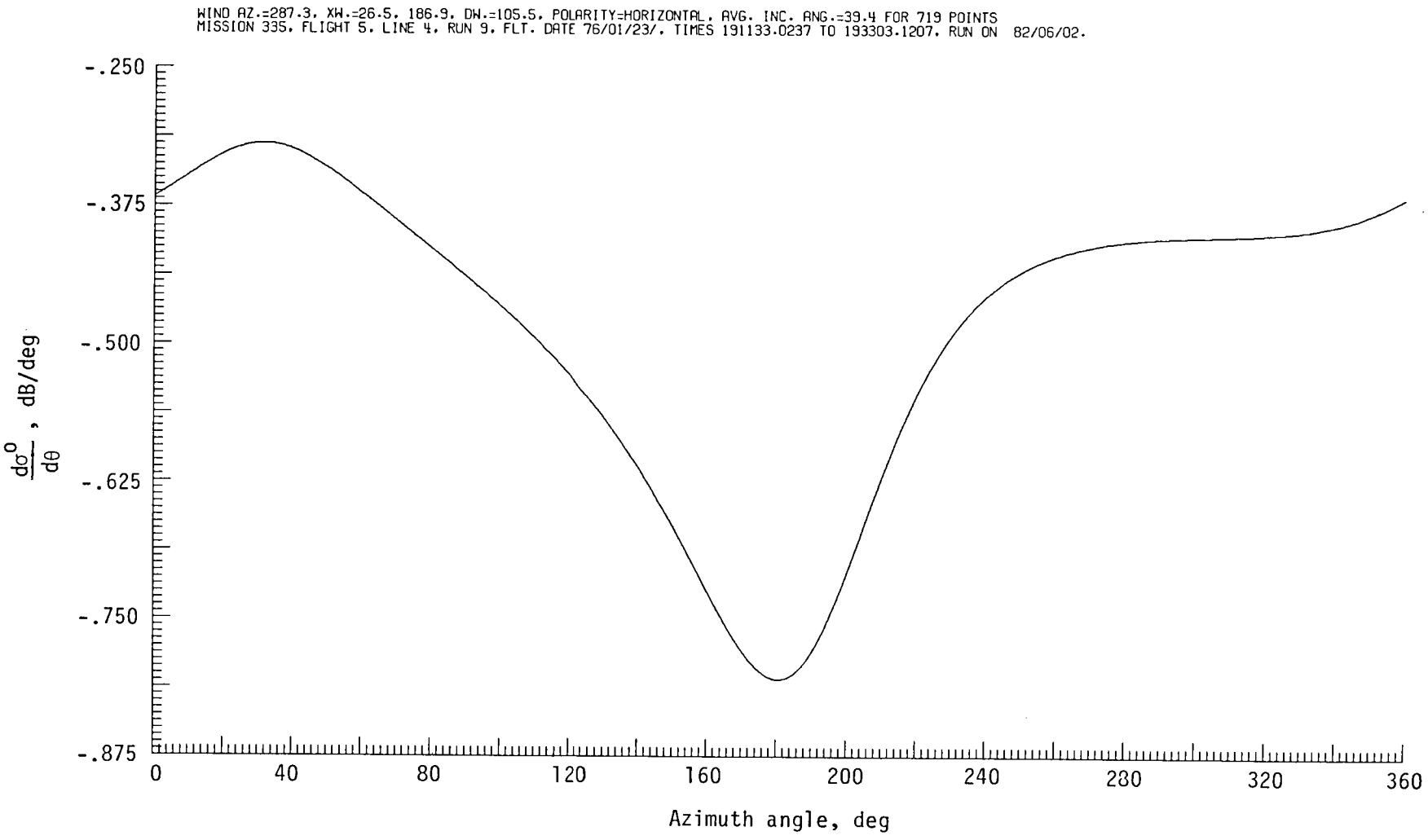

Figure 8.- Rate of change of NRCS with incidence angle d(NRCS)/dθ versus azimuth for ninth-order regression fit of typical RADSCAT circle flight line. Mission 335, flight 5; θ = 39°; horizontal polarization.

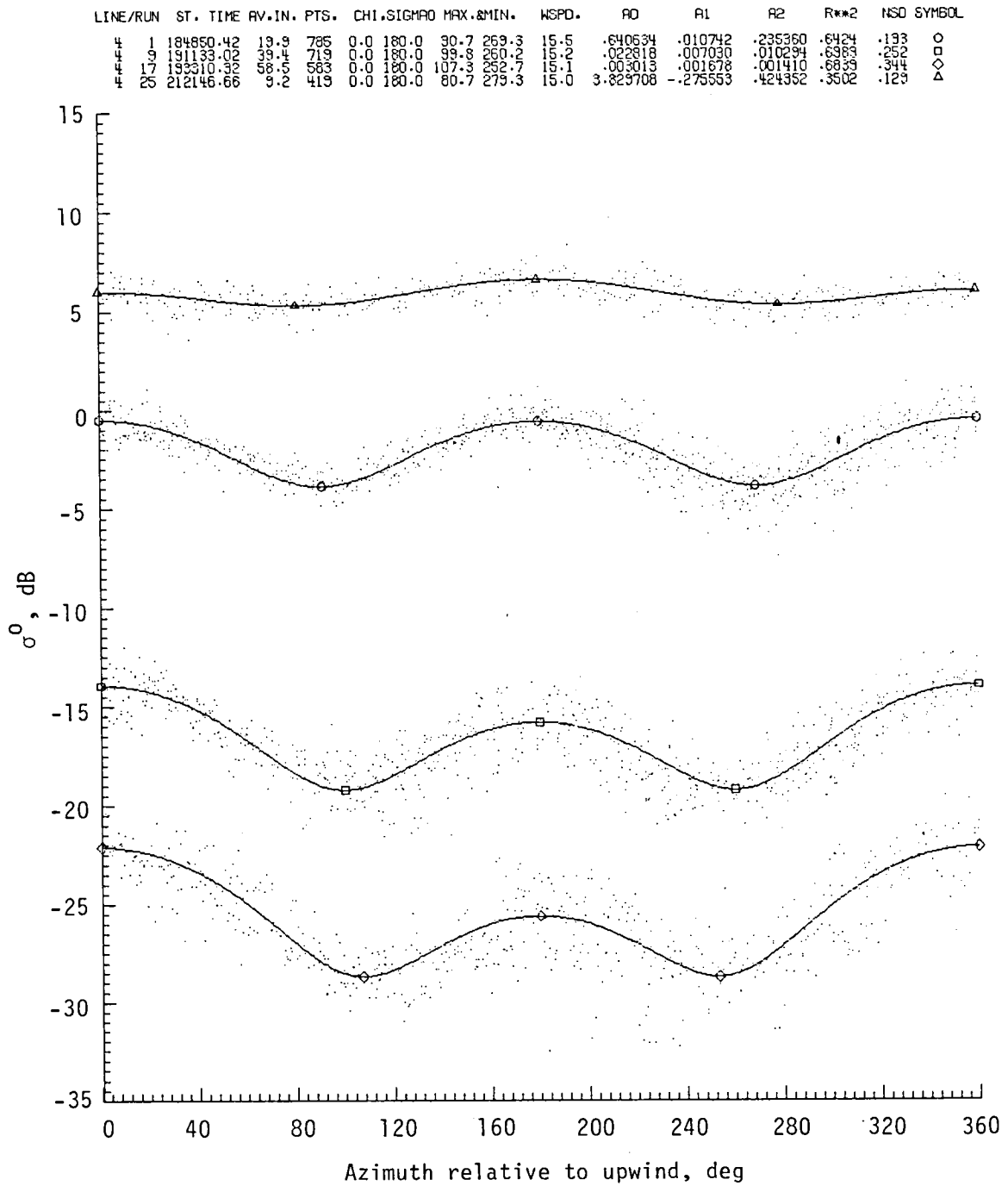

(a) Horizontal polarization.

Figure 9.- Second-order regression fit of NRCS versus azimuth relative to upwind for typical RADSCAT circle flight line. Mission 335, flight 5.

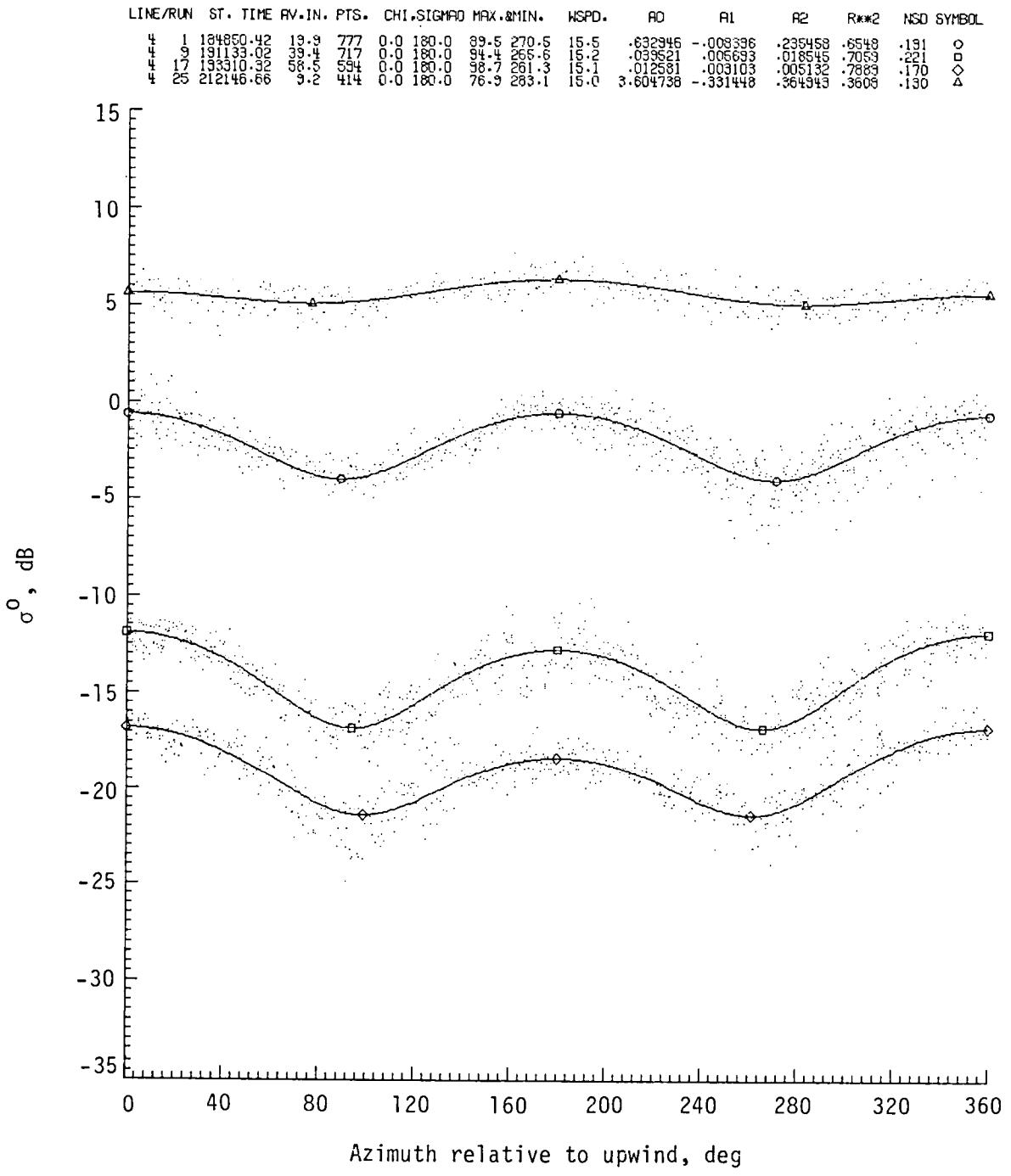

(b) Vertical polarization.

Figure 9.- Concluded.

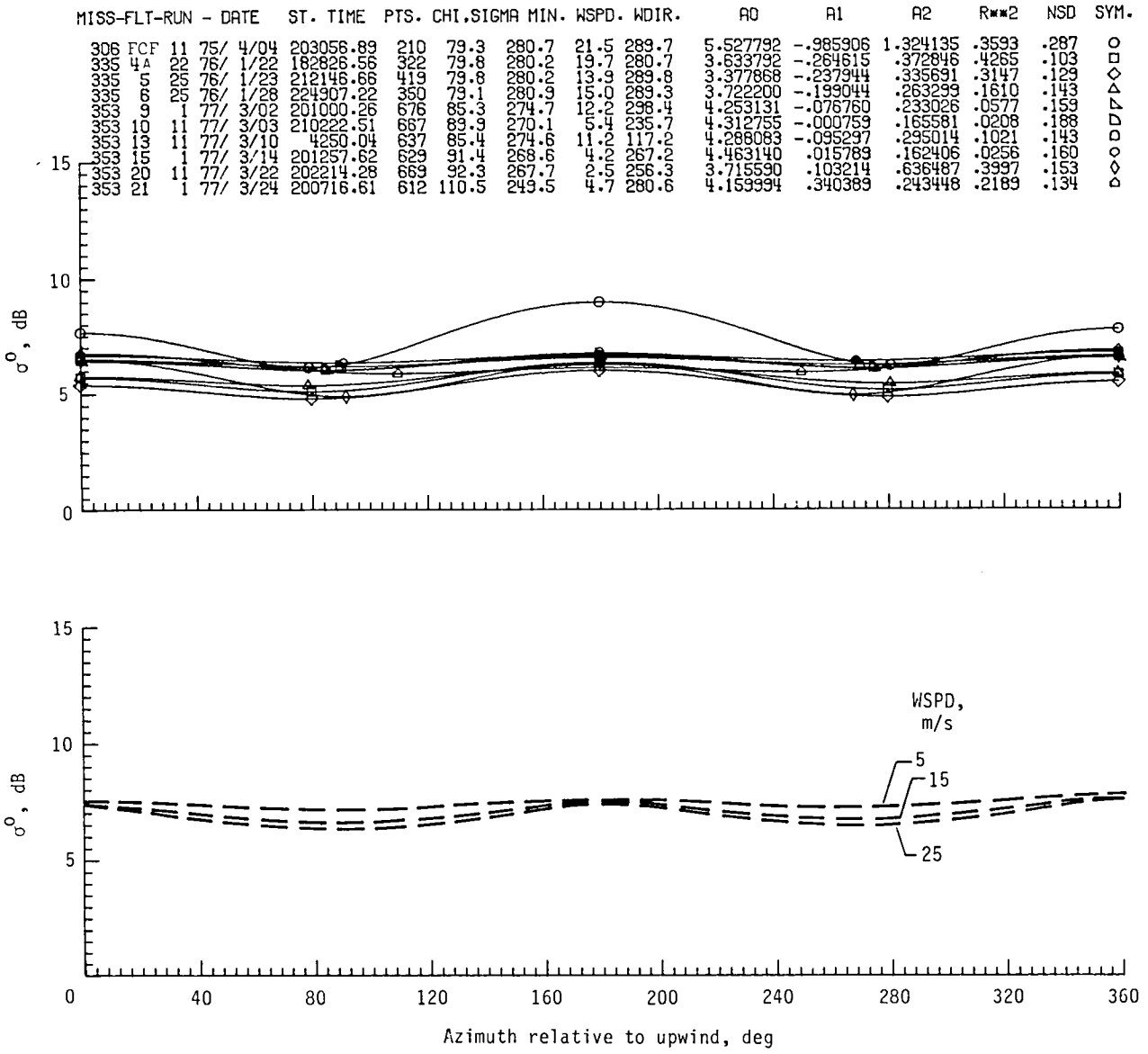

(a) Horizontal polarization.

Figure 10.- Second-order regression fit of NRCS versus azimuth relative to upwind for all RADSCAT circle flight lines at $\theta = 10°$, with SASS I regression lines (dashed) for comparison.

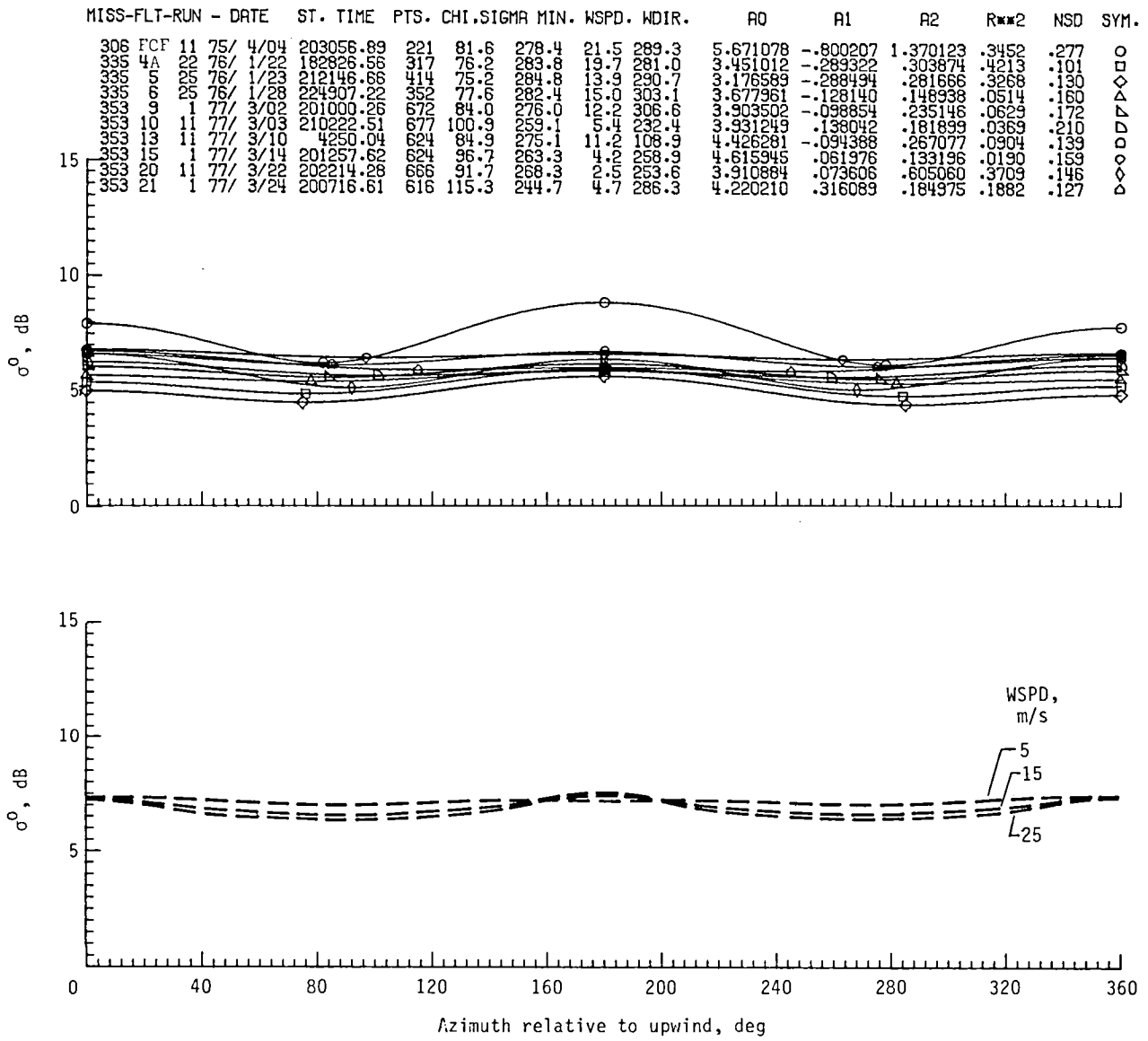

(b) Vertical polarization.

Figure 10. Concluded.

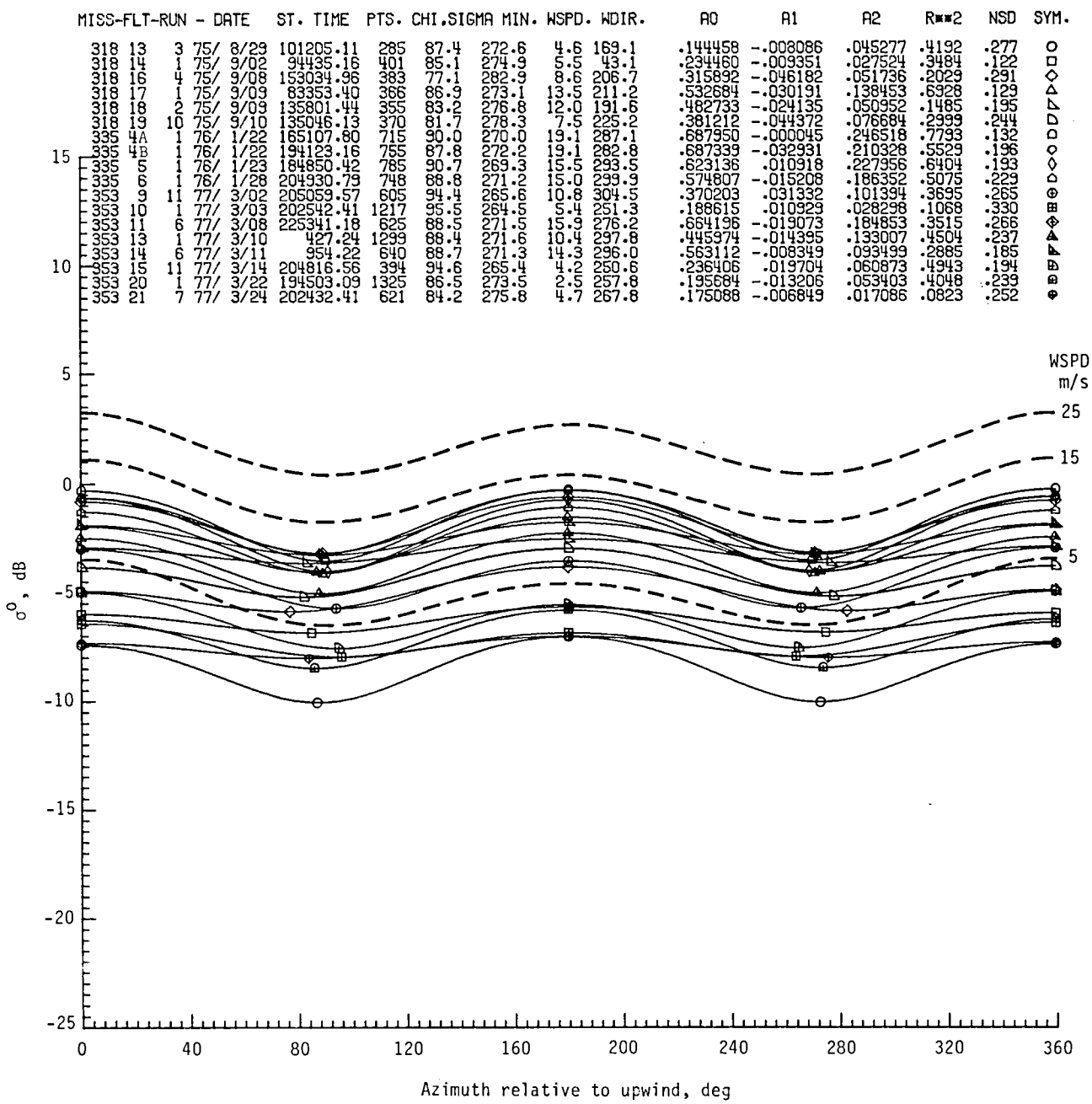

(a) Horizontal polarization.

Figure 11.- Second-order regression fit of NRCS versus azimuth relative to upwind for all RADSCAT circle flights at $\theta = 20°$, with SASS I regression lines (dashed) for comparison.

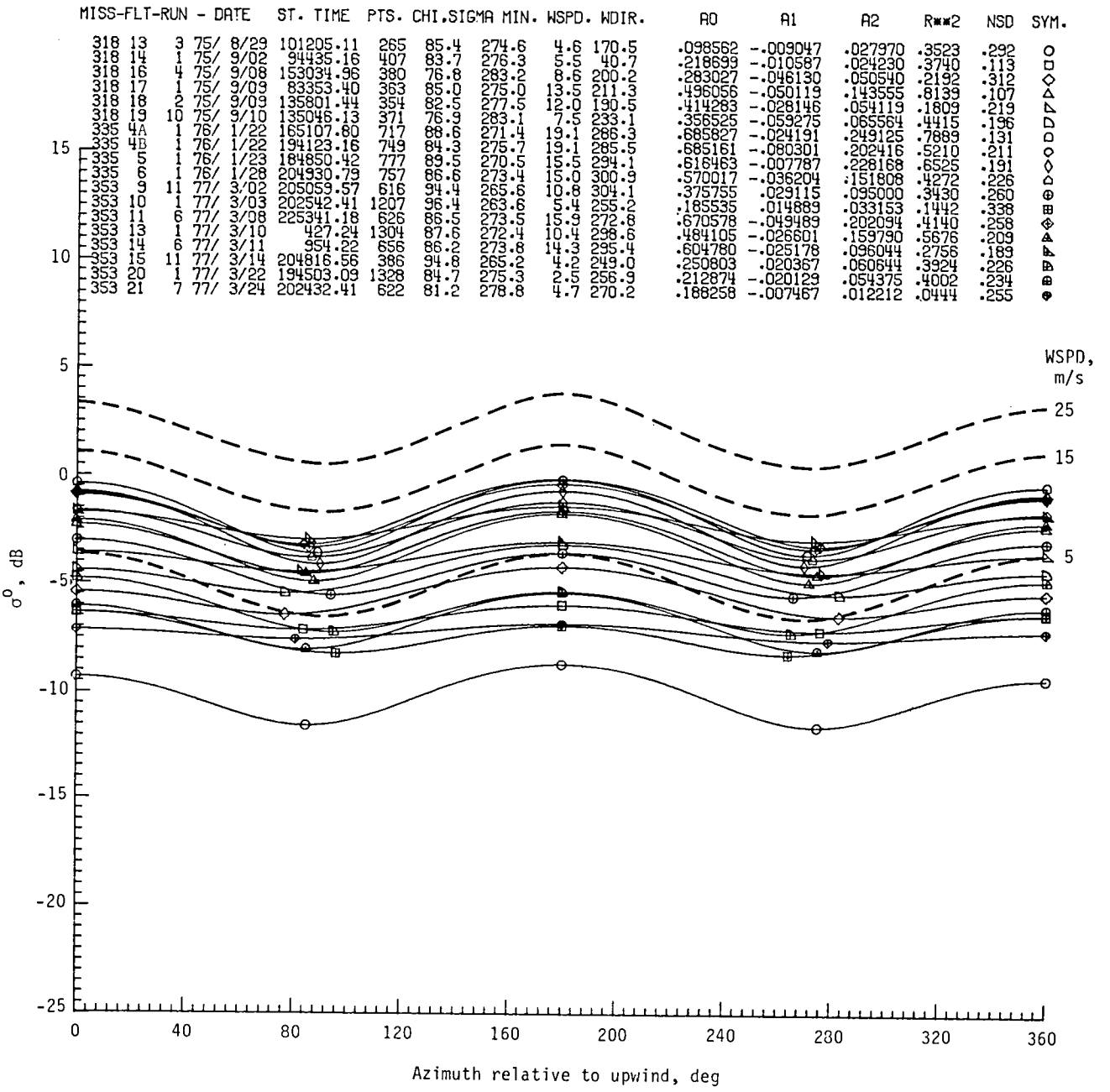

(b) Vertical polarization.

Figure 11.- Concluded.

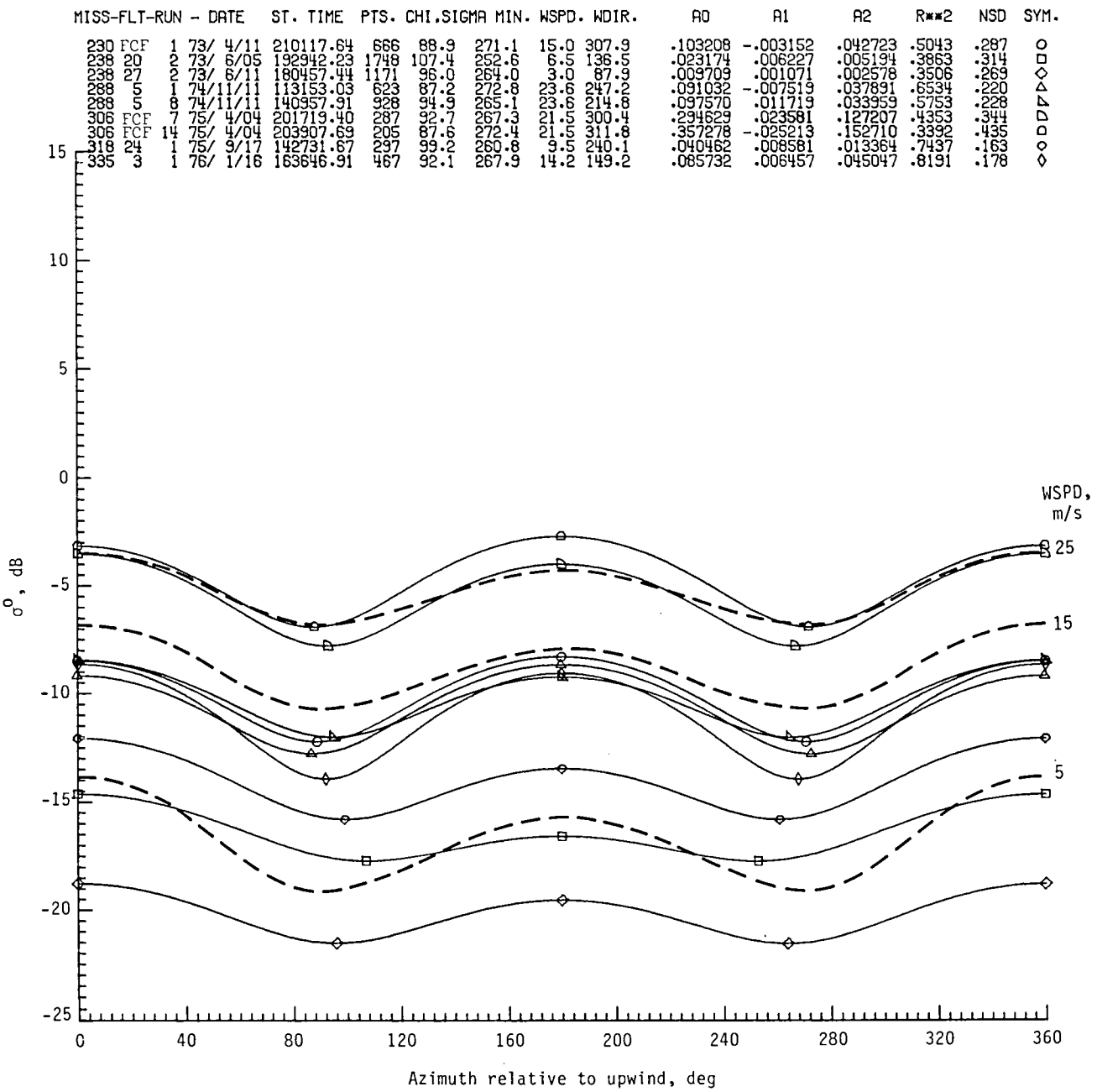

(a) Horizontal polarization.

Figure 12.- Second-order regression fit of NRCS versus azimuth relative to upwind for all RADSCAT circle flights at $\theta = 30°$, with SASS I regression lines (dashed) for comparison.

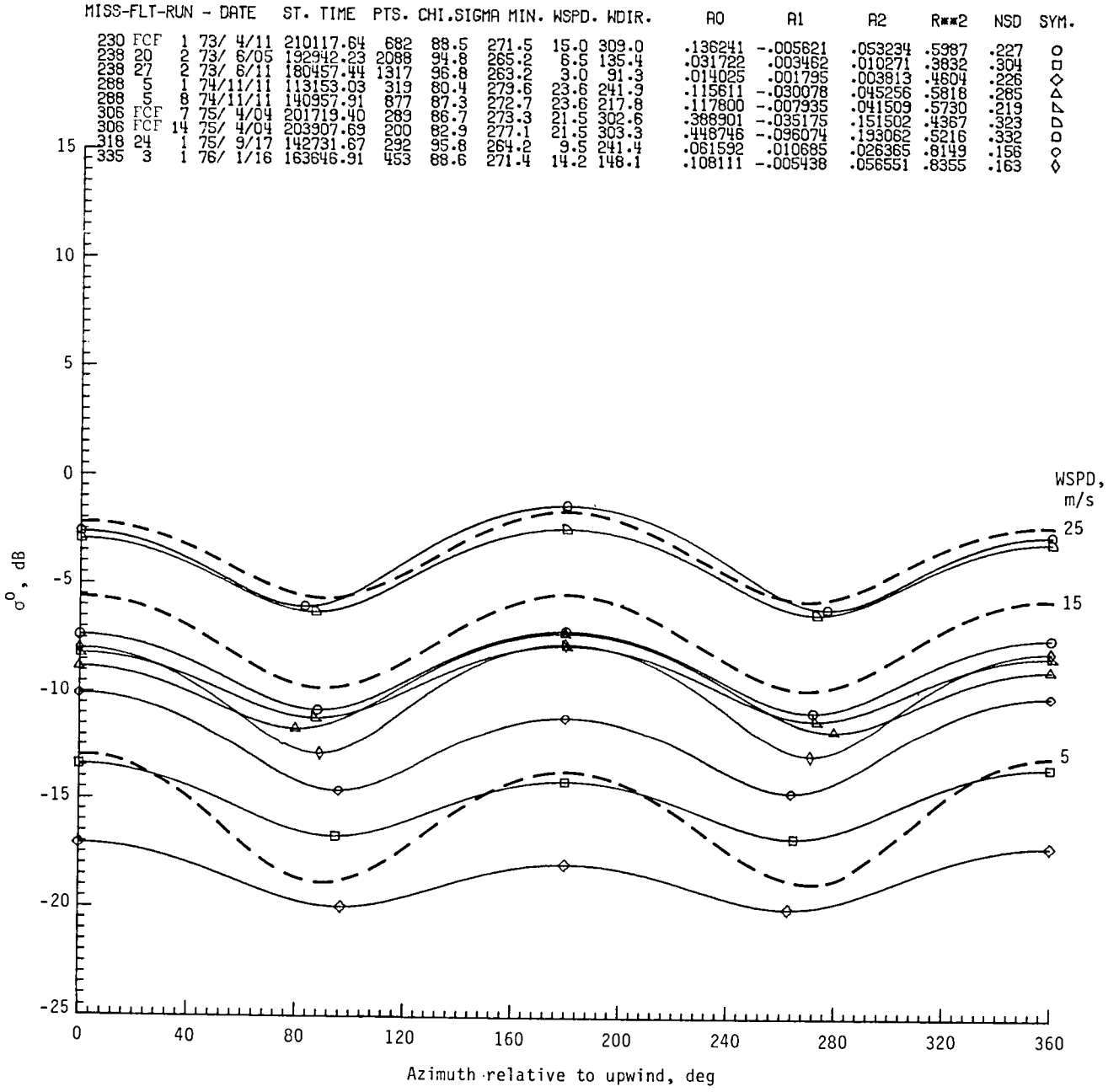

(b) Vertical polarization.

Figure 12.- Concluded.

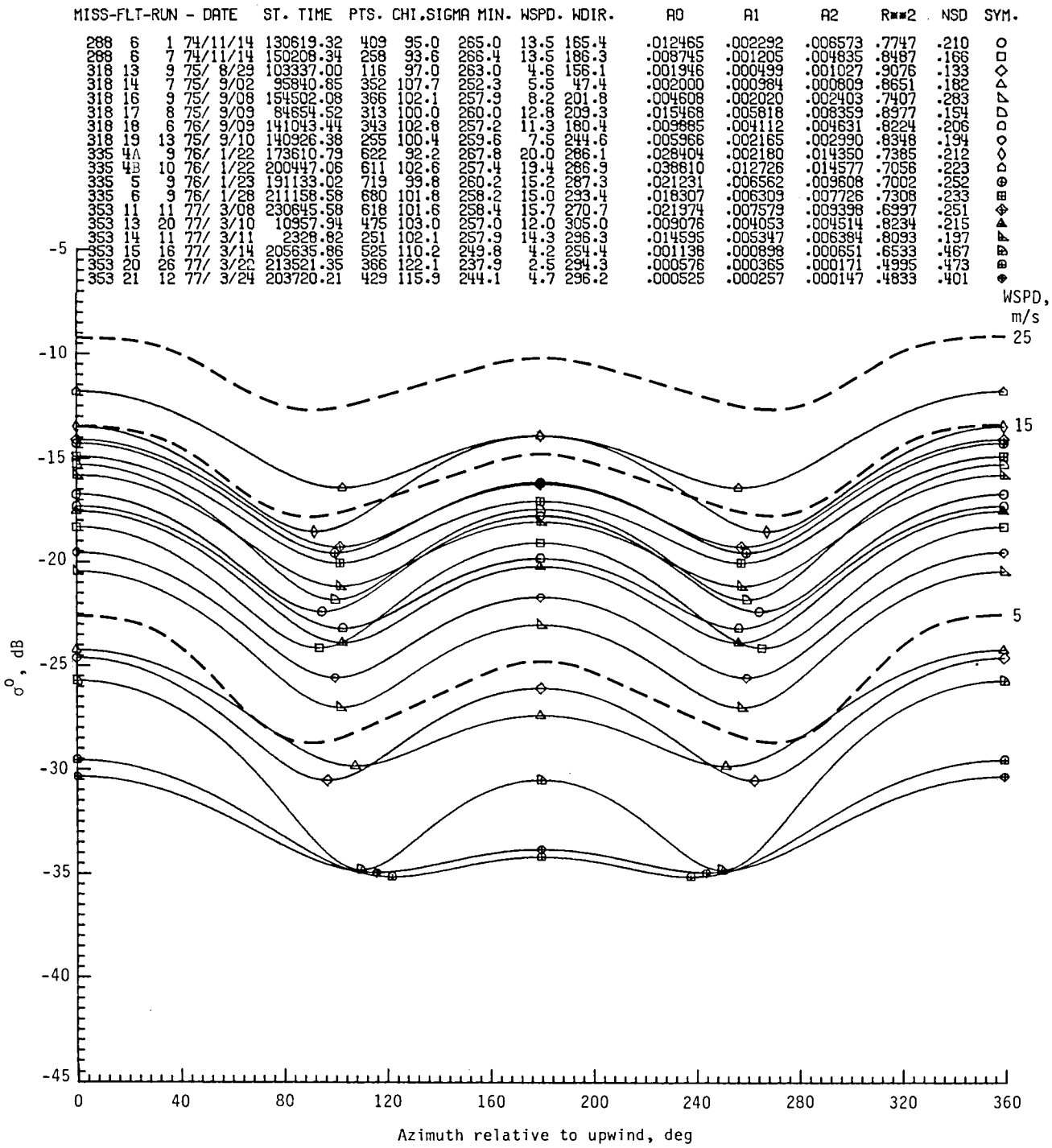

(a) Horizontal polarization.

Figure 13.- Second-order regression fit of NRCS versus azimuth relative to upwind for all RADSCAT circle flights at $\theta = 40°$, with SASS I regression lines (dashed) for comparison.

MISS-FLT-RUN	DATE	ST. TIME	PTS.	CHI.SIGMA	MIN. WSPD.	WDIR.	A0	A1	A2	R**2	NSD	SYM.
288 6 1	74/11/14	130619.32	410	89.3	270.7	13.5 178.5	.023316	-.000667	.012798	.8578	.154	○
288 6 7	74/11/14	150208.34	345	90.3	269.7	13.5 182.3	.015020	.000136	.007016	.7912	.167	□
318 13 9	75/ 8/29	103337.00	121	90.1	269.9	4.6 155.6	.002959	.000010	.001743	.9170	.122	◇
318 14 7	75/ 9/02	95840.85	347	96.4	263.6	5.5 46.4	.003937	.000798	.001785	.7617	.205	△
318 16 9	75/ 9/08	154502.08	369	93.8	266.2	8.2 198.2	.008682	.001462	.005475	.7408	.271	▽
318 17 8	75/ 9/09	84654.52	329	93.8	266.2	12.8 208.9	.027165	.004273	.016263	.9104	.134	▷
318 18 6	76/ 9/09	141043.44	344	95.4	264.6	11.3 181.8	.017963	.004822	.012917	.8759	.201	□
318 19 13	75/ 9/10	140926.38	247	92.1	267.9	7.5 245.1	.011510	.001037	.007176	.8815	.164	○
335 4A 9	76/ 1/22	173610.79	622	90.1	269.9	20.0 287.4	.051188	.000238	.024890	.7614	.192	◇
335 4B 10	76/ 1/22	200447.06	621	97.9	262.1	19.4 287.3	.062603	.013754	.024930	.7177	.198	△
335 5 9	76/ 1/23	191133.02	717	94.4	265.6	15.2 287.1	.037770	.005449	.017797	.7073	.221	⊕
335 6 9	76/ 1/28	211158.58	680	95.5	264.5	15.0 291.1	.035187	.006225	.016179	.7472	.206	⊞
353 11 11	77/ 3/08	230645.58	620	95.5	264.5	15.7 270.6	.040917	.007075	.018602	.7916	.173	◈
353 13 20	77/ 3/10	10957.94	478	94.6	265.4	12.0 305.0	.022954	.004202	.012998	.8100	.201	▲
353 14 11	77/ 3/11	2328.82	254	95.4	264.6	14.3 295.7	.029803	.005388	.014406	.7887	.187	◭
353 15 16	77/ 3/14	205635.86	603	99.2	260.8	4.2 255.0	.002649	.000936	.001465	.5515	.411	▣
353 20 26	77/ 3/22	213521.35	573	103.7	256.3	2.5 284.4	.001227	.000344	.000363	.2722	.466	⊠
353 21 12	77/ 3/24	203720.21	578	104.4	255.6	4.7 288.4	.001109	.000302	.000302	.3479	.375	◆

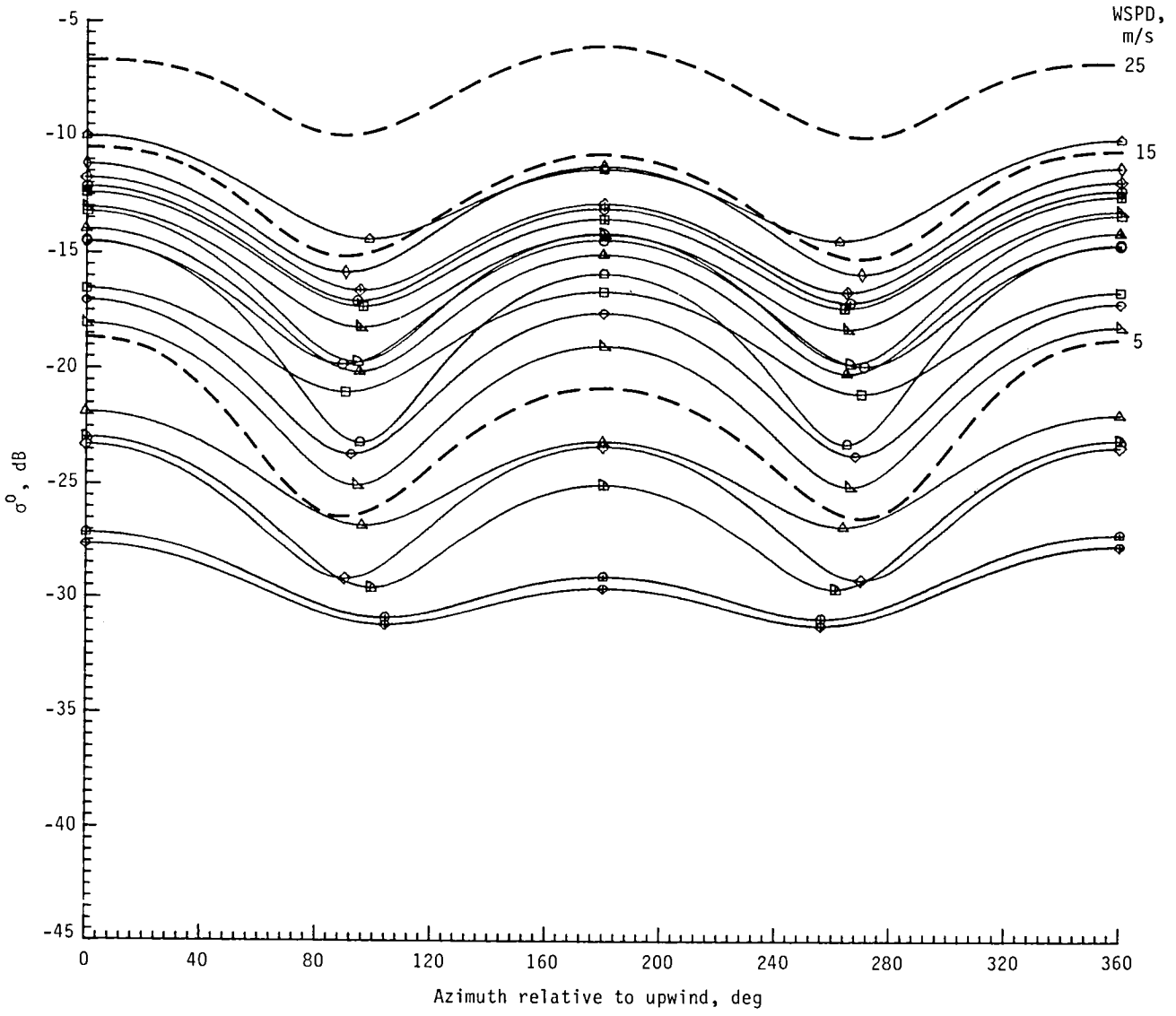

(b) Vertical polarization.

Figure 13.- Concluded.

MISS-FLT-RUN	DATE	ST. TIME	PTS.	CHI.SIGMA	MIN. WSPD.	WDIR.	A0	A1	A2	R**2	NSD	SYM.
306 FCF 1	75/ 4/04	200131.71	225	82.6	277.4	21.5 303.6	.033683	-.006943	.013563	.6894	.215	○
318 13 11	75/ 8/29	103903.80	269	105.8	254.2	4.6 154.7	.000321	.000266	.000244	.8961	.234	□
335 3 6	76/ 1/16	165006.91	376	94.6	265.4	14.2 147.6	.006159	.000799	.002468	.7350	.177	◇

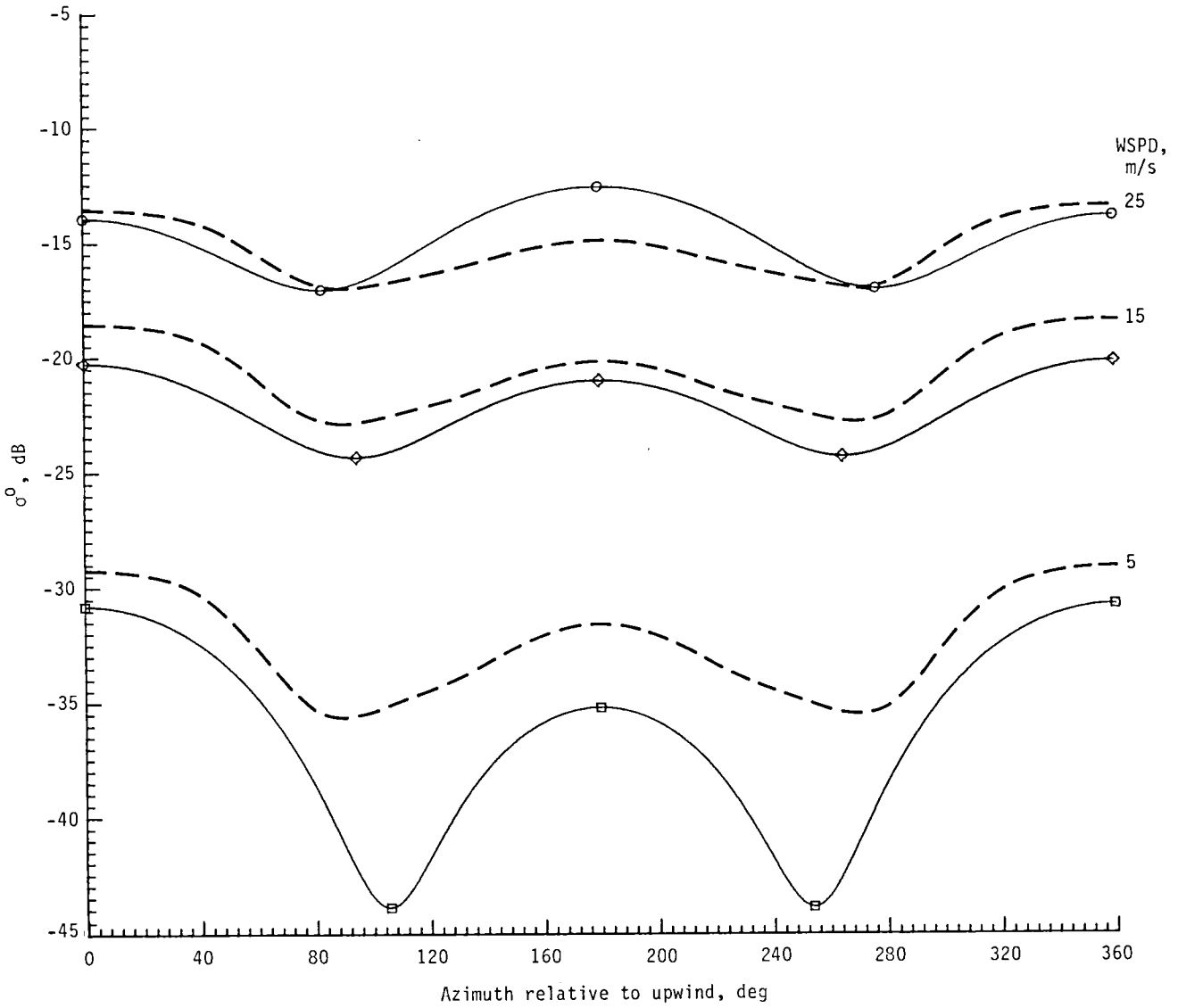

(a) Horizontal polarization

Figure 14.- Second-order regression fit of NRCS versus azimuth relative to upwind for all RADSCAT circle flights at $\theta = 50°$, with SASS I regression lines (dashed) for comparison.

MISS-FLT-RUN	DATE	ST. TIME	PTS.	CHI.SIGMA	MIN.	WSPD.	WDIR.	A0	A1	A2	R**2	NSD	SYM.
306 FCF 1	75/ 4/04	200131.71	214	85.4	274.6	21.5	300.7	.076882	-.008269	.025509	.6757	.172	○
318 13 11	75/ 8/29	103903.80	306	96.1	263.9	4.6	156.8	.001140	.000337	.000789	.8866	.192	□
335 3 6	76/ 1/16	165006.91	383	89.5	270.5	14.2	150.0	.018335	-.000300	.008394	.8678	.124	◇

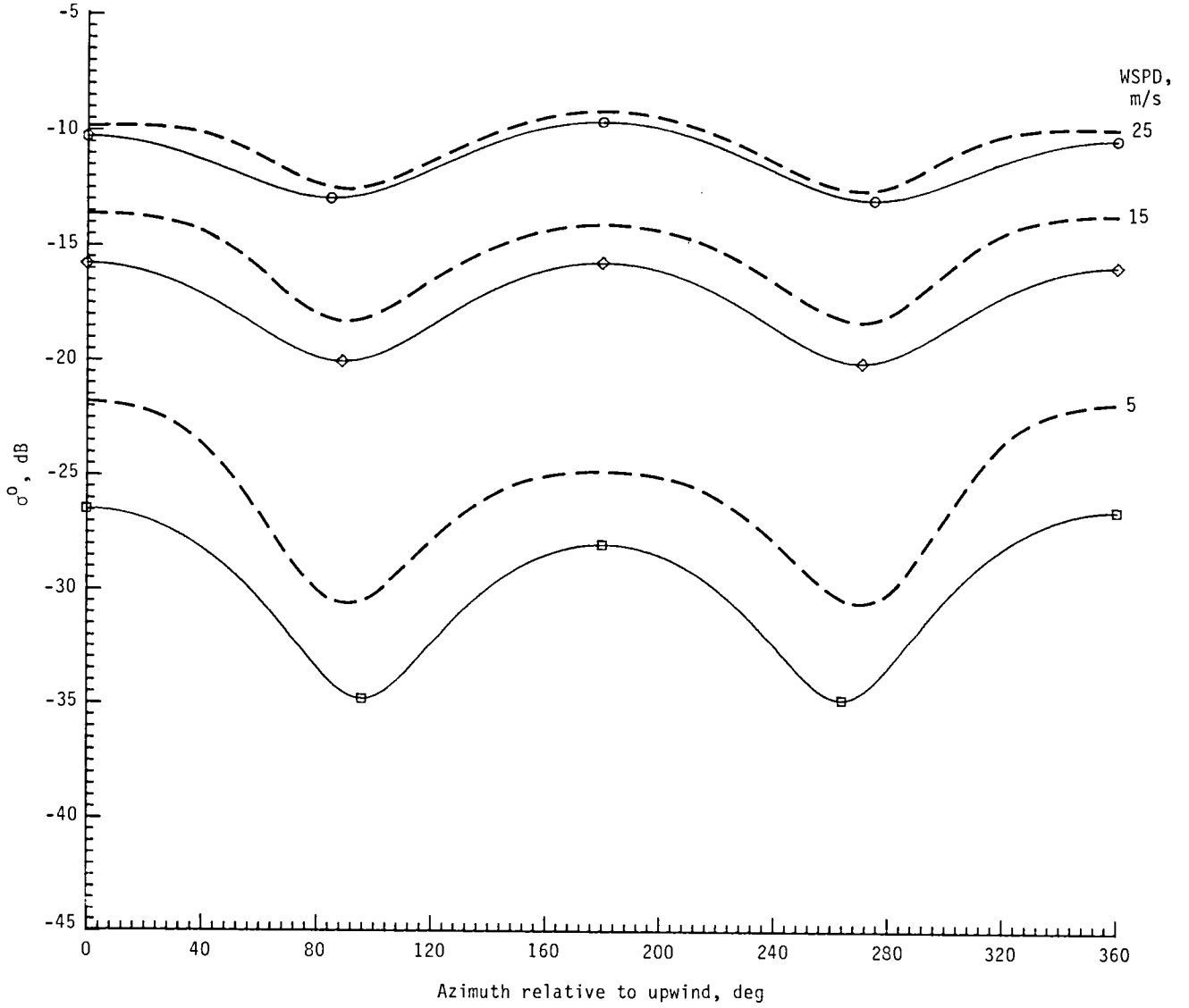

(b) Vertical polarization.

Figure 14.- Concluded.

MISS-FLT-RUN	DATE	ST. TIME	PTS.	CHI.SIGMA	MIN. WSPD.	WDIR.	A0	A1	A2	R**2	NSD	SYM.
306 FCF 4	75/ 4/04	200953.31	168	89.9	270.1	21.5 292.0	.014797	-.000041	.008698	.7826	.223	○
335 4A 17	76/ 1/22	181328.37	361	112.3	247.7	19.8 284.1	.003575	.001877	.001236	.7210	.266	□
335 5 17	76/ 1/23	193310.32	583	107.9	252.1	15.1 286.7	.002579	.001452	.001181	.6818	.346	◇
335 6 13	76/ 1/28	212223.98	622	108.0	252.0	15.0 293.2	.002388	.001162	.000939	.7870	.232	△

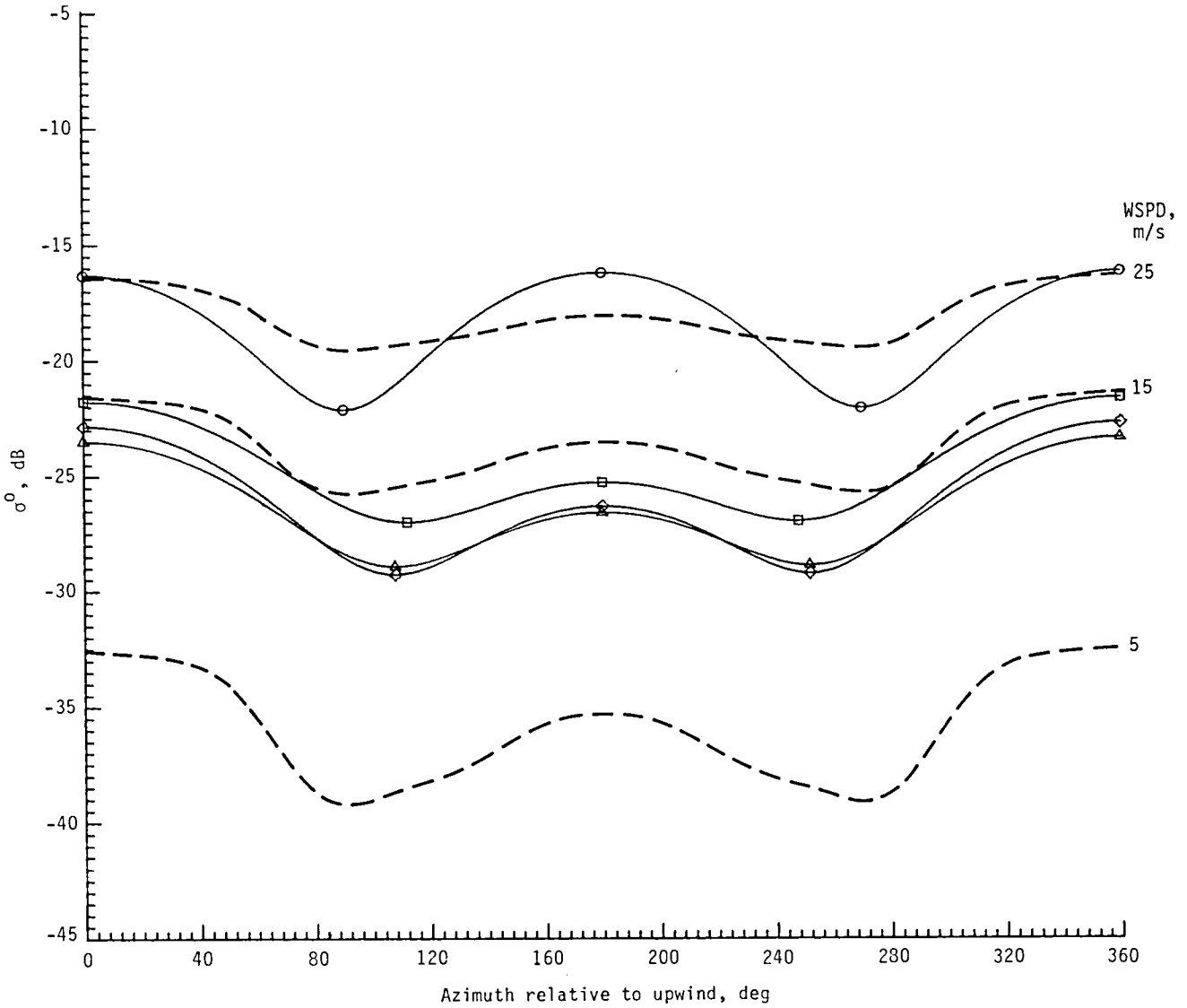

(a) Horizontal polarization.

Figure 15.- Second-order regression fit of NRCS versus azimuth relative to upwind for all RADSCAT circle flights at $\theta = 60°$, with SASS I regression lines (dashed) for comparison.

MISS-FLT-RUN - DATE	ST. TIME	PTS.	CHI.SIGMA	MIN.	WSPD.	WDIR.	A0	A1	A2	R**2	NSD	SYM.
306 FCF 4 75/ 4/04	200953.31	170	84.1	275.9	21.5	315.0	.047766	-.004582	.011216	.4540	.196	○
335 4A 17 76/ 1/22	181328.37	368	102.4	257.6	19.8	286.1	.013461	.004219	.004905	.7700	.178	□
335 5 17 76/ 1/23	193310.32	594	98.8	261.2	15.1	289.1	.011482	.002866	.004684	.7891	.170	◇
335 6 13 76/ 1/28	212223.98	621	99.3	260.7	15.0	291.4	.010771	.002812	.004369	.8469	.145	△

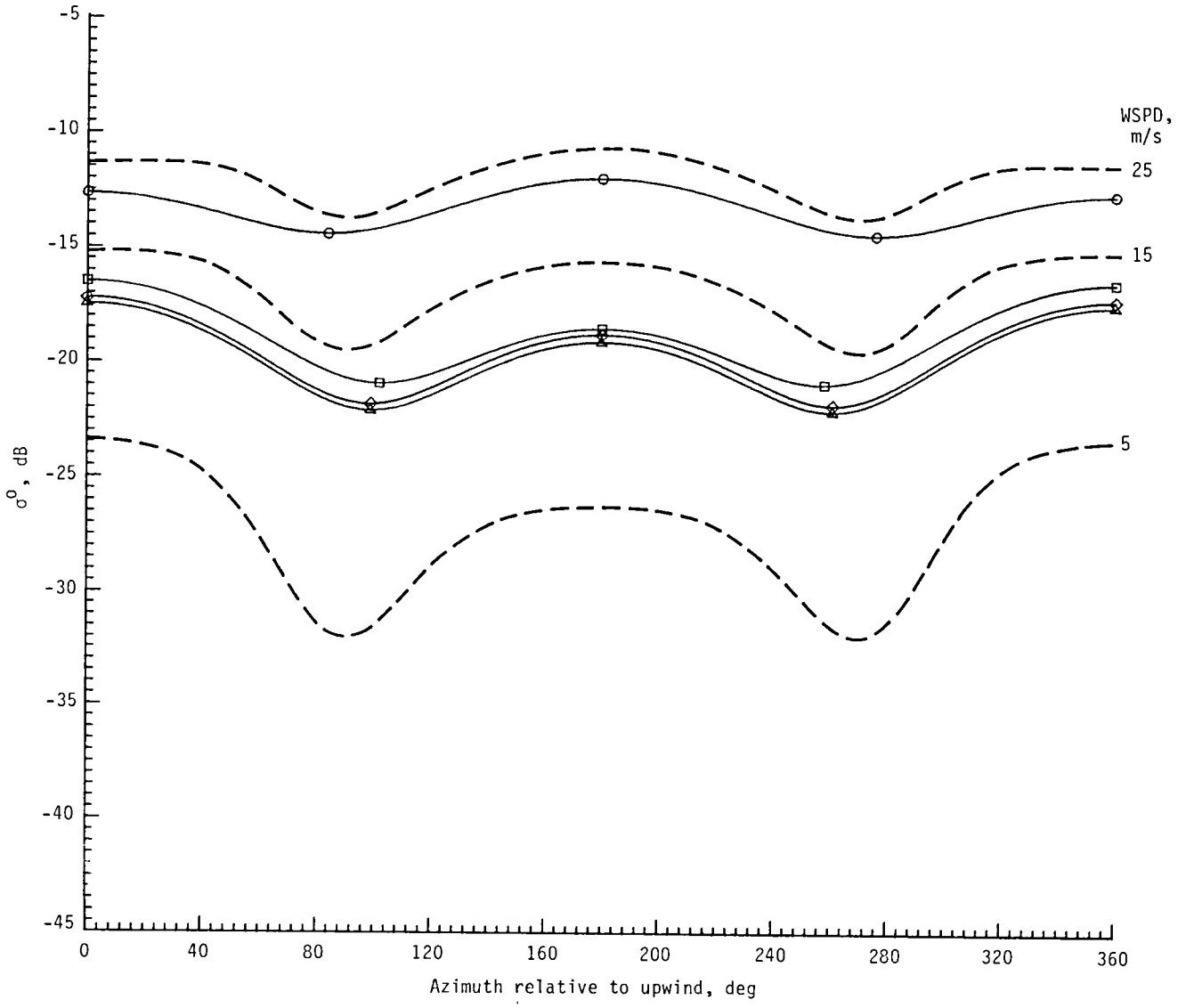

(b) Vertical polarization.

Figure 15.- Concluded.

MISS-FLT-RUN	DATE	ST. TIME	PTS.	CHI,SIGMA	MIN. WSPD.	WDIR.	A0	A1	A2	R**2	NSD	SYM.
318 14 12	75/ 9/02	101226.95	214	115.8	244.2	5.5 53.5	.000133	.000050	.000029	.4577	.334	○
318 16 14	75/ 9/08	155914.00	214	100.6	259.4	8.9 212.7	.000195	.000087	.000118	.7356	.270	□
318 17 12	75/ 9/09	85941.83	256	112.1	247.9	12.3 209.4	.000861	.000599	.000398	.9138	.167	◇
318 18 11	75/ 9/09	142321.43	195	94.1	265.9	10.5 193.7	.000850	.000145	.000505	.8669	.178	△
353 11 1	77/ 3/08	224044.38	505	110.5	249.5	16.0 262.1	.001065	.000789	.000563	.7719	.328	▽

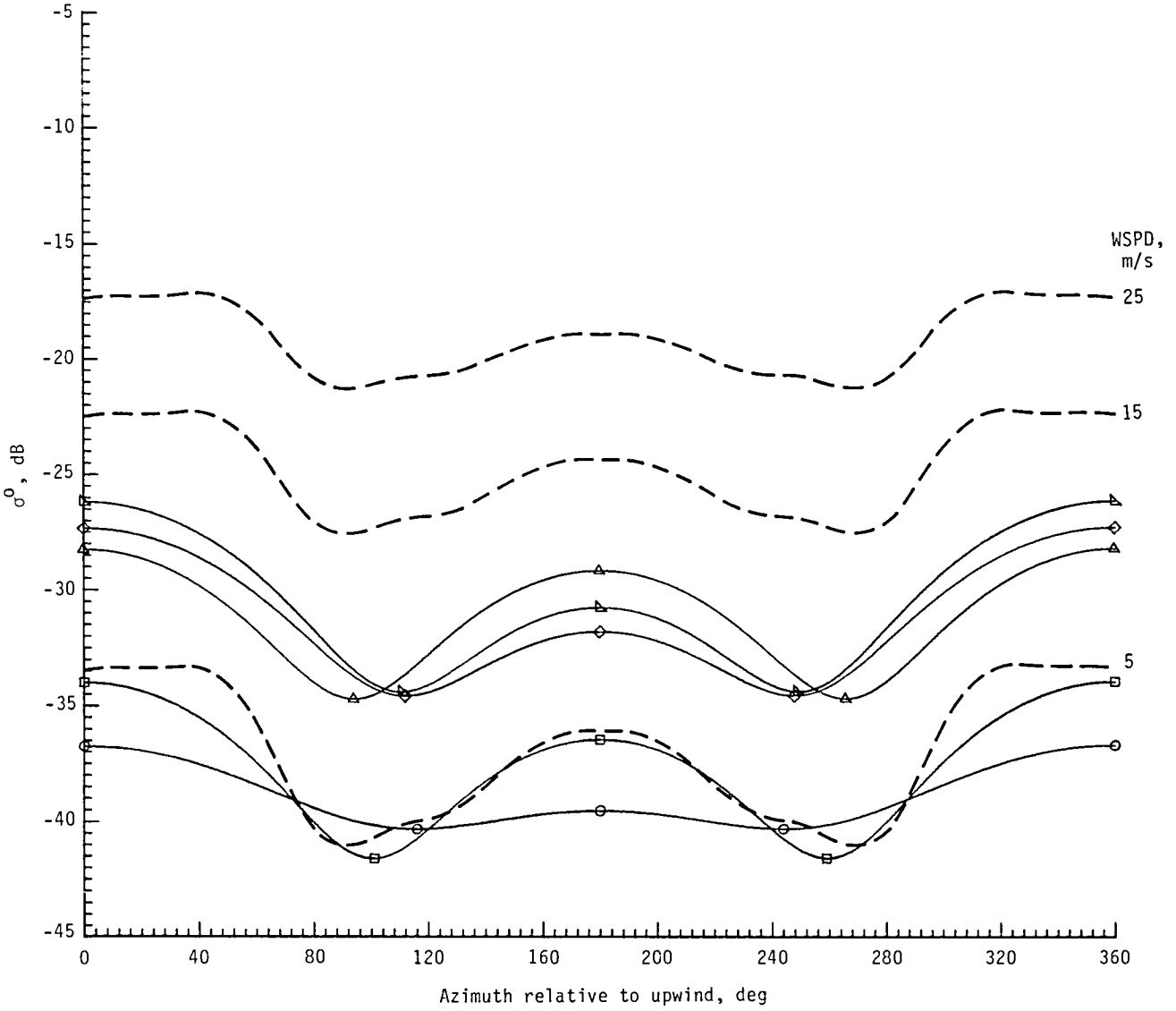

(a) Horizontal polarization.

Figure 16.- Second-order regression fit of NRCS versus azimuth relative to upwind for all RADSCAT circle flights at $\theta = 70°$, with SASS I regression lines (dashed) for comparison.

MISS-FLT-RUN	DATE	ST. TIME	PTS.	CHI.SIGMA	MIN. WSPD.	WDIR.	A0	A1	A2	R**2	NSD	SYM.
318 14 12	75/ 9/02	101226.95	267	92.8	267.2	5.5 50.7	.000705	.000072	.000369	.8722	.151	o
318 16 14	75/ 9/08	155914.00	272	85.7	274.3	8.9 206.8	.002614	-.000624	.002082	.8537	.244	□
318 17 12	75/ 9/09	85941.83	258	95.5	264.5	12.3 211.6	.006320	.001430	.003735	.9134	.128	◇
318 18 11	75/ 9/09	142321.43	189	87.6	272.4	10.5 192.5	.007073	-.000860	.005103	.8881	.181	△
318 19 17	75/ 9/10	141950.98	279	90.2	269.8	7.5 243.8	.002550	.000027	.001850	.7923	.263	◁
353 11 1	77/ 3/08	224044.38	621	99.9	260.1	16.0 265.1	.007033	.002241	.003243	.7900	.205	▷
353 13 16	77/ 3/10	5942.14	492	98.0	262.0	11.7 305.2	.003974	.001635	.002923	.8920	.203	▽
353 14 1	77/ 3/11	235637.93	639	98.1	261.9	14.3 275.5	.006400	.001867	.003298	.8056	.206	◇

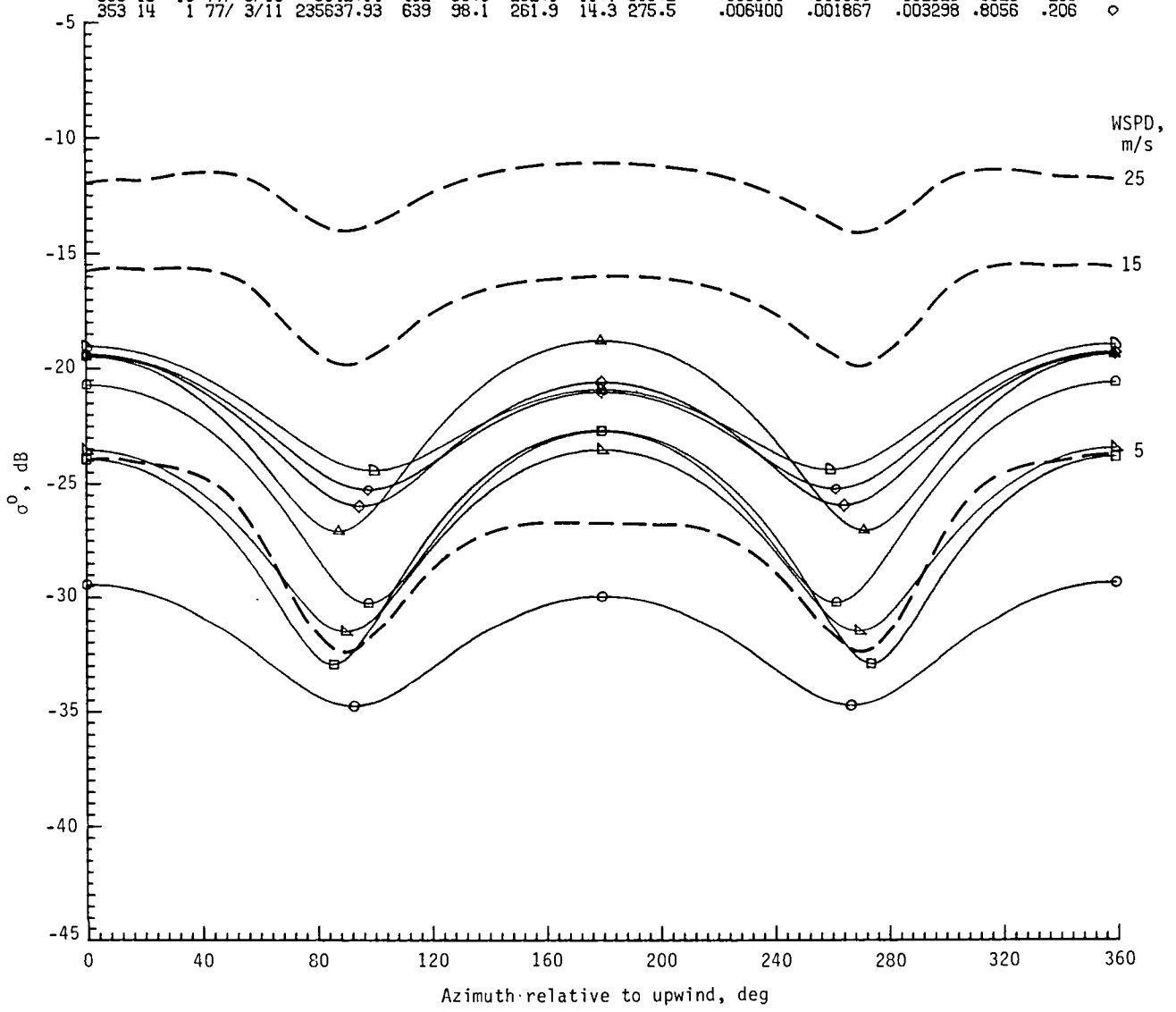

(b) Vertical polarization.

Figure 16.- Concluded.

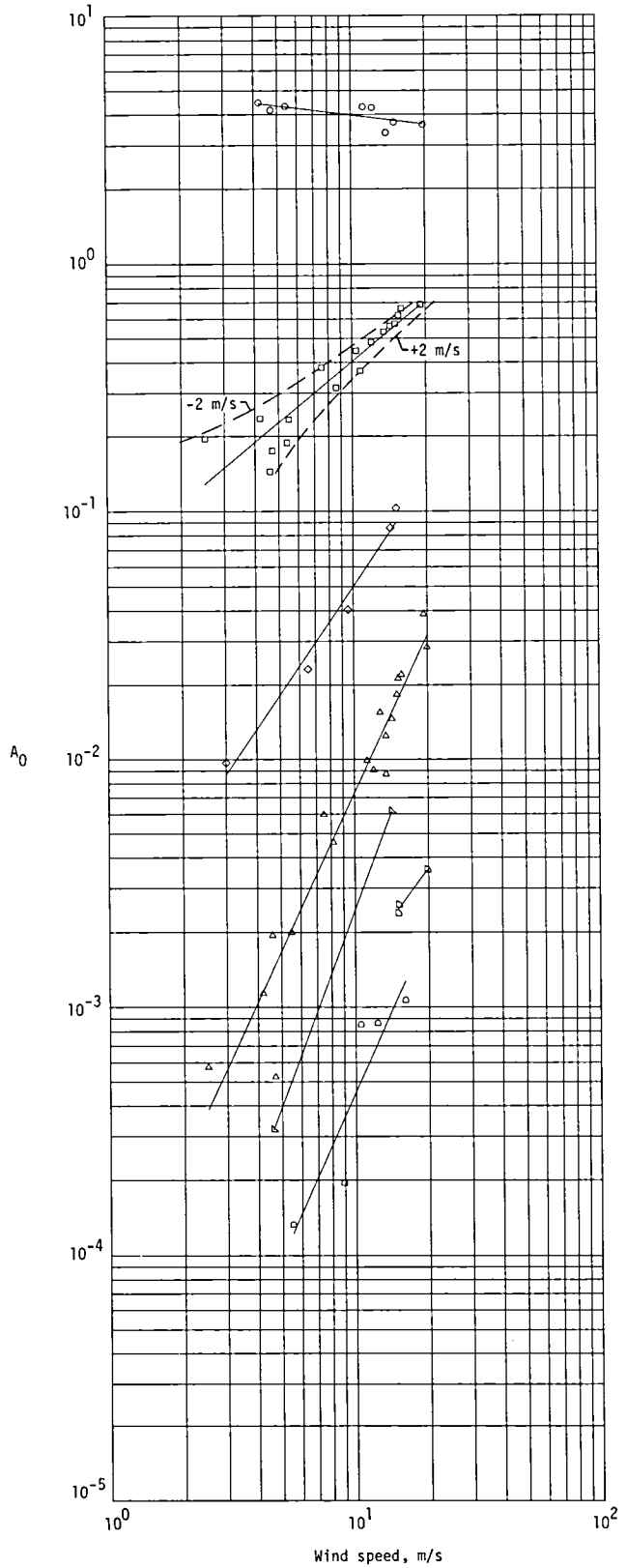

Symbol	Miss	Fl	Run	Wind speed, m/s	Coefficient
$\theta = 10^o$; $B_0 = 0.7218$; $B_1 = -0.1221$; $(SR)^2 = 0.0064$					
○	335	4A	22	19.7	3.6338
	335	5	25	13.9	3.3779
	335	6	25	15.0	3.7222
	353	9	1	12.2	4.2531
	353	10	11	5.4	4.3128
	353	13	11	11.2	4.2881
	353	15	1	4.2	4.4631
	353	21	1	4.7	4.1600
$\theta = 20^o$; $B_0 = -1.2168$; $B_1 = 0.8221$; $(SR)^2 = 0.1067$					
□	318	13	3	4.6	1.4446E-1
	318	14	1	5.5	2.3446E-1
	318	16	4	8.6	3.1589E-1
	318	17	1	13.5	5.3268E-1
	318	18	2	12.0	4.8273E-1
	318	19	10	7.5	3.8121E-1
	335	4A	1	19.1	6.8795E-1
	335	4B	1	19.1	6.8734E-1
	335	5	1	15.5	6.2314E-1
	335	6	1	15.0	5.7481E-1
	353	9	11	10.8	3.7020E-1
	353	10	1	5.4	1.8861E-1
	353	11	6	15.9	6.6420E-1
	353	13	1	10.4	4.4597E-1
	353	14	6	14.3	5.6311E-1
	353	15	11	4.2	2.3641E-1
	353	20	1	2.5	1.9568E-1
	353	21	7	4.7	1.7509E-1
$\theta = 30^o$; $B_0 = -2.7546$; $B_1 = 1.4532$; $(SR)^2 = 0.0133$					
◇	230	FCF	1	15.0	1.0321E-1
	238	20	2	6.5	2.3174E-2
	238	27	2	3.0	9.7091E-3
	318	24	1	9.5	4.0462E-2
	335	3	1	14.2	8.5732E-2
$\theta = 40^o$; $B_0 = -4.2562$; $B_1 = 2.1204$; $(SR)^2 = 0.3661$					
△	288	6	1	13.5	1.2465E-2
	288	6	7	13.5	8.7445E-3
	318	13	9	4.6	1.9462E-3
	318	14	7	5.5	1.9997E-3
	318	16	9	8.2	4.6082E-3
	318	17	8	12.8	1.5468E-2
	318	18	6	11.3	9.8850E-3
	318	19	13	7.5	5.9665E-3
	335	4A	9	20.0	2.8404E-2
	335	4B	10	19.4	3.8810E-2
	335	5	9	15.2	2.1231E-2
	335	6	9	15.0	1.8307E-2
	353	11	11	15.7	2.1974E-2
	353	13	20	12.0	9.0757E-3
	353	14	11	14.3	1.4595E-2
	353	15	16	4.2	1.1382E-3
	353	20	26	2.5	5.7620E-4
	353	21	12	4.7	5.2545E-4
$\theta = 50^o$; $B_0 = -5.2296$; $B_1 = 2.6200$; $(SR)^2 = 2.7667E-26$					
◺	318	13	11	4.6	3.2129E-4
	335	3	6	14.2	6.1587E-3
$\theta = 60^o$; $B_0 = -4.1784$; $B_1 = 1.3358$; $(SR)^2 = 4.3389E-4$					
◺	335	4A	17	19.8	3.5753E-3
	335	5	17	15.1	2.5785E-3
	335	6	13	15.0	2.3881E-3
$\theta = 70^o$; $B_0 = -5.5335$; $B_1 = 2.1922$; $(SR)^2 = 0.1302$					
◻	318	14	12	5.5	1.3282E-4
	318	16	14	8.9	1.9502E-4
	318	17	12	12.3	8.6053E-4
	318	18	11	10.5	8.4958E-4
	353	11	1	16.0	1.0646E-3

Figure 17.- Second-order regression coefficient A_0 versus wind speed (log-log scale) for horizontal polarization.

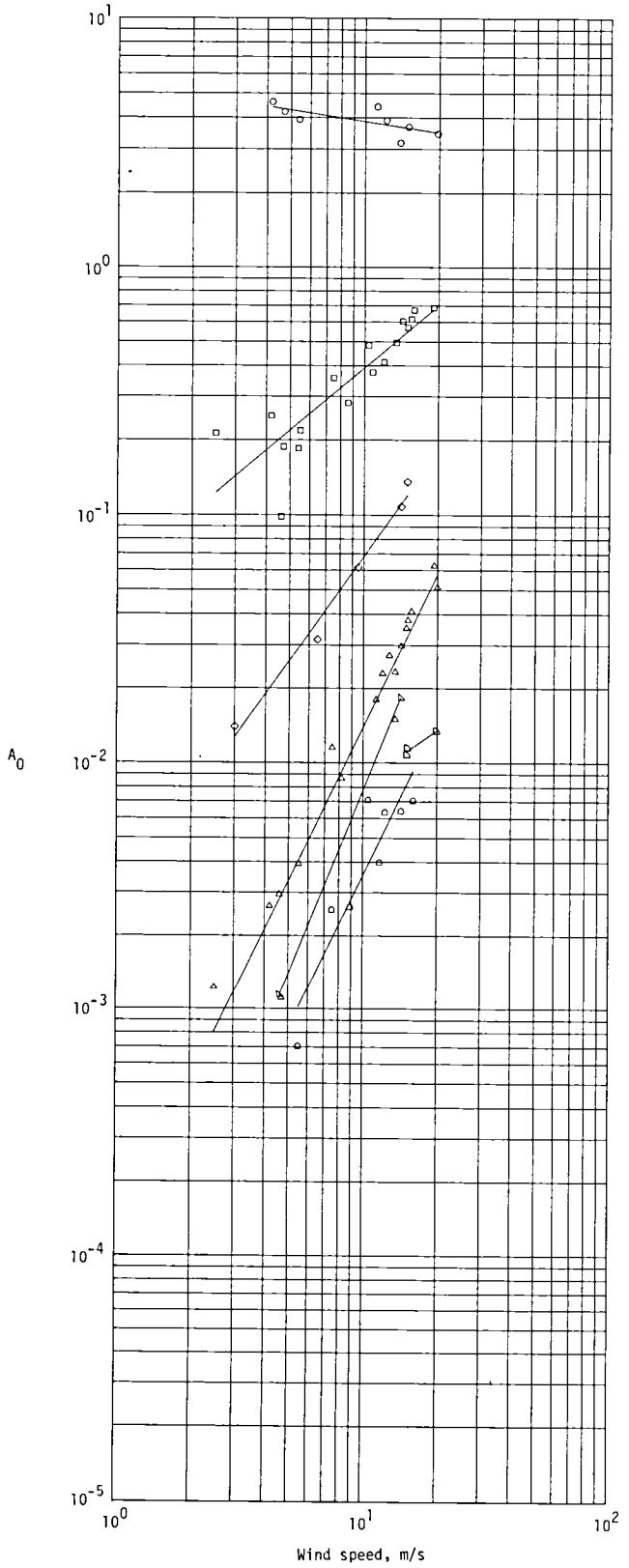

Symbol	Miss	Fl	Run	Wind speed, m/s	Coefficient
$\theta = 10^o$; $B_0 = 0.7377$; $B_1 = -0.1510$; $(SR)^2 = 0.0104$					
○	335	4A	22	19.7	3.4510
	335	5	25	13.9	3.1766
	335	6	25	15.0	3.6780
	353	9	1	12.2	3.9035
	353	10	11	5.4	3.9312
	353	13	11	11.2	4.4263
	353	15	1	4.2	4.6160
	353	21	1	4.7	4.2202
$\theta = 20^o$; $B_0 = -1.2416$; $B_1 = 0.8354$; $(SR)^2 = 0.2166$					
□	318	13	3	4.6	9.8562E-2
	318	14	1	5.5	2.1870E-1
	318	16	4	8.6	2.8303E-1
	318	17	1	13.5	4.9606E-1
	318	18	2	12.0	4.1428E-1
	318	19	10	7.5	3.5652E-1
	335	4A	1	19.1	6.8583E-1
	335	4B	1	19.1	6.8516E-1
	335	5	1	15.5	6.1646E-1
	335	6	1	15.0	5.7002E-1
	353	9	11	10.8	3.7576E-1
	353	10	1	5.4	1.8553E-1
	353	11	6	15.9	6.7058E-1
	353	13	1	10.4	4.8410E-1
	353	14	6	14.3	6.0478E-1
	353	15	11	4.2	2.5080E-1
	353	20	1	2.5	2.1287E-1
	353	21	7	4.7	1.8826E-1
$\theta = 30^o$; $B_0 = -2.5590$; $B_1 = 1.3927$; $(SR)^2 = 0.0102$					
◇	230	FCF	1	15.0	1.3624E-1
	238	20	2	6.5	3.1722E-2
	238	27	2	3.0	1.4024E-2
	318	24	1	9.5	6.1592E-2
	335	3	1	14.2	1.0811E-1
$\theta = 40^o$; $B_0 = -3.9088$; $B_1 = 2.0522$; $(SR)^2 = 0.3297$					
△	288	6	1	13.5	2.3316E-2
	288	6	7	13.5	1.5020E-2
	318	13	9	4.6	2.9594E-3
	318	14	7	5.5	3.9375E-3
	318	16	9	8.2	8.6815E-3
	318	17	8	12.8	2.7165E-2
	318	18	6	11.3	1.7983E-2
	318	19	13	7.5	1.1510E-2
	335	4A	9	20.0	5.1188E-2
	335	4B	10	19.4	6.2603E-2
	335	5	9	15.2	3.7770E-2
	335	6	9	15.0	3.5187E-2
	353	11	11	15.7	4.0917E-2
	353	13	20	12.0	2.2954E-2
	353	14	11	14.3	2.9803E-2
	353	15	16	4.2	2.6489E-3
	353	20	26	2.5	1.2274E-3
	353	21	12	4.7	1.1089E-3
$\theta = 50^o$; $B_0 = -4.5766$; $B_1 = 2.4645$; $(SR)^2 = 3.1554E-26$					
◺	318	13	11	4.6	1.1398E-3
	335	3	6	14.2	1.8335E-2
$\theta = 60^o$; $B_0 = -2.7783$; $B_1 = 0.7000$; $(SR)^2 = 0.3306E-3$					
◺	335	4A	17	19.8	1.3460E-2
	335	5	17	15.1	1.1482E-2
	335	6	13	15.0	1.0771E-2
$\theta = 70^o$; $B_0 = -4.5218$; $B_1 = 2.0668$; $(SR)^2 = 0.1390$					
◺	318	14	12	5.5	7.0460E-4
	318	16	14	8.9	2.6136E-3
	318	17	12	12.3	6.3198E-3
	318	18	11	10.5	7.0732E-3
	318	19	17	7.5	2.5502E-3
	353	11	1	16.0	7.0326E-3
	353	13	16	11.7	3.9740E-3
	353	14	1	14.3	6.3999E-3

Figure 18.- Second-order regression coefficient A_0 versus wind speed (log-log scale) for vertical polarization.

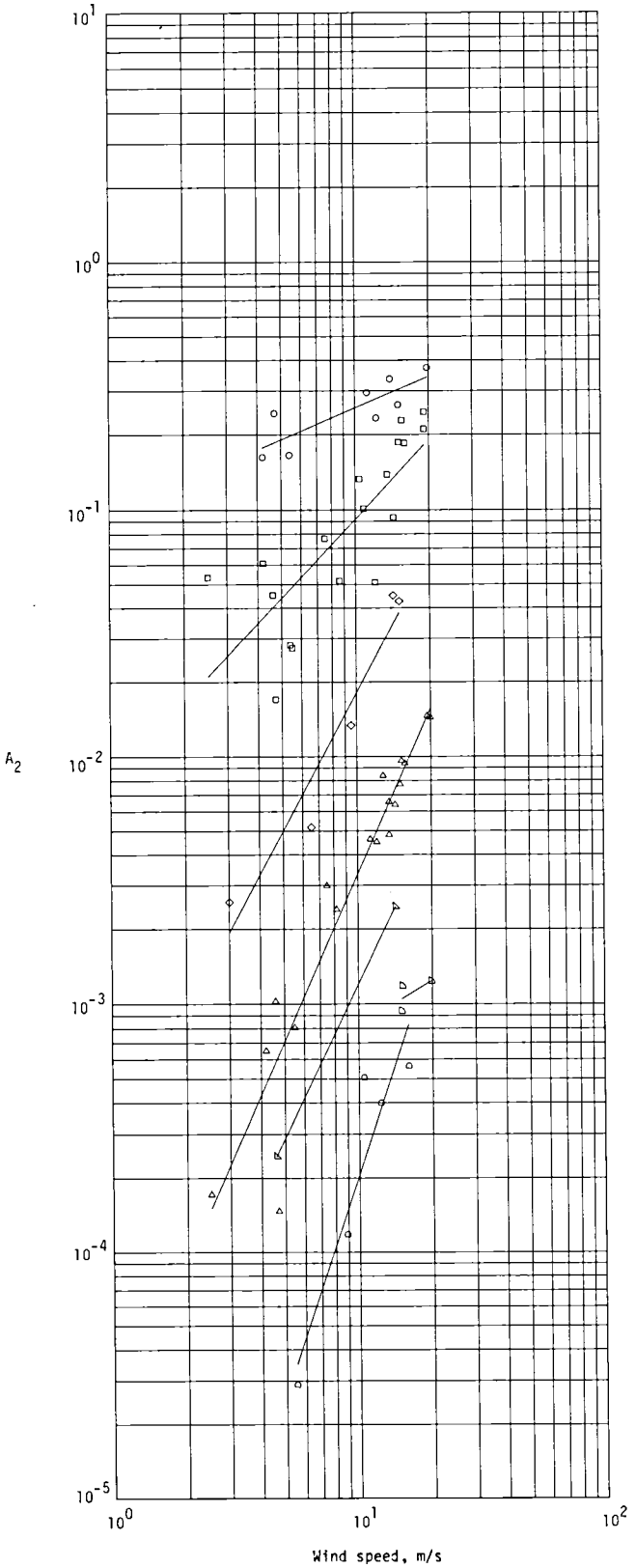

Symbol	Miss	Fl	Run	Wind speed, m/s	Coefficient
$\theta = 10^o$; $B_0 = -1.0156$; $B_1 = 0.4238$; $(SR)^2 = 0.0372$					
○	335	4A	22	19.7	3.7284E-1
	335	5	25	13.9	3.3569E-1
	335	6	25	15.0	2.6330E-1
	353	9	1	12.2	2.3302E-1
	353	10	11	5.4	1.6558E-1
	353	13	11	11.2	2.9501E-1
	353	15	1	4.2	1.6240E-1
	353	21	1	4.7	2.4345E-1
$\theta = 20^o$; $B_0 = -2.0976$; $B_1 = 1.0595$; $(SR)^2 = 0.7517$					
□	318	13	3	4.6	4.5277E-2
	318	14	1	5.5	2.7524E-2
	318	16	4	8.6	5.1736E-2
	318	17	1	13.5	1.3845E-1
	318	18	2	12.0	5.0952E-2
	318	19	10	7.5	7.6684E-2
	335	4A	1	19.1	2.4652E-1
	335	4B	1	19.1	2.1033E-1
	335	5	1	15.5	2.2796E-1
	335	6	1	15.0	1.8635E-1
	353	9	11	10.8	1.0139E-1
	353	10	1	5.4	2.8298E-2
	353	11	6	15.9	1.8485E-1
	353	13	1	10.4	1.3301E-1
	353	14	6	14.3	9.3498E-2
	353	15	11	4.2	6.0873E-2
	353	20	1	2.5	5.3403E-2
	353	21	7	4.7	1.7086E-2
$\theta = 30^o$; $B_0 = -3.5954$; $B_1 = 1.8525$; $(SR)^2 = 0.0766$					
◇	230	FCF	1	15.0	4.2723E-2
	238	20	2	6.5	5.1939E-3
	238	27	2	3.0	2.5784E-3
	318	24	1	9.5	1.3364E-2
	335	3	1	14.2	4.5047E-2
$\theta = 40^o$; $B_0 = -4.7096$; $B_1 = 2.2324$; $(SR)^2 = 0.5808$					
△	288	6	1	13.5	6.5727E-3
	288	6	7	13.5	4.8354E-3
	318	13	9	4.6	1.0274E-3
	318	14	7	5.5	8.0858E-4
	318	16	9	8.2	2.4032E-3
	318	17	8	12.8	8.3585E-3
	318	18	6	11.3	4.6308E-3
	318	19	13	7.5	2.9900E-3
	335	4A	9	20.0	1.4350E-2
	335	4B	10	19.4	1.4577E-2
	335	5	9	15.2	9.6084E-3
	335	6	9	15.0	7.7255E-3
	353	11	11	15.7	9.3975E-3
	353	13	20	12.0	4.5144E-3
	353	14	11	14.3	6.3837E-3
	353	15	16	4.2	6.5146E-4
	353	20	26	2.5	1.7148E-4
	353	21	12	4.7	1.4669E-4
$\theta = 50^o$; $B_0 = -4.9716$; $B_1 = 2.0515$; $(SR)^2 = 1.9589E-26$					
◺	318	13	11	4.6	2.4436E-4
	335	3	6	14.2	2.4678E-3
$\theta = 60^o$; $B_0 = -3.6855$; $B_1 = 0.6006$; $(SR)^2 = 0.0048$					
◺	335	4A	17	19.8	1.2363E-3
	335	5	17	15.1	1.1809E-3
	335	6	13	15.0	9.3863E-4
$\theta = 70^o$; $B_0 = -6.6550$; $B_1 = 2.9694$; $(SR)^2 = 0.1512$					
◻	318	14	12	5.5	2.8901E-5
	318	16	14	8.9	1.1790E-4
	318	17	12	12.3	3.9837E-4
	318	18	11	10.5	5.0542E-4
	353	11	1	16.0	5.6283E-4

Figure 19.- Second-order regression coefficient A_2 versus wind speed (log-log scale) for horizontal polarization.

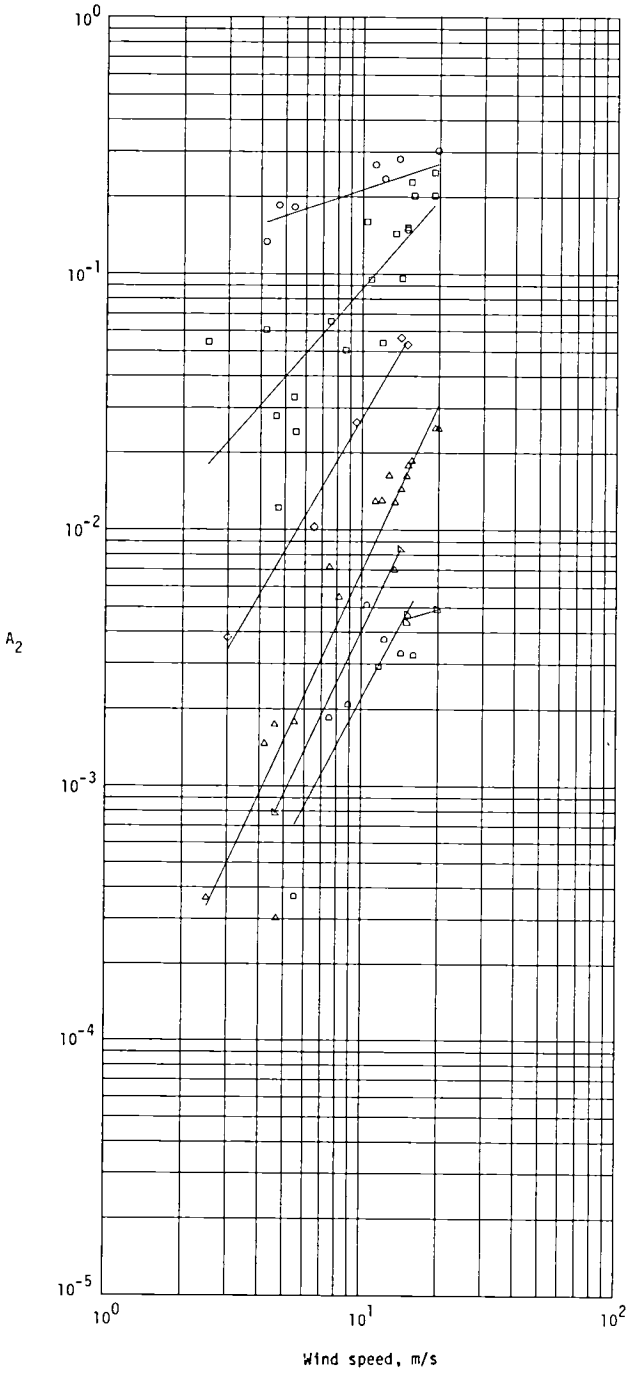

Symbol	Miss	Fl	Run	Wind speed, m/s	Coefficient
$\theta = 10^o$; $B_0 = -1.0108$; $B_1 = 0.3396$; $(SR)^2 = 0.0702$					
○	335	4A	22	19.7	3.0387E-1
	335	5	25	13.9	2.8167E-1
	335	6	25	15.0	1.4894E-1
	353	9	1	12.2	2.3515E-1
	353	10	11	5.4	1.8190E-1
	353	13	11	11.2	2.6708E-1
	353	15	1	4.2	1.3320E-1
	353	21	1	4.7	1.8497E-1
$\theta = 20^o$; $B_0 = -2.1985$; $B_1 = 1.1436$; $(SR)^2 = 0.9063$					
□	318	13	3	4.6	2.7970E-2
	318	14	1	5.5	2.4230E-2
	318	16	4	8.6	5.0540E-2
	318	17	1	13.5	1.4355E-1
	318	18	2	12.0	5.4119E-2
	318	19	10	7.5	6.5564E-2
	335	4A	1	19.1	2.4912E-1
	335	4B	1	19.1	2.0242E-1
	335	5	1	15.5	2.2817E-1
	335	6	1	15.0	1.5181E-1
	353	9	11	10.8	9.5000E-2
	353	10	1	5.4	3.3153E-2
	353	11	6	15.9	2.0209E-1
	353	13	1	10.4	1.5979E-1
	353	14	6	14.3	9.6044E-2
	353	15	11	4.2	6.0644E-2
	353	20	1	2.5	5.4375E-2
	353	21	7	4.7	1.2212E-2
$\theta = 30^o$; $B_0 = -3.2881$; $B_1 = 1.7261$; $(SR)^2 = 0.0162$					
◇	230	FCF	1	15.0	5.3234E-2
	238	20	2	6.5	1.0271E-2
	238	27	2	3.0	3.8128E-3
	318	24	1	9.5	2.6364E-2
	335	3	1	14.2	5.6551E-2
$\theta = 40^o$; $B_0 = -4.3357$; $B_1 = 2.1719$; $(SR)^2 = 0.6942$					
△	288	6	1	13.5	1.2798E-2
	288	6	7	13.5	7.0158E-3
	318	13	9	4.6	1.7427E-3
	318	14	7	5.5	1.7854E-3
	318	16	9	8.2	5.4755E-3
	318	17	8	12.8	1.6263E-2
	318	18	6	11.3	1.2917E-2
	318	19	13	7.5	7.1757E-3
	335	4A	9	20.0	2.4890E-2
	335	4B	10	19.4	2.4930E-2
	335	5	9	15.2	1.7796E-2
	335	6	9	15.0	1.6179E-2
	353	11	11	15.7	1.8602E-2
	353	13	20	12.0	1.2998E-2
	353	14	11	14.3	1.4406E-2
	353	15	16	4.2	1.4651E-3
	353	20	26	2.5	3.6338E-4
	353	21	12	4.7	3.0245E-4
$\theta = 50^o$; $B_0 = -4.4935$; $B_1 = 2.0980$; $(SR)^2 = 1.4944E-26$					
▽	318	13	11	4.6	7.8881E-4
	335	3	6	14.2	8.3943E-3
$\theta = 60^o$; $B_0 = -2.6974$; $B_1 = 0.2995$; $(SR)^2 = 4.3048E-4$					
▷	335	4A	17	19.8	4.9048E-3
	335	5	17	15.1	4.6836E-3
	335	6	13	15.0	4.3689E-3
$\theta = 70^o$; $B_0 = -4.5460$; $B_1 = 1.8875$; $(SR)^2 = 0.2827$					
◁	318	14	12	5.5	3.6891E-4
	318	16	14	8.9	2.0816E-3
	318	17	12	12.3	3.7349E-3
	318	18	11	10.5	5.1034E-3
	318	19	17	7.5	1.8499E-3
	353	11	1	16.0	3.2432E-3
	353	13	16	11.7	2.9230E-3
	353	14	1	14.3	3.2979E-3

Figure 20.- Second-order regression coefficient A_2 versus wind speed (log-log scale) for vertical polarization.

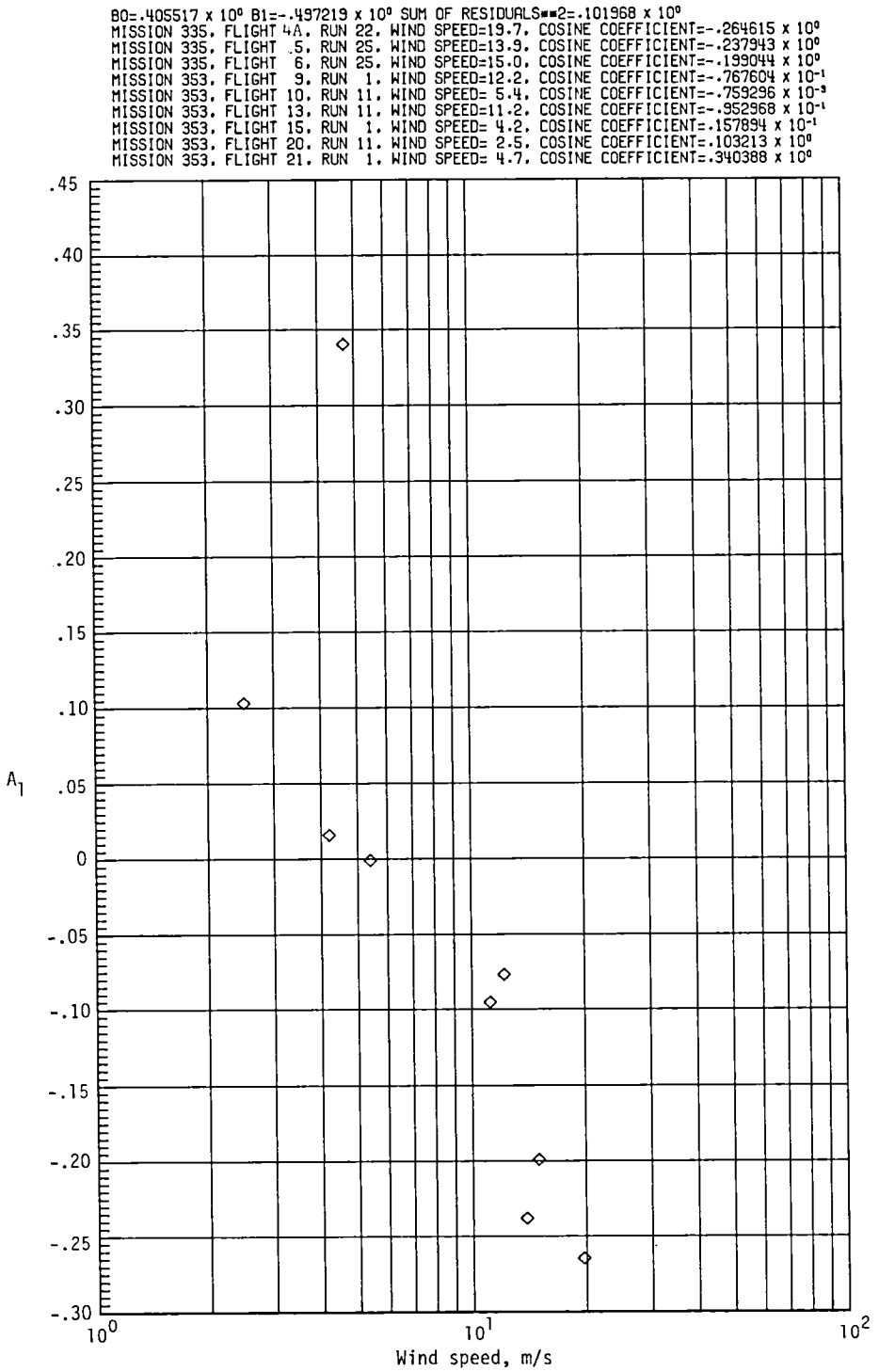

(a) $\theta = 10°$.

Figure 21.- Second-order regression coefficient A_1 versus log (Wind speed) for horizontal polarization.

B0=.167065 x 10^{-2} B1=-.133593 x 10^{-1} SUM OF RESIDUALS**2=.711647 x 10^{-2}
MISSION 318, FLIGHT 13, RUN 3, WIND SPEED= 4.6, COSINE COEFFICIENT=-.808644 x 10^{-2}
MISSION 318, FLIGHT 14, RUN 1, WIND SPEED= 5.5, COSINE COEFFICIENT=-.93514 x 10^{-2}
MISSION 318, FLIGHT 16, RUN 4, WIND SPEED= 8.6, COSINE COEFFICIENT=-.461818 x 10^{-1}
MISSION 318, FLIGHT 17, RUN 1, WIND SPEED=13.5, COSINE COEFFICIENT=-.301908 x 10^{-1}
MISSION 318, FLIGHT 18, RUN 2, WIND SPEED=12.0, COSINE COEFFICIENT=-.241349 x 10^{-1}
MISSION 318, FLIGHT 19, RUN 10, WIND SPEED= 7.5, COSINE COEFFICIENT=-.443721 x 10^{-1}
MISSION 335, FLIGHT 4A, RUN 1, WIND SPEED=19.1, COSINE COEFFICIENT=-.448269 x 10^{-4}
MISSION 335, FLIGHT 4B, RUN 1, WIND SPEED=19.1, COSINE COEFFICIENT=-.32931 x 10^{-1}
MISSION 335, FLIGHT 5, RUN 1, WIND SPEED=15.5, COSINE COEFFICIENT=.109179 x 10^{-1}
MISSION 335, FLIGHT 6, RUN 1, WIND SPEED=15.0, COSINE COEFFICIENT=-.152076 x 10^{-1}
MISSION 353, FLIGHT 9, RUN 11, WIND SPEED=10.8, COSINE COEFFICIENT=.313322 x 10^{-1}
MISSION 353, FLIGHT 10, RUN 1, WIND SPEED= 5.4, COSINE COEFFICIENT=.109286 x 10^{-1}
MISSION 353, FLIGHT 11, RUN 6, WIND SPEED=15.9, COSINE COEFFICIENT=-.190725 x 10^{-1}
MISSION 353, FLIGHT 13, RUN 1, WIND SPEED=10.4, COSINE COEFFICIENT=-.143949 x 10^{-1}
MISSION 353, FLIGHT 14, RUN 6, WIND SPEED=14.3, COSINE COEFFICIENT=-.834852 x 10^{-2}
MISSION 353, FLIGHT 15, RUN 11, WIND SPEED= 4.2, COSINE COEFFICIENT=.197039 x 10^{-1}
MISSION 353, FLIGHT 20, RUN 1, WIND SPEED= 2.5, COSINE COEFFICIENT=-.132059 x 10^{-1}
MISSION 353, FLIGHT 21, RUN 7, WIND SPEED= 4.7, COSINE COEFFICIENT=-.684929 x 10^{-2}

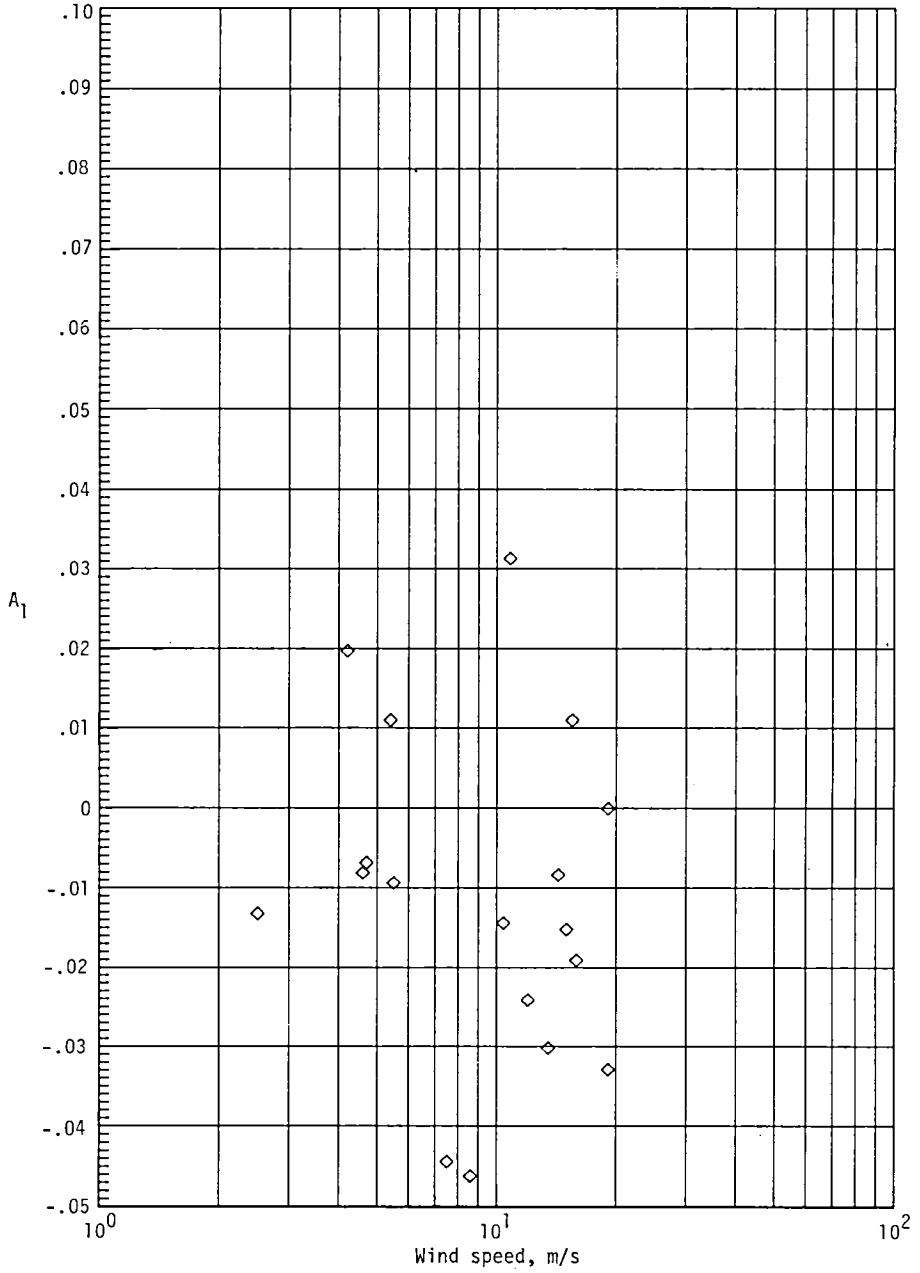

(b) $\theta = 20°$.

Figure 21.- Continued.

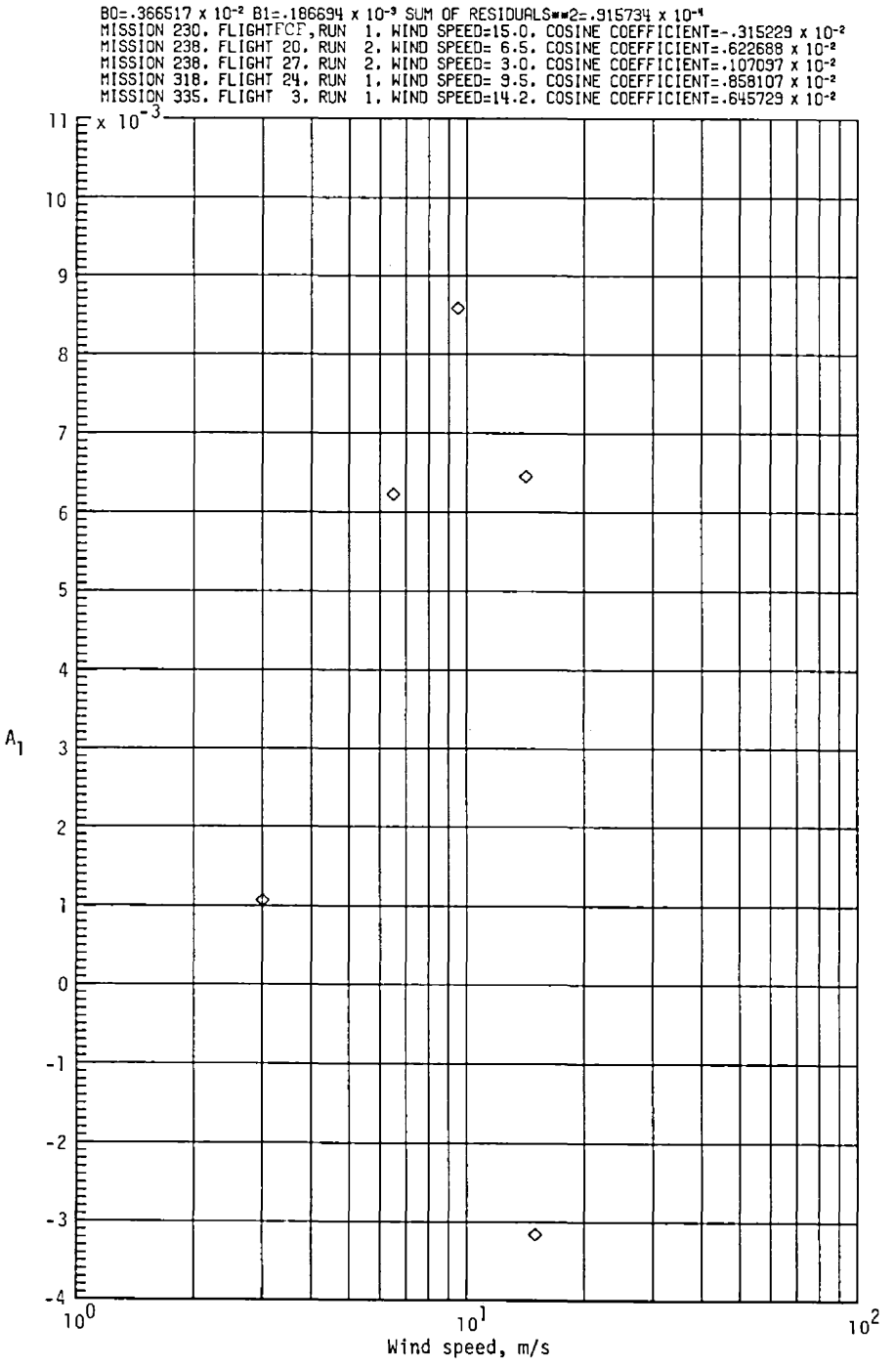

(c) $\theta = 30°$.

Figure 21.- Continued.

B0=-.496574 x 10^{-2} B1=.875131 x 10^{-2} SUM OF RESIDUALS**2=.938496 x 10^{-4}
MISSION 288, FLIGHT 6, RUN 1, WIND SPEED=13.5, COSINE COEFFICIENT=.2292 x 10^{-2}
MISSION 288, FLIGHT 6, RUN 7, WIND SPEED=13.5, COSINE COEFFICIENT=.120528 x 10^{-2}
MISSION 318, FLIGHT 13, RUN 9, WIND SPEED= 4.6, COSINE COEFFICIENT=.499285 x 10^{-3}
MISSION 318, FLIGHT 14, RUN 7, WIND SPEED= 5.5, COSINE COEFFICIENT=.983697 x 10^{-3}
MISSION 318, FLIGHT 16, RUN 9, WIND SPEED= 8.2, COSINE COEFFICIENT=.201962 x 10^{-2}
MISSION 318, FLIGHT 17, RUN 8, WIND SPEED=12.8, COSINE COEFFICIENT=.581798 x 10^{-2}
MISSION 318, FLIGHT 18, RUN 6, WIND SPEED=11.3, COSINE COEFFICIENT=.411159 x 10^{-2}
MISSION 318, FLIGHT 19, RUN 13, WIND SPEED= 7.5, COSINE COEFFICIENT=.21645 x 10^{-2}
MISSION 335, FLIGHT 4A, RUN 9, WIND SPEED=20.0, COSINE COEFFICIENT=.217982 x 10^{-2}
MISSION 335, FLIGHT 4B, RUN 10, WIND SPEED=19.4, COSINE COEFFICIENT=.127264 x 10^{-1}
MISSION 335, FLIGHT 5, RUN 9, WIND SPEED=15.2, COSINE COEFFICIENT=.65622 x 10^{-2}
MISSION 335, FLIGHT 6, RUN 9, WIND SPEED=15.0, COSINE COEFFICIENT=.6309 x 10^{-2}
MISSION 353, FLIGHT 11, RUN 11, WIND SPEED=15.7, COSINE COEFFICIENT=.757874 x 10^{-2}
MISSION 353, FLIGHT 13, RUN 20, WIND SPEED=12.0, COSINE COEFFICIENT=.405294 x 10^{-2}
MISSION 353, FLIGHT 14, RUN 11, WIND SPEED=14.3, COSINE COEFFICIENT=.534718 x 10^{-2}
MISSION 353, FLIGHT 15, RUN 16, WIND SPEED= 4.2, COSINE COEFFICIENT=.898057 x 10^{-3}
MISSION 353, FLIGHT 20, RUN 26, WIND SPEED= 2.5, COSINE COEFFICIENT=.364762 x 10^{-3}
MISSION 353, FLIGHT 21, RUN 12, WIND SPEED= 4.7, COSINE COEFFICIENT=.256576 x 10^{-3}

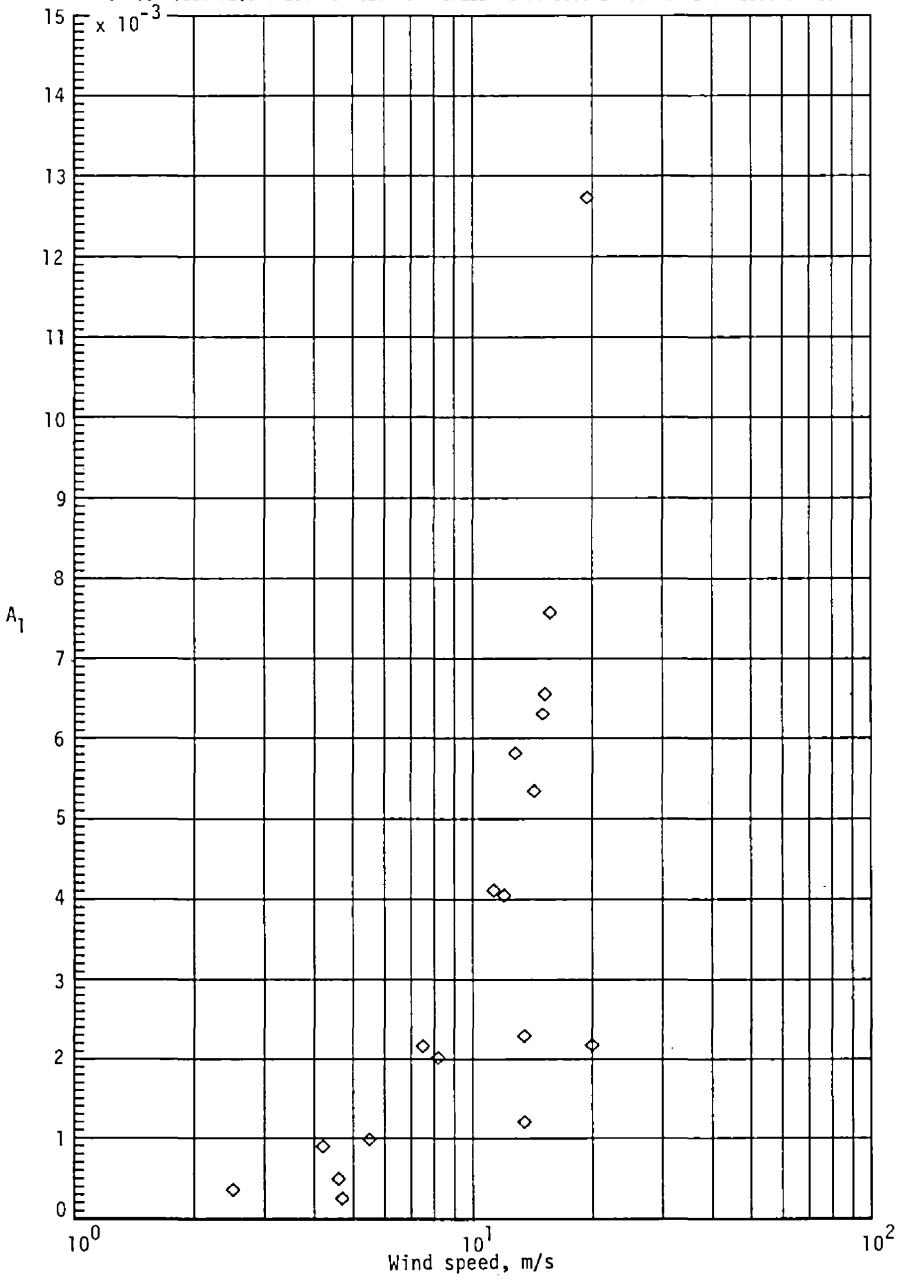

(d) $\theta = 40°$.

Figure 21.- Continued.

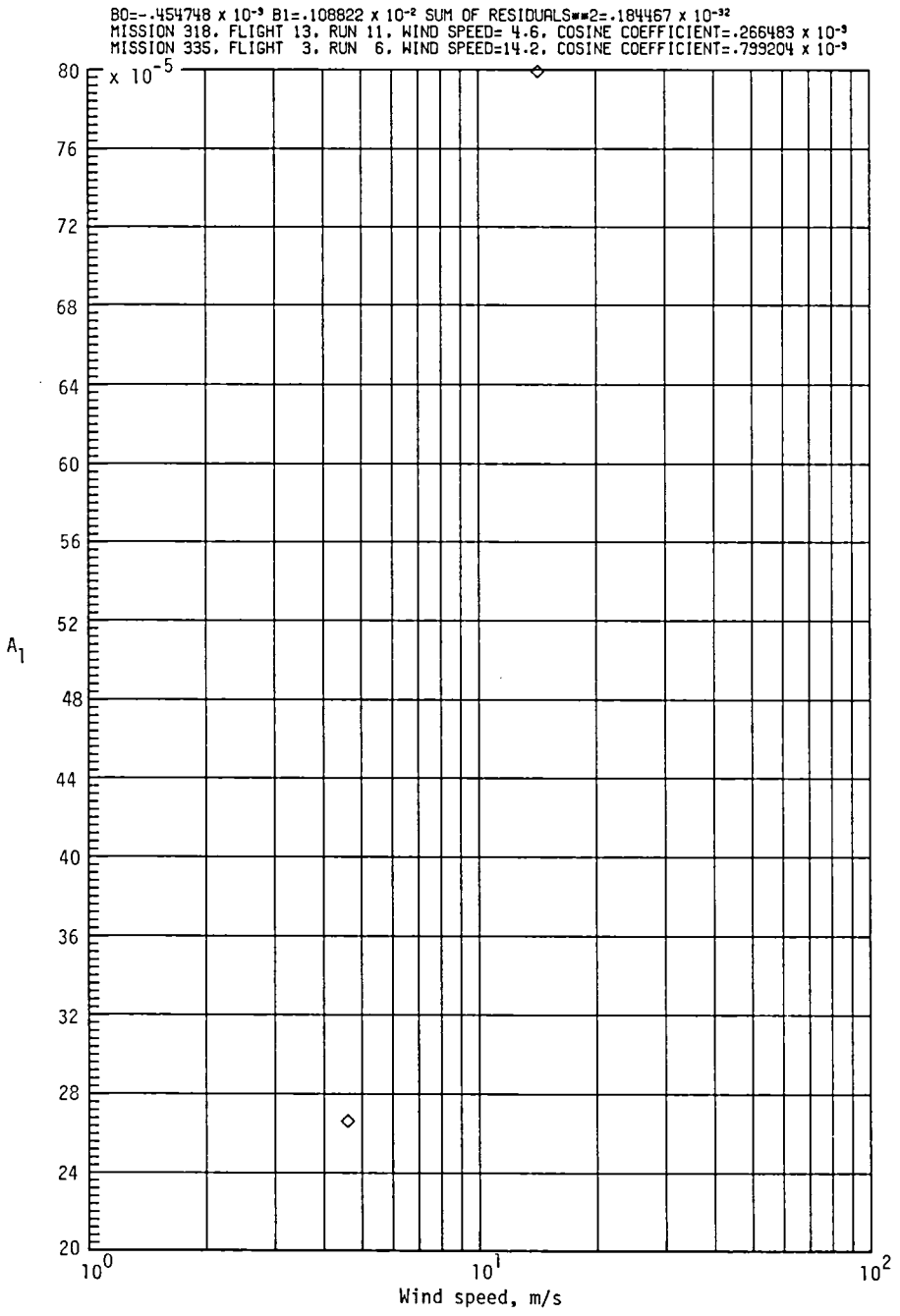

(e) $\theta = 50°$.

Figure 21.- Continued.

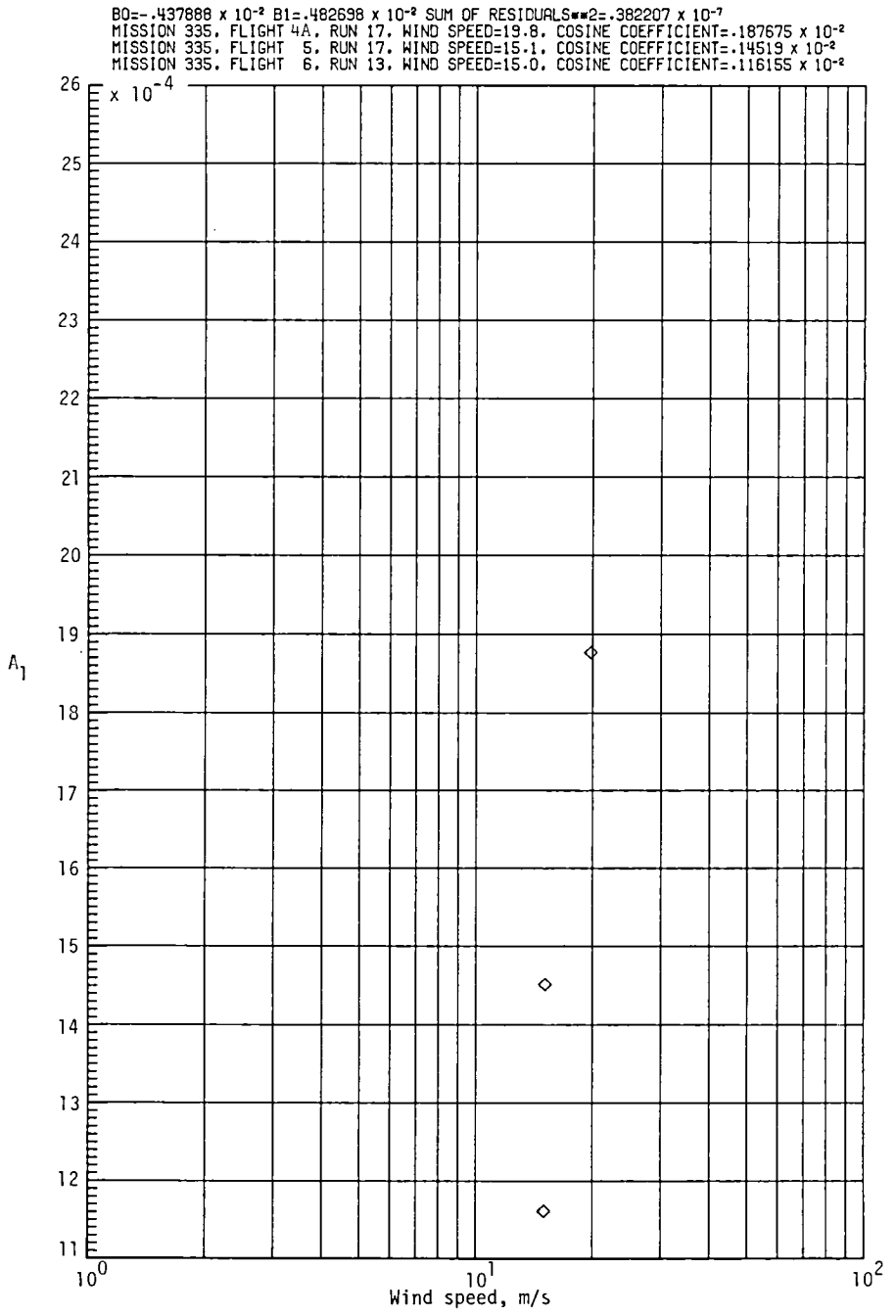

(f) $\theta = 60°$.

Figure 21.- Continued.

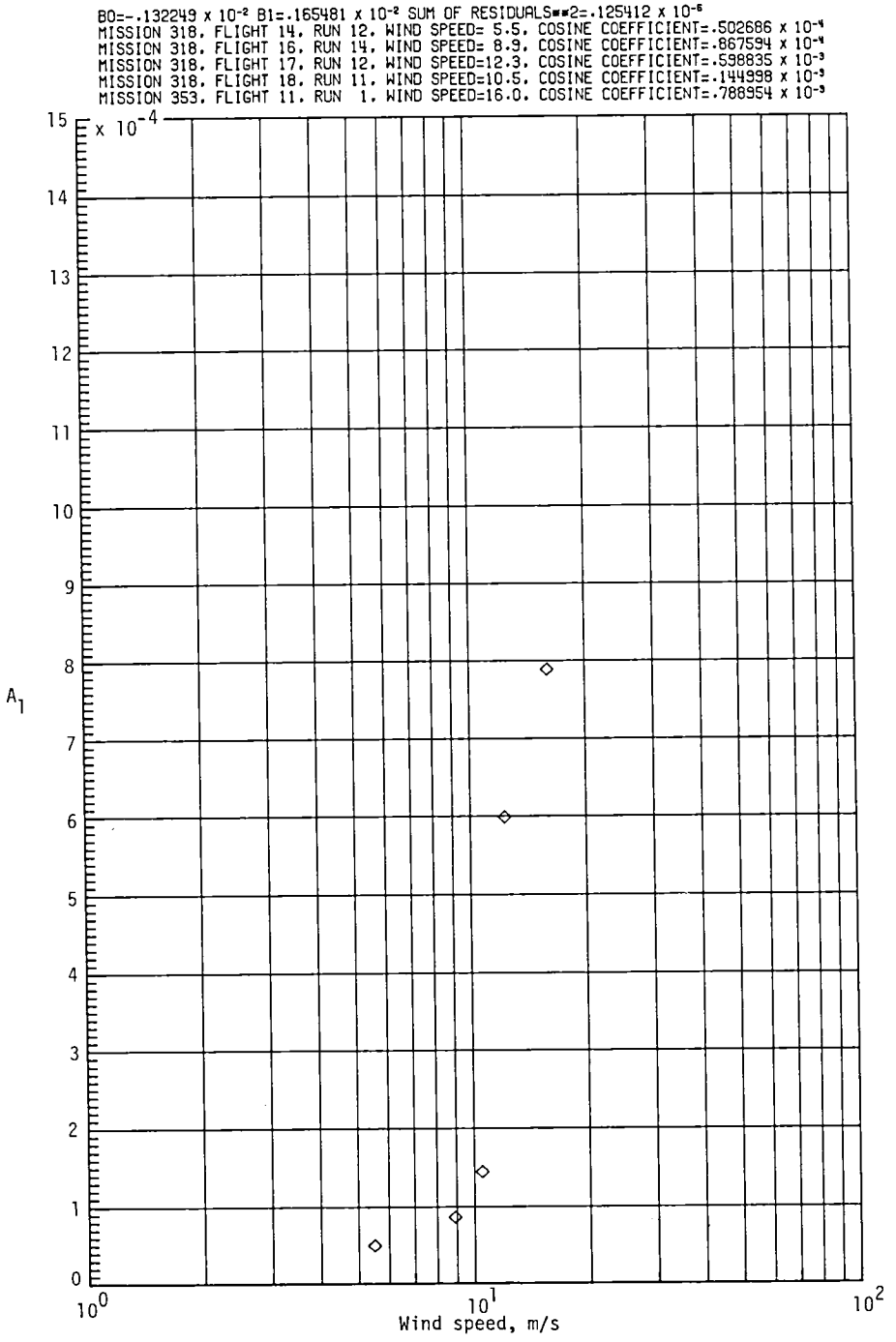

(g) $\theta = 70°$.

Figure 21.- Concluded.

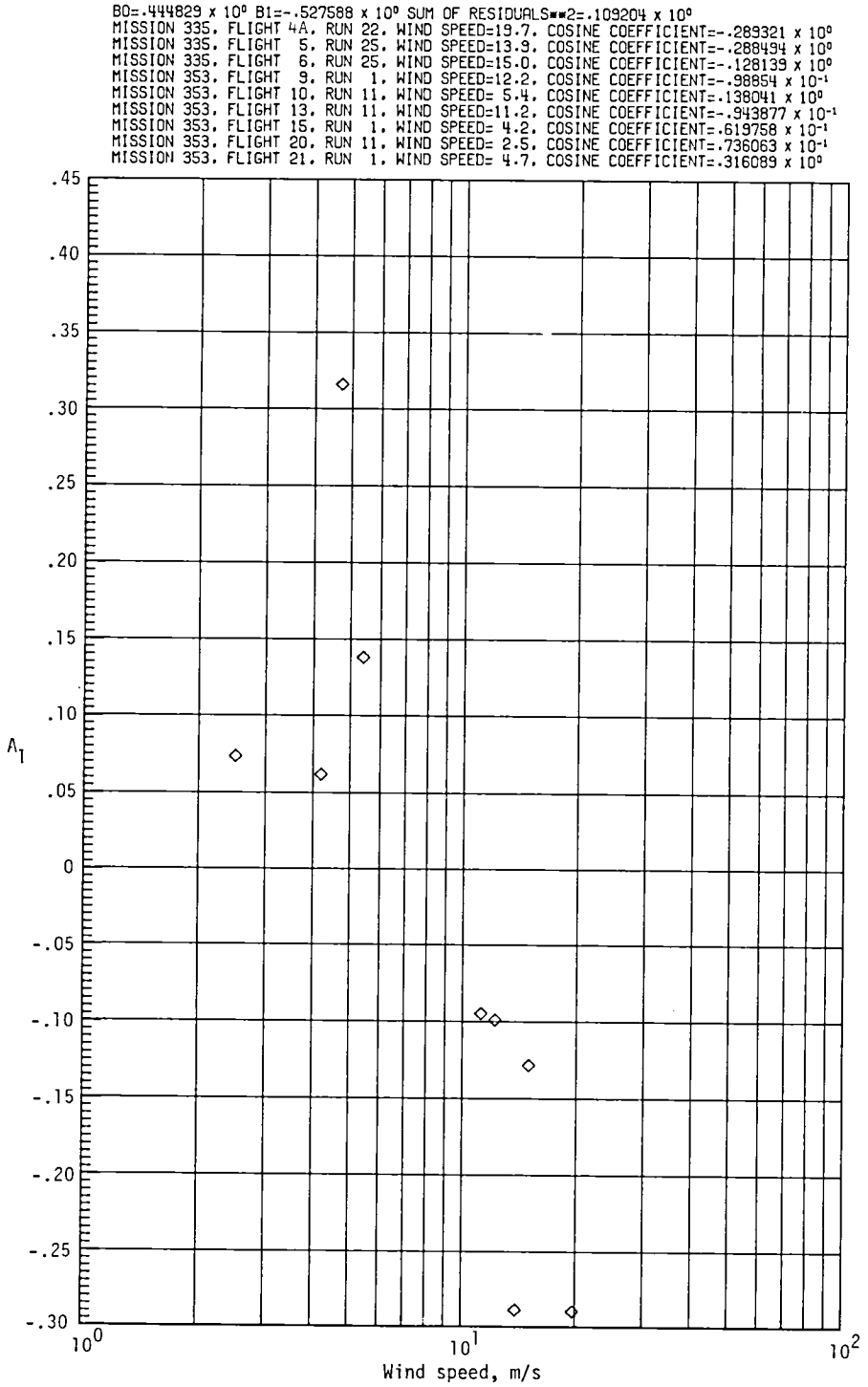

(a) $\theta = 10°$.

Figure 22.- Second-order regression coefficient A_1 versus log (Wind speed) for vertical polarization.

B0=.254113 x 10^{-1} B1=-.508442 x 10^{-1} SUM OF RESIDUALS**2=.106488 x 10^{-1}
MISSION 318, FLIGHT 13, RUN 3, WIND SPEED= 4.6, COSINE COEFFICIENT=-.904734 x 10^{-2}
MISSION 318, FLIGHT 14, RUN 1, WIND SPEED= 5.5, COSINE COEFFICIENT=-.105874 x 10^{-1}
MISSION 318, FLIGHT 16, RUN 4, WIND SPEED= 8.6, COSINE COEFFICIENT=-.461303 x 10^{-1}
MISSION 318, FLIGHT 17, RUN 1, WIND SPEED=13.5, COSINE COEFFICIENT=-.501188 x 10^{-1}
MISSION 318, FLIGHT 18, RUN 2, WIND SPEED=12.0, COSINE COEFFICIENT=-.28146 x 10^{-1}
MISSION 318, FLIGHT 19, RUN 10, WIND SPEED= 7.5, COSINE COEFFICIENT=-.59275 x 10^{-1}
MISSION 335, FLIGHT 4A, RUN 1, WIND SPEED=19.1, COSINE COEFFICIENT=-.241912 x 10^{-1}
MISSION 335, FLIGHT 4B, RUN 1, WIND SPEED=19.1, COSINE COEFFICIENT=-.803014 x 10^{-1}
MISSION 335, FLIGHT 5, RUN 1, WIND SPEED=15.5, COSINE COEFFICIENT=-.778731 x 10^{-2}
MISSION 335, FLIGHT 6, RUN 1, WIND SPEED=15.0, COSINE COEFFICIENT=-.362037 x 10^{-1}
MISSION 353, FLIGHT 9, RUN 11, WIND SPEED=10.8, COSINE COEFFICIENT=.291152 x 10^{-1}
MISSION 353, FLIGHT 10, RUN 1, WIND SPEED= 5.4, COSINE COEFFICIENT=.148893 x 10^{-1}
MISSION 353, FLIGHT 11, RUN 6, WIND SPEED=15.9, COSINE COEFFICIENT=-.494885 x 10^{-1}
MISSION 353, FLIGHT 13, RUN 1, WIND SPEED=10.4, COSINE COEFFICIENT=-.26601 x 10^{-1}
MISSION 353, FLIGHT 14, RUN 6, WIND SPEED=14.3, COSINE COEFFICIENT=-.251775 x 10^{-1}
MISSION 353, FLIGHT 15, RUN 11, WIND SPEED= 4.2, COSINE COEFFICIENT=.203669 x 10^{-1}
MISSION 353, FLIGHT 20, RUN 1, WIND SPEED= 2.5, COSINE COEFFICIENT=-.20129 x 10^{-1}
MISSION 353, FLIGHT 21, RUN 7, WIND SPEED= 4.7, COSINE COEFFICIENT=-.746688 x 10^{-2}

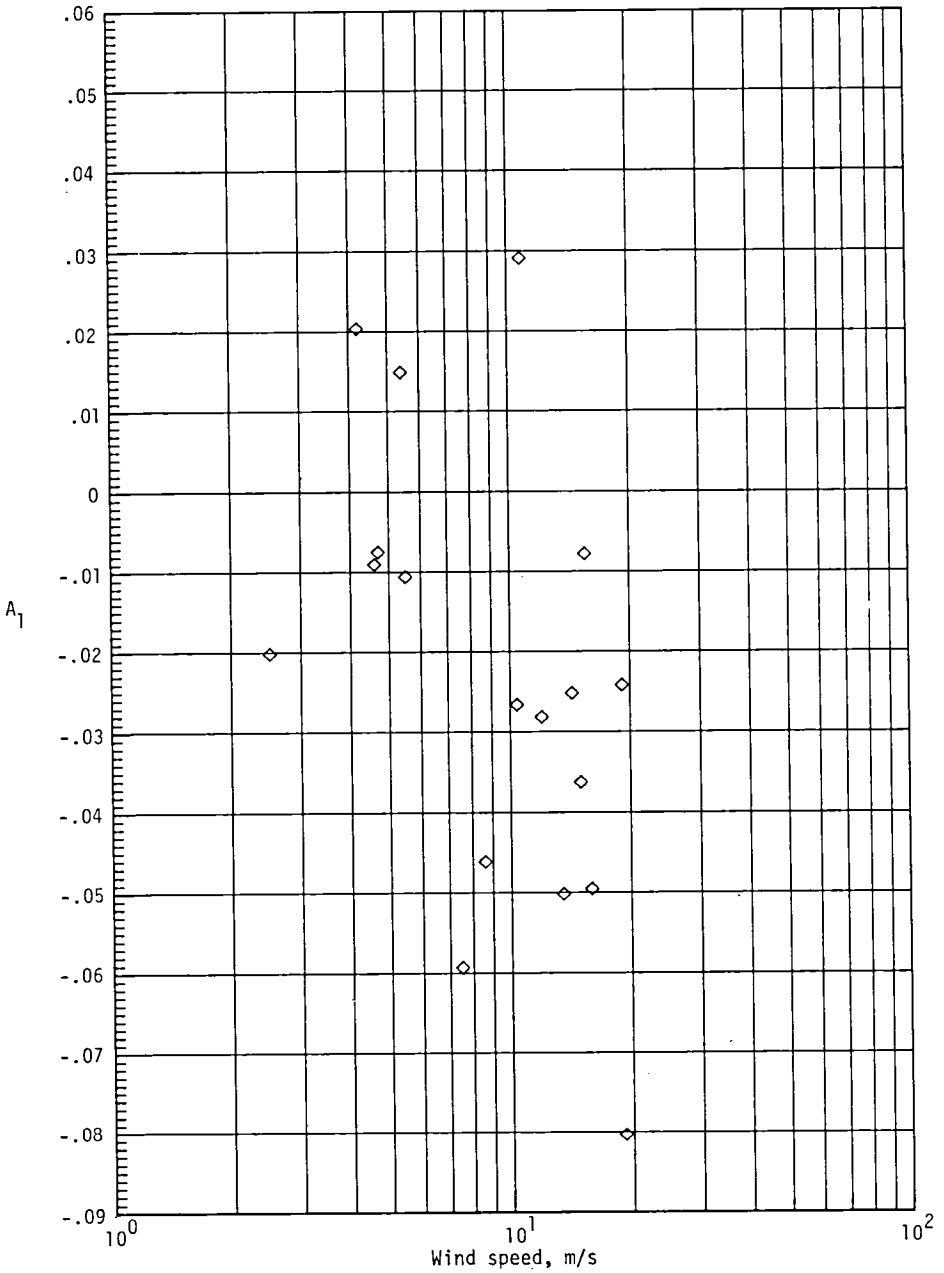

(b) $\theta = 20°$.

Figure 22.- Continued.

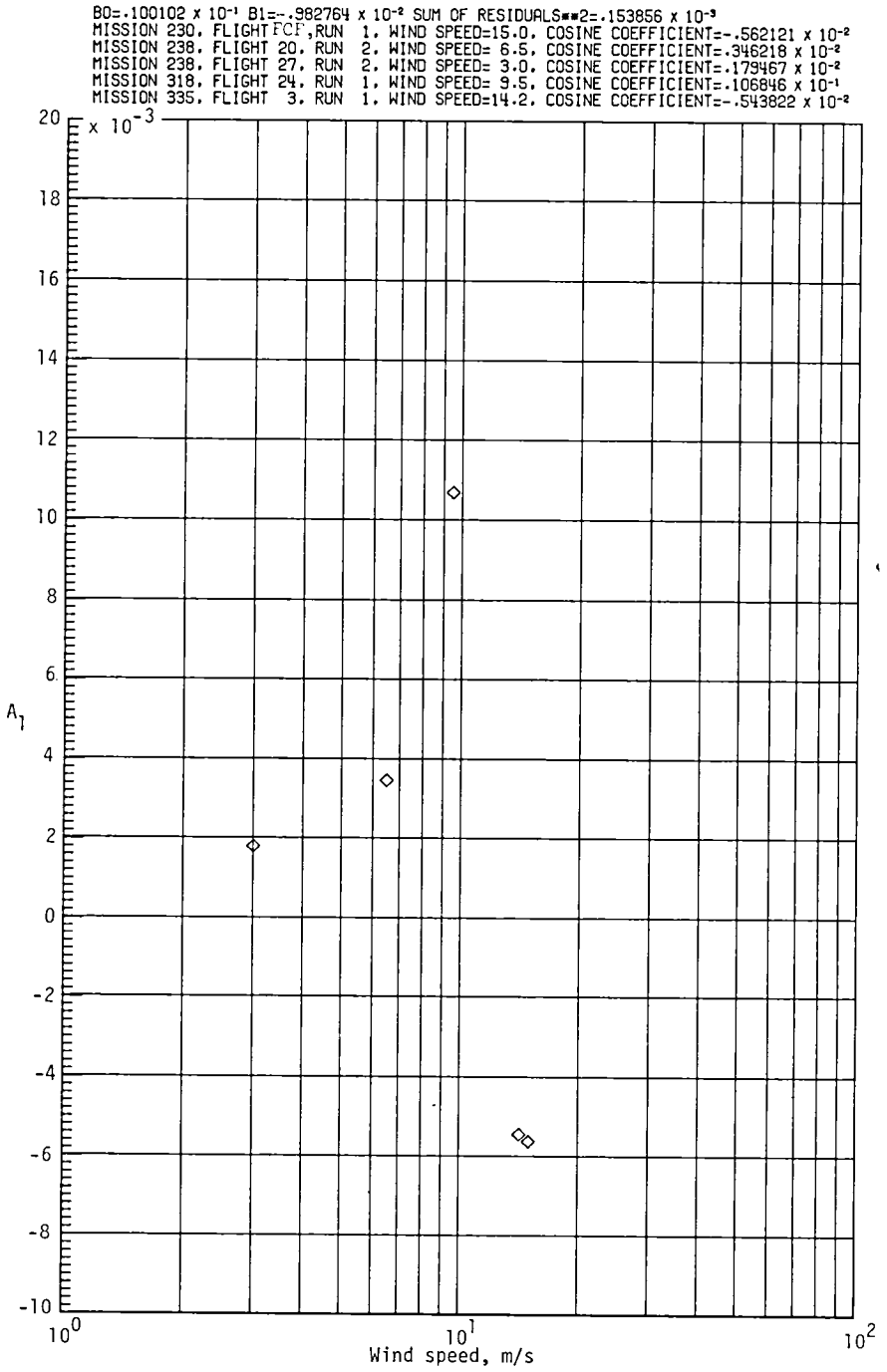

(c) $\theta = 30°$.

Figure 22.- Continued.

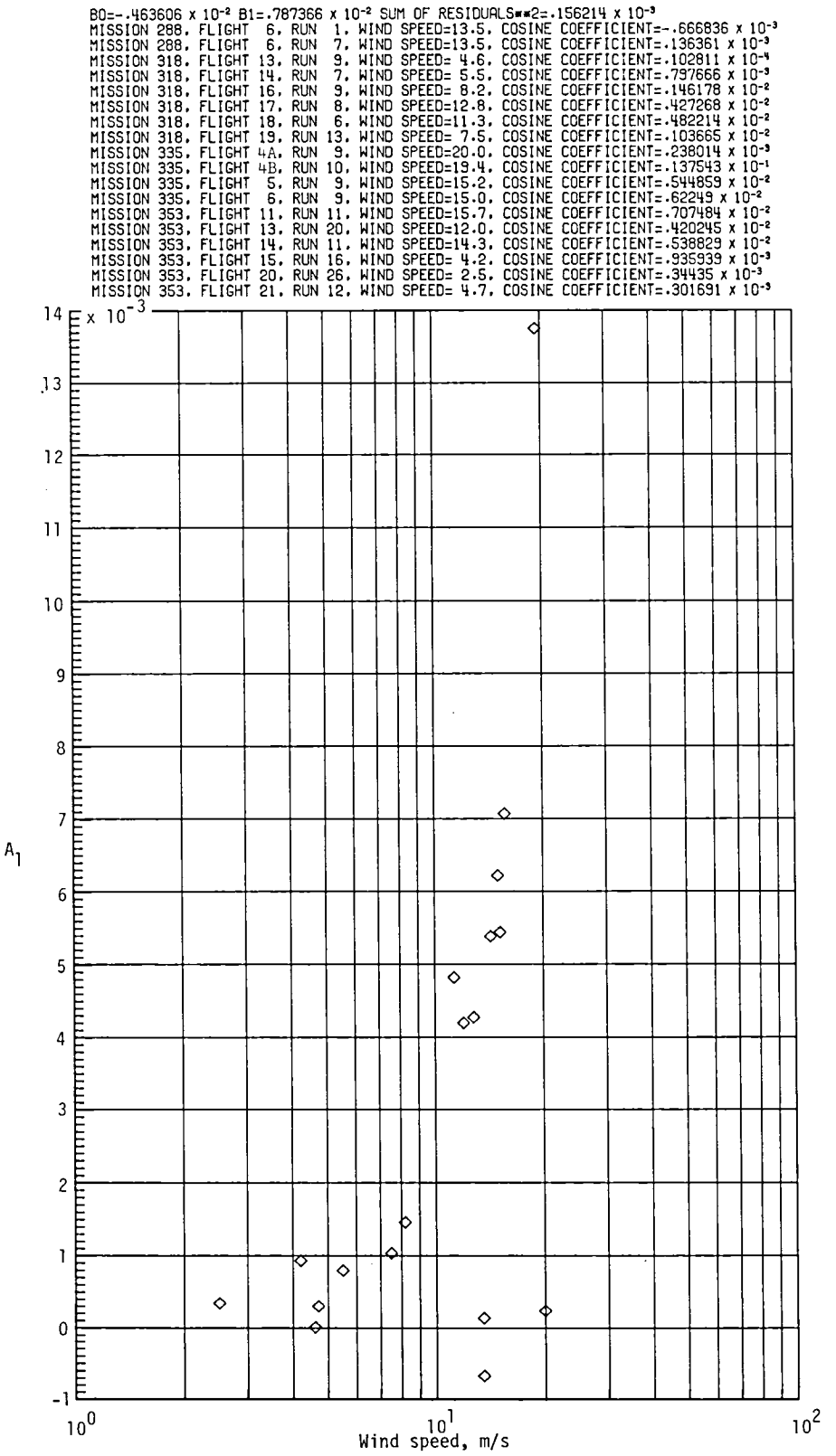

(d) $\theta = 40°$.

Figure 22.- Continued.

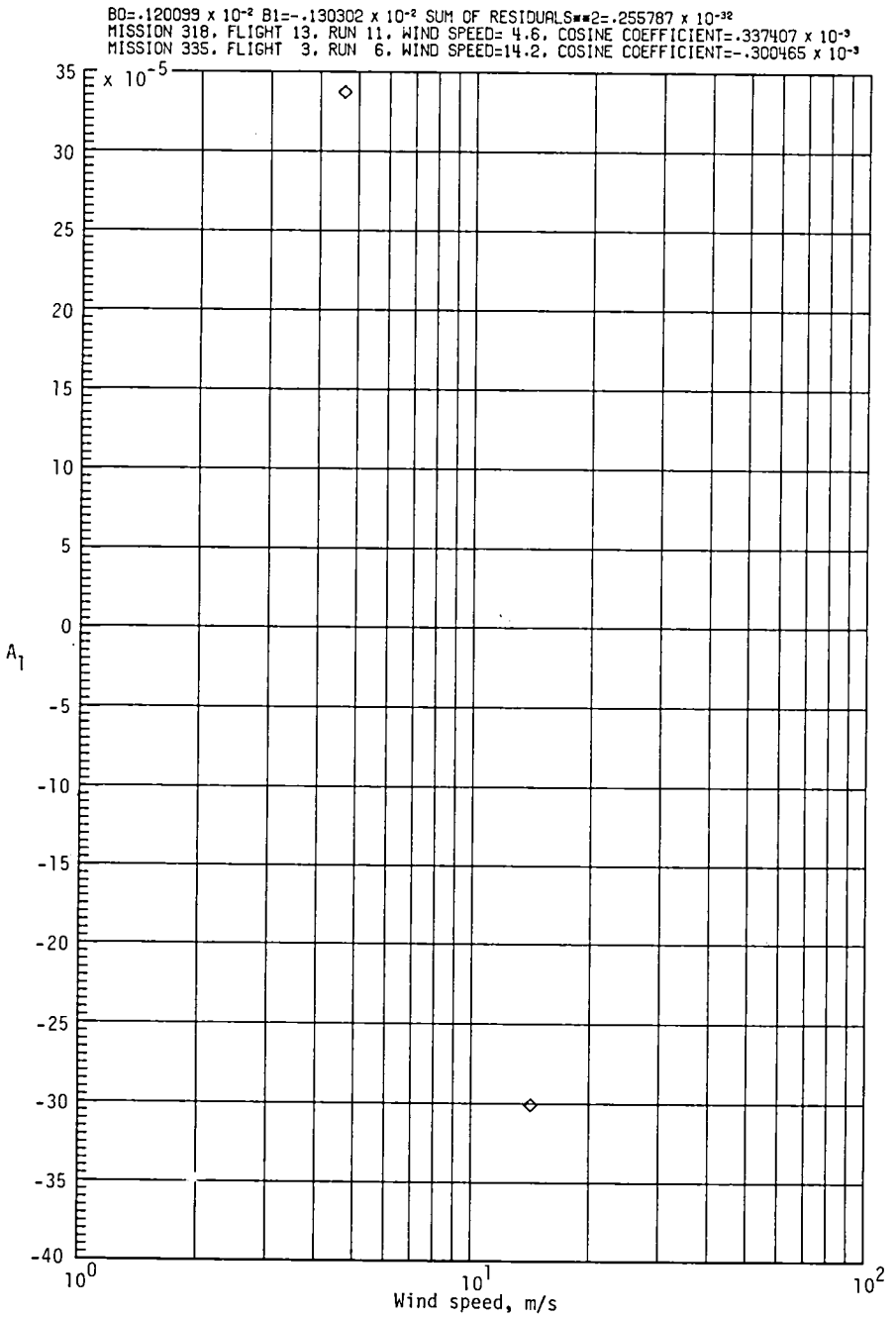

(e) $\theta = 50°$.

Figure 22.- Continued.

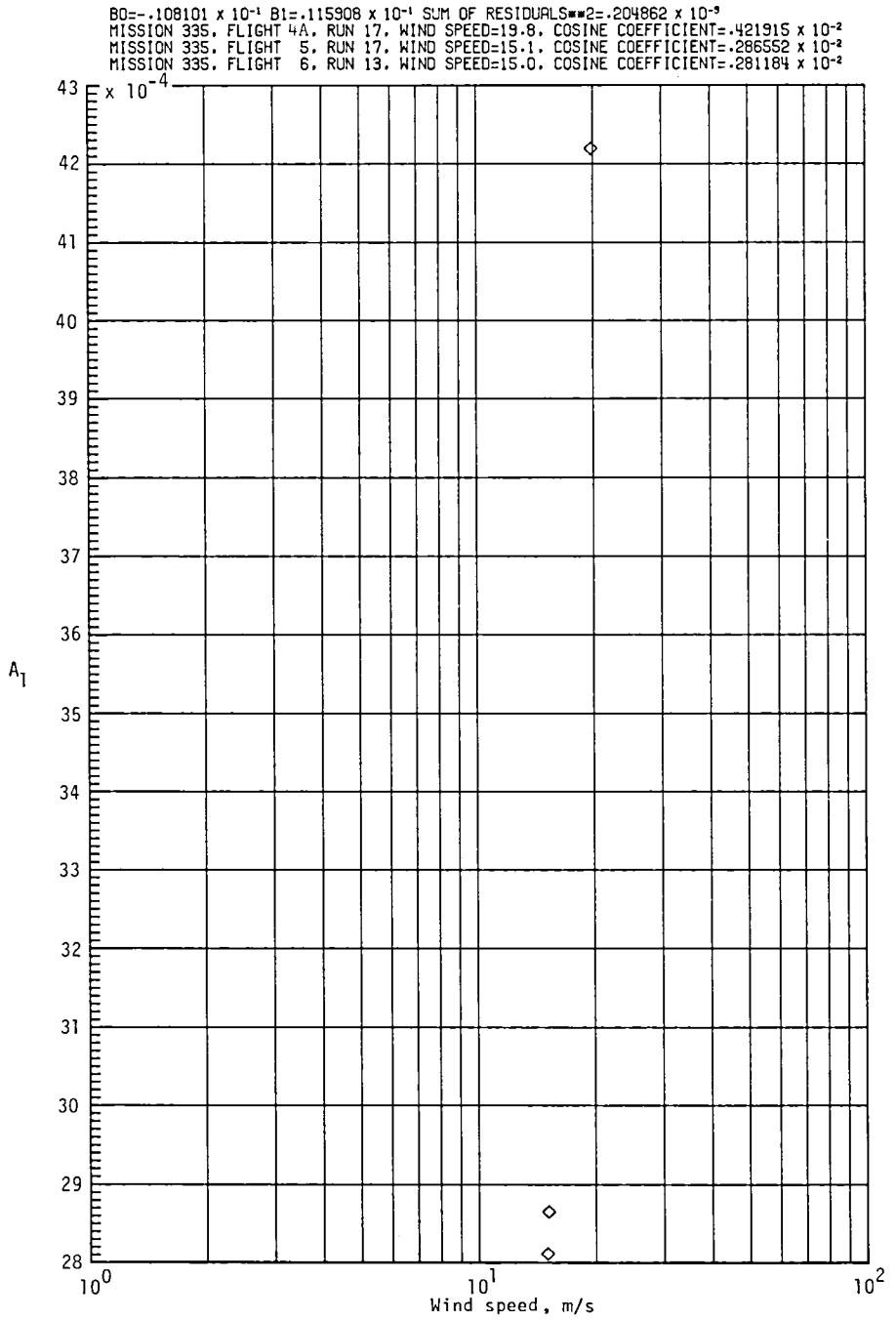

(f) $\theta = 60°$.

Figure 22.- Continued.

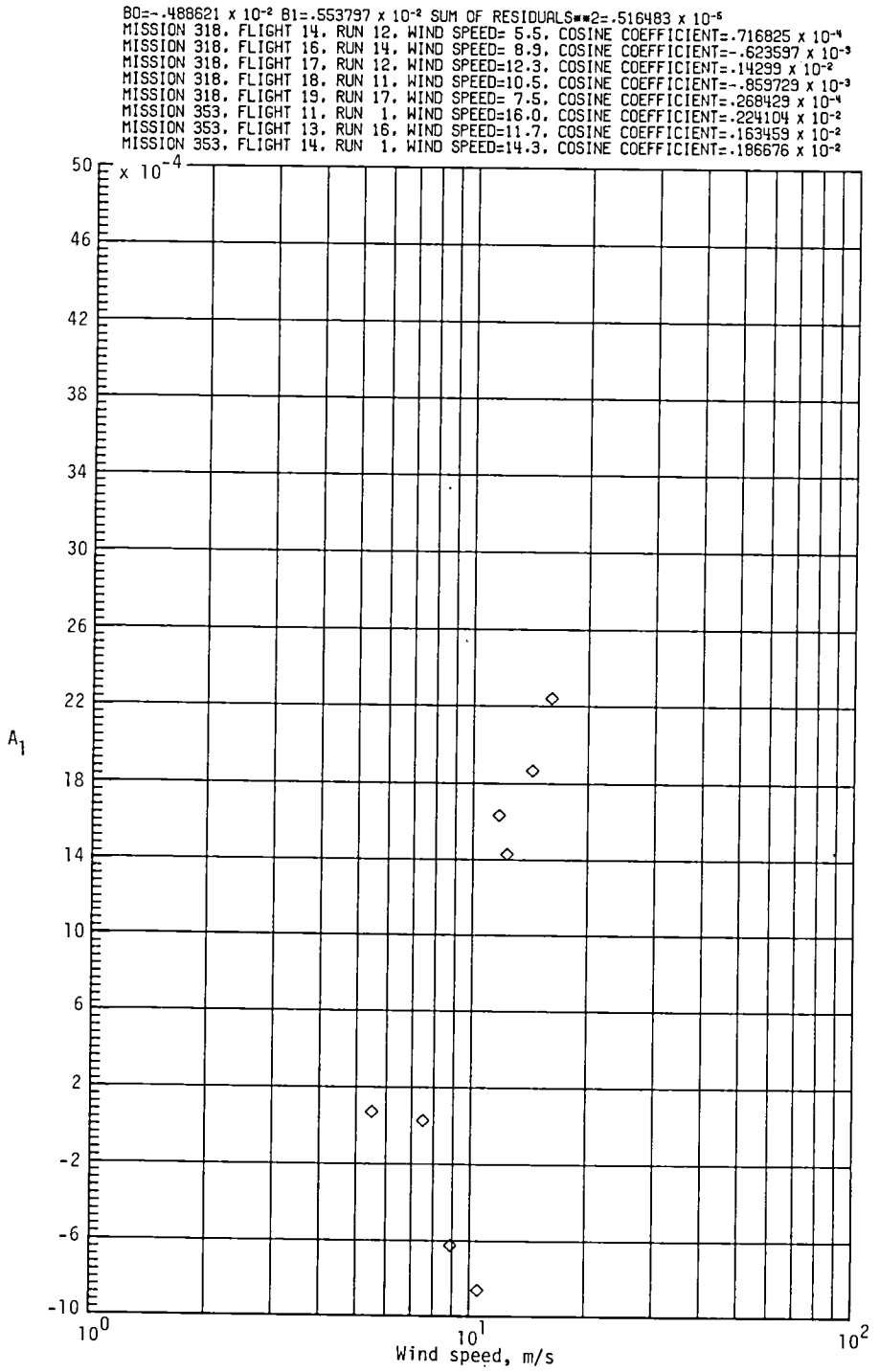

(g) $\theta = 70°$.

Figure 22.- Concluded.

1. Report No.	2. Government Accession No.	3. Recipient's Catalog No.
NASA TM-85646		

4. Title and Subtitle	5. Report Date
FLIGHT MEASUREMENT AND ANALYSIS OF AAFE RADSCAT WIND SPEED SIGNATURE OF THE OCEAN	January 1984
	6. Performing Organization Code 146-40-05-05

7. Author(s)	8. Performing Organization Report No.
Lyle C. Schroeder, W. Linwood Jones, Philip R. Schaffner, and John L. Mitchell	L-15651
	10. Work Unit No.

9. Performing Organization Name and Address	11. Contract or Grant No.
NASA Langley Research Center Hampton, VA 23665	

12. Sponsoring Agency Name and Address	13. Type of Report and Period Covered
National Aeronautics and Space Administration Washington, DC 20546	Technical Memorandum
	14. Sponsoring Agency Code

15. Supplementary Notes

Lyle C. Schroeder: Langley Research Center, Hampton, Virginia.
W. Linwood Jones: Satellite Television Corporation, Princeton Junction, New Jersey.
Philip R. Schaffner: Research Triangle Institute, Hampton, Virginia.
John L. Mitchell: Kentron International, Inc., Hampton, Virginia.

16. Abstract

About 10 years ago, the Advanced Aerospace Flight Experiment Radiometer Scatterometer (AAFE RADSCAT) made its first successful measurements of ocean radar scattering cross section from a NASA C-130 aircraft. This instrument was developed as a research tool to evaluate the use of microwave frequency remote sensors (particularly radars) to provide wind speed information at the ocean surface. The AAFE RADSCAT helped establish the feasibility of the satellite scatterometer for measuring both wind speed and direction. Probably the most important function of the AAFE RADSCAT was to provide a data base of ocean normalized radar cross section (NRCS) measurements as a function of surface wind vector at 13.9 GHz. NRCS measurements over a wide parametric range of incidence angles, azimuth angles, and winds were obtained in a series of RADSCAT aircraft missions from 1973 to 1977. In this report, analyses of data are presented from 26 of these flights during which the quality of the sensor and the surface wind measurements were felt to be understood. This data base was used to model the relationship between k_u-band radar signature and ocean surface wind vector. The models developed therefrom are compared with those used for inversion of the SEASAT-A satellite scatterometer (SASS) radar measurements to wind speeds. This report represents a comprehensive analysis of the complete RADSCAT data base.

17. Key Words (Suggested by Author(s))	18. Distribution Statement
k_u-band scatterometer Ocean wind sensor Radar cross section	Unclassified - Unlimited Subject Category 48

19. Security Classif. (of this report)	20. Security Classif. (of this page)	21. No. of Pages	22. Price
Unclassified	Unclassified	148	A07

For sale by the National Technical Information Service, Springfield, Virginia 22161

NASA-Langley, 1984

National Aeronautics and
Space Administration

Washington, D.C.
20546

Official Business
Penalty for Private Use, $300

THIRD-CLASS BULK RATE

Postage and Fees Paid
National Aeronautics and
Space Administration
NASA-451

NASA

POSTMASTER: If Undeliverable (Section 158 Postal Manual) Do Not Return